National Technical University of Athens

School of Electrical and Computer Engineering

Division of Communication, Electronic and Information Engineering

Network Management and Optimal Design Laboratory

Resource Allocation and Incentive Mechanism Design in Next Generation Wireless Communication and Mobile Computing Networks

Dissertation submitted for the degree of Doctor of Philosophy

of

Maria Diamanti

Athens
November 6, 2023

National Technical University of Athens
School of Electrical and Computer Engineering
Division of Communication, Electronic and Information Engineering
Network Management and Optimal Design Laboratory

Resource Allocation and Incentive Mechanism Design in Next Generation Wireless Communication and Mobile Computing Networks

Dissertation submitted for the degree of Doctor of Philosophy

of

Maria Diamanti

Advisory Committee: Prof. Symeon Papavassiliou *(Supervisor)*
Prof. Dimitrios Askounis
Prof. Theodora Varvarigou

Approved by the seven-member committee on 6th November, 2023

.....	.....	.....
Symeon Papavassiliou	Dimitrios Askounis	Theodora Varvarigou
Professor, NTUA	Professor, NTUA	Professor, NTUA
.....	.....	.....
Ioanna Roussaki	Eirini Eleni Tsiropoulou	Nikolaos Mitrou
Associate Professor, NTUA	Associate Professor, UNM	Professor, NTUA
.....		
Athanasios Panagopoulos		
Professor, NTUA		

Athens, November 2023

.....
Μαρία Διαμαντή
Διδάκτωρ Ηλεκτρολόγος Μηχανικός και Μηχανικός Υπολογιστών ΕΜΠ

Abstract

In light of the broader vision for digitalization and smart-X vertical industries (e.g., smart city, healthcare, manufacturing), an unprecedented increase of data-hungry and compute-intensive applications takes place, imposing stringent communication and computing requirements on the network. As a means of extending connectivity, increasing spectral and energy efficiency, and reducing latency, several prominent technologies and architectural paradigms emerge as key enablers of the Next Generation (NextG) 5G wireless networks. In this context, the simplistic adoption of existing solutions to traditional resource management problems is inefficient in exploring and exploiting the network's capabilities. On the contrary, several degrees of freedom should be concurrently determined about the nature and type of the resources to be allocated while accounting for the multifaceted competition between different stakeholders.

In this thesis, we tackle the problem of efficient resource allocation in heterogeneous and multi-tier wireless communication and mobile computing networks in a holistic, though distributed, manner. In the direction of self-organizing networks, where each network entity makes autonomous decisions regarding its resource utilization and allocation, we develop novel frameworks that capture the interdependencies between different network entities' behaviors, interactions, and decisions by accounting for their different and/or conflicting objectives and the existence of incompleteness of information between them. To provide such a real-life spirit in modeling the resource management problems, we resort to Game Theory and Contract Theory, which result in low-complexity methodologies and algorithms for solving the formulated problems.

First, multi-variable resource allocation problems are studied in heterogeneous and multi-tier wireless communication networks. Targeting to address the problem of incomplete/partial Channel State Information (CSI) from the Base Stations' (BSs') behalf, as well as the user-BS conflict regarding the users' uplink transmission power investment, a synergistic approach based on the principles of Contract Theory is initially introduced. The BSs design a menu of contracts based on their statistical knowledge about the users' CSI, which comprise indicative power levels along with a corresponding reward, such that the designed power levels enable the decoding of the users' transmitted signals at the BSs' receivers via the combination of Non-Orthogonal Multiple Access (NOMA) and Successive Interference Cancellation (SIC). The users autonomously select the one contract out of the menu that best fits their experienced channel conditions while employing a Reinforcement Learning (RL) algorithm to distributively determine the most beneficial BS association.

Taking one step further to the underlying network architecture and employed technologies, we aim to concurrently account for and properly configure the resources across the wireless access and backhaul network parts of an Unmanned Aerial Vehicle (UAV)-assisted and Reconfigurable Intelligent Surface (RIS)-aided communication network. By capitalizing on the structural hierarchy between the UAV-mounted BS and the users, a Stackelberg game is formulated to distributively deal with a highly combinatorial resource management problem. The UAV, acting as leader, determines the RIS's phase shifts such that the sum users' signal strength is maximized in the uplink and, in a second phase, jointly calculates the bandwidth and uplink transmission power allocation in the backhaul link to the core network. In the third phase, the users, acting as the followers, optimize their uplink transmission powers to the UAV in a distributed manner. The second and third phases are iteratively repeated to conclude with the game's Stackelberg equilibrium point, at which the end-to-end energy efficiency is maximized.

Respecting the need for converged radio and computing resource allocation frameworks within the context of NextG 5G networks, a multi-tier mobile computing topology is considered, and the joint problem of computation task offloading and uplink transmission/offloading power allocation is studied. In contrast to the existing literature, where single-tier computing networks are modeled, consisting of an edge, a fog, or a cloud service layer, concurrently utilizing a wide range of computing capabilities and options is pursued. Given the users' selfish behavior towards offloading to the edge due to the latter's proximity, an incentivization mechanism based on Contract Theory is designed to motivate them to allow a percentage of their initially offloaded tasks to the edge to be further forwarded and processed at the fog. Having determined this percentage, the ultimate users' computation task offloading and uplink transmission power to edge are jointly derived in a distributed manner by playing a game among them. By utilizing multiple computing service layers, an energy-efficient solution is derived while extending the edge service layer's computing capacity.

Finally, aiming to further study the distribution of computation tasks horizontally, i.e., within the same computing tier, while considering multiple servers, a multi-server Multi-Access Edge Computing (MEC) network is modeled. The users leverage the different available Radio Access Networks (RANs) nearby to offload their compute-intensive and latency-critical applications to multiple MEC servers simultaneously. To address the critical interference management problem under the resulting multi-user multi-server network topology while being motivated by the advancements in the non-orthogonal multiple access techniques, the application of Rate-Splitting Multiple Access (RSMA) is scrutinized. In this context, the minimization of the sum of the users' maximum experienced delay among the different MEC servers is pursued by jointly optimizing their computation task offloading ratios, rate, uplink transmission power, and computing resource allocation across the offloading MEC servers. The formulated joint optimization problem is analytically solved using conventional optimization techniques based on the Karush-Kuhn-Tucker (KKT) conditions. This complements the ultimate purpose of this thesis to provide a holistic approach and view to the converged wireless communication and mobile computing networks.

The considered resource management problems are thoroughly evaluated via modeling and simulation. The proposed frameworks' pure operational characteristics and the designed algorithms' convergence behavior are examined under different scenarios and values, while comparative results against other benchmarking and state-of-the-art solutions are provided to demonstrate the proposed frameworks' effectiveness and efficiency.

Keywords: Resource Allocation, Incentive Mechanisms, Non-Orthogonal Multiple Access, Rate-Splitting Multiple Access, Reconfigurable Intelligent Surface, Multi-access Edge Computing, Multi-variable Optimization, Distributed Optimization, Game Theory, Contract Theory

Περίληψη

Υπό το πρίσμα του ευρύτερου οράματος για ψηφιοποίηση και μετασχηματισμό των κάθετων βιομηχανιών (π.χ. έξυπνες πόλεις, έξυπνο σύστημα υγείας, έξυπνα εργοστάσια), σημειώνεται μια άνευ προηγουμένου αύξηση των εφαρμογών με εντατικές απαιτήσεις ως προς τον όγκο των δεδομένων που διαχειρίζονται και την αναγκαία υπολογιστική ισχύ για την επεξεργασία αυτών. Αυτό έχει ως αποτέλεσμα την επιβολή αυστηρών απαιτήσεων που αφορούν το ασύρματο δίκτυο. Ως μέσο επέκτασης της συνδεσιμότητας, αύξησης της φασματικής και ενεργειακής απόδοσης και μείωσης του λανθάνοντος χρόνου, μια πληθώρα τεχνολογιών και αρχιτεκτονικών παραδειγμάτων αναδεικνύονται ως μέσα ενεργοποίησης των ασύρματων δικτύων 5G επόμενης γενιάς. Σε αυτό το πλαίσιο, η απλοϊκή υιοθέτηση υφιστάμενων λύσεων σε παραδοσιακά προβλήματα κατανομής πόρων είναι αναποτελεσματική για την εξερεύνηση και την εκμετάλλευση των δυνατοτήτων του δικτύου. Αντίθετα, αρκετοί βαθμοί ελευθερίας πρέπει να καθορίζονται ταυτόχρονα σχετικά με τη φύση και το είδος των πόρων που κατανέμονται στο δίκτυο, λαμβάνοντας υπόψιν τον πολύπλευρο ανταγωνισμό μεταξύ των ενδιαφερόμενων μερών (π.χ. συνδρομητές, πάροχοι).

Σε αυτή τη διατριβή, αντιμετωπίζουμε το πρόβλημα της κατανομής πόρων σε ετερογενή και πολυεπίπεδα ασύρματα δίκτυα επικοινωνιών και κινητών υπολογισμών με έναν ολιστικό, αλλά κατανεμημένο, τρόπο. Σύμφωνα με τα αυτο-οργανωμένα δίκτυα, όπου κάθε δικτυακή οντότητα λαμβάνει αυτόνομες αποφάσεις σχετικά με τη χρήση και την κατανομή των πόρων της, αναπτύσσουμε πλαίσια που αντικατοπτρίζουν τις αλληλεξαρτήσεις μεταξύ των συμπεριφορών, των αλληλεπιδράσεων και των αποφάσεων των διαφορετικών διακτυακών οντοτήτων, λαμβάνοντας υπόψιν τους διαφορετικούς ή/και αντικρουόμενους στόχους τους, καθώς και την ύπαρξη ελλιπούς πληροφόρησης μεταξύ τους. Προκειμένου να προσδοθεί μια τέτοια ρεαλιστική χρειά στη μοντελοποίηση των προβλημάτων κατανομής πόρων, καταφεύγουμε στη Θεωρία Παιγνίων (Game Theory) και στη Θεωρία Συμβολαίων (Contract Theory), οι οποίες οδηγούν σε μεθοδολογίες και αλγόριθμους χαμηλής πολυπλοκότητας για την επίλυση των αντίστοιχων προβλημάτων.

Αρχικά, μελετώνται προβλήματα κατανομής πόρων πολλαπλών μεταβλητών σε ετερογενή και πολυεπίπεδα ασύρματα δίκτυα επικοινωνιών. Με στόχο την αντιμετώπιση του προβλήματος της ελλιπούς/μερικής πληροφόρησης των σταθμών βάσης σχετικά με την κατάσταση καναλιού (Channel State Information - CSI), καθώς και της αντίφασης μεταξύ των χρηστών και των σταθμών βάσης σχετικά με το επίπεδο ισχύος μετάδοσης στη ζεύξη ανόδου, εισάγεται μια συνεργατική προσέγγιση μεταξύ των δύο αυτών μερών, η οποία βασίζεται στις αρχές της Θεωρίας Συμβολαίων. Οι σταθμοί βάσης σχεδιάζουν ένα σύνολο συμβολαίων που αποτελούνται από ενδεικτικά επίπεδα ισχύος για τη ζεύξη ανόδου μαζί με μια αντίστοιχη ανταμοιβή προς τους χρήστες, κάνοντας χρήση της στατιστικής τους γνώσης σχετικά με την κατάσταση του καναλιού των χρηστών. Τα επίπεδα ισχύος των συμβολαίων επιλέγονται με τέτοιο τρόπο ώστε να επιτρέπουν την αποκωδικοποίηση των μεταδιδόμενων σημάτων των χρηστών από τους δέκτες των σταθμών βάσης, κάνοντας χρήση των τεχνικών μη ορθογωνικής πολλαπλής πρόσβασης (Non-Orthogonal Multiple Access - NOMA) και διαδοχικής ακύρωσης παρεμβολών (Successive Interference Cancellation - SIC). Οι χρήστες επιλέγουν αυτόνομα το συμβόλαιο που ταιριάζει καλύτερα στις συνθήκες καναλιού τους. Επιπλέον, αναπτύσσεται ένας αλγόριθμος ενισχυτικής μάθησης (Reinforcement Learning - RL) προκειμένου κάθε χρήστης να προσδιορίζει αυτόνομα και κατανεμημένα την πιο ωφέλιμη για αυτόν συσχέτισή του με ένα σταθμό βάσης.

Πηγαίνοντας ένα βήμα παραπέρα όσον αφορά την υποκείμενη αρχιτεκτονική δικτύου και τις χρησιμοποιούμενες τεχνολογίες, στοχεύουμε να κατανείμουμε βέλτιστα τους πόρους στα τμήματα ασύρματης πρόσβασης (access network) και οπισθόζευξης (back-haul network) ενός δικτύου υποβούμενου από ένα μη επανδρωμένο εναέριο όχημα (Unmanned Aerial Vehicle - UAV) και μια αναδιαμορφώσιμη έξυπνη επιφάνεια (Reconfigurable Intelligent Surface - RIS). Αξιοποιώντας τη

δομική ιεραρχία του δικτύου, διαμορφώνεται ένα παίγνιο Stackelberg μεταξύ του σταθμού βάσης που φέρει το UAV και των χρηστών για την κατανεμημένη επίλυση του ακόλουθου συνδυαστικού προβλήματος κατανομής πόρων. Το UAV, ενεργώντας ως ηγέτης, καθορίζει τις μετατοπίσεις φάσης του RIS έτσι ώστε η ισχύς του σήματος του συνόλου των χρηστών στη ζεύξη ανόδου να μεγιστοποιείται. Επίσης, το UAV, σε δεύτερη φάση, υπολογίζει την από κοινού κατανομή εύρους ζώνης συχνοτήτων και ισχύος στη ζεύξη ανόδου του οπισθοζευκτικού δικτύου προς το δίκτυο κορμού (core network). Σε τρίτη φάση, οι χρήστες, ενεργώντας ως ακόλουθοι, βελτιστοποιούν την ισχύ τους στη ζεύξη ανόδου του δικτύου πρόσβασης προς το UAV, επίσης με κατανεμημένο τρόπο. Η δεύτερη και τρίτη φάση επαναλαμβάνονται έως ότου βρεθεί η ισορροπία Stackelberg όπου μεγιστοποιείται η ενεργειακή απόδοση του δικτύου από άκρο σε άκρο.

Σεβόμενοι την ανάγκη για από κοινού μηχανισμούς κατανομής πόρων σε ασύρματα δίκτυα επικοινωνιών και δίκτυα κινητών υπολογισμών, εξετάζεται μια πολυεπίπεδη τοπολογία κινητών υπολογισμών και μελετάται το από κοινού πρόβλημα της εκφόρτωσης εργασιών υπολογισμού και κατανομής ισχύος μετάδοσης/εκφόρτωσης. Σε αντίθεση με την υπάρχουσα βιβλιογραφία, όπου μοντελοποιούνται δίκτυα υπολογισμών ενός επιπέδου, δηλαδή αποτελούμενα είτε από ένα επίπεδο υπολογιστικής άκρης (edge), ομίχλης (fog) ή νέφους (cloud), επιδιώκεται η χρήση ενός ευρέος φάσματος υπολογιστικών δυνατοτήτων. Δεδομένης της εγωιστικής συμπεριφοράς των χρηστών προς την εκφόρτωση στην άκρη του δικτύου λόγω της εγγύτητας του τελευταίου, σχεδιάζεται ένας μηχανισμός κινήτρων μέσω της Θεωρίας Συμβολαίων για να παρακινήσει τους χρήστες να επιτρέψουν ένα ποσοστό των αρχικών εκφορτωμένων εργασιών τους στο επίπεδο της άκρης να προωθηθούν περαιτέρω και να επεξεργαστούν στην ομίχλη. Έχοντας καθορίσει αυτό το ποσοστό, το τελικό ποσοστό εκφόρτωσης εργασιών, καθώς και η ισχύς μετάδοσης κατά την εκφόρτωση από τους χρήστες προς την άκρη του δικτύου, υπολογίζονται με κατανεμημένο τρόπο μέσω ενός μη συνεργατικού παιγνίου. Με τη χρήση πολλών επιπέδων υπολογισμών, βελτιώνεται η ενεργειακή απόδοση, ενώ επεκτείνεται η υπολογιστική ικανότητα του δικτύου.

Τέλος, με στόχο την μελέτη της κατανομής των εργασιών υπολογισμού εντός του ίδιου επιπέδου υπολογισμών, μοντελοποιείται ένα δίκτυο υπολογιστικών συστημάτων στην άκρη του δικτύου (Multi-access Edge Computing - MEC) πολλαπλών διακομιστών. Οι χρήστες αξιοποιούν τα διαθέσιμα δίκτυα ραδιοπρόσβασης (Radio Access Networks - RAN) για να εκφορτώσουν τις υπολογιστικά απαιτητικές και χρονικά κρίσιμες εφαρμογές τους σε πολλαπλούς διακομιστές MEC. Για την αντιμετώπιση του προβλήματος διαχείρισης παρεμβολών μεταξύ πολλαπλών διακομιστών και πολλαπλών χρηστών, καθώς και υποκινούμενοι από τις εξελίξεις στις τεχνικές μη ορθογωνικής πολλαπλής πρόσβασης, εξετάζεται η εφαρμογή της τεχνικής πολλαπλής πρόσβασης διαίρεσης ρυθμού (Rate-Splitting Multiple Access - RSMA). Υπό αυτό το πλαίσιο, επιδιώκεται η ελαχιστοποίηση του αθροίσματος της μέγιστης μετρούμενης καθυστέρησης των χρηστών μεταξύ των διαφορετικών διακομιστών MEC μέσω της από κοινού βελτιστοποίησης των ποσοστών εκφόρτωσης υπολογιστικών εργασιών, του ρυθμού και της ισχύος μετάδοσης/εκφόρτωσης στη ζεύξη ανόδου και της κατανομής υπολογιστικών πόρων από τους διακομιστές MEC προς τους χρήστες. Το πρόβλημα επιλύεται αναλυτικά μέσω των συνθηκών Karush-Kuhn-Tucker (KKT) και έτσι επιτυγχάνεται ο απώτερος σκοπός της διατριβής να παράσχει μια ολιστική προσέγγιση ως προς την κατανομή πόρων σε ασύρματα δίκτυα επικοινωνιών και κινητών υπολογισμών.

Τα εξεταζόμενα προβλήματα διαχείρισης πόρων αξιολογούνται μέσω μοντελοποίησης και προσομοίωσης. Τα λειτουργικά χαρακτηριστικά των προτεινόμενων πλαισίων και η συμπεριφορά σύγκλισης των σχεδιαζόμενων αλγορίθμων εξετάζονται κάτω από διαφορετικά σενάρια και τιμές, ενώ παρέχονται συγκριτικά αποτελέσματα έναντι άλλων λύσεων από την υπάρχουσα πρόσφατη βιβλιογραφία για να καταδειχθεί η αποτελεσματικότητα και αποδοτικότητά τους.

Λέξεις Κλειδιά: Κατανομή Πόρων, Μηχανισμοί Κινήτρων, Μη Ορθογωνική Πολλαπλή Πρόσβαση, Πολλαπλή Πρόσβαση Διαίρεσης Ρυθμού, Αναδιαμορφώσιμες Έξυπνες Επιφάνειες, Υπολογιστικά Συστήματα Άκρης, Πολυμεταβλητή Βελτιστοποίηση, Κατανεμημένη Βελτιστοποίηση, Θεωρία Παιγνίων, Θεωρία Συμβολαίων

for my parents, Fotis and Liana
and my brother, Zafiris

Contents

List of Abbreviations

AP	Access Point
AWGN	Additive White Gaussian Noise
BC	Broadcast Channel
BRD	Best Response Dynamics
BS	Base Station
CPU	Central Processing Unit
CR	Cognitive Radio
CSI	Channel State Information
CT	Contract Theory
D2D	Device-to-Device
DDPG	Deep Deterministic Policy Gradient
DFRC	Dual-Function Radar Communication
DRL	Deep Reinforcement Learning
DTN	Delay-Tolerant Network
ER	Energy Receiver
GT	Game Theory
HAPS	High Altitude Platform Station
IC	Incentive Compatibility
IoE	Internet of Everything
IoT	Internet of Things
IR	Individual Rationality
IRS	Intelligent Reflecting Surface
ISP	Internet Service Provider
ITU	International Telecommunication Union
KKT	Karush-Kuhn-Tucker
LIS	Large Intelligent Surface
LoS	Line-of-Sight
LTE	Long Term Evolution
MC	Multi-Carrier
MCC	Mobile Cloud Computing
MEC	Multi-access Edge Computing
MFC	Mobile Fog Computing
MIMO	Multiple-Input Multiple-Output
MISO	Multiple-Input Single-Output
mmWave	Millimeter Wave
MNO	Mobile Network Operator
NE	Nash Equilibrium
NextG	Next Generation
NLoS	Non-Line-of-Sight

NOMA	Non-Orthogonal Multiple Access
OFDMA	Orthogonal Frequency Division Multiple Access
OMA	Orthogonal Multiple Access
PIC	Pairwise Incentive Compatibility
QoS	Quality of Service
RAN	Radio Access Network
RB	Resource Block
RIS	Reconfigurable Intelligent Surface
RL	Reinforcement Learning
RNC	Radio Network Controller
RSMA	Rate-Splitting Multiple Access
SDMA	Space Division Multiple Access
SDN	Software-Defined Network
SIC	Successive Interference Cancellation
SINR	Signal-to-Interference-plus-Noise Ratio
SISO	Single-Input Single-Output
SWIPT	Simultaneous Wireless Information and Power Transfer
TDD	Time Division Duplex
TDMA	Time Division Multiple Access
THz	Terahertz
UAV	Unmanned Aerial Vehicle
ULA	Uniform Linear Array
URLLC	Ultra-Reliable Low Latency
WiFi	Wireless Fidelity

Preface

Acknowledgements

While pursuing my Ph.D., I dedicated a significant amount of personal effort and commitment. However, this journey would have been impossible without certain people's invaluable assistance and unwavering support, to whom I would like to express my heartfelt gratitude.

First and foremost, I would like to express my heartfelt gratitude to my supervisor, Prof. Symeon Papavassiliou, for his unwavering support during these years. Prof. Papavassiliou has a deep knowledge and understanding of my working scientific field, allowing for an intuitive grasp of my concerns and complex thoughts. He is always approachable and welcoming, offering instant solutions to my problems and soothing my worries. I would especially like to thank him for his skill in identifying, unveiling, and amplifying a person's particular strengths and abilities. With his guidance, I started working in a scientific field previously unfamiliar to me, where I now feel confident and find it to be a defining aspect of me. I am fortunate to work under his supervision and receive his support.

Regarding the hands-on and step-by-step guidance throughout these years, I feel truly grateful to work with Prof. Eirini-Eleni Tsiropoulou. Prof. Tsiropoulou is always present whenever I ask for her help and ready to solve any problem with paper and pencil. She has taught me valuable lessons in work planning and time management, and her enthusiasm serves as a powerful motivator, inspiring my commitment and the pursuit of my goals.

In addition to my advisors, there are colleagues with whom I have collaborated closely throughout these years, and I wish to extend my gratitude to them as well. I want to thank Vassilis and Grigoris, who first introduced me to the realm of a European-funded project, Christos, whose mathematical insights were a valuable addition to my thesis, and Panagiotis, who is my research collaborator in the NETMODE laboratory.

I deeply thank all my colleagues in the NETMODE laboratory who turned the workplace into a constant source of joy and laughter and cultivated a family-like environment, with shared meals being a cherished part of it every noon. In this workplace, I am fortunate to have made friends who can meet outside work and engage in meaningful discussions. Special thanks to Dimitris and Giannis, my "classmates" forever, Margarita and Georgia, my cultural events buddies, Grigoris, Kostas, Giorgos, Vassilis, and Dimitris. I also thank Marios for being there for many of these years.

Another thanks to my friends for providing me with an escape from work. A special thanks to Dina, whom I admire for her energy and autonomy, managing to make every engagement we have a unique and memorable experience, Eugenia for always being there and checking on how I am doing, and Dora for being the embodiment of logical reasoning in our conversations. I am sure my life would not have been the same without them.

This thesis is dedicated to my beloved parents, Fotis and Liana, for whom I will forever be their little kid, surrounding me with love and support by all means for me to be happy, and my brother, Zafiris, being kind and loving and always trying to make me laugh.

Structure

The thesis is structured as follows.

In **Chapter 1**, a general introduction to the topics that concern this thesis is provided, along with a description of the environment that motivated this research. Also, the contributions made therein by this thesis are presented.

In **Chapter 2**, the basic mathematical background that is deemed necessary to understand the solution methodologies used for the problems under investigation is set. Additional information is provided in the main part of the thesis whenever it is needed.

The following chapters constitute the main chapters of the thesis. Each chapter deals with a different problem that we consider worth investigating and aim to tackle. First, a general setting specific to the corresponding problem and the related work around the topic is provided. Then, the considered system model, problem formulation, and proposed solution framework are presented, while an in-depth evaluation of the proposed framework concludes each chapter.

In **Chapter 3**, the joint problem of user-to-base-station association and uplink transmission power control is considered and solved in a heterogeneous Non-Orthogonal Multiple Access (NOMA) wireless network. In particular, the case of incomplete/partial Channel State Information (CSI) at the base stations is considered, and a contract-theoretic solution is proposed to solve the power control problem. Also, a Reinforcement Learning (RL) algorithm is introduced to allow the users to self-associate with the available base stations.

In **Chapter 4**, the joint resource allocation in the fronthaul and backhaul parts of a network is considered while accounting for the existence of Reconfigurable Intelligent Surfaces (RISs) that further promote the propagation environment's reconfigurability. Specifically, the joint problem of RIS elements' phase-shift configuration, bandwidth splitting between the fronthaul and backhaul, and uplink power control in both the fronthaul and the backhaul networks is formulated and distributively solved by the adoption of Game Theory.

In **Chapter 5**, a contract-theoretic incentivization mechanism is designed to prevent the overexploitation of the network edge due to the users' selfish behavior by motivating them to allow part of their offloaded computation tasks to be further forwarded and processed at the fog based on their delay (in)sensitivity level. The outcome of this stage is then utilized to solve the joint task offloading and uplink power control problem from the users to the edge, promoting the efficient use of the whole spectrum of the computing continuum.

In **Chapter 6**, a multi-server Multi-Access Edge Computing (MEC) network is studied where the users are allowed to concurrently offload different parts of their computation tasks to the available servers in a non-orthogonal manner via the adoption of the Rate-Splitting Multiple Access (RSMA) technique. Subsequently, the joint problem of optimizing the users' computation task assignment ratios, rates, uplink transmission powers, and computing resource allocation across the different MEC servers is formulated and solved.

Finally, in **Chapter 7**, the problems addressed in this thesis are summarized, giving the reader a comprehensive overview of the most important conclusions drawn. Then, recommendations for future work and ideas for problems worth exploring in the future are presented as an extension of this thesis.

Chapter 1

Introduction

Next Generation (NextG) 5G wireless communication networks are facing an unprecedented increase in mobile data traffic and the number of subscribed users and devices. Quantitatively speaking, based on the recent statistics published by the International Telecommunication Union (ITU), the global mobile data traffic is expected to increase to 607 Exabytes (EBs) per month by 2025 and 5016 EBs by 2030 [1]. As per each subscriber, the amount of data traffic is estimated to grow to 607 EBs per month by 2025 and 5016 EBs by 2030. These numbers refer to the 70% of the global population that is expected to have subscribed to mobile services and use mobile Internet by that point, without accounting for the connected applications and devices within the context of the Internet of Everything (IoE) [2]. This huge data traffic demand is steered by the broader vision for digitalization and smart-X vertical industries (e.g., smart city, healthcare, manufacturing, transportation, education) and is consequently accompanied by stringent requirements for heterogeneous service provisioning support, full coverage, and ultra high-bandwidth wireless communications with ultra-high reliability and ultra-low latency [3, 4].

To provide extended coverage and ameliorate their spectral and energy efficiency, NextG wireless networks are equipped with novel technologies that range from the underlying physical layer to the overlying architecture of the network infrastructure. NextG wireless networks are founded upon heterogeneity - an architectural paradigm initially introduced by Long-Term Evolution (LTE) - in the sense that low-power Base Stations (BSs), such as femto, pico, or micro BSs coexist within the macrocells and contribute to increasing network capacity while providing the required Quality of Service (QoS) to the users [5, 6]. The latter paradigm is not limited to terrestrial communications but accounts also for airborne (non-terrestrial) platforms, such as Unmanned Aerial Vehicles (UAVs), High Altitude Platform Stations (HAPSs), and satellites that provide connectivity to the users [7, 8]. A high-level overview of the NextG 5G wireless network's architecture is presented in Figure 1.1.

Nevertheless, cell densification is yet insufficient by itself to address the coverage and spectral efficiency problem when moving to higher frequency bands, such as Millimeter Wave (mmWave) [9] or Terahertz (THz) [10], as intended in the NextG wireless networks. On the one hand, shorter-range communications reduce the degrees of freedom offered by the physical wireless channel due to the reduced number of scattering objects in the environment. On the other hand, high frequencies are characterized by high signal attenuation, affecting the communication reliability between the transmitter and the receiver. A reasonable solution for enriching the multi-path propagation environment based on the general advancements in active antenna design is passive beamforming, practically realized by Reconfigurable Intelligent Surfaces (RISs) [11]. Complementary to the aforementioned technologies, other interventions to the physical layer in the context of NextG networks regard the development

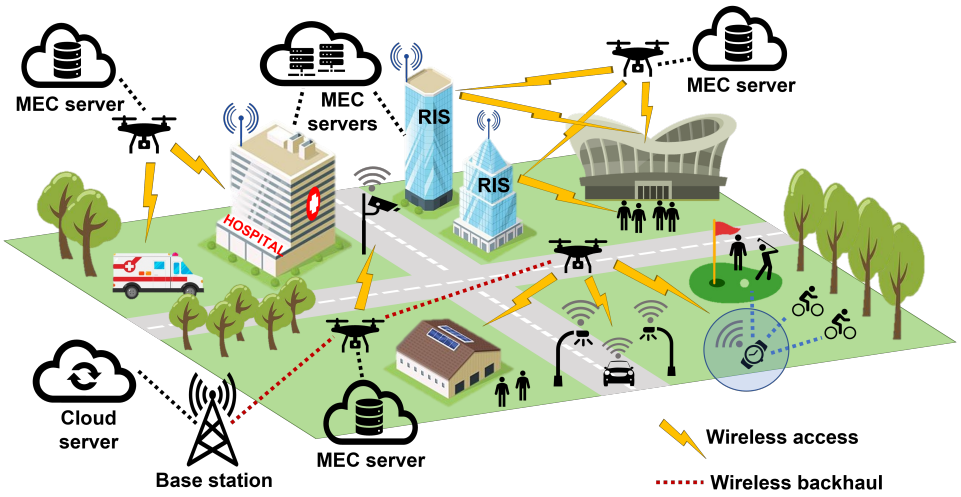

Figure 1.1: Overview of NextG 5G wireless communication and mobile computing networks.

of advanced and robust modulation and multiple access techniques, aiming to efficiently manage the interference sensed at the receivers and the signal decoding complexity.

The ubiquitous connectivity enabled by the NextG 5G wireless communication networks is, thus, progressively shaping the frontier of an ambient intelligence era. Striving to reap the benefits of the surrounding intelligence has provoked the increase of ever-more computationally intensive user applications. To facilitate the computationally and battery-constrained user devices to meet the application's response time and their energy consumption requirements, the concept of computation offloading of resource-intensive tasks to remote servers has become extremely popular [12, 13]. In particular, the NextG networks are envisioned to become a computer that would combine ubiquitous communication and computation, as a whole, among other functions such as storage, sensing, and control, to support disruptive user applications. Especially among the different computing capabilities and options existing within the computing continuum, i.e., fog [14] and cloud [15, 16] computing, the Multi-Access Edge Computing (MEC) [17] that is implemented within the Radio Access Network (RAN) (see Figure 1.1), has revolutionized the successful completion of low-latency and high-intensity applications, giving birth to the use-case scenario of Ultra Reliable Low Latency Communications (URLLC) [18].

NextG wireless communication and computing networks constitute competitive environments where the users evolve in a physical, digital, or virtual space with others, sharing the same resources, and numerous stakeholders with conflicting objectives should coordinate with each other. Although significant achievements have been made in the direction of studying such interconnected systems, there remain challenges to be addressed regarding the realistic conceptualization and modeling of the deep interdependencies among the behaviors, interactions, and decisions of the network entities, including but not limited to users, Mobile Network Operators (MNOs), Internet Service Providers (ISPs), cloud service providers. Concrete theoretical frameworks that provide a real-life spirit and more pragmatic approach to the resource management process and deal with the challenges of distributed decision-making, conflicting goals, and partial information availability should be implemented and span across the user plane, the radio access and edge network to the core network and the cloud. This form of ambient intelligence is considered a key enabler in making NextG 5G networks more intelligent and achieving dynamic network management and optimization.

1.1 New Air Interface

1.1.1 New Multiple Access Techniques

Within this congested and demanding wireless communications environment, the problem of efficiently, wisely, and sparingly using the system and users' available resources and capabilities becomes even more challenging and urgent. From the wireless network's perspective, this need is reflected in efficiently utilizing the available spectrum resources. From the users' side, they have to intelligently manage their mobile devices' power investment for performing different communication and computing tasks. Indeed, the multiple access technique that is used to multiplex the different transmissions that take place either in the downlink or the uplink is critical for the network's spectral and energy efficiency.

Previous deployments of wireless networks, e.g., 1G, 2G, 3G, exclusively relied on Orthogonal Multiple Access (OMA) techniques [19], according to which the available Resource Blocks (RBs) within each cell are divided orthogonally either in the time, frequency, or code domains and appropriately allocated such that the interference among adjacent RBs is suppressed. Although OMA techniques allow for simple signal detection at the receiver, they are significantly restrictive in the number of concurrent transmissions that can be accommodated due to the finite number of available RBs [20], and, thus, result in poor spectrum utilization. Besides, potential channel impairments along with the random nature of the wireless propagation environment cannot guarantee the success of data transmission even under orthogonally allocated spectrum resources. Therefore, the design and development of advanced and robust multiple access techniques has been constantly explored over the past years, giving rise to the introduction of Non-Orthogonal Multiple Access (NOMA) [21].

Non-Orthogonal Multiple Access (NOMA)

NOMA is a key enabling technique to efficiently exploit the available radio resources and serve multiple users simultaneously over the same time-frequency RB by multiplexing them in the power domain [22] or by spreading code in the code domain [23]. For example, in the downlink power-domain NOMA [24], the transmit signals at the BS are superposed and transmitted to multiple users using different power levels. The users of relatively high channel gain decode the interfering signals before decoding the signal intended for them by employing the Successive Interference Cancellation (SIC) technique, whereas the users of low channel gain treat the interference as noise. In the uplink power-domain NOMA [24], the decoding of the superposed signal received by the BS starts from the high channel gain user since its signal is more likely the strongest one. The high-channel gain users experience interference from all other users in the system, whereas the low-channel gain users enjoy an interference-free transmission. Given that the users are distinguished based on the quality of their wireless link and the corresponding power investment to the transmission that is, in turn, implied by their QoS requirement, NOMA provides an effective method to achieve fairness between the different users. However, the achievements of NOMA in terms of spectral, energy efficiency, and fairness come with the cost of increased signal decoding complexity at the receivers in contrast to the traditional OMA techniques.

Rate-Splitting Multiple Access (RSMA)

RSMA belongs to the broader category of non-orthogonal transmissions and is practically seen as the successor of NOMA, providing a more general and powerful transmission framework than its predecessor [25, 26]. Following this technique, user messages are split into common and private parts at the transmitter, such that part of the interference is decoded at the receiver while the remaining is treated as noise. In this way, RSMA enables softly

bridging and, therefore, reconciling the two extreme interference management strategies of treating interference as noise (as suggested by Space Division Multiple Access (SDMA) and MIMO implementations) and fully decoding interference, as suggested by NOMA. For example, in downlink RSMA [27], the message transmitted by the BS to multiple users is split into a common message and a private message. The common message is intended for and decoded by all the involved users in the transmission, whereas the private message is intended for each user separately. As a result, when decoding the private message, the interference stemming from the other users' private messages is treated as noise. In this way, a good balance between efficient spectrum usage, interference management, and signal processing complexity can be achieved, ameliorating the wireless network's performance.

1.1.2 Reconfigurable Intelligent Surfaces (RISs)

Aiming to deal with the problem of coverage extension, as presented earlier in Section 1, the technology of RISs has emerged as another key enabler of NextG 5G wireless networks. The introduction of RISs as a way to manipulate the wireless propagation environment constitutes a preliminary step towards the broader vision of Software-Defined Networking (SDN), according to which networks can be controlled remotely through the use of programmable software [28]. Besides, the design of RISs satisfies the essential requirement for flexible, feasible, and cost-effective solutions in terms of deployment, maintenance, and control, and hence, several research works can be found in the literature that study different aspects of their design, deployment and optimization under the additional terms of Intelligent Reflecting Surfaces (IRSs) [29] and Large Intelligent Surfaces (LISs) [30]. Practically, an RIS is a software-controlled metasurface of low thickness and shape of a two-dimensional planar array consisting of a massive number of low-cost passive reflecting elements. Each individual reflecting element can independently reflect the incident signals towards a desired destination that is determined by digitally controlling their adjustable amplitude and phase shifts via a smart controller. The cumulative goal behind controlling the reflecting elements may regard the spectral efficiency maximization [31], the power consumption minimization [32], or the URLL service provisioning [33]. Meanwhile, RISs may be deployed anywhere by coating ground surfaces [34] or even airborne platforms [35] and can assist applications beyond pure communications, such as positioning, navigation, and timing [36, 37], or computation offloading [38].

1.2 New Architecture

So far, all legacy and existing wireless networks have been designed to substantially accommodate bit-oriented communications, in contrast to the task-oriented nature of NextG wireless communications. NextG networks should support direct human-to-machine and machine-to-machine interactions via text, speech, and image, as well as augmented and virtual reality to align with the digitalization and smart-X vertical industries. The latter requirement calls for the convergence of communication and computing, resulting in a profound shift in the overall network architecture.

Several computing paradigms have been proposed over the past years by the research community that form the so-called computing continuum, whose ultimate purpose is to address the issues of high-bandwidth, geographically dispersed, ultra-low latency, and privacy-sensitive applications. The most popular paradigms, though, are the Mobile Cloud Computing (MCC) [15, 16] , Mobile Fog Computing (MFC) [14] , and the Mobile/Multi-Access Edge Computing (MEC) [17]. The common denominator among these paradigms is the deployment of cloud computing-like capabilities at the network edge in the form of data

centers, while they are distinguished from an architectural point of view concerning the location where their computing power is placed. In particular, in the edge computing model, the computational power and intelligence are implemented exactly at the network edge (e.g., local edge), while in the fog computing case, this functionality may be offered at different locations between the network edge and the core network connecting to the cloud, thus, exploiting the power of the whole digital continuum (e.g., main edge servers). It is, therefore, possible to create a hierarchical multi-tiered architecture, interconnected by the wireless network infrastructure, which allows for the individual data centers' cooperation with each other. Any customer – from third-party service providers to end users and the infrastructure providers themselves – can make use of this computing continuum and offload their computation tasks for remote execution, by leveraging the existing underlying wireless network infrastructure.

1.2.1 Multi-access Edge Computing (MEC)

In particular, MEC has been introduced for bringing cloud services and resources closer to the end user, where the term "closer" implies its direct implementation within the RAN. Precisely, indicative deployment locations considered by the MEC ISG include but are not limited to the LTE/5G BSs (eNodeBs/gNodeBs), 3G Radio Network Controllers (RNC), and multi-Radio Access Technology (3G/LTE/WLAN) cell aggregation sites [39], integrating, also, other networking and storage resources in the form of a MEC platform. Consequently, owing to the dense deployment of the MEC servers and their proximity to the users, MEC provides a promising solution to the problems of scalability, mobility support, security, and privacy, apart from supporting vast communications and remote computation executions, for which was initially destined. The NextG mobile computing networks should be able to serve billions of moving devices, and hence, the dynamic and seamless management of their number and movement is needed to maintain a high QoS. Additionally, MEC follows the general principles of distributed architectural designs, similar to the architectural shift of pure wireless communication networks, enhancing the overall network's security and privacy by alleviating single points of failure.

It is remarkable, though, noting that regardless of the MEC's appealing and prevailing features compared to other computing paradigms, it is crucial to be accounted for and utilized as a complement to the cloud computing model and not as a replacement for the latter. MEC constitutes another common pool of resources that should be efficiently, wisely, and sparingly used to unleash its benefits, similar to the shared spectrum resources within the context of pure wireless communications, as analyzed in Section 1.1.1. Otherwise, its overexploitation will gradually lead to its performance degradation.

1.3 Realizing Intelligence

The unparalleled growth in data traffic and burden in computation tasks is leading to the radio and computing resources becoming a critical bottleneck in the NextG 5G wireless communication and mobile computing networks. One sort of intelligence in the context of NextG networks lies in their ability to perform dynamic resource management and optimization. Given their distributed nature, this sort of intelligence should span across the user plane, the radio access and edge computing network part, to the core network and the cloud, in the sense that each network entity should be able to make autonomous decisions regarding its personal resource utilization. Meanwhile, from an economic and market perspective, NextG networks comprise a competitive environment, where multiple stakeholders, e.g., MNOs, ISPs, and cloud service providers cooperate or even compete in the provisioning of similar services by pursuing their personal goals. The latter goals may be different and/or

interdependent, such as the network's energy or spectral efficiency maximization, interference mitigation, delay minimization, or the profit increase just to name a few of them. At the same time, the multidimensionality of the resource management problem concerning the type and nature of the resources to be managed and the QoS requirements of each user to be served, motivate the need for common scientific tools and methodologies, and approaches that precisely and realistically capture the behavior of the network under investigation.

The ultimate goal, however, in realizing intelligence should be the delivery of holistic solutions to the converged radio and computing resource management problems. The MEC paradigm relies heavily on the air interface that practically facilitates computation task offloading when considering mobile implementations. This implies that the performance of mobile computing is interwoven with the quality of wireless communication, and thus, the corresponding resource management problems should be studied jointly.

1.3.1 Game-theoretic Modeling

A well-established method in the literature to formulate and solve distributed resource management problems is Game Theory [40]. In its most commonly used setting, the resource management problem is formulated as a non-cooperative game among the players, where each player is considered a greedy individual who independently seeks to maximize his/her perceived utility. However, cooperative game formulations exist where the individual players pursue a common goal from the personal or the network's perspective. The players participating in the game can map to any network entity or stakeholder of the network, competing in sharing a common pool of resources that can range from radio and computing resources to the number of subscribed users when referring to the competition between MNOs or ISPs.

The main benefits of the distributed resource management framework in general that especially apply in the context of game-theoretic modeling are (i) the ability of the users to decide autonomously and cognitively the most beneficial mode of operation; (ii) the alleviation of the burden of a single point of failure that characterizes the centralized solutions; (iv) the decrease in the computation complexity of the solutions, which is shared among multiple autonomous entities; (v) the improvement of the security and privacy levels as the decision-making process is shared among different devices, which exchange a limited amount of information; (vi) the support of the smooth operation of the overall system when providers and users with heterogeneous economic incentives are involved.

1.3.2 Contract-theoretic Modeling

Nevertheless, it is common knowledge that game theoretic models assume the rationality of the participating players in the game, which is impractical or even impossible as the size of the network grows. A novel framework from the field of economics that has been scrutinized over the past years is Contract Theory (CT) [41]. Contract Theory (CT), lying in the area of Labor Economics, provides the mathematical foundations to create mutually agreeable contracts or arrangements between economic players, i.e., principal/employer(s) and agents/employees, under the presence of incomplete information (often referred to as asymmetric information). The incompleteness of information refers to the unknown by the principal agents' private characteristics that under typical circumstances steer the contract formulation. Under this concept, the principal creates contract bundles based on the statistical knowledge of the potential agents' private information, i.e., the agents' types, to motivate them to provide back their effort and hence, reveal their actual type. Consequently, Contract Theory can provide more realistic modeling of the different network entities' and stakeholders' interdependent behaviors, interactions, and decisions, without assuming complete knowledge between them and while trying to reconcile their potentially conflicting

goals. A characteristic example of such a case from the network's side constitutes its effort to increase the network's capacity and efficient utilization of the spectrum resources, aided by technologies such as Device-to-Device (D2D) communications, Cognitive Radio (CR), or small cells. Towards satisfying their utility, the users will more likely avoid cooperating with other neighboring devices and thus, share/consume their resources, i.e., battery capacity, computing power, and available spectrum. Additionally, they will more likely circumvent the communication with a low-power small cell BS, minimizing the risk of being exposed to higher interference due to the small BS's reduced spectrum resources compared to a macrocell. Generally, any macro/small BS, MNO, or ISP can play the role of the principal that is in charge of designing the contract bundles intended for the prospective agents, such as end-user devices or other BSs [42, 43, 44]. Under this concept, a wide variety of optimization problems can be formulated and solved, rethinking the overall traditional resource management approaches in the fields of wireless communications and mobile computing.

1.4 Challenges and Motivation

Following the discussion so far, it is clear that the NextG wireless networks exhibit multiple degrees of freedom in terms of controlling the radio and computing environment to achieve the required QoS from the users' and/or the network's perspective. However, this increased level of flexibility brings new challenges that must be carefully considered. This thesis attempts to encompass novel approaches that provide a real-life and pragmatic spirit in modeling resource management problems. Subsequently, holistic solutions are derived by concurrently accounting for multiple types of resources related to wireless communications and mobile computing. The main pillars upon which this thesis has been constructed are summarized as follows:

- **Resource management & optimization:** Resource allocation has been critical since previous generations of wireless networks and becomes even more imperative as the complexity of the network increases in the number of users and applications, the stringency of QoS requirements, the deployed technologies, and the type of resources. Simply adopting already proposed solutions on traditional resource management problems, such as the typical downlink/uplink sum-rate maximization problem, is infeasible due to the incompatibility with the NextG 5G network's key enabling technologies, i.e., new multiple access techniques, Reconfigurable Intelligent Surfaces (RISs), Multi-access Edge Computing (MEC). Besides, the intelligence behind the proposed resource management solutions must evolve to cope with the complexity of the underlying networking environment. Therefore, resource management and optimization constitute the main drive behind this thesis.

- **Distributed decision-making:** The distributed nature of the NextG 5G network not only promotes but also imposes the formulation of resource management problems in a distributed manner. Such solutions allow for the modeling of the heterogeneity in the behavior and the subjectivity in the perception of the QoS by the network entities while providing flexible and scalable alternatives as the complexity of the network grows. The existence of central entities that accumulate the underlying network's knowledge is unrealistic in most modern application scenarios. Thus, scientific frameworks that allow for the different entities' autonomous decision-making lead to more viable solutions.

- **Contradictory objectives:** From an economic and market perspective, NextG 5G networks comprise a competitive environment, where multiple users and other stakeholders involved in communication and mobile computing service provisioning should

coordinate. It is, therefore, crucial to concurrently model their economic and technological interplay and account for their different and potentially conflicting goals to render more realistic solutions to the ultimate resource management and optimization problem. In this context, effective frameworks from the field of economics can be utilized to reconcile their goals and conclude mutually agreeable arrangements between them.

- **Incompleteness of information:** Apart from being highly heterogeneous, the emerging NextG 5G network constitutes a highly dynamic environment (i.e., stochastic or time-varying), which is an additional factor that imposes practical restrictions on the level of knowledge that a network entity can have about the actions of the rest of the competing entities. Hence, the applicability and accuracy of traditional distributed decision-making approaches founded on the individual player's, i.e., corresponding network entity's, rationality suffer from the incomplete and partial available information that each player possesses. Solutions restricted to each player's information about their own decisions and/or incomplete and uncertain information about the surrounding environment are significantly important.

- **Holistic solutions:** NextG 5G networks provide several degrees of freedom concerning the nature and type of resources to be managed, ranging from radio (e.g., spectrum, transmission powers, data rates, RISs' phase shifts, and amplitudes) to computing (e.g., computing frequency and power) resources. Unilaterally tackling resource management problems does not allow for exploiting the full potential and prospect of the underlying wireless communication and computing network. To reveal the network's limits, a more holistic treatment of resource allocation problems is required by adding more degrees of freedom and resorting to more scalable and generic problem design models. The added value of holistic solutions is multifold and not restricted only to the networking and computing field but can also provide insights for tackling similar combinatorial optimization problems in other disciplines.

1.5 Contributions

This thesis aims to tackle the aforementioned challenges that arise in the emerging NextG 5G wireless communication and mobile computing networks by proposing realistic solutions to several use-case scenarios. The main focus is placed on the decision-making process of the different network entities, where individual user devices and remote servers need to act autonomously and make choices regarding their resource utilization and investment inside their operating environment. The key contributions of this thesis can be summarized as follows:

1. **Multi-dimensional system modeling:** NextG 5G wireless networks have evolved into a complex system of numerous interconnections between users and different types of providers (e.g., infrastructure, service) due to the former's active enrollment in several wireless communication and mobile computing services. A major novelty of this thesis lies in the fact that the different network entities can determine multiple degrees of freedom during the resource allocation process. To achieve this, various network layers, architectures, and diverse services are considered, shifting, in this way, the modeling of the underlying system beyond traditional "flat" topologies. In the following, several resources to be allocated are concurrently considered at each application scenario and resource management problem, steadily progressing from pure wireless communication environments to converged communication and mobile computing settings.

2. **Resource allocation and incentive mechanism design in NOMA wireless networks:** Initially, the focus is placed on pure wireless communication network topologies – that are highly heterogeneous, though – and the application of novel Non-Orthogonal Multiple Access (NOMA) techniques is examined therein. In contrast to the large body of literature that assumes the complete Channel State Information (CSI) knowledge from the heterogeneous BSs' behalf, this thesis deals with the problem of statistical CSI. Particularly, the joint problem of user scheduling to the different available BSs and uplink transmission power control in NOMA-based heterogeneous wireless communication networks is formulated and solved under the incompleteness of CSI from the BSs' behalf by adopting the Contract Theory framework as a major enabler. Besides, the contract-theoretic modeling allows for the users' autonomous decision-making regarding the power level invested in their uplink transmission while resulting in mutually beneficial agreements with the BSs that possess partial/incomplete CSI. The overall framework is complemented by a Reinforcement Learning (RL)-based user-to-BS association mechanism that further promotes the users' self-adaptation and scheduling.

3. **Resource allocation in RIS-assisted NOMA wireless networks:** Apart from horizontally modeling the multi-dimensionality and heterogeneity of NextG networks by considering different types of cells within the wireless access network part, the problem of wireless backhaul connectivity of the cells to the core network is also studied in this thesis. This problem particularly applies to UAV-assisted communications, where the UAVs rely upon wireless backhaul links to connect to the core network, and calls for dynamic spectrum management frameworks. As a means of enhancing the spectrum utilization and energy efficiency across the fronthaul and backhaul of a UAV-assisted communications network, we scrutinize the prospect of Reconfigurable Intelligent Surfaces (RISs) for the first time in the literature. In this context, the joint optimization problem of a) the RIS elements' phase shifts, b) the bandwidth splitting among the fronthaul and backhaul network parts, c) the users' uplink transmission power to the UAV, and d) the UAV's uplink transmission power to the macro BS/core network, is formulated as a Stackelberg game and solved in a distributed manner by the different network entities. Consequently, a flavor of reconfigurability and adaptability is added to the end-to-end wireless propagation environment spanning from the access to the core.

4. **Resource allocation and incentive mechanism design in multi-tier computing networks:** Respecting the need for converged wireless communication and mobile computing solutions, a multi-tier mobile computing network is subsequently modeled and studied. The considered network is hierarchically organized into an edge service layer and a fog service layer to facilitate the computing demands of the computationally and battery-constrained user devices. The fundamental novelty of this work lies in the fact that the whole range of computing capabilities and options (i.e., edge and fog layers) is appropriately utilized according to the user applications' level of delay tolerance to prevent the potential degradation of the edge service layer's performance due to overexploitation. The latter goal is achieved by properly designing an incentivization mechanism following the principles of Contract Theory (CT), based on which the users are motivated to allow a percentage of their initially offloaded tasks to the edge to be further forwarded and processed at the fog. Given the latter percentage, the joint computation task offloading to the edge and uplink transmission power control problem of the users is tackled, such that the energy overhead stemming from both wireless transmission/offloading and task processing is minimized at both the user device and the edge service layer. The joint optimization problem is formulated as a

Stackelberg and solved in a distributed manner by the different network entities.

5. **Resource allocation in RSMA multi-server multi-access edge computing networks:** Aiming to further distribute the users' offloaded computation tasks horizontally (i.e., within the same computing tier) to multiple servers, a multi-server Multi-Access Edge Computing (MEC) network is then considered. Motivated by the distributed deployment of MEC servers within the RAN and the advancements in next-generation non-orthogonal multiple access techniques, we scrutinize the application of Rate-Splitting Multiple Access (RSMA) to enable the users' concurrent computation task offloading to the multiple MEC servers. In this context, a holistic solution to the joint task offloading, and radio and computing resource allocation problem is pursued such that the sum of users' maximum experienced delay among the different MEC servers is minimized. For the calculation of the latter, the delay stemming from both the wireless transmission/offloading and computation task processing at the different MEC servers is again taken into account. The formulated min-max-sum problem is analyzed and equivalently transformed to more easily conclude a tractable solution using conventional optimization techniques based on the Karush–Kuhn–Tucker (KKT) conditions.

6. **Evaluation of proposed frameworks with numerical results via modeling and simulation:** Extensive numerical results are presented that are obtained via appropriate modeling and simulation of the networking environment and the examined problem to demonstrate the effectiveness and efficiency of the proposed frameworks and resulting solutions.

In the following, Chapter 2 introduces some preliminary notions and concepts about the adopted scientific methodologies by this thesis. Then, each chapter focuses on one of the aforementioned settings and use-case scenarios, presenting the related work in this respective field and introducing the developed solutions along with a numerical evaluation of their effectiveness and efficiency.

Chapter 2

Background

In this chapter, we elaborate on the main scientific frameworks adopted in the following to tackle the emerging resource management problems, while specific information that applies to the respective application case will be provided in the main part of the thesis.

2.1 Game Theory

Game Theory is the theoretic study of strategic decision-making among rational decision-makers [40]. The foundations of a full-fledged theory were laid by the work of John von Neumann and Oskar Morgenstern in the book "Theory of Games and Economic Behavior" [45], while it was further enriched and formalized by John Nash with his work on non-cooperative games and the introduction of Nash Equilibrium (NE) [46]. Nash proved that every finite n-player non-zero-sum non-cooperative game admits an NE in mixed strategies, constituting a more widely applicable criterion to a variety of games compared to the one proposed by von Neumann and Morgenstern. Although Game Theory was initially developed as a theoretical tool related to social and economic disciplines [47], its applications span across many sciences, including but not limited to evolutionary biology [48], computer science, security [49], international politics, sociology [48], business, and wireless networks [50].

In Game Theory, a game is considered as the interaction between different rational stakeholders, namely players, each of which has a set of strategies on how to play or behave in the game. The strategies are characterized as either pure, meaning that only one strategy is selected at all times, or mixed when multiple strategies are considered based on a probability distribution. The combined behavior of the players results in a certain payoff for each player, which practically represents the corresponding player's level of satisfaction in terms of gains or losses based on its decision. The function that gives the value of the payoff is named as payoff or utility function.

Among the different forms of games in Game Theory, the most common representation of a game is the so-called "game in normal/strategic form", which is defined as the tuple:

$$G = \{N, A_{i \in N}, U_{i \in N}\} \tag{2.1}$$

where N is the set of players, A_i is the strategy set of each player i, and U_i is the utility/payoff function of player i.

The NE of a game that involves two or more players is a solution concept, at which no player has any incentive to unilaterally change his/her strategy, meaning he/she cannot achieve higher utility/payoff, whether the rest of the players keep their strategies unchanged. The best response is the strategy that yields the most favorable immediate outcome for

a player, i.e., the one strategy that maximizes his/her payoff, taking the other players' strategies as given. As a result, the NE can be expressed as the set of strategies, such that each player is playing the best response to the other players' strategies.

A simple example widely used to explain the concept of a game and its equilibrium strategy is the so-called "Prisoner's Dilemma". The game regards the hypothetical scenario of two suspects who are arrested for a crime. The police do not possess enough information to convict either of them and, for this reason, decide to offer them the following deal:

- If one testifies for the prosecution against the other and the other remains silent, the betrayer goes free and the accomplice receives the full 10-year sentence.
- If both choose to stay silent, the police can sentence both prisoners to only 6 months for a minor charge.
- If both choose to betray the other, they will each receive 5 years of sentence.

The prisoners have no information about the decisions of each other and have to autonomously decide on whether to betray the other or remain silent.

Table 2.1 visualizes the payoff of the prisoners, where the first and second numbers within a cell correspond to the payoff of the first and second prisoner, respectively, depending on the specific system state. A higher payoff value represents a higher gain earned by the respective prisoner, and, thus, a full 10-year sentence is assumed to result in a payoff equal to 0. A 5-year sentence yields a payoff of 1, while a 6-month sentence results in a payoff of 3. The situation of leaving without any charges concludes with a payoff equal to 5.

Table 2.1: Prisoner's Dilemma.

	Prisoner B silent	Prisoner B betrays
Prisoner A silent	$3, 3$	$0, 5$
Prisoner A betrays	$5, 0$	$1, 1$

Considering both prisoners' benefits, the most favorable outcome for them would be to stay silent and cumulative achieve a payoff of 6. Nevertheless, based on the definition of NE, each of the players would try to deviate from this state and betray to achieve a payoff of 5. As a result, the pure NE of the Prisoner's Dilemma game is that both players betray each other and get a payoff equal to 1. Indeed, none of the prisoners would try to unilaterally deviate from this decision since its payoff would decrease to 0. The state (1,1) constitutes the set of strategies that each player plays the best response to the other player's strategy. Apparently, the NE is not always the optimal solution for the play, even though it provides the only stable state of the system.

Another popular game is the "Matching Penny" game. In this game, two players, i.e., A and B, have to choose either heads or tails on a coin toss. Player A wins a dollar from player B if their choices match and loses a dollar to player B if they don't. The players' payoffs can be visualized as shown in Table 2.2.

Table 2.2: Matching Penny.

	Player B heads	Player B tails
Player A heads	$1, -1$	$-1, 1$
Player A tails	$-1, 1$	$1, -1$

The Matching Penny game does not admit a pure NE since playing consistently a strategy, would allow the other player to choose a strategy that maximizes his/her payoff at the first player's expense. The particular game has a unique mixed NE, implying that each player has to choose each action with a probability of one-half. In this way, player A is indifferent among all the actions that he/she selects, i.e., heads, tails, or any randomization between the two, given that player B chooses each action with one-half probability, and vice versa. As a result, both players should choose their actions with a probability of one-half to state at the NE point.

2.1.1 Game Theory Taxonomies

Depending on the way that the players' interactions are captured and modeled, the games can be categorized into the following classes:

- **Zero-sum and Non-zero-sum games:** In a zero-sum game, the benefit of one player yields at an equivalent loss to the other player, maintaining the sum of the players' utilities equal to zero (or a constant). The games for which this property does not hold are called non-zero-sum games.
- **Static and Dynamic games:** In a static game, the players have certain knowledge (information assumptions, behavior assumptions) that remains stable throughout the game, whereas, in a dynamic game, the players can utilize information from previous decisions or observations that can steer current and future decisions and actions.
- **Non-Stochastic and Stochastic games:** A stochastic game is played in stages, and at each stage, the game transits to a state that evolves according to a certain probabilistic/stochastic rule. This property does not hold for non-stochastic games.
- **Non-Cooperative and Cooperative games:** In a cooperative game, the players form alliances to achieve a common goal and compete against other coalitions or individual players. In a non-cooperative game, each player acts selfishly towards maximizing its utility/payoff, competing in this way with the others that may have conflicting goals.
- **Complete information and Incomplete information games:** In a complete information game, the available information among the players is common knowledge, meaning that every player knows that the available information is also known by any other player in the game. The opposite holds for incomplete information games (i.e., Bayesian games), where the players have only incomplete/partial information about the game.
- **Perfect information and Imperfect information games:** In a perfect information game, the players have full knowledge of the history of the game, in contrast to the imperfect information games where the players miss information regarding the decisions made at previous iterations of the game.

2.2 Contract Theory

Contract theory has been a highly successful and active research area in economics, finance, management, and corporate law for decades. Contract theory allows for studying the interaction between the employer(s) and employee(s) by introducing cooperation between them [41]. The performance of employees tends to be better when they work harder, and the probability of bad performance will be lower if employees place more dedication or focus on

the work. In contrast, if an employee's compensation is independent of their performance, the employee will be less likely to put effort into the work. At the same time, there exists some private information on the employees' behalf unknown to the employer, who makes the decision on the adequate level of compensation that motivates good work. The design of appropriate incentive mechanisms, which take at the same time into account such an asymmetry/incompleteness of information between the two parties, plays an important role in addressing the problem of incentives.

Contract Theory was first introduced around the 1960s, while its significance was very recently recognized when Jean Tirole was awarded a Nobel prize in Economic Sciences 2014 "for his analysis of market power and regulation" [51]. Two years later, a Nobel prize in Economic Sciences 2016 was awarded to Oliver Hart and Bengt Holmström "for their contributions to contract theory" [52]. In general, Contract Theory has been widely applied in different disciplines, such as industrial economics and public economics, banking, agriculture [53], and telecommunications [54]. In the following, we adopt the general terminology of "principal" and "agents" to capture any relationship between the contracting parties.

In contract theory, the solution obtained is a menu of contracts intended for the agents, aiming to maximize the principal's utility/payoff. In most cases, the problem is formulated as maximizing an objective function that represents the principal's payoff, subject to the incentive compatibility constraint that each agent's expected payoff is maximized when participating in the contract and the individual rationality constraint that each agent's payoff under this contract is larger than or equal to its reservation payoff when not participating at all.

2.2.1 Adverse Selection Problem

One of the most common incompleteness-of-information problems that arise between a principal and an agent is the so-called "Adverse Selection" problem, under which the agent's desired performance/effort by the principal and the principal's reward back to the agent are agreed upon. Specifically, the principal is unaware of the prospective agent's capabilities, i.e., the agent's private information, and tries to elicit this private information via its contract offer. Following the revelation principle, the principal can offer multiple employment contracts destined to different-capability agents, and each agent selects the appropriate contract offer for its type, i.e., the one that maximizes its utility. As such, the agent indirectly reveals its actual type to the principal.

Let us consider that there are N different agent types, denoted as $\theta_i, i \in \{1, \cdots, N\}$ that bear different private information. Although there exists incompleteness of information between the principal and the agents, the principal has statistical knowledge regarding the existence/occurrence of different agent types. Hence, we define as λ_i the probability of facing the agent type θ_i, such that $\sum_{i=1}^{N} \lambda_i = 1$. The contract bundle designed and offered by the principal to each agent i is denoted as $\{p_i, r_i\}$, where p_i corresponds to the agent's effort wanted by the principal and r_i is the principal's reward provided back to the agent.

The principal's expected utility function is formulated as its expected profit from the agents' efforts minus their provided rewards, i.e., $U_{pr} = \sum_{i=1}^{N}[\lambda_i \cdot (p_i - \mathcal{C} \cdot r_i)]$, where $\mathcal{C} \in \mathbb{R}^+$ is the principal's unit cost of its provided reward to each agent. Similarly, the agent's i personal utility function is defined as $U_i = \theta_i \cdot e(r_i) - p_i$, where the first term expresses the agent's evaluation of its received reward minus its provided effort. Specifically, the agent's evaluation function of reward $e(r_i)$ is usually assumed to be strictly increasing and concave with respect to the agent's i received reward (i.e., $e(0) = 0$, $e'(r_i) > 0$, $e''(r_i) < 0$) and is commonly modeled as $\sqrt{r_i}$ or $\log(1 + r_i)$, in order to capture the indifference of the agent regarding its utility as its effort increases.

Following the adverse selection problem formulation, the principal's utility function U_{pr}

is maximized subject to the agents' satisfaction of their personal utilities U_i, $\forall i \in \{1, \ldots, N\}$, expressed by the Individual Rationality (IR) and Incentive Compatibility (IC) constraints, as described below.

Definition 2.1. ***(Individual Rationality (IR))*** *A contract bundle $\{p_i, r_i\}$ satisfies the individual rationality constraint if each agent receives a non-negative utility, i.e.,*

$$\theta_i \cdot e(r_i) - p_i \geq 0, \forall i \in \{1, \ldots, N\}. \tag{2.2}$$

Definition 2.2. ***(Incentive Compatibility (IC))*** *Each agent must select the contract bundle $\{p_i, r_i\}$ that is designed specifically for their own type θ_i, i.e.,*

$$\theta_i \cdot e(r_i) - p_i \geq \theta_i \cdot e(r_i') - p_i', \forall i, i' \in \{1, \ldots, N\}, i \neq i'. \tag{2.3}$$

The IR constraint ensures the participation of each agent in the contract agreement by marginally satisfying the agent's utility function, while the IC constraint guarantees that each agent can only receive the highest utility when selecting the contract bundle designed for its type. Therefore, the optimization problem to be solved can be written as

$$\max_{\{p_i, r_i\}_{\forall i \in \{1, \ldots, N\}}} \quad U_{pr} = \sum_{i=1}^{N} [\lambda_i \cdot (p_i - \mathcal{C} \cdot r_i)] \tag{2.4a}$$

$$\textbf{s.t.} \quad \theta_i \cdot e(r_i) - p_i \geq 0, \forall i \in \{1, \ldots, N\}, \tag{2.4b}$$

$$\theta_i \cdot e(r_i) - p_i \geq \theta_i \cdot e(r_{i'}) - p_{i'}, \forall i, i' \in \{1, \ldots, N\}, i \neq i'. \tag{2.4c}$$

A fundamental application of the adverse selection optimization problem to perform transmission power control and computation offloading in wireless communication and mobile computing networks can be found in [55, 56]. It should be noted that the adverse selection problem model presented in the current section corresponds to the discrete agent type case and can also be generalized to the continuous agent type case to fit into more realistic scenarios. A corresponding extension to the transmission power control problem in wireless networks considering continuous agent types is presented in [57].

2.2.2 Moral Hazard Problem

In the adverse selection problem formulation, the notions of agent effort and agent performance were interchangeably used, assuming that a specific amount of effort yields a proportional performance. However, in several realistic scenarios, the agent's effort is costly, and its ultimate performance observed by the principal differs from the effort that has been exerted. To model such problems, where the agent's effort is hidden, and only the final performance is observable by the principal, the moral hazard problem formulation is adopted.

According to the basic moral hazard model, the agent's performance q is defined as a noisy signal of its actual provided effort a, such as $q = a + \varepsilon_q$, where $\varepsilon_q \sim N(\mu_q, \sigma_q^2)$. Given that the principal is unaware of the agent's effort, the principal has to strategically reward the agent based on a double compensation scheme that includes a fixed t and a variable s reward. The fixed amount of reward is intended to incentivize the agent to provide its best effort and, hence, is offered while "signing" the contract. On the contrary, the variable reward is offered as long as the principal observes the agent's ultimate performance and its purpose is to compensate the agent's incurred cost of providing its best effort. Thus, the total reward provided to the agent is defined as $r = t + s \cdot q$.

The agent is assumed to have Constant Absolute Risk-Averse (CARA) preferences, meaning that the agent's attitude toward risk is constant as its reward increases. Based on this modeling, the agent's utility is formulated as $U_a = -e^{-\eta[r - \psi(a)]}$, where $\eta > 0$ is the agent's

coefficient of absolute risk aversion ($\eta = -U_a^{''}/U_a^{'}$), the higher the value of which corresponds to less incentives for the agent to exert an effort. Also, the term $\psi(a)$ corresponds to the agent's cost function of providing its effort, while a common form of function chosen is the quadratic, such as $\psi(a) = \frac{1}{2}ca^2$, in order to capture the agent's sensitivity in the exerted effort. The principal's utility function is modeled as the evaluation of the agent's ultimate performance minus its total offered compensation, i.e., $U_{pr} = q - r = (1 - s) \cdot a - t$.

Considering the problem description above, the contract bundle designed and offered by the principal to the agent is denoted as $\{a, r\}$, where a corresponds to the agent's actual effort and r is the principal's total provided reward. Similarly to the adverse selection model, the principal's utility U_{pr} is maximized subject to the agent's satisfaction of its utility U_a. Thus, the optimization problem to be solved can be written as follows

$$\max_{a,t,s} \quad U_{pr} = (1 - s) \cdot a - t \tag{2.5a}$$

$$\textbf{s.t.} \quad E[-e^{-\eta[r-\psi(a)]}] \geq U_{min}, \tag{2.5b}$$

$$a \in \underset{a}{\operatorname{argmax}}\, E[-e^{-\eta[r-\psi(a)]}], \tag{2.5c}$$

where U_{min} is the minimum acceptable utility for the agent to "sign" the contractual agreement. In accordance with the adverse selection model, the principal has to reassure the agent's marginal participation in the contract by satisfying its utility function, as imposed by the first constraint of the optimization problem, i.e., the IR constraint. The second constraint maps to the IC constraint and guarantees that the agent can maximize its utility when selecting the right amount of effort. A fundamental application of the moral hazard optimization problem in computing networks can be found in [56], while the case where the problems of adverse selection and moral hazard are jointly considered under a collaborative mobile edge computing networks framework is presented in [58].

2.2.3 Contract Theory Taxonomies

Based on their inherent properties, the different contractual agreements can be categorized into the following major classes of contracts:

- **Static or Repeated contracts:** A static contract represents the one-shot trading between the different parties and is usually realized by offering a take-it-or-leave-it contract to the agent, to which the agent has to respond whether he/she accepts it or rejects it. As a result, every signing of a contract does bear information about previous trading histories. Repeated contracts, on the other hand, regard the renegotiation of long-term contractual agreements, such as long-term employment contracts.

- **Bilateral or Multilateral contracts:** A bilateral contract refers to the typical one-to-one contract between a single principal and a single agent, whereas the case when multiple agents are concurrently involved in the contractual agreement is known as a multilateral contract.

- **One-dimensional or Multi-dimensional contracts.** Under a one-dimensional contract, only one personal characteristic of the agent is regarded as its private information, and only one task of the agent is accounted as its provided effort to the principal. Consequently, only one type of reward is offered back to the agent by the principal. The opposite holds for the multi-dimensional contract.

- **Complete or Incomplete contracts.** In a complete contract, the legal consequences of every possible state of the environment are specified when "signing" the contract,

whereas the opposite holds for incomplete contracting cases where it is impossible to describe beforehand future uncertainties.

Chapter 3

Resource Allocation and Incentive Mechanism Design in NOMA Wireless Networks

3.1 General Setting

Despite the plethora of research works that have adopted and exploited the application of NOMA in heterogeneous wireless networks, there are still important challenges to be addressed, pertinent to its realization. Given the intrinsic interference caused by different users transmitting over the same resources, advanced interference management techniques are crucial to guarantee the performance gain of NOMA. The latter, in turn, heavily depends on the coupled problems of user scheduling and power control, stressing the need for joint resource optimization schemes. However, one of the key challenges faced by the existing resource allocation approaches, directly affecting their effectiveness and applicability, is the lack of perfect knowledge of the Channel State Information (CSI) at the Base Station (BS). Owing to the inherent uncertainty introduced by the rapidly varying channels and the increased backhaul signaling overhead induced by the deluge of user devices, perfect CSI is practically difficult to achieve. Nevertheless, when considering the situation where only statistical CSI is available at the BS, the private information of the user device regarding its experienced channel gain could be utilized to steer the resource allocation procedure. In that sense, the problem of resource allocation under statistical CSI can be modeled and treated as an incomplete information problem.

In this chapter, a synergistic approach between the BSs and their serving user devices is introduced to accommodate the incompleteness of CSI on the BSs' behalf and treat the timely resource allocation problem of joint user association and power allocation in NOMA-based wireless networks from the users' perspective. Such a user-centric resource allocation mechanism aims to additionally ameliorate users' satisfaction and facilitate temporal network deployments, such as Networked Flying Platforms (NFPs), against a continuously evolving heterogeneous environment. Our work targets to provide a consolidated framework to deal with the research gaps related to the distributed (i.e., user-centric) decision-making, the incompleteness of information, the contradictory objectives between the users and the BSs, and the delivery of holistic solutions in terms of the joint user scheduling and uplink power control in heterogeneous NOMA-based wireless communication networks. To this end, in the following, the theoretical frameworks of Contract Theory (CT) and Reinforcement Learning (RL) are adopted to properly capture and model the relationships between the

"actors" involved in this resource allocation process and the operation of the latter process as such.

3.2 Related Work

Driven by the fundamental concept of NOMA to multiplex users in the power domain, several research works have been devoted, so far, to the essential problem of power control in NOMA-operated networks. Early work by the authors in [59] introduced a fixed power allocation strategy that was further extended in [60] to account for the distinct channel state of each multiplexed user. Towards overcoming the drawbacks of fixed power allocations, dynamically adjusted power allocation schemes were designed in [61, 62] for two-user and multiple-user NOMA systems, respectively. Based on this groundwork, more recent efforts targeted addressing various joint resource allocation problems in NOMA-based networks, such as joint rate and power control [63], joint spectrum and power control [64], or even power splitting in dual-connectivity-enabled networks [65].

Nonetheless, when employing NOMA in a multi-cell network scenario, the interdependence between user-to-cell association and power allocation should be taken into account. Centralized solutions that iteratively optimize user association and power allocation have been presented in [66, 67], based on game theory (e.g., coalition formation and matching games) and advanced optimization techniques. Considering that such centralized approaches usually fail to apply in more complex systems, significant attention has also been drawn to the design of distributed solutions. A semi-distributed approach towards user association, transmission mode selection, and power allocation has been developed in [68]. Moreover, a cluster formation and power-bandwidth allocation algorithm executed exclusively by each cell is proposed in [69]. Despite their distributed structure and reduced computational complexity, both works in [68, 69] optimize the subsequent problems under investigation at different stages and independently of each other, instead of jointly addressing them. More importantly, though, all aforementioned works [66, 67, 68, 69] presume perfect CSI at the BSs during the resource allocation procedure, which significantly limits their exploitability and applicability.

Meanwhile, the issue of imperfect/partial CSI has received considerable attention to secure the performance gain of NOMA in practical implementations. Based on the long-term statistics of channel realizations, stochastic methods that model either the CSI or the channel estimation error have been extensively used in the literature to evaluate the performance of NOMA and to design effective resource allocation schemes. Primary efforts focused on identifying the impact of partial CSI on different performance metrics, such as the outage probability and the average sum rate [70], or the user fairness [62]. Power allocation strategies under statistical CSI have also been derived by the works in [71, 72], while more combinatorial resource allocation frameworks for networks operating under Multi-Carrier NOMA (MC-NOMA) have been proposed in [73, 74]. All the aforementioned resource allocation works (i.e., [71, 72, 73, 74]) formulate centralized optimization problems using probabilistic constraints on some outage event. Following a series of observations and appropriate simplifications, the constraints are subsequently reduced, and the corresponding problems are transformed into non-probabilistic ones.

An alternative formal method to mathematically formulate resource allocation problems under statistical CSI, that promotes users' involvement in the allocation procedure, has been recently introduced in the literature of wireless networks, based on the framework of Contract Theory (CT). Contract theory is a field of economics that provides the mathematical foundations to create mutually agreeable contracts or arrangements between economic players in the presence of complete or incomplete information (often referred to as asymmetric information) [41]. Under this concept, a principal/employer creates contract bundles based

on agents'/employees' private information, i.e., type, to motivate them to provide back their effort and, hence, reveal their actual type. In wireless communications, contract theory has been already used to provide mutual agreements between network/service providers and user devices. Exemplified works in [42, 75] have applied contract theory in Device-to-Device (D2D) and cognitive communications, respectively, to incentivize users' participation and contribution towards enhancing the network's capacity.

Consequently, contract theory constitutes a particularly prominent way to design resource allocation schemes that consider imperfect/partial CSI, under a user-centric flavor. Preliminary contract-based solutions of relevant resource allocation schemes have been discussed in [76, 77, 78]. Both [76] and [78] model the problem of relay node selection in wireless networks, while each research work employs a different multiple access technique, namely NOMA and Orthogonal Frequency Division Multiple Access (OFDMA), respectively. In these settings, the CSI of the prospective relay nodes is regarded as their private information and only the probability distribution of their types, i.e., channel gains, is known at the BS. Embracing the idea of probabilistic CSI at the BS, the authors in [77] confront the joint user association, and spectrum and power allocation problem from a contract-theoretic perspective, while aiming at mitigating the resulting interference in OFDMA networks. Nevertheless, the OFDMA-based specific formulation assumed in [77] renders this approach inapplicable in NOMA-operated networks, while its centralized nature restricts its applicability in terms of network scalability.

3.3 Contributions & Outline

To the best of our knowledge, our work is the first one in the literature that aims at exactly filling the aforementioned research gaps, by removing the corresponding assumptions of perfect CSI knowledge and treating the emerging challenges associated with resource allocation in NOMA-operated heterogeneous networks. In particular, we propose a novel framework that jointly tackles the user-to-BS association and uplink power allocation in heterogeneous wireless networks. The problem is formulated and solved under an incomplete CSI scenario, by introducing formal methods based on Reinforcement Learning (RL) and Contract Theory (CT). The main contributions of this work can be summarized as follows.

1. An RL mechanism is introduced to enable the distributed and autonomous user-to-BS association. Each user selects a BS to be associated with, aiming at optimizing its provided feedback from the communications environment that captures the network-related and social characteristics of the respective association. With the term social characteristics, we refer to the long-term BSs' reputation formulated by the users' expressed subjective opinion regarding the service that they enjoy, when associated with them. To truthfully elicit the users' subjective opinion, the novel use of the Bayesian Truth Serum mechanism is proposed, further allowing the expression of BSs' reputations as a Bayesian belief.

2. A contract-theoretic power allocation mechanism is proposed between each BS and its associated/communicating users, accounting for the imperfect CSI on the former's behalf. The users are distinguished into different types depending on their experienced channel conditions and different contract bundles are designed by the BSs tailored to them. The contract bundles comprise the requested effort by the BS from its communicating users, which is mapped to their uplink transmission power, and a corresponding reward. The overall uplink power allocation is iteratively optimized and determined, while the RL-based user-to-BS association procedure is realized.

3. Detailed numerical results, obtained via modeling and simulation, are presented to

demonstrate the proper operation and effectiveness of the proposed framework. Particularly, the inherent characteristics of the contract-theoretic power allocation mechanism are studied, under the cases of complete and incomplete CSI, while the operation of the RL-based user-to-BS association mechanism is illustrated in terms of its convergence to beneficial association points. A comparative numerical evaluation of the proposed approach against other user-to-BS association mechanisms is performed, showing the benefits of the overall proposed framework in terms of the achieved data rate and fairness among the users within the heterogeneous wireless network.

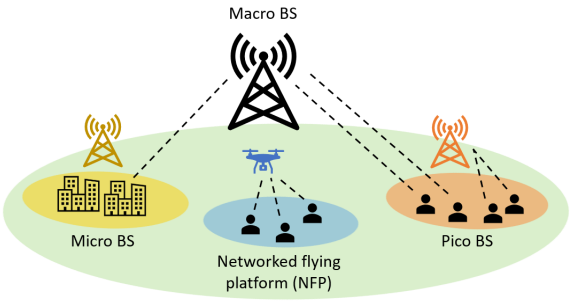

Figure 3.1: Heterogeneous wireless network topology.

3.4 System Model

We consider the uplink communication of a heterogeneous wireless network consisting of $|C|$ BSs and let us denote the corresponding set by $C = \{1, \ldots, |C|\}$. Each BS in the network, depending on its physical characteristics, features, and capabilities, can be of different types. Indicative examples of such different types of BSs are macro BSs, small BSs (i.e., micro, pico, or femto), or NFPs, as illustrated in Fig. 3.1. Let $U = \{1, \ldots, |U|\}$ denote the set of users to be served by the network. Subsequently, a set $\mathbb{U}_c$ of cardinality $|\mathbb{U}_c|$ represents the users associated with a BS c at any given time. As a means of efficiently managing complexity and interference mitigation, we assume that the total available system bandwidth B is sub-divided into $|C|$ different orthogonal frequency chunks, where accordingly bandwidth B_c has been allocated to each BS c, such that $B = \sum_{c=1}^{C} B_c$. Moreover, we presume that the allocated frequency chunks (i.e., channels) are exposed to frequency-flat block fading, meaning that they can be considered constant over their bandwidth, but can vary independently with each other. Following NOMA principles, multi-user spectrum sharing within the assigned bandwidth of a specific BS is achieved through power-domain multiplexing, capitalizing on the exploitation of channel gain difference among users. As a result, the users associated with a BS c transmit their signals on the entire BS's available bandwidth B_c, and distinguish themselves according to their transmission power level, while the SIC technique is applied at the receiver side to have the signals properly decoded.

Let us define as p_u^c the uplink transmission power of user u communicating with BS c and G_u^c the channel power gain of their wireless link. It is, also, noted that within the scope of this work and analysis, all the BSs are considered to be equipped with a single antenna. Based on the principle of SIC and without loss of generality, the channel gains observed by a BS c are sorted in ascending order as $G_1^c \leqslant \cdots \leqslant G_u^c \leqslant \cdots \leqslant G_{|\mathbb{U}_c|}^c$ and the signal of the highest channel gain user is decoded first. When a signal is decoded, it is subtracted from the superposition signal before further decoding takes place. Hence, the interference sensed

by a user u associated with BS c can be expressed as:

$$I_u^c = \sum_{u'=1}^{u-1} G_{u'}^c \, p_{u'}^c + I_0, \tag{3.1}$$

where I_0 is the power of zero-mean Additive White Gaussian Noise (AWGN). Adopting Shannon's capacity formula, the achievable data rate of user u pertinent to BS c is

$$R_u^c = B_c \, \log_2 \left(1 + \gamma_u^c\right) [bps], \tag{3.2}$$

where γ_u^c corresponds to the Signal-to-Interference-plus-Noise Ratio (SINR) given by

$$\gamma_u^c = \frac{G_u^c \, p_u^c}{I_u^c}. \tag{3.3}$$

3.4.1 Contract Bundle

Given a user-to-BS association, each BS incentivizes its serving users to transmit with an appropriately selected power level that enables the decoding of their signal, by offering them a contract bundle of {effort, reward}. The contract bundle $\{p_u^c, r_u^c\}$ designed by a BS c for a user $u \in \mathbb{U}_c$ consists of the user's effort, i.e., transmission power p_u^c, and its offered reward by the BS c, denoted by r_u^c. The offered reward is considered proportional to the user's sensed interference I_u^c, defined as $r_u^c = \rho \cdot I_u^c$, where $\rho \in \mathbb{R}^+$ is a reward factor. It is noted that the user's sensed interference I_u^c is determined by applying the SIC technique at the receiver, i.e., BS, as described earlier in Section 3.4, and it is computed and determined following Eq. (3.1). The physical meaning and interpretation of the reward is that the BS provides a greater reward to users who experience more interference, i.e., the higher channel gain users, since it expects greater transmission power to decode their signals. At the same time, the BS discourages the lower channel gain users from transmitting with high power levels that prevent the proper decoding of higher channel gain users' signals. Such a design allows for maintaining the distinctness among the received signals at the corresponding BS for the latter's receiver to properly perform the SIC technique. Apparently, the overall contract-theoretic power control mechanism provides appropriate incentives to the users to adapt their transmission power levels towards enabling their transmitted signals to be decoded by the receiver without burdening the overall communication environment with excessive interference. This process is further detailed later in Section 3.4.3.

3.4.2 User Type

Each user associated with a BS is characterized by a type that captures its private information related to its established channel quality. We define the type of a user $u \in \mathbb{U}_c$ communicating with BS c as $t_u^c = \left(G_u^c / \sum_{u=1}^{|\mathbb{U}_c|} G_u^c\right)^{1/2}, t_u^c \in (0, 1]$, where G_u^c corresponds to its channel gain. The proposed novel formulation of the user's type captures the user's relative quality of its channel gain within the examined wireless communication environment with respect to the rest of the users. It is noted that the introduced user type is unique for each user within the system and acts as its personal identity and characteristic. In the following analysis, we consider a fully heterogeneous networking environment in terms of users' channel gain characteristics and their corresponding types. Specifically, each user is characterized by a unique type and thus, there are $|\mathbb{U}_c|$ types of users associated with a BS c. The user types follow the order of the users' channel gains, i.e., $t_1^c < \cdots < t_u^c < \cdots < t_{|\mathbb{U}_c|}^c$, meaning that a user experiencing better channel conditions is of higher type. Naturally, a higher type implies that the user invests greater effort (i.e., transmission power) and thus, is rewarded more by the BS.

3.4.3 User's and BS's Utility

We define the user's utility function U_u^c that depicts its perceived satisfaction from the reward r_u^c provided by the BS c, as well as its cost to provide its effort to the BS, i.e., transmission power p_u^c, as follows:

$$U_u^c(p_u^c) = t_u^c \cdot e(r_u^c) - p_u^c. \tag{3.4}$$

The first term expresses the user's satisfaction depending on its type t_u^c and its evaluation function of reward $e(r_u^c)$. The evaluation function is strictly increasing and concave with respect to the user's received reward (i.e., $e(0) = 0, e'(r_u^c) > 0, e''(r_u^c) < 0$). For demonstration purposes and without loss of generality, in the following, we consider $e(r_u^c) = \sqrt{r_u^c}$. The physical meaning of the user's utility function captures the user's "profit" by transmitting its data to the BΣ within a fully heterogeneous NOMA-based communications environment.

Similarly, a BS c experiences a utility $U_c^u = p_u^c - \mathcal{C} \cdot r_u^c$ by each user's u provided effort, while accounting for its cost to provide the reward to the user, with $\mathcal{C} \in \mathbb{R}^+$ representing its unit cost. For simplicity in the presentation and without loss of generality, we consider that all the BSs experience the same unit cost $\mathcal{C}$. However, the rest of the analysis would hold even if each BS was characterized by a personalized unit cost $\mathcal{C}_c$, as the latter is a constant value. Also, it is noted that the BSs should sophisticatedly evaluate their unit cost $\mathcal{C}$ to guarantee that the users' available battery is sufficient to participate in the personalized contract bundles. In the typical and realistic scenario that the BS is unaware of the user's type, the BS c estimates the probability λ_u^c that the user u is of type t_u^c, with $\sum_{u=1}^{|\mathbb{U}_c|} \lambda_u^c = 1$. Therefore, for a number of $|\mathbb{U}_c|$ users communicating with BS c, its utility function is represented as follows:

$$U_c = \sum_{u=1}^{|\mathbb{U}_c|} \left[\lambda_u^c \cdot (p_u^c - \mathcal{C} \cdot r_u^c)\right]. \tag{3.5}$$

The physical meaning of the BS's utility function captures the probabilistic "profit" that the BS will experience by incentivizing the users to adapt their transmission power levels to avoid creating excessive interference in the overall system while enabling the BS to decode their received signals.

3.5 Contract-theoretic Power Allocation

In the following, the proposed contract-theoretic power allocation mechanism, under both complete and incomplete CSI scenarios is presented, based on the already defined contract bundles, user types, and user and BS utilities. The power allocation is formulated as a fully distributed optimization problem executed by each BS of the system independently. The objective of this distributed optimization problem is to maximize the respective BS's utility function subject to its corresponding users' constraints, which in turn ensure their acceptance of the contract. As stated before, the contract designed by a BS c for a user $u \in \mathbb{U}_c$ consists of the user's transmission power (i.e., user's effort), and its corresponding offered reward by the BS c. Accordingly, a set of contract bundles between the BS and its serving users is the outcome that we seek from this procedure. A thorough analysis of how to derive optimal contract bundles, meeting the optimization objectives defined under complete and incomplete information scenarios, is pursued in the subsequent sections. It is noted here that in the following subsections, we assume that the users have already been associated with a specific BS. However, later on, in Section 3.6, we provide a fully distributed user-to-BS association procedure and framework.

3.5.1 Optimal Contract under Complete Information

In this section, the complete information scenario is considered and analyzed, in the sense that the BS knows a priori the type of its serving users. This ideal case serves as a baseline to verify the effectiveness of the resource allocation performed under the incomplete CSI scenario. Indeed, since the BS is assumed to be completely aware of the users' types and corresponding channel characteristics, it can fully exploit their effort and maximize its utility, while guaranteeing that the users accept its offered contract. In other words, the BS has to ensure that the users experience a non-negative utility, i.e., the optimal contract bundles satisfy the individual rationality condition, as defined formally below.

Definition 3.1. ***(Individual Rationality (IR))*** *A contract bundle $\{p_u^c, r_u^c\}$ satisfies the individual rationality constraint if each user receives a non-negative utility, i.e.,*

$$t_u^c \cdot e(r_u^c) - p_u^c \geq 0, \forall c \in C, \forall u \in \mathbb{U}_c. \tag{3.6}$$

Therefore, the problem of determining the optimal contracts for a BS c under the complete information of the users' types, can be written as follows:

$$\max_{\{p_u^c, r_u^c\}_{\forall u \in \mathbb{U}_c}} U_c^u = p_u^c - \mathcal{C} \cdot r_u^c, \forall c \in C \tag{3.7a}$$

$$\textbf{s.t.} \quad t_u^c \cdot e(r_u^c) - p_u^c \geq 0, \forall u \in \mathbb{U}_c. \tag{3.7b}$$

In the contract design under complete CSI, the BS will target to maximize its utility, by providing the minimum acceptable utility to its serving users. In this case, it will decrease r_u^c until $t_u^c \cdot e(r_u^c) - p_u^c = 0$, meaning that the constraint of Eq. (3.7b) can be considered as equality. Accordingly, solving the equality of Eq. (3.7b) with respect to r_u^c and substituting in Eq. (3.7a), we get $U_c^u = p_u^c - \mathcal{C} \cdot (p_u^c / t_u^c)^2$. Thus, a closed-form solution can be derived for the optimization problem of Eq. (3.7a)-3.7b by solving the following equation:

$$\frac{\partial U_c^u}{\partial p_u^c} = 0, \forall c \in C, \forall u \in \mathbb{U}_c. \tag{3.8}$$

Consequently, under the assumption of complete CSI availability at a BS, it can be easily found that the optimal contract bundles between each BS c and its serving users are given by $\{p_u^c, r_u^c\} = \left\{ \frac{(t_u^c)^2}{2\mathcal{C}}, (\frac{t_u^c}{2\mathcal{C}})^2 \right\}$.

3.5.2 Feasible Contract under Incomplete Information

In this section, we elaborate on the necessary and sufficient conditions to determine a feasible contract under the realistic scenario of incomplete CSI. The purpose of this analysis is to derive optimal contracts subsequently in Section 3.5.3.

In a scenario of incomplete CSI, the BS has to ensure that the users are provided not only with a non-negative utility but also with the maximum utility when selecting the contract designed for their type. The former refers to the Individual Rationality (IR) condition given by Eq. (3.6), while the latter corresponds to the Incentive Compatibility (IC) condition defined formally below.

Definition 3.2. ***(Incentive Compatibility (IC))*** *Each user must select the contract bundle $\{p_u^c, r_u^c\}$ that is designed specifically for their own type t_u^c, i.e.,*

$$t_u^c \cdot e(r_u^c) - p_u^c \geq t_u^c \cdot e(r_{u'}^c) - p_{u'}^c, \forall c \in C, \forall u, u' \in \mathbb{U}_c, u \neq u'. \tag{3.9}$$

Hence, it can be easily inferred that when a contract satisfies the IR and IC constraints, the users have adequate incentives to truthfully reveal their private type, by choosing the contract bundle designed for them. Apart from ensuring incentive compatibility, several additional conditions should hold to render a contract feasible.

Proposition 3.1. *For any feasible contract* $\{p_u^c, r_u^c\}$*, the following must hold true:* $r_u^c > r_{u'}^c \iff t_u^c > t_{u'}^c$ *and* $r_u^c = r_{u'}^c \iff t_u^c = t_{u'}^c$, $\forall u, u' \in \mathbb{U}_c$, $u \neq u'$.

Proof. Initially, we prove the sufficiency of the proposition, i.e., $t_u^c > t_{u'}^c \implies r_u^c > r_{u'}^c$, by using the IC constraint in Eq. (3.9). Based on the IC constraint in Eq. (3.9), we have

$$t_u^c \cdot e(r_u^c) - p_u^c \geq t_u^c \cdot e(r_{u'}^c) - p_{u'}^c, \tag{3.10}$$

$$t_{u'}^c \cdot e(r_{u'}^c) - p_{u'}^c \geq t_{u'}^c \cdot e(r_u^c) - p_u^c. \tag{3.11}$$

Adding appropriately the corresponding terms of the inequalities of Eq. (3.10) and Eq. (3.11), we obtain

$$t_u^c \cdot e(r_u^c) + t_{u'}^c \cdot e(r_{u'}^c) \geq t_u^c \cdot e(r_{u'}^c) + t_{u'}^c \cdot e(r_u^c). \tag{3.12}$$

By performing simple factorization, inequality Eq. (3.12) is recasted into the following one:

$$(t_u^c - t_{u'}^c) \cdot \big[e(r_u^c) - e(r_{u'}^c)\big] \geq 0. \tag{3.13}$$

Given that $t_u^c > t_{u'}^c$ and $e(r_u^c)$ is a strictly increasing function with respect to r_u^c, it is concluded from Eq. (3.13) that $r_u^c > r_{u'}^c$.

Thereafter, we prove the necessity of the proposition, i.e., $r_u^c > r_{u'}^c \implies t_u^c > t_{u'}^c$. Since $r_u^c > r_{u'}^c$ and $e(r_u^c)$ is strictly increasing with r_u^c, it holds that $e(r_u^c) - e(r_{u'}^c) > 0$. Hence, from Eq. (3.13) we obtain that $t_u^c > t_{u'}^c$. As a result, it has been proven that $r_u^c > r_{u'}^c \iff t_u^c > t_{u'}^c$.

Following a similar procedure and argumentation, it can be easily proven that $r_u^c = r_{u'}^c \iff t_u^c = t_{u'}^c$, which completes the proof. □

The rationale behind Proposition 3.1 is that a higher type t_u^c user, which represents a user of better channel conditions will receive a greater reward from the associated BS c to be incentivized to establish a connection and transmit its data.

Proposition 3.2. ***(Monotonicity)*** *A user of higher type, i.e.,* $t_1^c < \cdots < t_u^c < \cdots < t_{|\mathbb{U}_c|}^c$*, will receive a greater reward from the BS* c*, i.e.,* $r_1^c < \cdots < r_u^c < \cdots < r_{|\mathbb{U}_c|}^c$*, as it will contribute a greater effort, i.e.,* $p_1^c < \cdots < p_u^c < \cdots < p_{|\mathbb{U}_c|}^c$.

Proof. Given our assumption that user types follow an ascending order $t_1^c < \cdots < t_u^c < \cdots < t_{|\mathbb{U}_c|}^c$, the first part of this proposition readily stems from Proposition 3.1. Subsequently, we prove that for any feasible contract $\{p_u^c, r_u^c\}$, the following holds true: $p_u^c > p_{u'}^c \iff r_u^c > r_{u'}^c$, $\forall u, u' \in \mathbb{U}_c$, $u \neq u'$.

First, we prove that if $p_u^c > p_{u'}^c$ then $r_u^c > r_{u'}^c$. According to the IC constraint in Eq. (3.9), we have $t_u^c \cdot e(r_u^c) - p_u^c \geq t_u^c \cdot e(r_{u'}^c) - p_{u'}^c \Leftrightarrow t_u^c \cdot \big(e(r_u^c) - e(r_{u'}^c)\big) \geq p_u^c - p_{u'}^c$. Since $p_u^c > p_{u'}^c$ and given that $e(r_u^c)$ is a strictly increasing function of r_u^c, it holds that $r_u^c > r_{u'}^c$. Similarly, in order to prove that if $r_u^c > r_{u'}^c$ then $p_u^c > p_{u'}^c$, we follow the IC constraint in Eq. (3.9), and we have $t_{u'}^c \cdot e(r_{u'}^c) - p_{u'}^c \geq t_{u'}^c \cdot e(r_u^c) - p_u^c \Leftrightarrow p_u^c - p_{u'}^c \geq t_{u'}^c \cdot \big(e(r_u^c) - e(r_{u'}^c)\big)$. Since $r_u^c > r_{u'}^c$ and $e(r_u^c)$ is a strictly increasing function with respect to r_u^c, we conclude that $p_u^c > p_{u'}^c$. This completes the proof of the monotonicity condition. □

Proposition 3.3. *A user of higher type, i.e.,* $t_1^c < \cdots < t_u^c < \cdots < t_{|\mathbb{U}_c|}^c$*, will receive higher utility to be incentivized by the BS* c*, i.e.,* $U_1^c < \cdots < U_u^c < \cdots < U_{|\mathbb{U}_c|}^c$.

Proof. We examine two users $u, u' \in \mathbb{U}_c$, $u \neq u'$ of types $t_u^c > t_{u'}^c$. Based on the IC condition in Eq. (3.9), we have

$$t_u^c \cdot e(r_u^c) - p_u^c \geq t_u^c \cdot e(r_{u'}^c) - p_{u'}^c > t_{u'}^c \cdot e(r_{u'}^c) - p_{u'}^c. \tag{3.14}$$

Then, it holds that $U_u^c > U_{u'}^c$ when $t_u^c > t_{u'}^c$ and thus, for $t_1^c < \cdots < t_u^c < \cdots < t_{|\mathbb{U}_c|}^c$ we conclude that $U_1^c < \cdots < U_u^c < \cdots < U_{|\mathbb{U}_c|}^c$. □

Based on the above-analyzed conditions that guarantee the feasibility of a contract under an incomplete information scenario, the optimization problem executed by each BS c can, then, be formulated. The objective of each BS is to maximize its utility to be able to collect and properly decode the users' transmitted signals (as dictated by the received SINR). At the same time, all associated users' constraints should be satisfied for the users to be willing to be served by the specific BS. Therefore, the following distributed optimization problem, which captures both the BS's and corresponding users' requirements, is formulated at each BS as follows:

$$\mathbf{P1:} \max_{\{p_u^c, r_u^c\}_{\forall u \in \mathbb{U}_c}} U_c = \sum_{u=1}^{|\mathbb{U}_c|} \left[\lambda_u^c \cdot (p_u^c - \mathcal{C} \cdot r_u^c)\right], \forall c \in C \tag{3.15a}$$

$$\textbf{s.t.} \quad t_u^c \cdot e(r_u^c) - p_u^c \geq 0, \forall u \in \mathbb{U}_c, \tag{3.15b}$$

$$t_u^c \cdot e(r_u^c) - p_u^c \geq t_u^c \cdot e(r_{u'}^c) - p_{u'}^c, \forall u, u' \in \mathbb{U}_c, u \neq u', \tag{3.15c}$$

$$0 \leq r_1^c < \cdots < r_u^c < \cdots < r_{|\mathbb{U}_c|}^c, \tag{3.15d}$$

where Eq. (3.15b), (3.15c), (3.15d) represent the aforementioned IR, IC, and monotonicity constraints, respectively. Because problem **P1** is non-convex, the procedure described in Section 3.5.3 below, is carried out to reduce its constraints and obtain a tractable solution effectively.

3.5.3 Optimal Contract under Incomplete Information

In the following, the explanation and detailed analysis of the IR and IC constraints reduction is pursued, for a contract under incomplete information.

Step 1: IR Constraints Reduction

By considering the assumption about the user types ordering, i.e., $t_1^c < \cdots < t_u^c < \cdots < t_{|\mathbb{U}_c|}^c$ and the IC condition in Eq. (3.9), we can write $t_u^c \cdot e(r_u^c) - p_u^c \geq t_u^c \cdot e(r_{u'}^c) - p_{u'}^c \geq t_u^c \cdot e(r_1^c) - p_1^c$. Also, given that $t_u^c > t_1^c$ and based on the IR condition in Eq. (3.6), we have

$$t_u^c \cdot e(r_u^c) - p_u^c \geq t_u^c \cdot e(r_1^c) - p_1^c > t_1^c \cdot e(r_1^c) - p_1^c \geq 0. \tag{3.16}$$

As a result, we deduce that if the IR constraint of the lowest user type t_1^c is ensured (i.e., $t_1^c \cdot e(r_1^c) - p_1^c \geq 0$), all other IR constraints for the users with higher types will automatically be satisfied. Towards increasing BS's utility, the latter IR constraint can be considered alternatively as equality, i.e., $t_1^c \cdot e(r_1^c) - p_1^c = 0$. Hence, the $|\mathbb{U}_c|$ IR inequality constraints defined in problem **P1**, are reduced to one IR equality constraint.

Step 2: IC Constraints Reduction

To accommodate the IC constraint reduction process, additional terminology is used about the IC constraints defined between different user types. In particular, the IC constraints between user types u and u', $u' \in \{1, \ldots, u-1\}$ are termed as Downward IC (DIC) constraints. Specifically, the DIC constraint between adjacent user types u and $u-1$ is referred to as the local DIC constraint. Similarly, the IC constraints between user types u and u', $u' \in \{u+1, \ldots, |\mathbb{U}_c|\}$ are called Upward IC (UIC) constraints, while the UIC constraint between adjacent user types u and $u+1$ pertains to the local UIC constraint. Next, we will consecutively analyze how to reduce both the DIC and the UIC constraints to conclude a convex optimization problem.

Proposition 3.4. *All the DIC constraints can be represented by the local DIC constraints.*

Proof. We consider three adjacent user types, such that $t_{u-1}^c < t_u^c < t_{u+1}^c$. Then, the following two local DIC constraints can be derived:

$$t_{u+1}^c \cdot e(r_{u+1}^c) - p_{u+1}^c \geq t_{u+1}^c \cdot e(r_u^c) - p_u^c, \tag{3.17}$$

$$t_u^c \cdot e(r_u^c) - p_u^c \geq t_u^c \cdot e(r_{u-1}^c) - p_{u-1}^c. \tag{3.18}$$

Based on Proposition 3.1, we have $r_u^c > r_{u'}^c \iff t_u^c > t_{u'}^c$. Also, for $r_u^c > r_{u-1}^c \overset{e\nearrow}{\Longleftrightarrow} e(r_u^c) > e(r_{u-1}^c) \Leftrightarrow e(r_u^c) - e(r_{u-1}^c) > 0$. For $t_{u+1}^c > t_u^c$, the second inequality becomes

$$\begin{aligned} t_{u+1}^c \cdot \left[e(r_u^c) - e(r_{u-1}^c)\right] &> t_u^c \cdot \left[e(r_u^c) - e(r_{u-1}^c)\right] \\ &\geq^{Eq.\ (3.18)} p_u^c - p_{u-1}^c. \end{aligned} \tag{3.19}$$

From inequality Eq. (3.17) and with the use of Eq. (3.19) we have

$$\begin{aligned} t_{u+1}^c \cdot e(r_{u+1}^c) - p_{u+1}^c &\geq t_{u+1}^c \cdot e(r_u^c) - p_u^c \\ &\geq^{Eq.\ (3.19)} t_{u+1}^c \cdot e(r_{u-1}^c) - p_{u-1}^c \\ &\geq \dots \\ &\geq t_{u+1}^c \cdot e(r_1^c) - p_1^c. \end{aligned} \tag{3.20}$$

Therefore, if the DIC constraint between user types $u+1$ and u holds, then it, also, holds for user types $u+1$ and $u-1$. This property can be recursively extended downward from user types $u-1$ to 1, as dictated by Eq. (3.20).

If the local DIC constraints hold, then all the DIC constraints are automatically satisfied. In other words, all the DIC constraints can be equivalently captured by

$$t_u^c \cdot e(r_u^c) - p_u^c \geq t_u^c \cdot e(r_{u-1}^c) - p_{u-1}^c. \tag{3.21}$$

□

Proposition 3.5. *All the UIC constraints can be represented by the local DIC constraints.*

Proof. An identical procedure with Proposition 3.4 is followed, and the local UIC constraints between three adjacent user types, such as $t_{u-1}^c < t_u^c < t_{u+1}^c$, are written as:

$$t_{u-1}^c \cdot e(r_{u-1}^c) - p_{u-1}^c \geq t_{u-1}^c \cdot e(r_u^c) - p_u^c, \tag{3.22}$$

$$t_u^c \cdot e(r_u^c) - p_u^c \geq t_u^c \cdot e(r_{u+1}^c) - p_{u+1}^c. \tag{3.23}$$

Based on Proposition 3.1, we have $r_u^c > r_{u'}^c \iff t_u^c > t_{u'}^c$. For $t_u^c > t_{u-1}^c$, the second inequality becomes

$$\begin{aligned} p_{u+1}^c - p_u^c &\geq^{Eq.\ (3.23)} t_u^c \cdot \left[e(r_{u+1}^c) - e(r_u^c)\right] \\ &> t_{u-1}^c \cdot \left[e(r_{u+1}^c) - e(r_u^c)\right]. \end{aligned} \tag{3.24}$$

From inequality Eq. (3.22) and with the use of Eq. (3.24) we have

$$\begin{aligned} t_{u-1}^c \cdot e(r_{u-1}^c) - p_{u-1}^c &\geq t_{u-1}^c \cdot e(r_u^c) - p_u^c \\ &\geq^{Eq.\ (3.24)} t_{u-1}^c \cdot e(r_{u+1}^c) - p_{u+1}^c \\ &\geq \dots \\ &\geq t_{u-1}^c \cdot e(r_{|\mathbb{U}_c|}^c) - p_{|\mathbb{U}_c|}^c. \end{aligned} \tag{3.25}$$

Thus, if the UIC constraint between user types $u-1$ and u holds, then it, also, holds for user types $u-1$ and $u+1$. Similarly, this property can be extended upward from user type $u+1$ to $|\mathbb{U}_c|$, as dictated by Eq. (3.25).

Therefore, we have proved that if the local UIC constraints hold, then all UIC constraints are automatically satisfied and can be captured by

$$t_u^c \cdot e(r_u^c) - p_u^c \geq t_u^c \cdot e(r_{u+1}^c) - p_{u+1}^c. \tag{3.26}$$

To complete the proof, it is remarkable to observe that the local DIC constraint defined in Eq. (3.21), can easily imply the following local UIC constraint:

$$t_{u-1}^{c} \cdot e(r_{u-1}^{c}) - p_{u-1}^{c} \geq t_{u-1}^{c} \cdot e(r_{u}^{c}) - p_{u}^{c}. \tag{3.27}$$

In this respect, inequality Eq. (3.26) can be equivalently represented by Eq. (3.21), and thus, all UIC constraints are reduced to the local DIC constraint implied by Eq. (3.21). The latter constraint, i.e., Eq. (3.21), is considered as equality to each BS to achieve the maximum benefit from its serving users' effort. Hence, the $|\mathbb{U}_c| \cdot (|\mathbb{U}_c| - 1)$ IC inequality constraints defined in problem **P1**, are reduced to $|\mathbb{U}_c| - 1$ equality constraints, accordingly. □

Based on the reduced IR and IC constraints, the optimization problem **P1** can be rewritten as follows:

$$\mathbf{P2:} \max_{(r_u^c, p_u^c)_{\forall u \in \mathbb{U}_c}} U_c = \sum_{u=1}^{|\mathbb{U}_c|} \left[\lambda_u^c \cdot (p_u^c - \mathcal{C} \cdot r_u^c)\right], \forall c \in C \tag{3.28a}$$

$$\text{s.t.} \quad t_1^c \cdot e(r_1^c) - p_1^c = 0, \forall u \in \mathbb{U}_c, \tag{3.28b}$$

$$t_u^c \cdot e(r_u^c) - p_u^c = t_u^c \cdot e(r_{u-1}^c) - p_{u-1}^c, \forall u \in \mathbb{U}_c, \tag{3.28c}$$

$$0 \leq r_1^c < \cdots < r_u^c < \cdots < r_{|\mathbb{U}_c|}^c. \tag{3.28d}$$

It is noted that the resulting optimization problem **P2** is an equivalent transformation of the original problem **P1**, thus resulting in the same outcome, i.e., the optimal contracts established among the users and the BSs. We can easily prove that **P2** is a convex programming problem by checking the Hessian matrix. Thus, **P2** can be solved by applying the Karush–Kuhn–Tucker (KKT) conditions. Accordingly, the optimal users' uplink transmission power vector $\mathbf{p}_c^* = [p_1^{c*}, \ldots, p_{|\mathbb{U}_c|}^{c*}]$ and BS's rewards vector $\mathbf{r}_c^* = [r_1^{c*}, \ldots, r_{|\mathbb{U}_c|}^{c*}]$, can be determined.

The contract design and optimization are handled by each BS of the heterogeneous network independently, and the detailed process is summarized as part of the Algorithm 3.1, (as presented below in Section 3.6.3).

3.6 Autonomous User-to-BS Association

In this section, we introduce a fully distributed and user-centric user-to-BS association framework, where the users of the underlying network topology, acting as learning automata, autonomously select the BS to be associated with and transmit their data. To enhance the users' satisfaction with the provided communication service, their decision is probabilistically reinforced by considering the prospective BSs' network-related and social characteristics. Analytically, we introduce a mechanism based on the Bayesian Truth Serum (BTS) concept to truthfully elicit the users' perceived satisfaction when served by a certain BS. The users are allowed to express their subjective opinions regarding their achieved data rate after the contract-theoretic uplink power allocation is performed. The overall users' satisfaction reports contribute to the extraction of an objective outcome pertinent to each BS's service provisioning. This objective outcome is further utilized to formulate each BS's reputation as a Bayesian Belief and provide it back to the users as feedback for their BS selection. The concluded intelligent user-to-BS association mechanism, whose high-level overview is illustrated in Fig. 3.2, provides a tangible application example of Artificial Intelligence (AI) and Machine Learning (ML) toward solving a fundamental problem in 5G and beyond networks and has been characterized as a critical enabler therein [79]. Additional details with respect to each mechanism, are provided in the subsequent sections. Finally, a comprehensive analysis of the algorithmic complexity of the unified user association and power allocation scheme complements the section.

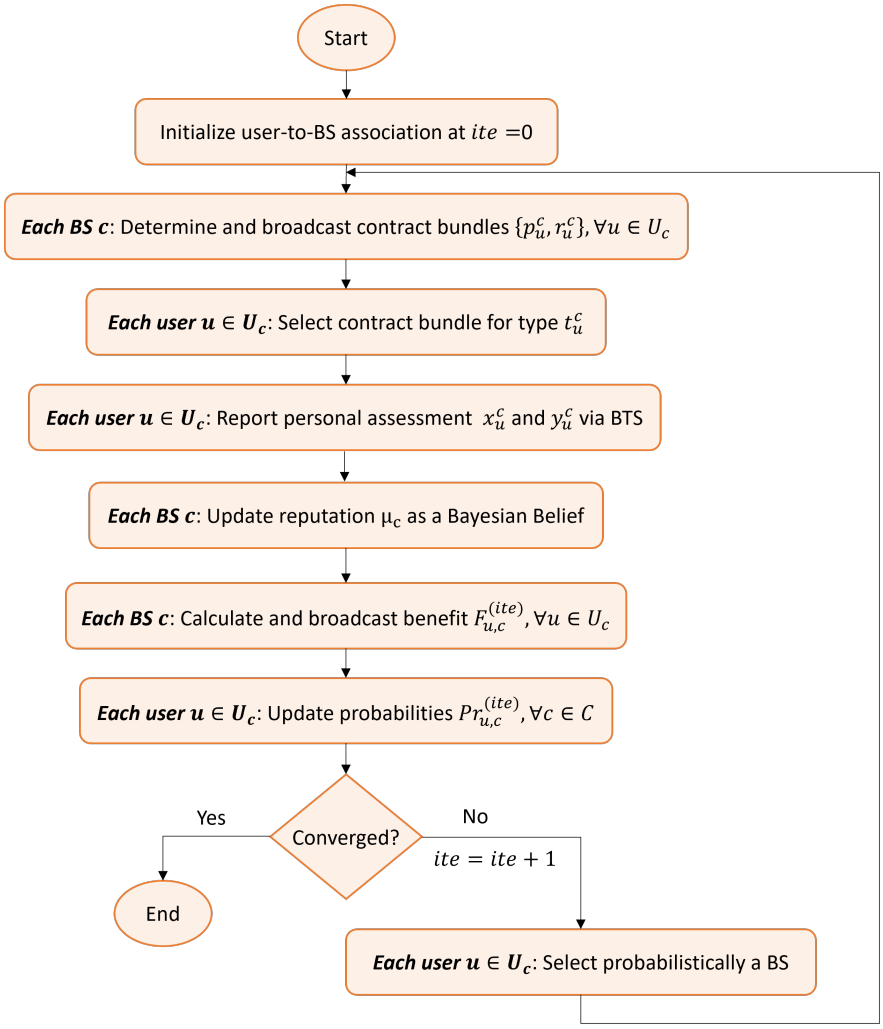

Figure 3.2: Unified user-to-BS and resource management framework overview.

3.6.1 Users' Satisfaction-related Information Truthfulness based on Bayesian Truth Serum

Undoubtedly, the primary concern when designing resource allocation mechanisms for 5G networks, is to enhance users' perceived satisfaction. Aligning with the user-centric flavor of the overall resource orchestration procedure, we introduce an assessment phase, where the users report their personal assessment about the service provided by the BS that they are associated with, revealing in this way their corresponding perceived satisfaction. As a means of eliciting truthful assessments from the users in a vastly heterogeneous network, we adopt the method of Bayesian Truth Serum (BTS) [80]. The BTS method is strict Bayes-Nash incentive compatible for $|\mathbb{U}_c| \to \infty$ and allows us to extract a holistic objective evaluation from the users' subjective reviews when the ground truth is unknown.

In particular, each user $u \in \mathbb{U}_c$ provides an answer regarding a binary question, i.e., "Are you satisfied with the experienced data rate when served by BS c?", by filing two reports:

- The information report $\mathbf{x}_u^c = \left[x_{u,c}^{NO}, x_{u,c}^{YES}\right]$, which is the user's answer to the aforemen-

tioned question. It holds true that $\sum_{i\in\{NO,YES\}} x_{u,c}^i = 1$, where $x_{u,c}^i \in \{0,1\}, \forall i \in \{NO, YES\}$.

- The prediction report $\mathbf{y}_u^c = \left[y_{u,c}^{NO}, y_{u,c}^{YES}\right]$, where $y_{u,c}^{YES}$ corresponds to the prediction regarding the proportion of the users which answered YES, i.e., $x_{u,c}^{YES} = 1$, while $y_{u,c}^{NO}$ is the prediction regarding the users whose answer is NO, i.e., $x_{u,c}^{NO} = 1$. It holds true that $\sum_{i\in\{NO,YES\}} y_{u,c}^i = 1$, where $y_{u,c}^i \in [0,1], \forall i \in \{NO, YES\}$.

Afterwards, the population endorsement frequencies $\overline{x}_c^i$ and the geometric mean of the users' predictions $\overline{y}_c^i$ for each of the available answers $i \in \{NO, YES\}$ can be calculated by

$$\overline{x}_c^i = \frac{1}{|\mathbb{U}_c|} \cdot \sum_{u=1}^{|\mathbb{U}_c|} x_{u,c}^i, \tag{3.29}$$

and

$$\log\left(\overline{y}_c^i\right) = \frac{1}{|\mathbb{U}_c|} \cdot \sum_{u=1}^{|\mathbb{U}_c|} \log\left(y_{u,c}^i\right). \tag{3.30}$$

As a consequence, the BTS score $s_{BTS,u}^c(\mathbf{x}_u^c, \mathbf{y}_u^c)$ of each user u, which corresponds to the truthfulness of the user's committed answer, can be expressed by

$$s_{BTS,u}^c\left(\mathbf{x}_u^c, \mathbf{y}_u^c\right) = \sum_i x_{u,c}^i \cdot \log\left(\frac{\overline{x}_c^i}{\overline{y}_c^i}\right) + \alpha \cdot \sum_i \overline{x}_c^i \cdot \log\left(\frac{y_{u,c}^i}{\overline{x}_c^i}\right), \tag{3.31}$$

where the parameter $\alpha \in \mathbb{R}^+$ controls the effect of the prediction score in the total BTS score. The first part of Eq. (3.31) is known as the information score, while the second part is the prediction score of the users. Regarding the information score, it increases with respect to how surprisingly common an answer is, i.e., how much greater the population endorsement frequency $\overline{x}_c^i$ is compared to the $\overline{y}_c^i$. It is noteworthy to mention that the surprisingly common criterion is based on the Bayesian Reasoning principle, according to which a user is of the opinion that the rest of the population will eventually underestimate its personal opinion, and hence, the user reports a higher prediction for its answer to further support it [81]. This is in line with the Bayesian argument, which concludes the fact that a user's truthful opinion is more likely to be surprisingly common. The prediction score formulation is based on a penalty that is proportional to the Kullback-Leibler divergence between the actual population endorsement frequencies $\overline{x}_c^i$ of the answers and the corresponding user's predictions $y_{u,c}^i, \forall i \in \{NO, YES\}$ [82].

As a result, the optimal prediction score (i.e., the lowest penalty) is equal to 0, which is achieved when the user's prediction $y_{u,c}^i$ is equal to the real users' proportion $\overline{x}_c^i$ of the answer i, i.e., $log\left(\frac{y_{u,c}^i}{\overline{x}_c^i}\right) \overset{y_{u,c}^i = \overline{x}_c^i}{=} log(1) = 0$, also known as absolute accuracy. Thus, the average BTS score of each answer $i \in \{NO, YES\}$, can be written as

$$\overline{u}_c^i = \frac{1}{|\mathbb{U}_c| \cdot \overline{x}_c^i} \cdot \sum_{u=1}^{|\mathbb{U}_c|} x_{u,c}^i \cdot s_{BTS,u}^c(\mathbf{x}_u^c, \mathbf{y}_u^c). \tag{3.32}$$

The final holistic and most truthful answer $x_{BTS,c}$ regarding the satisfaction of the users belonging to the set $\mathbb{U}_c$ and served by the BS c, is the one with the highest average BTS score, as follows

$$x_{BTS,c} = \underset{i\in\{NO,YES\}}{\arg\max}\ \overline{u}_c^i. \tag{3.33}$$

3.6.2 BSs' Reputation as a Bayesian Belief

After acquiring the users' personal assessment for a given BS association via the BTS method described in Section 3.6.1, we can eventually extrapolate the long-term social characteristics of the network, in terms of the users' perceived satisfaction, over several iterations of the user-to-BS association procedure. In our setting, to formulate the network's social characteristics we utilize the reputation μ_c for each BS c, which is a Bayesian model featuring adverse selection based on Bayesian updating of belief [83]. We assume that all users associated with a certain BS share the same prior belief distribution $\mu_{c,0} = \mu_0, \forall c \in C$, regarding the potential satisfaction that they might receive by getting associated with BS c. We consider that every BS c can offer either a satisfying or dissatisfying data rate with probabilities a_H and a_L, respectively, where it holds that $0 < a_L < a_H < 1$. After the BTS evaluation takes place (Section 3.6.1), an up-vote or down-vote $\forall c \in C$ occurs, creating a history for every BS throughout the time horizon. We introduce S_c and F_c to indicate the number of times that BS c satisfied ($x_{BTS,c} = YES$) and dissatisfied ($x_{BTS,c} = NO$) the users being associated with it, correspondingly, up to the present time instance. Thus, each BS's c posterior belief distribution can be expressed as follows:

$$\mu_c = \frac{\mu_0 \cdot a_H^{(S_c)} \cdot (1 - a_H)^{(F_c)}}{\mu_0 \cdot a_H^{(S_c)} \cdot (1 - a_H)^{(F_c)} + (1 - \mu_0) \cdot a_L^{(S_c)} \cdot (1 - a_L)^{(F_c)}}. \tag{3.34}$$

To prevent situations, where large S_c and F_c exponents lead to unrepresentable numbers, the S_c and F_c counters are updated with a step equal to 0.5, each time a user is satisfied or dissatisfied, respectively.

By observing Eq. (3.34), we deduce that the reputation μ_c is correlated with the BS's c history of the users' BTS evaluations, i.e., S_c and F_c, since it increases when the former increases and decreases when the latter increases.

3.6.3 Reinforcement Learning-enabled User-to-BS Association

In this section, we adduce the reinforcement learning approach based on the Stochastic Learning Automata (SLA) model [84], according to which each user selects the most beneficial BS to be associated with in a distributed and autonomous manner.

Inherently, the users within the considered wireless environment aim at minimizing their communication delay and, thus, exhibit a preference towards associating with a BS in their proximity. Furthermore, in our proposed solution, the users' association preference is affected by the BSs' bandwidth and reputation, leaning towards a resource-conscious utilization of BS's available frequency resources, by preventing the drawing of excessive network traffic. Considering a user-to-BS association at a specific iteration ite of the SLA algorithm, each BS c within the network determines a vector of personalized feedback signals $\boldsymbol{\mathcal{F}}_c^{(ite)} = \left[\mathcal{F}_1^{c,(ite)}, \ldots, \mathcal{F}_{|\mathbb{U}_c|}^{c,(ite)}\right]$ for each serving user u, and broadcasts them to the respective user devices. Naturally, the users' personalized feedback signals reflect their benefit from communicating with the specific BS c and are given by

$$\mathcal{F}_u^{c,(ite)} = \frac{\mu_c \cdot B_c / \sum\limits_{c=1}^{|C|} B_c}{d_u^c / \sum\limits_{u=1}^{|\mathbb{U}_c|} d_u^c}, \tag{3.35}$$

where μ_c is the BS's long-term reputation over the preceding SLA iterations, while $B_c / \sum_{c=1}^{|C|} B_c$ and $d_u^c / \sum_{u=1}^{|\mathbb{U}_c|} d_u^c$ correspond to the normalized BS's available bandwidth and user's distance

from the BS, respectively. Each user's personalized feedback signal in Eq. (3.35) is further normalized as $\hat{\mathcal{F}}_u^{c,(ite)} = \left(\mathcal{F}_u^{c,(ite)} / \sum_{u=1}^{|\mathbb{U}_c|} \mathcal{F}_u^{c,(ite)} \right)^{1/4}$, such that $\hat{\mathcal{F}}_u^{c,(ite)} \in [0,1]$.

After each BS in the network broadcasts the users' normalized feedback signals, each user u acts as a stochastic learning automaton and updates its personal action probabilities vector $\mathbf{Pr}_u^{(ite)} = \left[Pr_u^{1,(ite)}, \ldots, Pr_u^{|C|,(ite)} \right]$ at the end of iteration ite. Specifically, for a user u associated with a BS $c \in C$ at iteration ite, the probability of selecting the same BS c in the subsequent iteration $ite+1$ is defined as

$$Pr_u^{c,(ite+1)} = Pr_u^{c,(ite)} + b \cdot \hat{\mathcal{F}}_u^{c,(ite)} \cdot \left(1 - Pr_u^{c,(ite)}\right), \tag{3.36}$$

while the probability of selecting a different BS $c' \in C, c' \neq c$ at the next iteration is determined by

$$Pr_u^{c',(ite+1)} = Pr_u^{c',(ite)} - b \cdot \hat{\mathcal{F}}_u^{c,(ite)} \cdot Pr_u^{c',(ite)}, \tag{3.37}$$

where $0 < b \leq 1$ is the SLA algorithm's learning rate.

The users' update of their action probabilities concludes the overall resource orchestration procedure along one iteration of the proposed algorithm, initiating the subsequent algorithm's iteration with their updated BS selections, as demonstrated in Fig. 3.2. Throughout the time horizon, this iterative procedure enables the users to converge to the most beneficial selection of BS, as dictated by their normalized feedback signal. The optimization policy of the proposed reinforcement learning mechanism aims to optimize the long-term normalized personalized feedback received by each user, converging to a beneficial user-to-BS association, which is beneficial from the users' perspective. The convergence of the SLA algorithm is achieved when for all users $u \in U$ there is at least one action probability such that $Pr_u^{c,(ite+1)} \geq \varepsilon$, $\varepsilon \to 1$ [85, 86]. The complete process and operation of the proposed unified user association and power allocation scheme is summarized in Algorithm 3.1.

3.6.4 Complexity Analysis

First, to analyze the complexity of Algorithm 3.1, we investigate the contract-theoretic power allocation mechanism that is encapsulated in the overall user-to-BS association procedure. For a given iteration of the SLA algorithm, where all users in the network are associated with a prospective BS, the fully distributed optimization problem **P2**, presented in Section 3.5.3, is executed by each BS. Hence, in our complexity analysis, we presume that the contract-theoretic power allocation is performed in parallel by all BSs of the system.

The optimization problem **P2** can be solved via well-known existing methods for solving constrained non-linear optimization problems, and accordingly, obtain the optimal contracts under the incomplete information scenario. For demonstration purposes, we utilize the Sequential Quadratic Programming (SQP) method [87], along with the *fmincon()* [88] function implemented by the MATLAB Optimization Toolbox to return the constrained non-linear optimization problem's solution, the computational complexity of which is denoted as $\mathcal{O}(K)$ [89]. We also indicate as ITE the total number of the iterations required by the SLA algorithm to converge. Consequently, the SLA algorithm's complexity is calculated as: $\mathcal{O}\left(ITE \cdot (K + |U| + |U| \cdot |C|)\right)$, i.e., $\mathcal{O}\left(ITE \cdot (K + |U| \cdot |C|)\right)$, taking into account that the complexities of the BSs' selections and the users' action probabilities' updates at every SLA iteration are $\mathcal{O}(|U|)$ and $\mathcal{O}(|U| \cdot |C|)$, respectively. Finally, because both the complexities of the Bayesian Truth Serum and the reputations' updates are $\mathcal{O}(|U|)$, and since the rest of the SLA algorithm includes only algebraic calculations (of $\mathcal{O}(1)$ complexity), the overall complexity of Algorithm 3.1 is obtained as: $\mathcal{O}\left(ITE \cdot (K + |U| \cdot |C|)\right)$.

Algorithm 3.1 Unified User Association and Power Allocation.

Initialize a_L, a_H, $\mu_{c,0}$, b and set $ite = 0$, $S_c = 0$, $F_c = 0$, $\forall c \in C$.
Initialize the action probabilities vector $\mathbf{Pr}_u^{(0)}$, $\forall u \in U$ with equal probabilities for the BSs, in the coverage area of which each user belongs, otherwise set $\Pr_u^{c,(0)} = 0$.
repeat
  for $u = 1$ to $|U|$ **do**
    Choose a BS to associate with based on the action probabilities vector $\mathbf{Pr}_u^{(ite)}$.
  end for
  for $c = 1$ to $|C|$ **do**
    Sort the user types in ascending order.
    Obtain the optimal contract bundles by solving **P2**.
    Broadcast the optimal contract bundles to all associated users $u \in \mathbb{U}_c$.
    for $u = 1$ to $|\mathbb{U}_c|$ **do**
      Select the contract designed for its type.
      Execute the contract and transmit the data with uplink transmission power p_u^{c*}.
      Evaluate the achieved data rate R_u^c by broadcasting $\mathbf{x}_u^c$ and $\mathbf{y}_u^c$ reports to BS c.
    end for
    Calculate the holistic answer $x_{BTS,c}$ regarding the serving users' satisfaction based on Eq. (3.33).
    Update the counters S_c and F_c based on $x_{BTS,c}$, and thereafter, update the reputation μ_c based on Eq. (3.34).
    Calculate users' feedback signals $\boldsymbol{\mathcal{F}}_c^{(ite)}$ as in Eq. (3.35).
    Broadcast the users' normalized feedback signals vector $\hat{\boldsymbol{\mathcal{F}}}_{\boldsymbol{u}}^{\boldsymbol{c,(ite)}}$.
  end for
  for $u = 1$ to $|U|$ **do**
    Update the action probabilities vector $\mathbf{Pr}_u^{(ite+1)}$ based on Eq. (3.36) and Eq. (3.37).
  end for
until for all users $u \in U$ there is at least one action probability such that $Pr_u^{c,(ite+1)} \geq \varepsilon$, $\varepsilon \to 1$.

3.7 Performance Evaluation

In this section, the performance and effectiveness of the proposed unified user association and power allocation scheme is demonstrated by performing a detailed numerical evaluation, via modeling and simulation. First, in Section 3.7.1, we focus on validating the operation of the contract-theoretic mechanism in terms of the allocated optimal contract bundles and the obtained user and BS utilities. The specifics of the user-to-BS association procedure are further studied in Section 3.7.2, where we explore and analyze the characteristics that pertain to the operation of the pure autonomous user-to-BS association mechanism. Having verified and analyzed the pure performance of both the contract-theoretic power allocation and the RL and BTS-based user association in detail, Section 3.7.3 concludes our evaluation with some comparative results obtained from their seamless joint operation. In particular, a comparative analysis over different heuristic user-to-BS association mechanisms and under different spatial user distributions is provided, which demonstrates and explains the superiority of the proposed RL-enabled orchestration scheme in increased-density heterogeneous wireless deployments. For the latter, both uniform and non-uniform user distribution scenarios are evaluated over the network topology. The results of this work are also presented in [90].

Throughout our evaluation, we consider a densely deployed portion of a macrocell of

450-meter radius, consisting of one Macro BS (MBS) located in the center of the cell, as well as two Pico BSs (PBSs) and two Unmanned Aerial Vehicles (UAVs), serving as NFPs aiming at temporarily alleviating the excessive network traffic. The coverage radius of the PBSs and the UAVs is set to 300 m and 200 m, respectively. In that manner, the coverage areas of all BSs overlap with each other, forming the hybrid aerial-terrestrial communications environment that is graphically represented in Fig. 3.3. In the following, unless otherwise explicitly stated, we consider that the simulated network topology serves 50 users uniformly distributed with maximum uplink transmission power equal to 23 dBm. It should be noted that users associated with the same BS are further grouped and allocated different subchannels, following the work in [24], such that implementing the SIC technique is feasible. The specific simulation parameters are given in Table 3.1. Our setting is perfectly aligned with the heterogeneous system baseline simulation model defined by the Third-Generation Partnership Project (3GPP) in [91] and is further extended to account for UAV-assisted communications. We model the channel conditions of the ground-to-air links between the users and the UAVs according to the reference free-space path loss model, as proposed in [92]. Regarding the contract theory-related parameters, we consider that each BS c estimates its serving users' channel conditions, i.e., their types, following a uniform distribution, such that $\lambda_u^c = 1/|\mathbb{U}_c|$, $\forall c \in C$, $\forall u \in \mathbb{U}_c$. Each BS's c unit cost is set equal to $\mathcal{C} = 0.65$, while each user's $u \in U$ reward factor is $\rho = 100$. In the following results, for demonstration purposes, unless otherwise explicitly stated, the learning rate parameter of the SLA algorithm is set equal to $b = 0.7$. It is noted that the users and the UAVs remain stationary throughout a decision period, while the inclusion of the mobility aspect within the examined problem is part of our current and future work.

Table 3.1: Simulation Parameters.

Parameter	Value
MBS's bandwidth	1.8 MHz
PBSs' bandwidth	720 kHz
UAVs' bandwidth	360 kHz
MBS to user path loss	$128.1 + 37.6 \log_{10}(d[km])$ dB
PBS to user path loss	$140.7 + 36.7 \log_{10}(d[km])$ dB
UAV to user path loss	$92.45 + 20 \log_{10}(d[km])$ dB
Shadowing standard deviation	8 dB
AWGN power spectral density	-174 dBm/Hz
Users' max transmit power	23 dBm
Carrier frequency	2 GHz
UAVs' height	20 m

3.7.1 Contract-theoretic Mechanism Evaluation

In this section, the proper functioning and operation of the proposed contract-theoretic power allocation mechanism is examined under both complete and incomplete CSI scenarios. A complete execution of the unified user association and power allocation scheme is performed and the contract-theoretic results for the optimal user-to-BS association, where the algorithm converged, are obtained. In Fig. 3.4a-3.4e, we indicatively analyze and present the results of the contract-theoretic power allocation achieved for the MBS and its 16 associated users in total. Similar results and analysis are obtained for any BS of the considered wireless network topology.

The obtained optimal contract bundles are depicted in Fig. 3.4a-3.4b as a function of

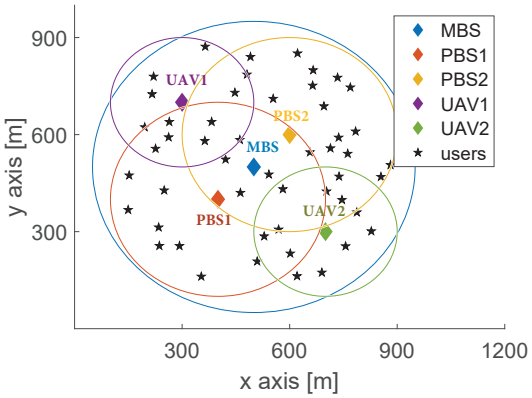

Figure 3.3: Wireless network simulation topology with uniform user distribution.

the user index, where a higher user index represents a higher type and, thus, channel gain user, considering the different users sorted in ascending order of their types/channel gains. Specifically, the user's invested transmission power (Fig. 3.4a) and the corresponding MBS's provided reward (Fig. 3.4b) are illustrated, under both cases of complete and incomplete CSI. Moreover, the MBS's attained utility U^u_{MBS} by each user's $u \in \mathbb{U}_{MBS}$ provided effort (i.e., uplink transmission power) and each user's utility U^{MBS}_u, when associated with the MBS, are presented in Fig. 3.4c and Fig. 3.4d, respectively. The results show that a user of a higher type, who experiences better channel conditions, transmits its data with higher power (Fig. 3.4a), maintaining the distinctness of the received signals by the MBS encouraged by power-domain NOMA. Thus, the MBS rewards the users of a higher type, with a higher reward (Fig. 3.4b), and consequently, those users achieve higher utility compared to users of a lower type (Fig. 3.4d). Apart from the increased users' achieved utility, MBS's utility is, also, increasing concerning the users' type (Fig. 3.4c).

Furthermore, comparing the results in Fig. 3.4a-3.4b between the scenarios of complete and incomplete CSI, it is inferred that the obtained contract bundles follow a similar behavior with respect to the users' types in both scenarios. Thus, the results verify the accuracy of the performed resource allocation in situations where there is the absence of complete CSI on the MBS's behalf. Nevertheless, the motivation behind the MBS's contract bundle allocation strategy along the different CSI scenarios, primarily differentiates the achieved users' and MBS's attained utilities, as revealed by the results in Fig. 3.4c-3.4d. Specifically, knowing a priori the users' types, the MBS fully exploits the users' effort to maximize its utility, providing them back with the minimum possible reward that marginally ensures the users' acceptance of the contract, i.e., the satisfaction of their rationality constraints. Consequently, based on Fig. 3.4c, the MBS's utility is higher under the complete CSI scenario, while at the same time, the utility achieved by all associated users is equal to zero (Fig. 3.4d).

To complement the evaluation of the contract feasibility under incomplete CSI, in Fig. 3.4e, the utilities of two selected users with indexes 5 and 10 are examined over each contract bundle designed by the MBS (represented in the horizontal axis by the user index) to showcase that the contract bundles are incentive compatible. The results confirm the IC condition satisfaction, in the sense that each user being part of the proposed contract-theoretic agreement is provided with adequate incentives to select the contract bundle designed for its type and experienced channel characteristics. By selecting the most appropriate contract for their type, the users on the one hand steer the power allocation procedure, while on

the other hand, they incidentally reveal their type and, thus, their CSI, contributing to the establishment of a common CSI knowledge with the MBS.

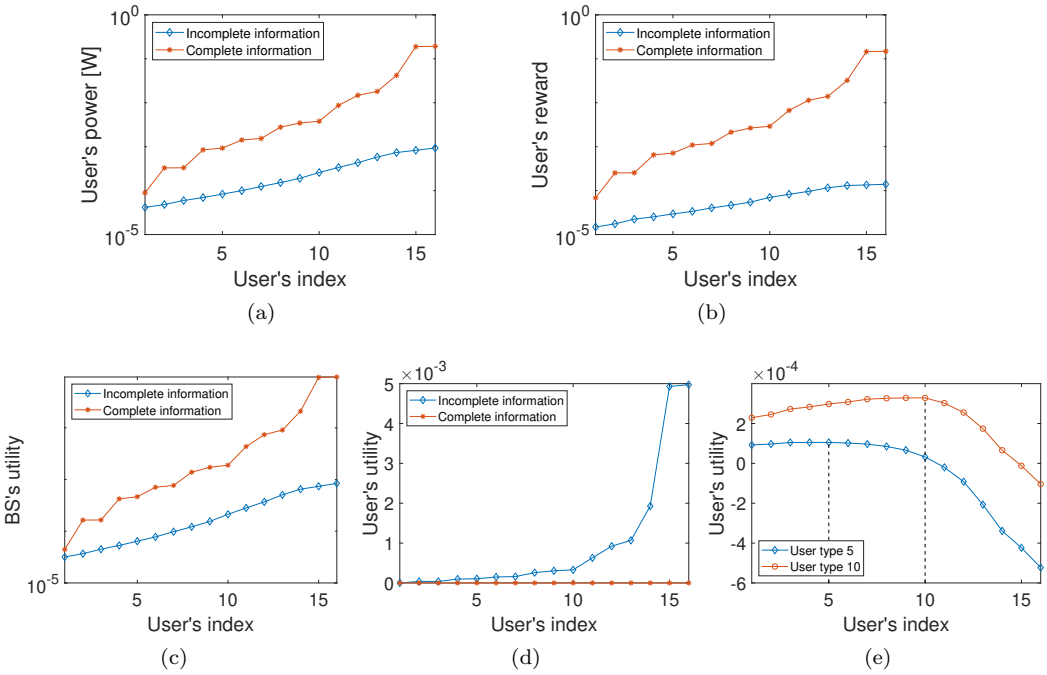

Figure 3.4: Pure contract-theoretic power allocation evaluation for MBS under complete and incomplete CSI scenarios.

3.7.2 User-to-BS Association Mechanism Evaluation

In this section, we aim to elucidate the operational characteristics of the pure autonomous user-to-BS association mechanism proposed. First, we target the evaluation of the RL-enabled association mechanism's external operation, i.e., its convergence behavior and achieved association outcome (Fig. 3.5a-3.5e). Afterward, we emphasize the internal features that guide the RL algorithm and thus, the users' behavior throughout the association process. In this regard, the impact of the users' satisfaction-related information elicitation via the BTS method on the overall association procedure is analyzed (Fig. 3.6a-3.6b). The results introduced for the rest of the Section 3.7 - unless otherwise explicitly stated - have been averaged over a number of 500 executions.

Initially, we study the convergence behavior of the proposed RL association mechanism based on the SLA algorithm. In Fig. 3.5a, the cumulative mean users' normalized feedback signal (Eq. (3.35)) is illustrated with respect to the SLA algorithm's iterations. The results reveal that after approximately 50 SLA iterations, the mean users' normalized feedback signal converges to its maximum value and, henceforth, the users persist in their BS association selection. Indeed, the convergence of the users' feedback signal directly implies the convergence of the users' personal action probabilities vector, determined by Eq. (3.36)-(3.37), which dictates the probability of selecting a specific BS. This observation is further verified by Fig. 3.5b, which demonstrates the action probabilities for one indicative user as a function of the SLA algorithm's iterations. Taking into consideration that the user under investigation is located within the coverage areas of the MBS, the PBS2, and the UAV2, an

equal number of approximately 50 SLA iterations is required for the user's action probabilities to converge. Eventually, the specific user's most beneficial BS association is the one, for which the user's action probability converges at 1, i.e., UAV2 in this case.

Concerning the overall RL-enabled association algorithm's speed of convergence, which actually refers to the speed of convergence of Algorithm 3.1, we conduct a Monte Carlo simulation over all possible values of the SLA algorithm's learning rate parameter $b \in [0.1, 0.9]$ and derive the resulting real execution time in [s], as well as the achieved mean users' normalized feedback signal (Fig. 3.5c). As the value of the learning rate parameter b decreases, the exploration of the possible user-to-BS association alternatives is becoming exhaustive. Consequently, the algorithm identifies user-to-BS associations that lead to improved user benefit, denoted by the increasing trend of the mean users' normalized feedback signal. Thus, the exploration of higher benefit user-to-BS associations is performed with the cost of increased real execution time. The learning rate parameter b can appropriately be controlled in realistic applications accounting for the tradeoff between the users' benefit and the time-critical decision-making.

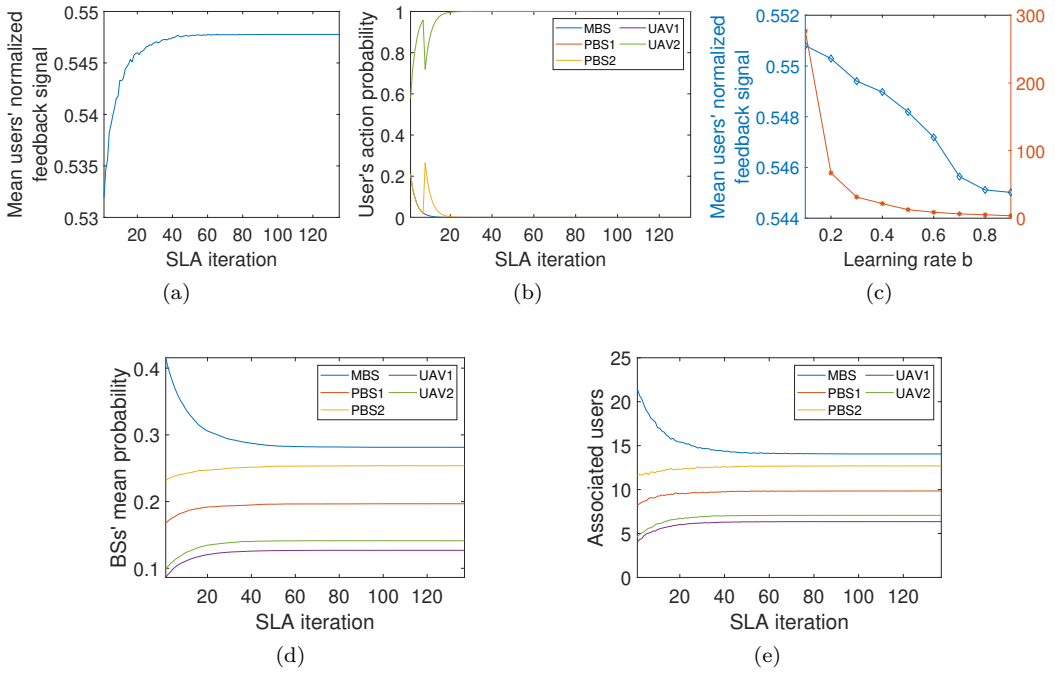

Figure 3.5: Pure reinforcement learning-enabled association mechanism's evaluation.

To gain more insight into the convergence behavior of the RL mechanism across the overall wireless network simulation topology, as presented in Fig. 3.3, we calculate the mean BSs' probabilities of being selected as a function of the SLA iterations (Fig. 3.5d). The corresponding results are next, correlated with the emerged total number of users associated with each BS versus the SLA iterations (Fig. 3.5e). Because the MBS provides complete coverage to the considered wireless network topology, the mean MBS's probability of being selected is higher compared to the rest of the BSs during the first SLA iterations. As a result, the total number of users associated with the MBS is, also, higher during the first SLA iterations. As the algorithm's execution evolves, part of the users that were initially assigned to the MBS are uniformly assigned to other BSs after assessing the tradeoff between

user-to-BS distance and BSs' bandwidth availability.

Targeting the interpretation of the RL-enabled association mechanism's internal features that steer such a user-to-BS association, we provide an analysis regarding the evolution of the BSs' reputation based on their history of users' BTS evaluations. Specifically, Fig. 3.6a presents the sum of users' BTS score for each BS (i.e., the sum of "YES" and "NO" answers) after the algorithm's convergence, which is captured by the counters S_c and F_c. Accordingly, Fig. 3.6b depicts each BS's reputation with respect to the SLA iterations. At this point, it should be recalled that for a total number of 120 SLA iterations, the sum BTS scores of "YES" and "NO" answers add up to 60, due to the S_c and F_c counters' increment with a step equal to 0.5. Following our analysis and focusing on the MBS, the dominance of its associated far-distanced users, whose achieved data rate is not satisfying enough, leads to an equal to zero "YES" BTS score (Fig. 3.6a), justifying the degradation of the MBS's reputation over the SLA iterations (Fig. 3.6b). On the contrary, the short-distanced users communicating with the PBSs, whose available bandwidth is adequate to provide them with a satisfying service, vote in favor of the PBSs, causing an increase in the reputation of the latter over the SLA iterations. However, this observation does not apply to the users served by the UAVs, mainly due to the restricted UAVs' available bandwidth.

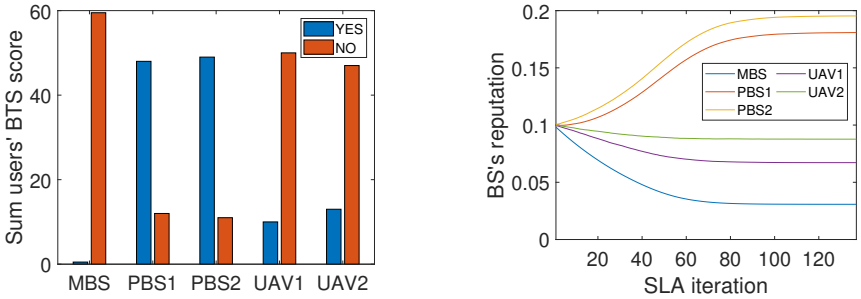

Figure 3.6: The impact of BSs' history of users' BTS evaluations on the evolution of BSs' reputation over the SLA iterations.

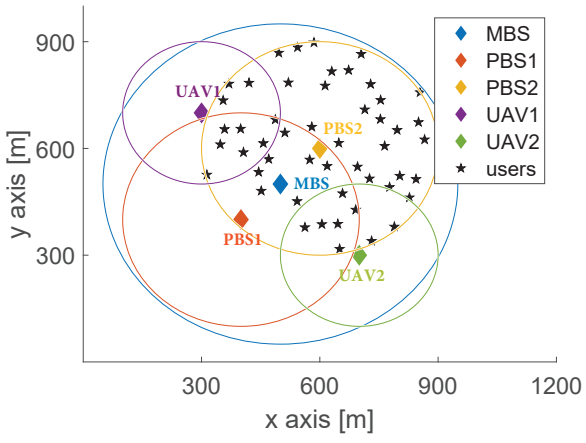

Figure 3.7: Wireless network simulation topology with non-uniform user distribution.

3.7.3 Comparative Evaluation

This section is devoted to demonstrating the effectiveness of the devised unified scheme towards the achieved users' fairness in the share of the available resources. Specifically, our proposed RL-based user-to-BS association mechanism is compared against other heuristic mechanisms, i.e., short-distance and random associations. Following the short-distance associations, the users are associated with the BS in their closest proximity, whereas based on the random association the users are randomly associated with a BS, given that they belong to its coverage area. After the association phase, for fairness in the comparison, the designed contract-theoretic power allocation is, also, applied to the derived short-distance and random user-to-BS associations. Apart from the different association mechanisms used for benchmarking purposes, we adduce an additional comparative analysis considering different spatial user distributions. The results presented encompass the cases of both uniform (Fig. 3.3) and non-uniform (Fig. 3.7) user distribution. Both wireless network deployments consist of the same number and type of BSs, as well as the same number of users.

Fig. 3.8a-3.8b present the resulting total number of associated users to each BS, as well as the sum of users' transmission power and achieved data rate per BS, after the application of each unified alternative scheme under the uniform user distribution case. Similar results are derived for the case of non-uniform user distribution in Fig. 3.9a-3.9b. A comparison between the resulting fairness in terms of the users' achieved data rates under each unified alternative scheme is introduced in Fig. 3.10a-3.10b. To evaluate the users' fairness, we consider the converged user-to-BS associations between the users $u \in U$ and BSs $c \in C$ and derive the system's overall fairness by applying the fairness criterion known as Jain's index [93], defined as follows

$$J = \frac{\left(\sum_{u=1}^{|U|} R_u^c\right)^2}{|U| \cdot \sum_{u=1}^{|U|} (R_u^c)^2}, \; J \in [0, 1]. \tag{3.38}$$

Nominally, Jain's index constitutes an independent scale criterion that measures how fair and even the performed share of throughput is in distributed computer systems. The higher the index, the fairer the resource allocation is. Hence, the maximum index value is obtained in the case when all users receive the same share of resources, which in our analysis corresponds to the equal share of the data rates.

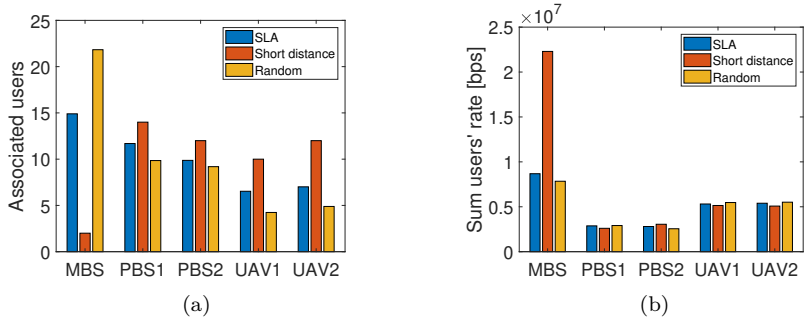

Figure 3.8: Comparative evaluation between SLA, short distance, and random association per BS, in terms of (a) total number of associated users and (b) sum of users' rates, under uniform users' distribution.

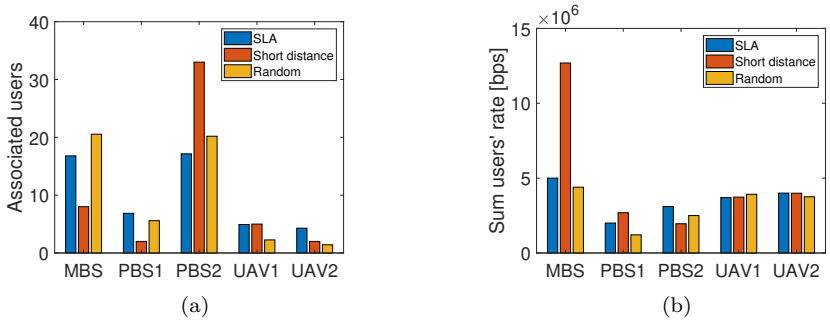

Figure 3.9: Comparative evaluation between SLA, short distance, and random association per BS, in terms of (a) total number of associated users and (b) sum of users' rates, under non-uniform users' distribution.

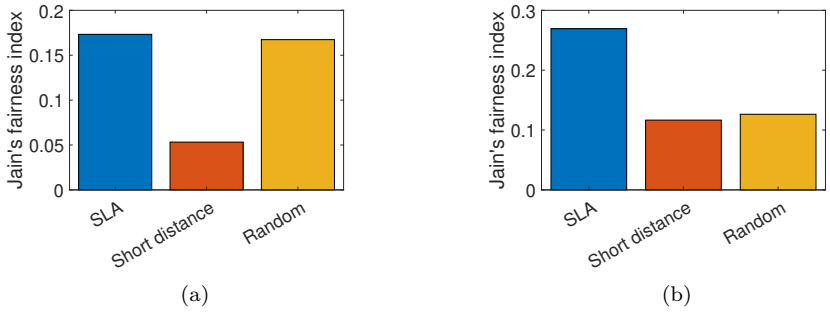

Figure 3.10: Comparative evaluation between SLA, short distance, and random association in terms of the overall achieved Jain's fairness index under (a) uniform users' distribution and (b) non-uniform users' distribution.

Considering the uniform user distribution case, there exists direct discrimination between the unified scheme employing short-distance compared to the SLA and random-based association mechanisms, stemming from the uneven user-to-BS association induced when applying short-distance (Fig. 3.8a). In more detail, due to the shortest intermediate distance between the users and the PBSs and UAVs, a significantly high number of users is ultimately served by the PBSs and UAVs, while an extremely low number of users is associated with the MBS. As a result, the low number of users served by the MBS achieves an extremely high data rate compared to the rest of the users served by the small BSs of restricted bandwidth resources (Fig. 3.8b) The unfair share in the users' data rate is further corroborated by the resulting Jain's fairness index, depicted in Fig. 3.10a. Indeed, the users' fairness when applying the short-distance association mechanism is very low, while the SLA-based and random-based unified schemes present similar behavior under the uniform user distribution.

Next, we examine the case of non-uniform user distribution (Fig. 3.7). Emphasizing the operation of the random-based unified scheme, we observe that there are no adequate incentives for the random association mechanism to uniformly associate the users with different BSs other than the PBS2 and MBS (Fig. 3.9a), in the proximity of which the majority of the users are located (as observed in Fig. 3.7). Hence, the remarkably high number of users associated with the PBS2 experience lower data rates compared to the rest of the users (Fig. 3.9b). Also, the large number of users associated with the MBS achieve low data rates,

which are balanced due to the high bandwidth availability that characterizes the MBS. This result is further confirmed by the obtained Jain's fairness index presented in Fig. 3.10b. The SLA-enabled user-to-BS association mechanism concludes with a more even and fair share of the users' achieved data rates, by uniformly associating them with different BSs. Also, the results reveal that the users' association with longer-distanced BSs from the users is performed with the cost of the increased sum of users' consumed powers (Fig. 3.9b).

Chapter 4

Resource Allocation in RIS-assisted NOMA Wireless Networks

4.1 General Setting

Taking one step further to the heterogeneity of the wireless network topology and, especially, placing our focus on UAV-assisted communications, several emerging technologies have been unveiled recently from the research community and the standardization bodies, leading to the latter's gradual maturity. A characteristic example of such a technology is the Integrated Access and Backhaul (IAB) network deployment [94]. This paradigm proposes that the Next Generation Node Bases (gNBs), referred to as IAB nodes , wirelessly relay the mobile traffic in a multi-hop manner to finally reach the IAB donor , which is connected to the core Internet with fiber infrastructure [95]. The principal idea behind the IAB paradigm is to efficiently utilize the 5G New Radio (NR) spectral resources across the fronthaul and backhaul network parts (including multiple intermediate hops), by utilizing advanced resource optimization and multiple access techniques. In this context, by increasing the UAV's (acting as an IAB node) degrees of freedom in terms of wireless service provisioning and its connectivity to the core network, the IAB network architecture is seen as one of the primary enablers of the vision of fully reconfigurable and energy-efficient wireless networks. Building upon the concept and potentials of the IAB networks, another technology that has lately received notable attention and is deeply related to the future wireless networks' attributes of reconfigurability and energy efficiency, is the Reconfigurable Intelligent Surface (RIS).

In this chapter, we capitalize on the joint benefits of IAB and RIS technologies, and we design and propose an end-to-end resource management framework, tailored to the converged RIS-aided and UAV-assisted network deployments. Such a converged network deployment is adapted to the future urban UAV-assisted communications, in which the wireless propagation environment can be appropriately controlled to account for different objectives, while the UAVs serve as an integral part of the network's infrastructure to provide end-to-end connectivity under adverse situations. In this context, we consider the uplink communications and treat the distinct objective of end-to-end energy efficiency maximization by jointly accounting for and controlling: a) the RIS elements' phase shifts, b) the bandwidth splitting among the fronthaul and backhaul network parts, c) the users' uplink transmission power to the UAV, and d) the UAV's uplink transmission power to the micro BS/core network.

To deal with this multivariable optimization problem in a distributed manner, we resort to the adoption of Game Theory and, especially, Stackelberg games, capturing the hierarchy between the users, UAV, and microcell, as imposed by the IAB network architectural deployment. Complementary to the above, and for better revealing the benefits and tradeoffs of the obtained solution when aiming at energy efficiency, we also analyze and evaluate the application of the proposed framework under a different optimization objective, namely the end-to-end data rate optimization.

4.2 Related Work

Although the paradigm of IAB deployment is still in its infancy, there exist research works in the literature that deal with timely resource allocation problems under the umbrella of IAB. In [96], a multi-hop IAB network that operates under the combination of Time (TDMA) and Frequency Division Multiple Access (FDMA) is considered to coordinate the transmissions along the different wireless links. The problem of subchannel and power allocation is formulated to maximize the sum system throughput, while insights regarding the optimal IAB node placement and user association are presented. Under a similar multi-IAB-node, though single-hop, network topology, the authors in [97] treat the problem of spectrum assignment to the different IAB nodes via a Deep Reinforcement Learning (DRL) approach while trying to maximize the sum users' throughput. Also, a joint traffic load balancing and interference mitigation optimization problem is introduced in [98], targeting the maximization of the overall network's capacity. The joint problem is organized into two sub-problems, which are iteratively solved following the successive convex approximation method.

Moving from the terrestrial network deployments to the promising inclusion of the UAVs within the concept of IAB, different challenges and considerations behind the idea of UAV-based communications in Millimeter Wave (mmWave) frequencies are discussed in [99], while investigating the effect of UAVs' and users' mobility to the network's performance. Other works that deal with backhaul-aware UAV-assisted networks can be found in [100, 101]. In the former, the joint problem of 3D UAV positioning, wireless backhaul sub-band assignment, and downlink transmission power allocation is formulated, such that the UAV's transmission power is minimized while accounting for the users' Quality of Service (QoS) prerequisites. On the other hand, the uplink communication is assumed in [101], and the joint user association, power, and bandwidth assignment are determined to maximize the sum system throughput. Targeting the interference mitigation at the access and backhaul links, the authors in [102] introduce a joint optimization problem of the users' association to the BSs, the downlink power allocation regarding the access and backhaul transmissions, and the UAV's deployment within the examined communications environment. Settings with multiple UAVs that belong to different providers and compete for service provisioning to multiple users are also considered, e.g., [103], further highlighting the heterogeneity of the emerging wireless networks and the usage of UAVs as temporary cellular infrastructure.

To further enhance the energy and spectral efficiency of 5G and beyond networks, significant attention has been paid to incorporating RIS technology under a plethora of different communication scenarios. Initial works, such as [104, 105, 106], focused on simple use cases and scrutinized the joint problems of power control and RIS elements' phase shift optimization. Both aforementioned works compared the performance gain incurred by the RIS considering different multiple access techniques, such as orthogonal and non-orthogonal, while targeting the users' power minimization and data rate maximization, respectively. Similar problems have been formulated for more complex setups, such as the Simultaneous Wireless Information and Power Transfer (SWIPT) case in [107] and the Multiple-Input Single-Output (MISO) NOMA network considered in [108]. In the latter work, the au-

thors addressed the sum users' data rate maximization problem under a combination of machine learning algorithms based on K-means Gaussian Mixture Model (K-GMM) and deep Q-Network (DQN) while optimizing the RIS's passive beamforming vector and the users' decoding order and power allocation, subject to their data rate prerequisites.

The majority of the relevant existing research works exclusively consider the downlink direction of the RIS-enabled communications, while only a few attempts have been made towards modeling and optimizing the wireless network's resources treating the uplink direction. Focusing on the uplink communication of a RIS-enabled wireless cellular network, the authors in [109] deal with the maximization problem of the sum rate of all users subject to their power constraints. In [110], a comparative study between OMA and NOMA RIS-enabled networks is presented, examining both the uplink and downlink communication for several fading characteristics of the communications environment. The authors conclude that the RIS-enabled network consistently achieves a high signal-to-noise ratio, while its increasing trend is not affected by the number of RIS elements and/or the fading parameters. Also, in [111], the tradeoff between the energy and spectral efficiency in the uplink communication is studied by jointly optimizing the users' transmit precoding and the RIS's reflective beamforming to maximize the resource efficiency.

Finally, the joint power of RIS and UAV-assisted communications has also been examined. In [112], the deployment of a RIS on the boundary of a UAV's serving area is considered, and the joint users' resource allocation and UAV's trajectory optimization are designed to take advantage of its existence. The authors in [113] introduce a machine learning approach to jointly determine the UAV's trajectory, the phase shifts of the RIS elements, the power allocation policy from the UAV to the users, and the dynamic decoding order, towards minimizing the overall system's energy consumption. The scenario of an RIS mounted on a UAV to maintain the Line-of-Sight (LoS) communication is studied in [114] and similarly, a joint resource allocation and UAV mobility problem is devised.

4.3 Contributions & Outline

Undoubtedly, the existing research has focused on different network optimization problems about the emerging technologies of UAVs, IAB, and RIS, and has identified their challenges and performance gains in a rather fragmented manner. To the best of our knowledge, there exists no work in the current literature that identifies the prospect of RIS and its added value in a backhaul-aware network optimization process, as the one revealed by the IAB paradigm. In this chapter, our objective is to address this issue and demonstrate the prospect of RIS in a UAV-assisted IAB network targeting its energy efficiency. In this way, we aim to introduce a dynamic, intelligent, and reconfigurable resource optimization framework, which jointly accounts for the access and backhaul resource optimization and operation towards ensuring end-to-end service provisioning for the users. Respecting the need for the design and deployment of decentralized resource management processes, we capitalize on the distributed nature of Game Theory models and, especially, Stackelberg games, and accordingly, we jointly treat the wireless propagation environment's adaptation and the network's resources' optimization under a low-complexity end-to-end framework. It is shown that RIS can provide significant improvements in terms of higher sum users' energy efficiency, driving the overall equilibrium and the UAV's performance at more energy-efficient points. The key contributions of this work are summarized as follows:

1. A system model capturing a RIS-aided and UAV-assisted IAB network is introduced, accounting for the communications established at the uplink of both the wireless access and wireless backhaul network parts (Section 4.4).

2. The problem of the IAB network's end-to-end resource management towards its energy efficiency optimization is formulated and treated via a distributed Stackelberg game-theoretic approach. The proposed approach comprises three stages, across which the following parameters are controlled and dynamically optimized: a) the RIS elements' phase shifts, b) the bandwidth splitting among the wireless access and backhaul network parts, and c) the users' and d) the UAV's uplink transmission powers (Section 4.5). The UAV, acting as leader, determines in the first stage the RIS elements' phase shifts that maximize the sum users' signal strength in the uplink, following a low-complexity heuristic approach (Section 4.5.2). Then, the UAV calculates the bandwidth splitting and its uplink transmission power to the IAB donor (Section 4.5.3). In the third stage, the users, i.e., the followers, optimize their uplink transmission powers to the UAV in a distributed manner (Section 4.5.4). The overall Stackelberg game-based algorithm is presented in Section 4.5.5.

3. The applicability and adaptation of the proposed resource management framework are also demonstrated for the treatment of the IAB network's end-to-end data rate optimization problem. The solution is obtained following a similar distributed Stackelberg game-theoretic approach with its energy efficiency-related counterpart (Section 4.6). This alternative optimization objective serves as the basis for highlighting the benefits and tradeoffs of the obtained solution when aiming at energy efficiency.

4. The overall network's performance is evaluated and extensive numerical results are presented that demonstrate the benefits introduced to both the users' and UAV's energy efficiency, by the joint exploitation of UAV, IAB, and RIS technologies (Section 4.7).

Notation Conventions: The notations used in the remainder of the chapter are listed as follows. The vectors and matrices are denoted by bold-face letters and are accompanied by their size. $\mathbb{C}^{X\times Y}$ represents the $X \times Y$ space of a complex-valued matrix. Given any matrix $\mathbf{G}$, $\mathbf{G}^T$ and $\mathbf{G}^H$ indicate the transpose and conjugate transpose of the general matrix $\mathbf{G}$, accordingly, while $G_{i,j}$ is the (i,j)-th element of the matrix. Given any vector $\mathbf{g}$, $diag(\mathbf{g})$ refers to the diagonal matrix, whose elements on the main diagonal are the elements of the vector $\mathbf{g}$. $\mathcal{CN}(\mu,\sigma^2)$ denotes the Circularly Symmetric Complex Gaussian (CSCG) distribution with mean μ and variance σ^2, and $\backsim$ stands for "distributed as". Considering a complex number g, $|g|$ denotes its absolute value and $\angle g$ its phase. Considering any function f, dom denotes the domain of the function f.

4.4 System Model

We consider the uplink communication of a RIS-aided and UAV-assisted two-tier IAB network, as illustrated in Fig. 4.1, consisting of $|N|$ users, with $N = \{1,\dots,n,\dots,|N|\}$ denoting their set, a UAV and a micro Base Station (mBS). The UAV, serving as an IAB node, collects the users' data in the first tier and the second tier and forwards this data to the mBS (i.e., the IAB donor) through the wireless backhaul. In this work, the position of the UAV is considered to be fixed throughout the operation of the resource management procedure. It should be noted that the problem of the UAV's trajectory optimization and its impact on resource management under different operation scenarios and requirements, though interesting and challenging by itself, is considered beyond the scope of this work and is part of our current and future research activities. All the involved transmitting/receiving entities, i.e., the users, the UAV, and the mBS, bear single-antenna transmitters and receivers. The IAB network operates in out-of-band mode, meaning that the wireless access and backhaul links use different frequency bands. Hence, the total system bandwidth W [Hz] is split into

two parts μW and $(1-\mu)W$ [Hz] to facilitate the wireless access and backhaul communications, respectively, where $\mu \in [0,1]$ is the corresponding bandwidth splitting ratio. The users' transmissions in the first tier are multiplexed using the combination of power-domain NOMA and SIC techniques.

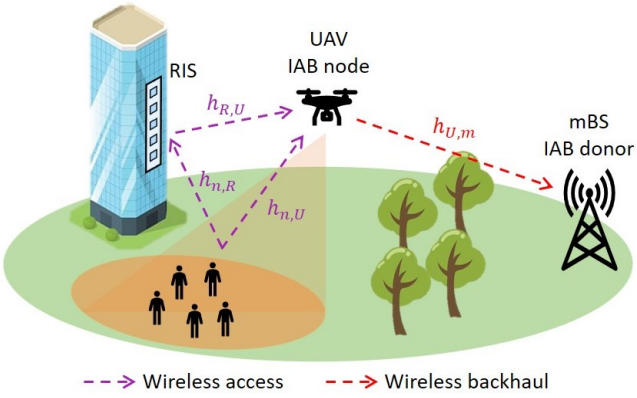

Figure 4.1: Overview of the RIS-aided and UAV-assisted Integrated Access and Backhaul (IAB) network.

4.4.1 Path Loss Model

In the considered IAB network, the path loss between any network entity and the UAV is stochastically determined to account for both the Line-of-Sight (LoS) and Non-LoS (NLoS) cases [101]. The probability that the wireless link between a network entity and the UAV is LoS derives from the function:

$$Pr^{LoS}(z_U, d) = \frac{1}{1 + \psi e^{-\beta(\theta - \psi)}}, \tag{4.1}$$

where $\theta = \frac{180}{\pi} sin^{-1}\left(\frac{z_U}{d}\right)$ [rad] is the elevation angle between the network entity and the UAV, with d [m] denoting their in-between Euclidean distance and z_U [m] representing the UAV's altitude. Also, $\psi, \beta \in \mathbb{R}^+$ are constants depending on the carrier frequency and the type of the communications environment, e.g., rural, urban, suburban. The path loss for the oLoS case between a network entity and the UAV is defined as a function of their in-between Euclidean distance d as:

$$PL^{LoS}(d) = \eta_{LoS}\left(\frac{4\pi f_c d}{c}\right)^{a_U}, \tag{4.2}$$

while the respective path loss model for the NLoS case is:

$$PL^{NLoS}(d) = \eta_{NLoS}\left(\frac{4\pi f_c d}{c}\right)^{a_U}, \tag{4.3}$$

where f_c [Hz] is the carrier frequency, c [m/s] is the speed of light, a_U is the path loss exponent and η_{LoS}, η_{NLoS} [dB] are the excessive path loss coefficients, such that $\eta_{NLoS} > \eta_{LoS} > 1$. The overall expected path loss is probabilistically given by:

$$\overline{PL}(z_U, d) = Pr^{LoS} PL^{LoS} + \left(1 - Pr^{LoS}\right) PL^{NLoS}. \tag{4.4}$$

Focusing on the first network tier, the prospect of RIS is scrutinized, and a Uniform Linear Array (ULA) consisting of a set of $M = \{1, \ldots, m, \ldots, |M|\}$ reflecting elements is

considered, placed at a height of z_R meters above the ground. For each reflecting element m of the RIS, we denote as $\omega_m \in [0, 2\pi)$ the phase shift of the reflection and we assume that no change in the amplitude of the incident signal is incurred, i.e., the amplitude of the reflection coefficient is equal to 1. The diagonal reflection matrix of the RIS elements is noted as $\mathbf{\Omega} = diag(e^{j\omega_1}, \ldots, e^{j\omega_{|M|}}) \in \mathbb{C}^{|M|\times|M|}$, while the first RIS element is used as a reference point for the performance of the subsequent calculations. The direct communication link between a user n and the UAV follows the probabilistic path loss modeling, such that $PL_{n,U} = \overline{PL}(z_U, d_{n,U})$, where $d_{n,U}$ [m] is the Euclidean distance between user n and the UAV. Thus, the corresponding channel gain coefficient $h_{n,U} \in \mathbb{C}$ is given as follows:

$$h_{n,U} = \sqrt{\frac{1}{PL_{n,U}}}\tilde{h}, \tag{4.5}$$

with $\tilde{h} \backsim \mathcal{CN}(0, 1)$ denoting the random scattering component captured by a zero-mean and unit-variance complex Gaussian random variable. The path loss between a user n and the RIS is $PL_{n,R} = \rho(d_{n,R})^{a_R}$, where ρ [dB] is the path loss at the reference distance 1m, $d_{n,R}$ [m] is the Euclidean distance between user n and the reference point of RIS and a_R is the path loss exponent [29]. Assuming that the RIS is in the users' proximity, the channel gain coefficient $\mathbf{h}_{n,R} \in \mathbb{C}^{|M|\times 1}$ between a user n and the RIS is:

$$\mathbf{h}_{n,R} = \sqrt{\frac{1}{PL_{n,R}}}\left[1, e^{-j\frac{2\pi}{\lambda}d_s\phi_{n,R}}, \ldots, e^{-j\frac{2\pi}{\lambda}(|M|-1)d_s\phi_{n,R}}\right]^T, \tag{4.6}$$

where λ [m] is the carrier wavelength, d_s [m] is the antenna separation and $\phi_{n,R}$ is the cosine of the angle of arrival of the user's signal to the RIS. The channel gain $\mathbf{h}_{R,U} \in \mathbb{C}^{|M|\times 1}$ of the RIS-to-UAV wireless link is modeled as:

$$\mathbf{h}_{R,U} = \sqrt{\frac{1}{PL_{R,U}}}\left(\sqrt{\frac{\kappa}{1+\kappa}}\mathbf{h}_{R,U}^{LoS} + \sqrt{\frac{1}{1+\kappa}}\mathbf{h}_{R,U}^{NLoS}\right), \tag{4.7}$$

where $PL_{R,U} = \overline{PL}(z_U - z_R, d_{R,U})$ is the link's path loss determined probabilistically and κ is the Rician factor. Also, $\mathbf{h}_{R,U}^{LoS} = \left[1, e^{-j\frac{2\pi}{\lambda}ds\phi_{R,U}}, \ldots, e^{-j\frac{2\pi}{\lambda}(|M|-1)ds\phi_{R,U}}\right]^T$ is the LoS component, with $\phi_{R,U}$ denoting the cosine of the angle of departure of the signal from the RIS to the UAV, and $\mathbf{h}_{R,U}^{NLoS} \backsim \mathcal{CN}(0, 1)$ is the NLoS component, which follows the complex Gaussian distribution. Subsequently, the total channel power gain between a user n and the UAV is given by:

$$G_n = \left|h_{n,U} + \mathbf{h}_{R,U}^H \mathbf{\Omega} \mathbf{h}_{n,R}\right|^2. \tag{4.8}$$

Concerning the second IAB network tier, the path loss of the wireless backhaul link between the UAV and the mBS follows the probabilistic model and is defined as $PL_{U,m} = \overline{PL}(z_U, d_{U,m})$, where $d_{U,m}$ [m] is the Euclidean distance between the UAV and the mBS. The channel gain coefficient $h_{U,m} \in \mathbb{C}$ between the UAV and the mBS is:

$$h_{U,m} = \sqrt{\frac{1}{PL_{U,m}}}\tilde{h'}, \tag{4.9}$$

with $\tilde{h'} \backsim \mathcal{CN}(0, 1)$ accounting for the random scattering, while the respective channel power gain is noted as:

$$G_U = \left|h_{U,m}\right|^2. \tag{4.10}$$

4.4.2 Communications Model

Focusing on the communication between the users and the UAV, the SIC technique is implemented at the UAV's receiver to decode the received signals. Without loss of generality, we assume that the users' total channel gains G_n are sorted as $G_1 \leq \cdots \leq G_n \leq \cdots \leq G_{|N|}$ and decoding starts from the highest channel gain user. Thus, a user's n achieved data rate through the wireless access R_n^{AC} is as follows:

$$R_n^{AC} = \mu W \log_2 \left(1 + \frac{G_n P_n}{\sum_{n'=1}^{n-1} G_{n'} P_{n'} + \mu W N_0}\right) [bps], \tag{4.11}$$

where P_n [W] denotes the uplink transmission power of user n, and N_0 [dBm/Hz] is the power spectral density of the zero-mean Additive White Gaussian Noise (AWGN).

Let P_U [W] indicate the UAV's transmission power for forwarding the users' data to the mBS, then the UAV's achieved data rate through the wireless backhaul R_U^{BH} is:

$$R_U^{BH} = (1-\mu) W \log_2 \left(1 + \frac{G_U P_U}{(1-\mu) W N_0}\right) [bps]. \tag{4.12}$$

From the cumulative UAV's achieved data rate R_U^{BH}, we adopt a proportionally fair approach and derive each user's n achieved data rate at the wireless backhaul R_n^{BH} as follows:

$$R_n^{BH} = \frac{R_n^{AC}}{\sum_{n=1}^{|N|} R_n^{AC}} R_U^{BH} [bps]. \tag{4.13}$$

Accordingly, the user's n end-to-end achieved data rate R_n^{E2E} is obtained by:

$$R_n^{E2E} = \min \left(R_n^{AC}, R_n^{BH}\right) [bps]. \tag{4.14}$$

4.5 End-to-End Energy Efficiency Optimization

4.5.1 Design for Reconfigurability and Efficiency

In the following, we elaborate on our proposed dynamic and reconfigurable resource management framework that targets the end-to-end energy efficiency optimization of the network topology under consideration. In particular, we seek to dynamically allocate the available spectrum and power resources in both the wireless access and wireless backhaul parts of the considered RIS-aided and UAV-assisted IAB network, while maximizing the overall IAB network's energy efficiency. Under this scope, the corresponding joint optimization problem is formulated, simultaneously accounting for and controlling: a) the RIS elements' phase shifts $\boldsymbol{\omega}$, b) the bandwidth splitting ratio parameter μ, c) the users' transmission power vector $\mathbf{P}$ to the UAV, and d) the UAV's transmission power P_U to the mBS. This joint optimization problem is formulated as a single-leader multiple-followers Stackelberg game and treated in three sequential stages. The UAV, acting as the leader, determines in the first stage the optimal RIS elements' phase shifts that enhance its overall received signal strength and broadcasts the appropriate control signals to the controller of the RIS. Then, in the second stage, the UAV calculates the bandwidth splitting ratio and its transmission power to the mBS that maximize its energy efficiency. The results of the second stage are fed back to the users, who are acting as the followers and determine in a distributed and autonomous manner their uplink transmission powers towards maximizing their energy efficiency. The second and third stages of the devised Stackelberg game are played iteratively to converge to the Stackelberg equilibrium. An overview of the proposed end-to-end resource management framework is illustrated in Fig. 4.2, in the form of a block diagram.

It is noted that in our introduced paradigm and resource management framework, the radio propagation environment, from simply being a passive exogenous entity, becomes a controllable and reconfigurable element with programmable properties, through the intelligent RIS's phase shifts' adaptation. In this way, the quality of the received signal strength is improved, combating the unfavorable propagation conditions due to the wireless channels' fading, while resulting in reduced transmission powers and interference. The inclusion of the RIS in the wireless environment provides an extra degree of freedom apart from the typical power and bandwidth control when seeking to maximize the end-to-end energy efficiency or data rate. Moreover, owing to the emergence of RISs and the advanced intelligent decision-making methods adopted, we treat the wireless environment and resources as part of the overall network design that can be adapted to satisfy specific system and user requirements in a dynamic manner (i.e., dynamic access and backhaul bandwidth splitting).

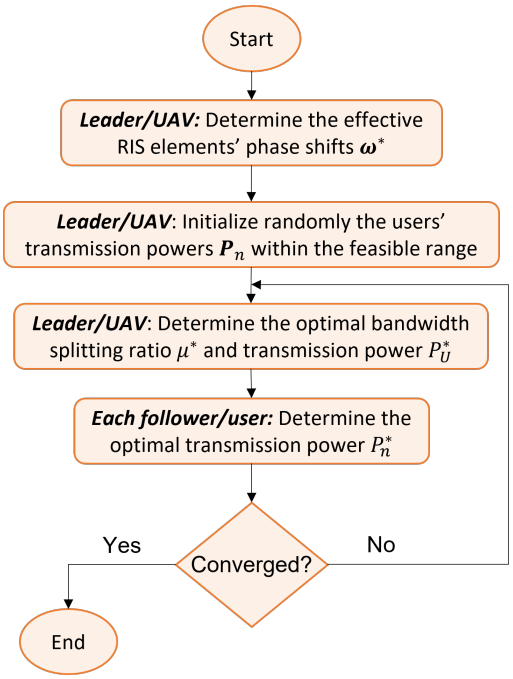

Figure 4.2: End-to-end resource management framework overview.

4.5.2 RIS Elements' Phase Shifts' Adaptation

As discussed earlier, the optimization of the wireless propagation environment, via the constructive beams created by reflection from the RIS, is used to assist and boost the network's resources' optimization procedure. To achieve this, the UAV determines the effective RIS elements' phase shifts $\boldsymbol{\omega}^* = [\omega_1, \ldots, \omega_m, \ldots, \omega_{|M|}]$ that enhance its overall received signal strength, towards further supporting the system's energy efficiency optimization via the optimal bandwidth splitting ratio μ^* and its optimal transmission power P_U^* to the mBS. For the UAV to maximize the overall received signal strength, it suffices to find the effective RIS elements' phase shifts $\boldsymbol{\omega}^*$ that maximize the overall channel power gain of the users. Hence,

the UAV treats the following optimization problem:

$$\max_{\boldsymbol{\omega}} \quad \sum_{n=1}^{|N|} \left| h_{n,U} + \mathbf{h}_{R,U}^{H} \boldsymbol{\Omega} \mathbf{h}_{n,R} \right|^2 \tag{4.15a}$$

$$\textbf{s.t.} \quad 0 \leq \omega_m < 2\pi, \forall m \in M. \tag{4.15b}$$

To easier handle the problem in Eq. (4.15a)-(4.15b), we denote as $v_m = e^{j\omega_m}, \forall m \in M$ and define the corresponding reflection-coefficient vector $\mathbf{v} = [v_1, \ldots, v_m, \ldots, v_{|M|}]$. Then, by substituting $\hat{\mathbf{h}}_{n,R}^{H} = \mathbf{h}_{R,U}^{H} diag(\mathbf{h}_{n,R}) \in \mathbb{C}^{1\times|M|}$, the problem in Eq. (4.15a)-(4.15b) is equivalently rewritten as:

$$\max_{\boldsymbol{v}} \quad \sum_{n=1}^{|N|} \left| h_{n,U} + \hat{\mathbf{h}}_{n,R}^{H} \mathbf{v} \right|^2 \tag{4.16a}$$

$$\textbf{s.t.} \quad |v_m| = 1, \forall m \in M, \tag{4.16b}$$

where Eq. (4.16b) is the unit-modulus equivalent constraint to the one expressed in Eq. (4.15b). Eq. (4.16a) is a non-concave function concerning the vector $\mathbf{v}$ and the unit-modulus constraint in Eq. (4.16b) defines, also, a non-convex set. Thus, the optimization problem in Eq. (4.16a)-(4.16b) is generally non-concave and there exists no standard method to derive a globally optimal solution [29, 115]. For this reason, we adopt an effective and low-complexity heuristic approach [104], as presented in the sequel.

Consider the case when a single user, denoted by $n = 1$, exists in the system. Then, it generally holds that this user's channel power gain is maximized when its signals arriving from different paths at the receiver of the UAV, i.e., the direct signal and the signal created by reflection from the RIS, are perfectly aligned and coherently combined [35, 104]. This happens when the phase shifts of the direct and the reflected signals are equal, such as:

$$\angle h_{1,U} = -\angle \hat{\mathbf{h}}_{1,R} + \angle \mathbf{v} \Leftrightarrow \angle \mathbf{v} = \angle h_{1,U} + \angle \hat{\mathbf{h}}_{1,R}, \tag{4.17}$$

concluding to the optimal $1 \times |M|$ phase-shift vector $\boldsymbol{\omega}^* = \angle \mathbf{v}$ for the single-user system.

As a logical consequence of Eq. (4.17), in the multiple-user case, there exists a different reflection-coefficient vector $\mathbf{v}_n = [v_{n,1}, \ldots, v_{n,m}, \ldots, v_{n,|M|}]$ for each user n that maximizes each individual user's n channel power gain, which is given by:

$$\mathbf{v}_n = e^{j\angle h_{n,U}} e^{j\angle \hat{\mathbf{h}}_{n,R}}, \forall n \in N. \tag{4.18}$$

Apparently, the reflection-coefficient vectors $\mathbf{v}_n$ of different users differ from each other, which suggests that there does not exist a single reflection-coefficient vector $\mathbf{v}$ maximizing all users' $|N|$ channel power gains concurrently.

Towards striking a balance between the different users' reflection-coefficient vectors $\mathbf{v}_n$ and obtaining a global solution for the RIS elements' phase shifts' adaptation problem, we introduce for each user n an appropriate weight factor $w_n \in [0, 1]$ and derive the linear combination of the overall users' reflection-coefficients $\mathbf{v}_n$ as follows:

$$\mathbf{v} = \sum_{n=1}^{|N|} w_n \mathbf{v}_n, \tag{4.19}$$

such that $\sum_{n=1}^{|N|} w_n = 1$ holds true.

Our ultimate objective is to determine the optimal value of the weight factor w_n of each term of the reflection-coefficient vector $\mathbf{v}$ in Eq. (4.19) that concludes to an increased

sum of the users' channel power gains, as imposed by Eq. (4.16a). Thus, the corresponding optimization problem to be addressed to derive an efficient and effective RIS elements' phase shifts' adaptation is formulated as:

$$\max_{\mathbf{w}} \sum_{n=1}^{|N|} |h_{n,U} + \mathbf{h}_{R,U}^{H} \mathbf{\Omega} \mathbf{h}_{n,R}|^2 \tag{4.20a}$$

$$\textbf{s.t.} \quad 0 \leq w_n \leq 1, \forall n \in N, \tag{4.20b}$$

$$\sum_{n=1}^{|N|} w_n = 1, \tag{4.20c}$$

where the reflection matrix $\mathbf{\Omega}$ is calculated with backward induction as $\mathbf{\Omega} = diag\left(e^{j\angle \mathbf{v}}\right)$. Also, $\mathbf{w} = [w_1, \ldots, w_n, \ldots, w_{|N|}]$ is the vector of the users' assigned weight factors. The optimization problem defined in Eq. (4.20a)-(4.20c) comprises a non-negative linear objective function and constraints, which can be optimized straightforwardly to conclude to the optimal weights $\mathbf{w}^*$.

The optimal weights' $\mathbf{w}^*$ derivation leads to a single and effective RIS elements' reflection-coefficient vector $\mathbf{v}^* = [v_1, \ldots, v_m, \ldots, v_{|M|}]$, and eventually determines the effective RIS elements' phase shifts $\boldsymbol{\omega}^* = [\omega_1, \ldots, \omega_m, \ldots, \omega_{|M|}]$.

4.5.3 Leader's Energy Efficiency Optimization

Following the RIS elements' phase-shift adaptation, the UAV playing the role of the leader, derives the optimal bandwidth splitting ratio μ^* and its optimal transmission power P_U^* to the mBS, given the users' uplink transmission power vector $\mathbf{P} = [P_1, \ldots, P_n, \ldots, P_{|N|}]$, towards maximizing its energy efficiency EE_U. The corresponding optimization problem, solved by the leader, is formulated as follows:

$$\max_{\mu, P_U} \quad EE_U(\mu, P_U) = \frac{\sum_{n=1}^{|N|} R_n^{AC} + R_U^{BH}}{P_U} \tag{4.21a}$$

$$\textbf{s.t.} \quad 0 \leq \mu \leq 1, \tag{4.21b}$$

$$P_U \leq P_U^{max}, \tag{4.21c}$$

$$R_n^{E2E} \geq R_{min}, \forall n \in N. \tag{4.21d}$$

Having the ability to control the network parameters that pertain to both the access and the backhaul network parts, the UAV pursues the maximization of the total achieved data rates at the access and the backhaul network (Eq. (4.21a)), while trying to minimize its transmission power to the mBS. Eq. (4.21b) refers to the feasible range of values of the bandwidth splitting ratio parameter μ. Also, Eq. (4.21c) guarantees that the UAV's optimal transmission power to the mBS does not exceed the UAV's maximum power budget P_U^{max}, while Eq. (4.21d) reassures that the optimal bandwidth splitting ratio satisfies the users' end-to-end achieved data rate QoS requirement R_{min}.

The outcome of the optimization problem described in Eq. (4.21a)-(4.21d) is the optimal bandwidth splitting ratio μ^* and the UAV's optimal transmission power P_U^* to the mBS. To establish the existence of an optimal solution (μ^*, P_U^*) for the specific problem, we observe that the numerator of $EE_U(\mu, P_U)$ consists of two terms, i.e., $\sum_{n=1}^{|N|} R_n^{AC}$ and R_U^{BH}. However, based on Eq. (4.11) and Eq. (4.12) and by calculating their derivatives with respect to the bandwidth splitting ratio parameter μ, it is concluded that the numerator of $EE_U(\mu, P_U)$ in Eq. (4.21a) is not always a concave function on μ, complicating twice the derivation of an optimal solution for the two-variable optimization problem in Eq. (4.21a)-(4.21d) [116].

To address this problem and provide a tractable solution, we decompose the optimization problem presented in Eq. (4.21a)-(4.21d) into an exhaustive search of the optimal value of μ over its strategy space, and an optimization problem concerning the optimal value of P_U. The optimization problem in Eq. (4.21a)-(4.21d) is solved with respect to P_U over different values of the parameter μ and ultimately, the values of μ and P_U that yield the maximum energy efficiency, based on Eq. (4.21a), are selected to serve as the optimal solution (μ^*, P_U^*). For all practical purposes, the partitioning of the bandwidth is typically performed into a finite discrete region (i.e., resource blocks or slices of predefined sizes), and therefore the μ takes discrete values in a finite strategy space. Thus, for demonstration purposes, we can consider some indicative discrete values of μ, e.g., $\mu = 0.05, 0.1, 0.15, \ldots, 0.95$, and determine the corresponding optimal values of P_U^*, as follows.

Lemma 4.1. *The energy efficiency function EE_U in Eq. (4.21a) is strictly quasi-concave with respect to P_U.*

Proof. As defined in [117], a function $f : \mathbb{R}^n \to \mathbb{R}$ is strictly quasi-concave if its sublevel set $S_a = \{\mathbf{x} | \mathbf{x} \in dom f, f(\mathbf{x}) \geq a\}$ is strictly convex for every a, where $\mathbf{x}$ is the corresponding vector of variables. Accordingly, the sublevel set S_a defined for the EE_U function in Eq. (4.21a) is:

$$S_a = \{P_U | P_U \in dom\, EE_U, \frac{g(P_U)}{P_U} \geq a\}, \tag{4.22}$$

where $g(P_U) = \sum_{n=1}^{|N|} R_n^{AC} + R_U^{BH}$ is the sum data rate function, for which it holds that it is strictly concave on P_U, since the term $\sum_{n=1}^{|N|} R_n^{AC}$ is independent of P_U, and the term R_U^{BH} is a concave function with respect to P_U. As a result, when $a \leq 0$, then S_a is obviously convex on P_U. In the case when $a > 0$, then the sublevel set in Eq. (4.22) is rewritten as:

$$S_a = \{P_U | P_U \in dom\, EE_U, aP_U - g(P_U) \leq 0\}. \tag{4.23}$$

Given that the sum rate function $g(P_U)$ is strictly concave with respect to P_U, it follows that $-g(P_U)$ is strictly convex on P_U, while the term aP_U increases linearly with P_U. As a result, the sublevel set S_a in Eq. (4.22) constitutes a strictly convex set. This completes the proof that the $EE_U(P_U)$ function is quasi-concave. □

Lemma 4.2. *The constraints in Eq. (4.21b)-(4.21d) form a compact, i.e., closed and bounded, and convex set.*

Proof. The constraint in Eq. (4.21b) generally forms a compact set, while for the rest of the constraints in Eq. (4.21c)-(4.21d) we consider the following functions:

$$\begin{aligned} s^{(1)} &= P_U - P_U^{max} \\ s_n^{(2)} &= R_{min} - R_n^{E2E}, \forall n \in N. \end{aligned} \tag{4.24}$$

It can be easily proved that the functions $s^{(1)}$ and $s_n^{(2)}, \forall n \in N$ are convex on P_U. Hence, their level sets, are defined generally as follows:

$$S_0 = \{\mathbf{x} | \mathbf{x} \in dom f, f(\mathbf{x}) = 0\}, \tag{4.25}$$

considering any function f and any vector of variables $\mathbf{x}$, are convex sets. This completes the proof. □

Based on Lemmas 4.1-4.2 and the preceding analysis, the optimization problem defined in Eq. (4.21a)-(4.21d) forms a quasi-concave program that belongs in the broader area of concave fractional programming and, thus, admits an optimal solution P_U^* [118]. The

solution can be obtained by appropriately transforming the quasi-concave problem into a series of concave problems via existing methods [117], and subsequently, by utilizing existing concave/convex optimization tools [88]. Overall, an effective, efficient, and well-established methodology is to employ Dinkelback's algorithm [119, 120].

4.5.4 Followers' Energy Efficiency Optimization

After the UAV reports back to the users the optimal bandwidth splitting ratio, the users' decision-making process takes place. Specifically, each user aims to distributively maximize its energy efficiency achieved at the access network part, by optimizing its uplink transmission power to the UAV. Hence, each user's n personal utility function is expressed as:

$$EE_n(P_n, \mathbf{P}_{-n}) = \frac{R_n^{AC}}{P_n}, \tag{4.26}$$

where $\mathbf{P}_{-n} = [P_1, \ldots, P_{n-1}, P_{n+1}, \ldots, P_{|N|}]$ is the vector of uplink transmission powers of all users except for user n. The interactions among the users are captured via a non-cooperative game $G = [N, \{A_n\}_{\forall n \in N}, \{EE_n\}_{\forall n \in N}]$, where N is the set of players, i.e., the users, $A_n = [0, P_n^{max}]$ is each user's strategy set, i.e., the set of feasible uplink transmission power levels, as indicated by the user's maximum power budget P_n^{max}, and EE_n is each user's payoff function, i.e., its energy efficiency. The non-cooperative game G is treated as a distributed utility maximization problem, in which each user n updates its uplink transmission power P_n selfishly, by having prior information about the rest of the users' transmission powers $\mathbf{P}_{-n}$ as broadcasted by the UAV, seeking to maximize its perceived satisfaction, i.e., its energy efficiency. The corresponding optimization problem that is solved by each user is formulated as:

$$\max_{P_n} \quad EE_n(P_n, \mathbf{P}_{-n}) = \frac{R_n^{AC}}{P_n}, \forall n \in N \tag{4.27a}$$

$$\textbf{s.t.} \quad P_n \leq P_n^{max}, \forall n \in N, \tag{4.27b}$$

$$G_n P_n - \sum_{n'=1}^{n-1} G_{n'} P_{n'} \geq P_{tol}, n = 2, \ldots, |N|, \tag{4.27c}$$

$$R_n^{AC} \geq R_{min}, \forall n \in N. \tag{4.27d}$$

Apart from the maximum power budget constraint that the user's uplink transmission power to the UAV should meet, as imposed by Eq. (4.27b), Eq. (4.27c)-(4.27d) denote the extra group of constraints that the users' n strategy P_n should satisfy. Eq. (4.27c) guarantees that the SIC technique is successfully performed at the UAV's receiver, according to the receiver's sensitivity/tolerance P_{tol}, while Eq. (4.27d) ensures the user's minimum acceptable data rate QoS requirement R_{min}.

Let us denote as Γ_n the strategy space of each user, formed by the inclusion of the extra set of constraints in Eq. (4.27c)-(4.27d), i.e., $\Gamma_n = \{(P_n)$ satisfies Eq. (4.27c)-(4.27d)$\}$. Then, each user's n overall feasible strategy space is reformulated as $\Delta_n = A_n \cap \Gamma_n, \forall n \in N$ and the non-cooperative game is restructured as $G = [N, \{\Delta_n\}_{\forall n \in N}, \{EE_n\}_{\forall n \in N}]$.

Towards solving the updated non-cooperative game G, the widely used concept of Nash equilibrium is adopted. The Nash equilibrium point is the users' strategy vector $\mathbf{P}^* = [P_1, \ldots, P_n, \ldots, P_{|N|}]$, from which no user has the incentive to deviate, given the strategies of the rest of the users.

To further accommodate our discussion regarding the existence of at least one Nash equilibrium point for the non-cooperative game G and, thus, the convergence of the users' strategies to the Nash equilibrium, we adopt the theory of the n-person generalized concave games [121].

Theorem 4.1. ***(Existence of Nash Equilibrium)*** *The non-cooperative game G is a n-person generalized concave game and admits at least one Nash equilibrium point if the following conditions hold [121]:*

1. *the strategy sets $\Delta_1, \ldots, \Delta_{|N|}$ are non-empty, compact, convex subsets of finite dimensional Euclidean spaces,*
2. *all payoff functions $EE_1, \ldots, EE_{|N|}$ are continuous on $\Delta = \Delta_1 \times \cdots \times \Delta_{|N|}$,*
3. *every payoff EE_n is a quasi-concave function of P_n over Δ_n if all the other strategies are held fixed.*

Proof. The Theorem 4.1 is proved by exploiting the content of Lemmas 4.1-4.2 introduced in Section 4.5.3, properly adapted to suit the energy efficiency function in Eq. (4.27a) and the constraints defined in Eq. (4.27b)-(4.27d). Condition 1 of Theorem 4.1 holds following a similar procedure to Lemma 4.2. Condition 2 holds given that the energy efficiency function is continuous on the users' strategy space Δ. Last, condition 3 holds following the analysis presented in Lemma 4.1, verifying that the energy efficiency function in Eq. (4.27a) is strictly quasi-concave. Therefore, the non-cooperative game G is a n-person generalized concave game and at least one Nash equilibrium point exists. □

The convergence of the users' strategies to the Nash equilibrium point is achieved by implementing a Best Response Dynamics algorithm [122], as shown in Algorithm 4.1. At each iteration of the Best Response Dynamics algorithm, the quasi-concave optimization problem defined in Eq. (4.27a)-(4.27d) for each user is equivalently transformed and treated as a series of convex optimization problems via the Dinkelbach's algorithm , following the procedure described earlier in Section 4.5.3.

4.5.5 Stackelberg Game-based Optimization Process

After the convergence of the users' strategies, their optimal uplink transmission powers $\mathbf{P}^*$, are fed back to the UAV to establish the next iteration of the Stackelberg game. In other words, the optimization problem in Eq. (4.21a)-(4.21d) and the non-cooperative game among the users are iteratively solved and the output of the one acts as input to the other, complying with the relationship between the leader and the followers. This iterative procedure results to the Stackelberg equilibrium $(\mu^*, P_U^*, \mathbf{P}^*)$ that concludes the preceding mathematical analysis in Sections 4.5.3 and 4.5.4.

The complete Stackelberg game-based optimization process and operation of the proposed dynamic resource management framework are summarized in Algorithm 4.1. Note that the superscript (i) is used to dictate the value of each variable after the i-th iteration of the leader's and followers' optimization stages, which are iteratively updated until convergence is reached, whereas the superscript (j) is used to indicate the iterations required for the nested non-cooperative game that is played among the users.

To calculate the computational complexity of the Stackelberg game-based optimization process presented in Algorithm 4.1, the following algorithmic complexities should be first considered alone. The complexity of the optimization problem in Eq. (4.20a)-(4.20c) can be regarded as $\mathcal{O}(M^x)$, where $1 \leq x \leq 4$, by employing an interior-point algorithm intended for linear programming [123]. The sorting of the users according to their channel power gain can be performed with complexity $\mathcal{O}(N^2)$ via the well-known Quicksort algorithm [124], while the search within the set $\mathcal{S}$ is of $\mathcal{O}(\log(K))$ complexity when using the Binary Search algorithm [124], where K denotes the number of bandwidth splitting ratio values tested (i.e., $K = 19$). Concerning the Dinkelbach's algorithm, it is known to have a super-linear convergence rate [119, 120], while the asymptotic complexity of each convex optimization

problem addressed at each iteration of the Dinkelbach's algorithm is polynomial in the number of optimization variables [111, 32]. Hence, our resulting single-variable problems have computational complexity equal to $\mathcal{O}(1)$. The remainder of the typical mathematical manipulations are of $\mathcal{O}(1)$ complexity and are omitted, while we also assume that the distributed non-cooperative game among the users is performed in parallel.

For representation purposes and following commonly used methodologies, let I_D^U and I_D^n denote the number of Dinkelbach's algorithm's iterations required to solve the UAV's and each user's n optimization problems in Eq. (4.21a)-(4.21d) and Eq. (4.27a)-(4.27d), respectively. Also, we indicate as I and J the total number of iterations required for the Stackelberg and the nested non-cooperative game to converge, accordingly. Consequently, the overall computational complexity of Algorithm 4.1 is equal to $\mathcal{O}\left(M^x + N^2 + I \cdot (K \cdot I_D^U \cdot 1 + log(K) + J \cdot I_D^n \cdot 1)\right)$. Indicative numerical results regarding the actual number of required Stackelberg game iterations, as well as the real execution time needed to converge to the Stackelberg equilibrium, are presented in Section 4.7, below.

Algorithm 4.1 Stackelberg game-based optimization process.

1: Initialize network simulation topology, including users', RIS's, UAV's, and mBS's locations.
2: Initialize ψ, β, η_{LoS}, η_{NLoS}, f_c, c, a_U, ρ, a_R, d_s, W, N_0, P_U^{max},P_n^{max}, P_{tol}, R_{min}.
3: Determine RIS elements' phase-shift adaptation by solving Eq. (4.20a)-(4.20c) and calculate $G_n, \forall n \in N$.
4: Sort users in ascending order according to G_n.
5: Initialize randomly $P_U \in [0, P_U^{max}]$.
6: Set $i = 0$.
7: **repeat**
8: Set $i = i + 1$.
9: **for** $\mu = 0.05 : 0.05 : 0.95$ **do**
10: Determine optimal uplink transmission power P_U^* by solving Eq. (4.21a)-(4.21d) with respect to P_U.
11: Add solution $\{(\mu, P_U^*), EE_U^*\}$ to $\mathcal{S}$.
12: **end for**
13: Select $\{(\mu^*, P_U^*), EE_U^*\}$ from $\mathcal{S}$, for which EE_U^* is the maximum in $\mathcal{S}$.
14: Set $\mu^{*(i)} = \mu^*$ and $P_U^{*(i)} = P_U^*$.
15: Initialize randomly $P_n \in \Delta_n, \forall n \in N$.
16: Set $j = 0$.
17: **repeat**
18: Set $j = j + 1$.
19: **for** $n \in N$ **do**
20: Determine optimal uplink transmission power $P_n^{*(j)}$ by solving Eq. (4.27a)-(4.27d).
21: **end for**
22: **until** $|P_n^{*(j)} - P_n^{*(j-1)}| \leq \epsilon, \forall n \in N$, where $\epsilon \approx 10^{-5}$.
23: **until** $|P_U^{*(i)} - P_U^{*(i-1)}| \leq \epsilon$, where $\epsilon \approx 10^{-5}$.

4.6 End-to-End Data Rate Optimization

In this section, we extend our proposed dynamic spectrum and power management framework, analyzed in detail in Section 4.5, to account for an alternative objective, namely the

end-to-end data rate optimization. On the one hand, we aim to corroborate the reconfigurability and adaptability of the devised resource optimization framework, under different optimization objectives, while revealing the benefits introduced by the proper manipulation of the wireless propagation environment. On the other hand, we seek to macroscopically identify and promote the significance of energy efficiency optimization.

Specifically, concerning the resource optimization framework design presented in Section 4.5, we subsequently introduce its counterpart towards maximizing the IAB network's end-to-end data rate. The joint optimization problem is formulated and solved in a distributed manner, following once again the principles of the Stackelberg games. Next, the three-stage optimization procedure adopted and explained in Fig. 4.2 is presented in a concise, though comprehensive manner, emphasizing the main differences arising from the different optimization objectives.

By the methodology followed in Section 4.5, the first stage of the dynamic resource management framework towards the end-to-end data rate optimization refers to the appropriate RIS elements' phase-shift adaptation by the UAV, which concludes with its increased received signal strength. The RIS elements' adaptation is performed following the proposed intelligent and low-complexity approach described in Section 4.5.2. Then, the second stage takes place and the UAV proceeds to the derivation of the optimal bandwidth splitting ratio and its transmission power to the mBS, which maximize the sum users' end-to-end data rate, given the users' uplink transmission powers. The corresponding optimization problem solved by the UAV is written as:

$$\max_{\mu, P_U} \quad \sum_{n=1}^{|N|} R_n^{E2E} \tag{4.28a}$$

$$\textbf{s.t.} \quad 0 \leq \mu \leq 1, \tag{4.28b}$$

$$P_U \leq P_U^{max}, \tag{4.28c}$$

$$R_n^{E2E} \geq R_{min}, \forall n \in N, \tag{4.28d}$$

where the constraints in Eq. (4.28b)-(4.28d) are in accordance with the ones introduced in the energy efficiency optimization problem counterpart. The problem defined in Eq. (4.28a)-(4.28d) is, once again, solved with respect to P_U under a range of values of the parameter μ, as discussed in Section 4.5.3. Thus, we derive the optimal solution (μ^*, P_U^*).

In the third stage, the users optimize in an autonomous and distributed manner their uplink transmission powers to the UAV, such that their data rate in the access network part is maximized. The optimization problem to be solved by each user is given by:

$$\max_{P_n} \quad R_n^{AC}(P_n, \mathbf{P}_{-n}), \forall n \in N \tag{4.29a}$$

$$\textbf{s.t.} \quad P_n \leq P_n^{max}, \forall n \in N, \tag{4.29b}$$

$$G_n P_n - \sum_{n'=1}^{n-1} G_{n'} P_{n'} \geq P_{tol}, n = 2, \ldots, |N|, \tag{4.29c}$$

$$R_n^{AC} \geq R_{min}, \forall n \in N. \tag{4.29d}$$

Once again, their in-between interactions are coordinated through a non-cooperative game, according to which each user n updates its uplink transmission power (i.e., its strategy) in a selfish way, given the other users' strategies $\mathbf{P}_{-n}$. The outcome of the non-cooperative game is the Nash equilibrium point of the users' strategies, i.e., the vector $\mathbf{P}^* = [P_1, \ldots, P_n, \ldots, P_{|N|}]$. The analysis, based on which the existence of at least one Nash equilibrium and the convergence at this point is ensured, follows the n-person concave games due to the objective function's strict concavity on $P_n, \forall n \in N$ and is analogous to the

one incorporated in Section 4.5.4. The second and third optimization stages are iteratively performed and updated between the UAV and the users to ultimately conclude the overall system's Stackelberg equilibrium point $(\mu^*, P_U^*, \mathbf{P}^*)$, as illustrated in Fig. 4.2.

4.7 Performance Evaluation

In this section, we evaluate the performance and effectiveness of the proposed end-to-end resource management framework, via modeling and simulation. First, the pure performance of the distributed Stackelberg game, as well as its convergence behavior to the Stackelberg equilibrium is demonstrated, targeting the energy efficiency of the considered IAB network. Then, a comparative analysis between the two distinct optimization objectives, namely the end-to-end energy efficiency optimization analyzed in Section 4.5 and the end-to-end data rate optimization approach summarized in Section 4.6, is enclosed. Finally, our proposed resource management framework is compared against different baseline resource management approaches in terms of both the RIS elements' phase shifts adaptation and the dynamic spectrum management solutions devised in this work. The results of this work are also presented in [125].

The simulation setting used to generate the numerical results presented in the remainder of this section is initialized as follows. Considering a three-dimensional coordinates system, the three main network entities of the RIS-aided and UAV-assisted IAB network, i.e., the RIS, the UAV, and the mBS, are located along the $y = x$ line, and their distances from the coordinates system's origin are set to 100 m, 200 m, and 400 m, respectively. The UAV hovers at 150 m above the ground, whereas the RIS, composed of $|M| = 100$ elements (unless mentioned otherwise), is placed at a height of 1.5 m and near the users. We consider a NOMA cluster of $|N| = 4$ users in total, placed with increasing distances from the RIS, denoted as d_1 [m], $d_1 + 10$ [m], $d_1 + 20$ [m], $d_1 + 30$ [m], respectively, where d_1 indicates the distance of the first user from the RIS and is generally set as $d_1 = 5$ m unless otherwise stated. The parameters that characterize the wireless propagation environment are configured as: $\psi = 11.95$, $\beta = 0.14$, $\eta_{LoS} = 3$ dB, $\eta_{NLoS} = 23$ dB, $f_c = 2$ GHz, $c = 3 \cdot 10^8$ m/s, $a_U = 2$, $\rho = 100$, $a_R = 2.8$, $d_s = \frac{\lambda}{2}$. The remaining communications-related simulation parameters are set as: $W = 5$ MHz, $N_0 = -174$ dBm/Hz, $P_n^{max} = 24$ dBm, $P_U^{max} = 46$ dBm, $P_{tol} = -114$ dBm, $R_{min} = 1$ Mbps, unless otherwise explicitly stated. Finally, for statistical purposes, the results have been averaged over 100 different channel model realizations.

4.7.1 Pure Evaluation of the Stackelberg Game-based Optimization Process

In Fig. 4.3, we study the performance of the overall Stackelberg game-based process towards the IAB network's energy efficiency optimization, while at the same time assessing its convergence behavior concerning the number of iterations I and the real execution time required to converge to the Stackelberg equilibrium point. Specifically, Fig. 4.3a depicts the sum of users' uplink transmission powers as a function of the required iterations and the real execution time in seconds. The different curves present an analysis over a different number of RIS elements $|M| = [100, 200, 300]$, while the term "no RIS" refers to the case where no RIS exists within the simulated network topology. The real execution time has been calculated as the mean execution time of the four different RIS elements' scenarios, as presented above. On the one hand, the results reveal that after a small number of iterations (e.g., $I = 5$ iterations or approximately 0.085 seconds in the case under consideration) the proposed approach converges to the optimal solution. On the other hand, it is confirmed that the use of RIS concludes to significantly lower power levels for the users, owing to the increased channel power gains incurred by the proper adaptation of the RIS elements' phase

shifts. Given that the optimization objective targeted is the network's energy efficiency, the decreased sum users' power levels lead apparently to the remarkable increase of the sum users' energy efficiency, as illustrated in Fig. 4.3b. The findings of Fig. 4.3b demonstrate that the use of RIS can provide almost 1.5 orders of magnitude higher sum users' energy efficiency, considering a number of $|M| = 300$ RIS elements, compared to the case where no RIS exists in the network topology. Although the RIS is deployed in the access network part, directly affecting the users' power and energy efficiency, it results in the end-to-end system's optimized performance, as indicated in Fig. 4.3c. Fig. 4.3c shows the pure UAV's energy efficiency, which is calculated as the fraction of the UAV's achieved data rate at the backhaul to its consumed uplink transmission power. Apparently, the access network's optimized performance steers the end-to-end system's Stackelberg equilibrium to more energy-efficient points. Furthermore, the introduction of a RIS deployed at a higher point above the ground and in LoS with the UAV, can further enhance the UAV's performance and strengthen the communications established at the backhaul network part.

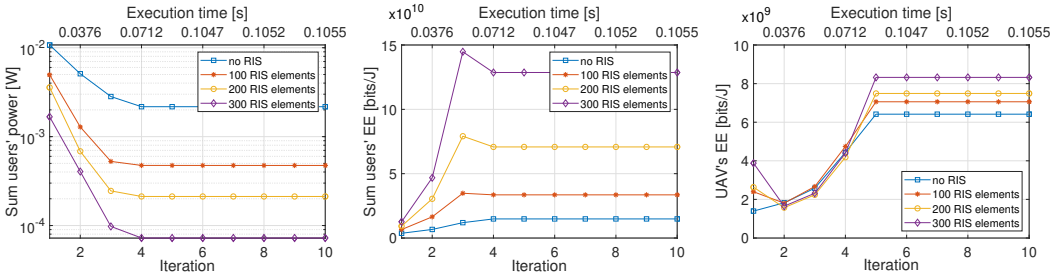

Figure 4.3: Evaluation of the performance and the convergence behavior of the Stackelberg game-based process towards the end-to-end energy efficiency optimization, under different number of RIS elements.

4.7.2 Comparative Evaluation of Different Network Optimization Objectives

To gain more insights regarding the significance of energy efficiency optimization objective in the wireless network's performance, we proceed to a comparative examination between the two distinct optimization objectives of end-to-end energy efficiency and end-to-end data rate maximization. In particular, in Fig. 4.4 we scrutinize the network's performance in terms of the sum users' transmission power levels and their achieved sum end-to-end data rates under the two different optimization objectives/approaches, which are denoted as "EE-Opt" and "DR-Opt". Furthermore, a study over different values $R_{min} = [0.5, 1.5, 3]$ Mbps of the users' minimum end-to-end data rate requirement accompanies our analysis, to further identify and highlight the network's enhanced performance under the energy efficiency optimization approach, considering different user QoS requirements.

Apparently, when the "DR-Opt" optimization approach is treated, the users are forced to transmit in the uplink using their maximum power budget regardless of their minimum data rate QoS requirement R_{min}, as properly presented in Fig. 4.4a. On the contrary, the sum users' transmission powers are approximately thirty times lower in the case of "EE-Opt" compared to "DR-Opt", while a slight increase is imposed as the minimum data rate requirement increases. The sum users' end-to-end data rates achieved by utilizing the sum power levels of Fig. 4.4a are accordingly shown in Fig. 4.4b. It can be easily observed that

the thirty-times increase in the users' power levels results in almost only three orders higher end-to-end data rates, verifying the significant gains provided by the "EE-Opt", mainly in terms of the resulting efficiency. Last, it should be noted that the small decrease in the sum users' end-to-end data rates, induced as the R_{min} requirement increases, is due to the need for a higher bandwidth portion in the access network part that is shared among the users which are interfering with each other, such that the remaining bandwidth part about the backhaul network part decreases.

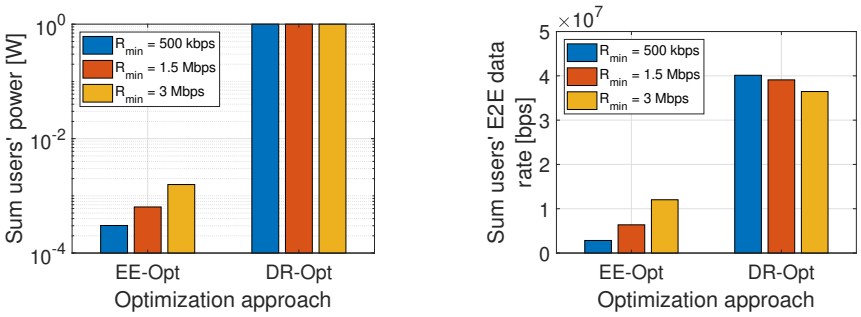

(a) (b)

Figure 4.4: Comparative evaluation between the two distinct end-to-end energy efficiency and data rate optimization approaches, under different users' minimum end-to-end data rate requirements.

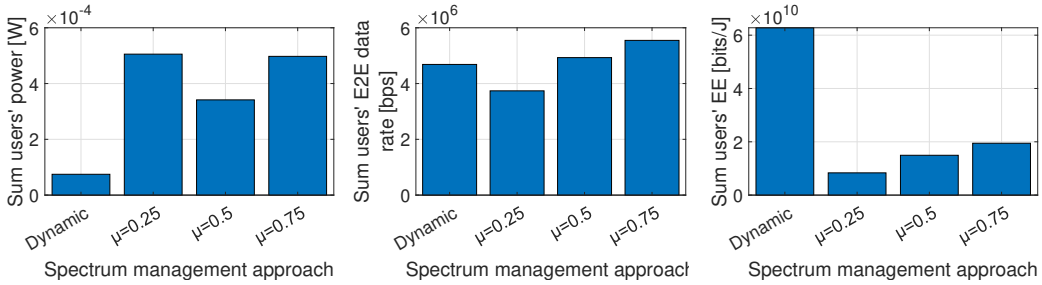

(a) (b) (c)

Figure 4.5: Comparative evaluation of the proposed dynamically allocated spectrum solution between the access and backhaul network parts, against different fixed bandwidth splitting approaches.

4.7.3 Evaluation of the Dynamic Spectrum Management

Subsequently, we aim to investigate the effectiveness and efficiency of the proposed end-to-end resource management framework concerning the dynamically allocated spectrum in the access and backhaul network parts, under our primarily targeted energy efficiency optimization objective. Towards this direction, our dynamic spectrum management solution is compared against other heuristic mechanisms that assume a fixed bandwidth partitioning between the two network parts (i.e., access and backhaul). For demonstration purposes, three different fixed bandwidth splitting schemes are considered with bandwidth splitting ratio parameter values equal to $\mu = [0.25, 0.5, 0.75]$. The outcome of this comparison is

presented in Fig. 4.5, where the term "Dynamic" refers to our proposed dynamically allocated spectrum procedure. The numerical results in Fig. 4.5 have been specifically averaged over 300 different IAB network topologies, considering different locations of the mBS, which range from 400 m to 700 m far from the origin of the three-dimensional coordinates system, to account for the potential different needs in terms of bandwidth splitting among the access and backhaul network parts. Evidently, the proposed dynamic spectrum management solution results in remarkably lower sum users' power levels compared to any of the fixed bandwidth splitting schemes, as demonstrated in Fig. 4.5a. Moreover, a small differentiation occurs in the achieved sum users' end-to-end data rates under the different spectrum management approaches (Fig. 4.5b). Nevertheless, the dominance of the dynamically allocated spectrum is identified, when considering the sum users' energy energy efficiency achieved, as presented in Fig. 4.5c.

4.7.4 Evaluation of the Proposed RIS Elements' Phase-Shift Adaptation

Our evaluation analysis is complemented with an extensive study pertinent to the performance gain provided by the introduction of the RIS within the network topology, as well as its proper configuration and phase-shift adaptation via our proposed method, as described in Section 4.5.2. To this end, we compare our proposed RIS elements' phase-shift adaptation method against a baseline approach, in which a random phase-shift configuration is selected for the RIS, referred to as "Random" in the following. In Fig. 4.6, appropriate results corresponding to the two different phase-shift configuration schemes, i.e., the "Proposed" one and the "Random" one, are extracted considering a different number of RIS elements $|M| = [100, 200, 300]$ and different distances of the users' from the RIS. The different users' distance scenarios from the RIS are indicated via the first user's distance d_1 [m] from the RIS along the x-axis. Also, the general case where no RIS exists within the network simulated topology is included as a reference scenario. In particular, in Fig. 4.6a, the sum of users' power levels is depicted as a function of the different phase-shift configuration schemes and the different users' distances. As the number of RIS elements increases, the sum users' uplink transmission powers decrease, resulting correspondingly in their increased sum achieved energy efficiency, as indicated by Fig. 4.6b.

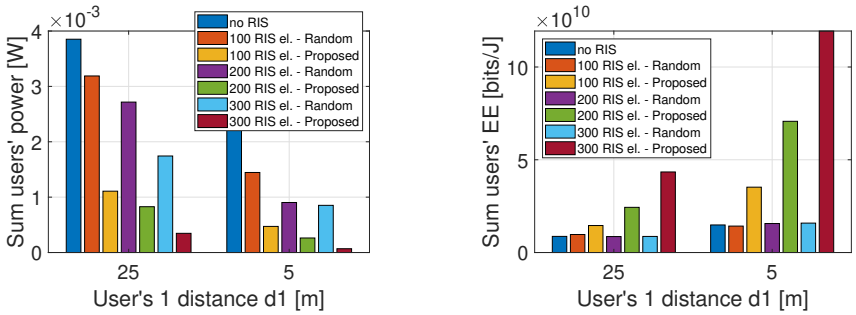

Figure 4.6: Comparative evaluation of the proposed RIS elements' phase-shift adaptation method against a random phase-shift configuration approach, under different numbers of RIS elements and distances of the users from the RIS.

Chapter 5

Resource Allocation and Incentive Mechanism Design in Multi-tier Computing Networks

5.1 General Setting

To facilitate the computationally and battery-constrained user devices to meet their applications' QoS requirements, the concept of computation offloading of resource-intensive tasks has become extremely popular. Especially, among the different computing capabilities and options existing within the computing continuum, the Multi-Access Edge Computing (MEC), often implemented within the Radio Access Network (RAN), has revolutionized the successful completion of low-latency applications. Nevertheless, driven by their appealing properties, the overexploitation of the edge computing networks will gradually lead to their performance degradation. To alleviate this issue and ameliorate the overall system's resource utilization, a heterogeneous multi-layer computing architecture should be pursued, where different computing entities of various capabilities across the network cooperate. Indeed, the diversity of the offloaded tasks in terms of their intensity, as well as the heterogeneity of the corresponding user applications' performance requirements regarding their delay (in)sensitivity and power consumption, create a solid ground for the proper utilization of the different computing options across the network. Nevertheless, despite the potential ability of the delay-tolerant tasks to be processed in the fog (or even the cloud) without degrading the QoS, edge computing's appealing features regarding its proximity to the users along with the users' selfish behavior, may prove to impede the realization of the envisioned heterogeneous multi-layer computing paradigm.

In this chapter, we aim to exactly address this challenge under a two-layer computing environment, consisting of an edge service layer and a fog service layer that are distinguished from an architectural point of view concerning the location where their computation power is placed (see Chapter 1 and Section 1.2). First, an incentive mechanism is designed and proposed based on multi-dimensional Contract Theory (CT). The edge server seeks to motivate its offloading users to allow part of their offloaded tasks to be further forwarded and processed at the fog, based on their distinct and heterogeneous applications' characteristics, as a means of improving the resource utilization efficiency across the network and increasing its overall service capacity, especially under the presence of delay-tolerant services. Accordingly, we utilize the outcome of the economic interplay between the users-edge-fog layers to tackle the challenging problem of a multi-layer computing environment's resource orchestra-

tion. Given the percentage of the initially offloaded tasks to the edge that are allowed to be further forwarded to the fog, the joint computation task offloading and uplink transmission power allocation problem between the users and the edge is addressed, considering the users' transmissions' multiplexing via the NOMA technique. Respecting the need for decentralized resource management approaches, the joint radio and computation task offloading problem is formulated as a Stackelberg game and solved in a distributed manner by the network entities.

5.2 Related Work

Several works exist in the literature, dealing with computation task offloading and resource allocation problems in multi-layer computing environments, e.g., [126, 127, 128, 129, 130]. In [126], the users' full offloading of their computation tasks to a primary fog server is assumed and the problem of invoking the assistance of other fog servers or the cloud is studied to complete the users' tasks within their time constraint. In [127], the multi-user decision problem of their computation tasks' execution either locally, at the fog, or the cloud is formulated and solved as a potential game, while other works consider similar offloading decision problems to multiple computing layers along with computing resource allocation [128], joint computing resource, uplink transmission power and radio resource allocation [129], or servers' service caching decision [130] problems. On the one hand, none of the existing works accounts for the three-level splitting (i.e., local, edge, and fog layers) of the users' computation tasks, while overlooking the economic and market perspective of the computation offloading as a service.

In this work, though the users are provided with a transparent computing service - meaning that the multiple service layers are viewed as a contiguous computing network - they can still smartly evaluate the emerging tradeoffs between delay tolerance and task intensity and size, which are directly affected by the available computing options. Shifting the selfish users' preference to upper computing layers according to their delay-tolerance levels calls for the creation and provisioning of appropriate incentives. In this context, a well-established method to deal with the problem of incentives comes from the field of labor economics and Contract Theory [41]. Among the wide variety of applications of Contract Theory in wireless communications and networking (e.g., cognitive radio networks [75], Device-to-Device (D2D) communications [131], crowdsourcing [132], resource allocation like Chpater 3 of this thesis), some effort has been made in the direction of computation offloading. In [133], the problem of incentivization of potential temporary edge nodes from an edge computing operator is examined under an MEC paradigm. Similar problems are considered in [134, 135] under the concept of vehicular edge/fog computing offered by vehicles to other traveling vehicles or roadside users. Different from the concept of computation offloading, but relevant to the incentivization of delay-tolerant users is the work in [136]. In this work, the users capitalize on their delay tolerance and cost sensitivity, and forward their traffic through the available Delay-Tolerant Networks (DTNs) or WiFi networks, in return for reduced service cost.

Focusing on the practical application of contract theory models, most of the existing works in the literature, including the aforementioned ones in [75, 131, 132, 133, 134, 135, 136], rely on one-dimensional user types that typically capture each user's level of willingness or ability to participate in the contract. Nevertheless, such an approach appears to be rather restrictive, since in most cases there is more than one distinguishing feature for each user that should steer the contract modeling, especially when these features are conflicting. Recently, the problem of multi-dimensional contract theory in terms of the number of user types that characterize each user has been investigated in [137, 138, 139]. In [137], the interplay between an advertiser and the users is modeled under a contract, in which different user types are devised to account for the users' enjoyment, disutility, and ad sensitivity,

respectively. In [138], the contractual agreement between a federated learning model owner and different UAVs that offer their computation capabilities is examined, in which each UAV is jointly distinguished based on its sensing, computation, and transmission costs. In [139], the problem of optimal wireless data plans offered by an MNO to its subscribing users is studied, by incorporating the users' satisfaction and network substitutability as two distinct user types in the model.

Concerning the computation offloading under single-layer computing environments, a wide variety of works exist in the literature. Indicative ones in [140, 89], treat unilaterally the problem of computation offloading from different perspectives, accounting for multi-server setups [140] or devising usage-based pricing policies [89]. Other attempts, e.g., [141, 142, 143], focus on the challenging joint communication and computing resource allocation under NOMA-enabled computing systems, by mainly proposing game-theoretic approaches to obtain a solution in a tractable manner and within polynomial time [144]. In [141], the authors aim to minimize the users' sum delay by optimizing their offloading strategies and uplink transmission powers to the edge server. Optimizing a similar set of variables, the minimization of the total energy is pursued in [142], while the concurrent minimization of the users' energy consumption and latency is achieved in [143], via a Stackelberg game. However, all aforementioned works in [140, 89, 141, 142, 143], consider this single layer as a practically infinite energy and resource computing layer compared to the users' constrained devices, whereas our approach removes this limitation, by taking the edge service layer's energy efficiency into account.

5.3 Contributions & Outline

It becomes apparent that although several efforts have been devoted to the joint task offloading and power control problem that pertain to different multi-layer computing settings, the overwhelming majority of them are founded on the effective and efficient execution of delay-sensitive tasks. In our work, in contrast to the rest of the research works, we aim to, first, study the problem of collaborative edge-fog computing from a market perspective and leverage the economic interplay between the involved parties to tackle the challenging two-layer computing environment's resource orchestration. Under this objective, our goal is to better utilize the available computing resources in such a heterogeneous and multi-layer computing setting, increasing in this way its computing service capacity, while minimizing the end-to-end energy overhead. Specifically, the key contributions of this work are summarized as follows:

1. A system model of a two-layer edge-fog computing environment is introduced, accounting for both the computing models of the users, the edge and fog servers, and the wireless users-to-edge and edge-to-fog communication models (Section 5.4).

2. An incentive mechanism is designed between the edge server and the users following the principles of multi-dimensional contract theory. Based on the heterogeneity of the users' applications and, hence, their multi-dimensional private information, the edge server derives a set of contract bundles, comprising the required efforts from the users and their offered rewards. Each user's effort represents the percentage of the initially offloaded task to the edge server that can be further transmitted and processed at the fog (Section 5.5).

3. A joint computation task offloading and uplink transmission power control problem is designed between the edge server and the users in the form of a Stackelberg game. The edge server, i.e., the leader, determines the users' optimal amounts of tasks to be offloaded to the edge, being aware of the percentage of each user's task that will

be processed at the fog. Subsequently, the users, i.e., the followers, being multiplexed via power-domain NOMA, derive their optimal uplink transmission powers to the edge. The edge server seeks to maximize its perceived satisfaction minus the end-to-end energy overhead from the users to the fog, while the users pursue their personal energy efficiency maximization under a non-cooperative game. The overall resource allocation procedure is iteratively executed until the Stackelberg equilibrium is reached (Section 5.6).

4. Based on the above theoretical foundations, we study the inherent operational characteristics of both the incentive mechanism and the resource allocation procedure, via modeling and simulation. Moreover, we prove the performance efficiency of the proposed incomplete information contract by comparison with the benchmark complete information case, while demonstrating, at the same time, the superiority of the proposed resource allocation approach, against different baseline offloading strategies (Section 5.7).

5.4 System Model

A two-layer computing environment is considered, consisting of a set of users $\mathcal{N} = \{1, \ldots, N\}$, an edge server , and a fog server . We assume that the edge server can be mobile, with consequently some limitation on its available energy, and, hence, can move near the users. On the other hand, the fog server lies between the edge and the cloud/core network, serving - among others - the purpose of computation alleviation/relaxation of the edge. It should be noted that the problem of the edge server placement, though interesting and challenging, is considered beyond the scope of this work, while the extension to the multi-edge server case is part of our future research activities. The focus of the current work is primarily placed on the interplay between the various computing layers (users-edge-fog) and their joint and collaborative exploitation. A high-level overview of the general users-edge-fog computing architecture, aligned with the system model considered in this work, is presented in Fig. 5.1. Fig. 5.1 highlights the architectural differentiation between the edge and fog computing layers, concerning the location where their intelligence and computation power is placed within the overall network [14, 145, 146, 147].

In this system, each user n has a computing application A_n, which can range from a typical smart city, transportation [148], healthcare, industry, and agriculture computing application (e.g., [149, 150]), as illustrated in Fig. 5.1. Each user's computing application's A_n specific characteristics are defined as $A_n = (D_n, \phi_n, T_n, E_n)$, where D_n [Bytes] denotes the application's total input bytes, ϕ_n [CPU cycles/Byte] indicates the application's intensity and T_n [s] is the end-to-end completion time requirement, which implicitly reveals the user's level of delay tolerance. Last, E_n [J] is the user device's energy constraint. Accordingly, the term $\phi_n D_n$ [CPU cycles] denotes the number of CPU cycles required for the application's execution, which is referred to as "task" in the following and can represent a number of images, videos, text, voice, or maps, depending on the user's computing application's nature. In this work, we pursue a realistic scenario, under which the user application's characteristics take values from discrete sets, such that $D_n \in \mathcal{D}$, $\phi_n \in \Phi$, $T_n \in \mathcal{T}$ and $E_n \in \mathcal{E}$, where $\mathcal{D}, \Phi, \mathcal{T}, \mathcal{E}$ are the corresponding discrete sets. Also, we assume that a task $\phi_n D_n$ can be arbitrarily partitioned into subsets of any size, which can be executed at either the user device, edge server, or fog server.

Owing to the edge server's appealing attributes, including its proximity to the users, we assume that each user n chooses to communicate with the edge server and offload part of its total task $\phi_n D_n$ for remote computation. We denote as $\phi_n d_n$ [CPU cycles] the part of the task that is actually offloaded by the user to the edge, where $d_n \in [0, D_n]$ [Bytes] is

the user's n offloading bytes. Based on the application's A_n characteristics, a percentage $x_n \in [0, 1]$ of the initially offloaded task $\phi_n d_n$ by the user n to the edge, is allowed to be further transmitted and processed at the fog. The value of the percentage x_n is derived from the contractual agreement between the edge server and the user n, which is analytically presented later in Section 5.5. As a result, considering a user n, a total amount of $x_n d_n$ [Bytes] is wirelessly transmitted from the edge to the fog, and $x_n \phi_n d_n$ [CPU cycles] are computed at the fog server, while the remaining $(1 - x_n)\phi_n d_n$ are ultimately processed at the edge. Finally, it is noted that $D_n - d_n$ bytes are reserved for local computation at the user's device.

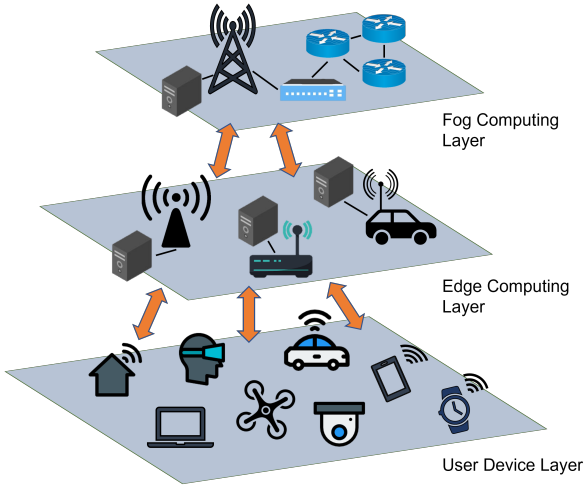

Figure 5.1: High-level overview of the two-layer computing environment's architecture.

5.4.1 Wireless Communication Model

Focusing on the communication model, we assume that the two-layer wireless network operates in out-of-band mode, meaning that the transmissions in the wireless access and backhaul network parts (e.g., user-to-edge and edge-to-fog) are performed using different frequency bands. We denote as W_e [Hz] the bandwidth of the wireless access and W_f [Hz] the bandwidth of the wireless backhaul that facilitates the transmission from the edge to the fog. The users' transmissions in the wireless access are multiplexed using the combination of power-domain NOMA and SIC techniques, while no interference is sensed by the edge server at the wireless backhaul network part.

In detail, regarding the wireless access of the users to the edge server, we denote by G_n the channel gain of a user n, which is defined as $G_n = \rho d_{n,e}^{-a_e}$, where ρ [dB] is the path loss at the reference distance of 1m, $d_{n,e}$ [m] is the Euclidean distance between the user n and the edge server and a_e is the path loss exponent. Without loss of generality, we assume that the users' channel gains are ordered in ascending manner, i.e., $G_1 \leq \cdots \leq G_n \cdots \leq G_N$, such that the decoding starts from the higher channel gain user when the SIC technique takes place at the receiver of the edge server. Hence, following the combination of NOMA and SIC, the user's n achieved data rate in the uplink direction to the edge server is:

$$R_n = W_e \log_2 \left(1 + \frac{G_n p_n}{\sum_{n'=1}^{n-1} G_{n'} p_{n'} + I_0} \right) [bps], \tag{5.1}$$

where $p_n \in [0, p_n^{max}]$ [W] indicates the user's n uplink transmission power that is constrained

by a maximum transmission power level p_n^{max}, and I_0 [dBm/Hz] is the power spectral density of zero-mean Additive White Gaussian Noise (AWGN). As a result, considering that a user n transmits d_n bytes to the edge server, we can define the transmission time and energy overheads that experiences as follows:

1. User's n offloading time overhead:

$$T_n^{off} = \frac{d_n}{R_n}[s]. \tag{5.2}$$

2. User's n offloading energy overhead:

$$E_n^{off} = \frac{d_n p_n}{R_n}[J]. \tag{5.3}$$

Regarding the wireless backhaul transmission from the edge to the fog, we define as $G_e = \rho d_{e,f}^{-a_f}$ the channel gain between the edge and fog servers, where $d_{e,f}$ [m] is the Euclidean distance between the two servers and a_f is the corresponding path loss exponent. Denoting as p_e [W] the uplink transmission power of the edge server to the fog, the edge server's achieved data rate is expressed as:

$$R_e = W_f \log_2 \left(1 + \frac{G_e p_e}{I_0}\right)[bps]. \tag{5.4}$$

Accordingly, we define the transmission time and energy overheads at the backhaul, experienced by the edge server, considering a single user n:

1. Edge server's offloading time overhead for user's n task:

$$T_e^{n,off} = \frac{x_n d_n}{R_e}[s]. \tag{5.5}$$

2. Edge server's offloading energy overhead for user's n task:

$$E_e^{n,off} = \frac{x_n d_n p_e}{R_e}[J]. \tag{5.6}$$

5.4.2 Computing Model

The two-layer edge-fog computing setting under consideration provides, apparently, three levels of different computing capabilities to its serving users. Analyzing these options from a bottom-up perspective, we denote as F_n [CPU cycles/s] the user n device's inherent (local) computing capability, and σ_n its processor's chip energy coefficient [151]. Considering that the user n executes locally a task of size $\phi_n(D_n - d_n)$ CPU cycles, the user's n corresponding computation/execution time and energy overheads are defined as follows [152, 153]:

1. User's n execution time overhead:

$$T_n^{exec} = \frac{\phi_n(D_n - d_n)}{F_n}[s]. \tag{5.7}$$

2. User's n execution energy overhead:

$$E_n^{exec} = \sigma_n \phi_n (D_n - d_n) F_n^2 [J]. \tag{5.8}$$

Adopting similar modeling for the subsequent computing layer, we indicate as F_e [CPU cycles/s] the edge server's computing capability, which is assumed to be higher than each user's n, but finite and more limited compared to the fog. Also, let σ_e denote its processor's chip energy coefficient. Considering that the edge servers' resources are sufficient and can facilitate the parallel computation of the users' tasks [154, 155], the edge server's incurred time and energy consumption overheads for each user n are:

1. Edge server's execution time overhead for user's n task:

$$T_e^{n,exec} = \frac{(1-x_n)\phi_n d_n}{F_e}[s]. \tag{5.9}$$

2. Edge server's execution energy overhead for user's n task:

$$E_e^{n,exec} = \sigma_e(1-x_n)\phi_n d_n F_e^2[J]. \tag{5.10}$$

As far as the fog computing layer is concerned, in this work, we assume that the processing capabilities of the fog server significantly excel both the edge server and the user devices, and hence, without loss of generality and for simplicity in the presentation, we assume that the fog induces practically zero time and energy costs compared to the other two lower computing layers. However, this analysis is still valid and can be easily extended to additionally account for these overheads at the fog computing layer.

5.4.3 Overall Framework

In this work, we aim to promote the utilization of the end-to-end users-edge-fog computing paradigm, under the case that the users' tasks are characterized by some form of delay tolerance. Considering that the users typically exhibit selfish and greedy behavior about their perceived satisfaction from the remote computation of their tasks, we first employ an incentive mechanism that targets to shift their preference from the prevailing edge server to the fog server. To this end, a multi-dimensional contract is designed by the edge server, which based on the edge server's statistical knowledge of the potential user applications' heterogeneous features, concludes to a set of optimal contract bundles $\mathbf{w}^* = \{\mathbf{x}^*, \mathbf{r}^*\}$ intended for the users. The term $\mathbf{x}^*$ indicates the vector of the users' required efforts, which are mapped to the percentage of each user's task $\phi_n d_n$ that is further offloaded to the fog, while the term $\mathbf{r}^*$ represents the vector of the corresponding rewards, which can be considered as a form of discount to the users' received computing service from the edge server. The exact definition of these parameters is provided later in Section 5.5.1. Based on its private information, i.e., user application characteristics, each user autonomously selects the contract bundle $w_n^* = \{x_n^*, r_n^*\}$ that best fits its type, revealing implicitly in this way its private information to the edge server.

Being aware of the percentage of task x_n^* that is allowed by each user n to be transmitted to the fog, the edge server can calculate the end-to-end system's total energy and time overhead from the users to the fog, as presented in Eq. (5.2)-(5.3) and Eq. (5.5)-(5.10). Targeting to maximize its perceived satisfaction minus the end-to-end computing environment's energy overhead, the edge server calculates each user's n optimal amount of offloaded task $\phi_n d_n^*$, having prior knowledge of the users' uplink transmission powers to the edge. The edge server's decision is fed back to the users, who accordingly determine their optimal uplink transmission power levels $p_n^*, \forall n \in \mathcal{N}$ in a distributed manner, by participating in a non-cooperative game among themselves. The optimization procedures of both the edge server and the users are iteratively updated, until convergence of this joint resource allocation is achieved, resulting in a Stackelberg game. A high-level overview of the individual

steps of the proposed incentive mechanism and resource allocation framework is presented in Fig. 5.2, revealing also the interactions that take place between the edge server and the users at each step.

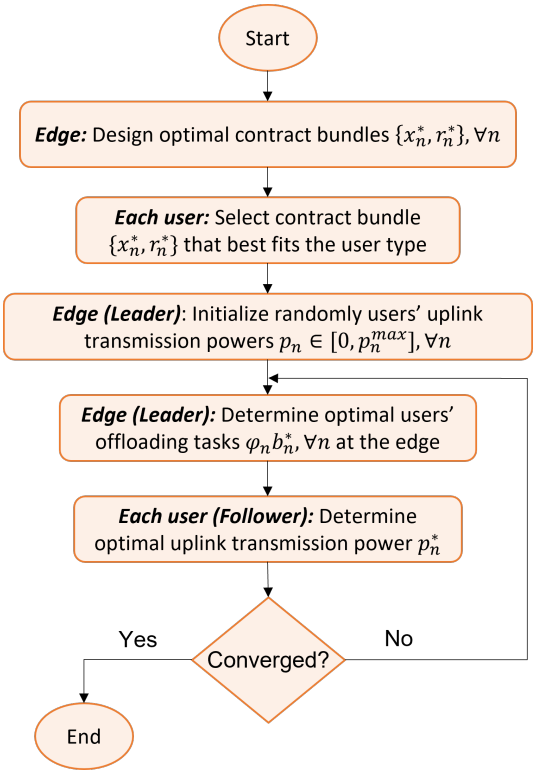

Figure 5.2: High-level overview of the overall incentive mechanism and resource allocation framework.

5.5 Multi-Dimensional Contract-based Incentive Mechanism Design

This section is devoted to the introduction and analytic description of the devised incentive mechanism, based on multi-dimensional contract theory. First, we define the multi-dimensional private information and user types that distinguish the users and reflect their heterogeneity, along with the designed contract bundles and utilities. Then, we study the problem of contract formulation and, gradually, we derive the optimal contracts.

5.5.1 User Types, Contract Bundles & Utilities

Following each user application's A_n heterogeneous characteristics, the users can be categorized into different user types that capture their ability and willingness to allow part of their initially offloaded tasks to the edge server to be forwarded to the fog. Assuming that the discrete sets $\mathcal{D}, \Phi, \mathcal{T}$ comprise K, L, M values, respectively, such that $\mathcal{D} = \{\mathcal{D}_k : 1 \leq k \leq K\}$, $\Phi = \{\Phi_l : 1 \leq l \leq L\}$ and $\mathcal{T} = \{\mathcal{T}_m : 1 \leq m \leq M\}$, there exist $K \times L \times M$ combinations of user types in the system, which derive from the Cartesian product $B \times \Gamma \times \Delta$ of the sets B, Γ, Δ analyzed in the following. Specifically, we categorize the users into

a set $B = \{\beta_k : 1 \leq k \leq K\}$ of K application size evaluation types, which are determined by the rule $\beta_k = \mathcal{D}_k / \max_{1 \leq k \leq K}\{\mathcal{D}_k\}$, a set $\Gamma = \{\gamma_l : 1 \leq l \leq L\}$ of L application intensity evaluation types that are derived as $\gamma_l = \Phi_l / \max_{1 \leq l \leq L}\{\Phi_l\}$, as well as a set $\Delta = \{\delta_m : 1 \leq m \leq M\}$ of M delay sensitivity evaluation types, such that $\delta_m = \left(\mathcal{T}_m / \max_{1 \leq m \leq M}\{1/\mathcal{T}_m\}\right)^{-1}$. For all user types it holds that $\beta_k, \gamma_l, \delta_m \in (0, 1], \forall k, l, m$. Without loss of generality, we assume that the user types are sorted in ascending order under all dimensions, i.e., $\beta_1 \leq \cdots \leq \beta_k \leq \cdots \leq \beta_K$, $\gamma_1 \leq \cdots \leq \gamma_l \leq \cdots \leq \gamma_L$, $\delta_1 \leq \cdots \leq \delta_m \leq \cdots \leq \delta_M$. Also, each combination of the $K \times L \times M$ user types is characterized by a joint probability mass function $Pr(\beta_k, \gamma_l, \delta_m), \forall k, l, m$. At this point, it should be reminded that the user types constitute the users' private information that is unknown to the edge server, whereas the edge server is only aware of the different user types' joint probability mass function, and should appropriately design the contract bundles relying on this partially complete (or incomplete) information.

As mentioned earlier, the edge server designs a set of optimal contract bundles $\mathbf{w}^* = \{\mathbf{x}^*, \mathbf{r}^*\}$ of the users' required efforts and offered rewards, respectively, based on its probabilistic knowledge of the potential users' types. Specifically, we denote as $x^n_{k,l,m} \in [0, 1]$ the effort of user n of type $(\beta_k, \gamma_l, \delta_m)$, and $r^n_{k,l,m} \in \mathbb{R}^+$ its corresponding reward. Apparently, different users from the set $\mathcal{N}$ can be of the same type $(\beta_k, \gamma_l, \delta_m)$, acquire the same contract bundle and, hence, experience the same utility. Since our analysis is focused on the differentiation of the contract bundles concerning the different user types, in the following, we drop the superscript n that points to a specific user for notation simplicity. In addition, we refer to the user type $(\beta_k, \gamma_l, \delta_m)$ as (k, l, m)-type user, whose corresponding contract bundle is $w_{k,l,m} = \{x_{k,l,m}, r_{k,l,m}\}$.

Given a (k, l, m)-type user's effort $x_{k,l,m}$ and its offered reward $r_{k,l,m}$, we define its perceived satisfaction from its participation in the contract by the following utility:

$$U_{k,l,m}(w_{k,l,m}) = r_{k,l,m} - (1.5 + \delta_m - \beta_k \gamma_l) q(x_{k,l,m}), \tag{5.11}$$

where $q(x_{k,l,m})$ is an increasing function of $x_{k,l,m}$, which together with the term $(1.5 + \delta_m - \beta_k \gamma_l)$ implies its evaluation of provided effort. Specifically, the term $\beta_k \gamma_l q(x_{k,l,m})$ indicates that the user's benefit from exerting its effort to the edge server increases as its β_k, γ_l types increase since a higher amount of task can be executed at the combination of edge-fog. On the contrary, the user's benefit decreases as its delay sensitivity evaluation δ_m increases, noted by the term $-\delta_m q(x_{k,l,m})$. The physical meaning and interpretation of the overall utility function is that the (k, l, m)-type user's satisfaction derives from its offered reward minus its provided effort, which, in turn, increases proportionally to its application's input bytes and intensity and is inversely proportional to its delay sensitivity. For ease of reference, we define as $Q_{k,l,m}(x_{k,l,m}) = -(1.5 + \delta_m - \beta_k \gamma_l) q(x_{k,l,m})$, and we rewrite the (k, l, m)-user type's utility as $U_{k,l,m}(w_{k,l,m}) = Q_{k,l,m}(x_{k,l,m}) + r_{k,l,m}$. Taking into account that $\beta_k, \gamma_l, \delta_m \in (0, 1]$ and that $q(x_{k,l,m})$ is an increasing function, it holds that $\frac{\partial Q_{k,l,m}}{\partial x_{k,l,m}} < 0$, and, thus, $Q_{k,l,m}(x_{k,l,m})$ is a decreasing function on $x_{k,l,m}$. For demonstration purposes and without loss of generality, in the following, we consider $q(x_{k,l,m}) = x^2_{k,l,m}$.

Concerning the utility that the edge server attains from a single (k, l, m)-type user's participation in the contract, this is modeled as $V_{k,l,m}(w_{k,l,m}) = h(x_{k,l,m}) - \xi r_{k,l,m}$, where $h(x_{k,l,m})$ is an increasing and concave function on $x_{k,l,m}$, accounting for the edge server's evaluation of received effort, while $\xi \geq 1$ is the edge server's cost of offered rewards. Obviously, the edge server's utility increases as the user's effort increases and decreases proportionally to its offered reward. As a result, the overall edge server's utility from the different user types' participation can be expressed as follows:

$$V(W) = \sum_{k=1}^{K} \sum_{l=1}^{L} \sum_{m=1}^{M} Pr_{k,l,m} \left(h(x_{k,l,m}) - \xi r_{k,l,m} \right), \tag{5.12}$$

where $W = \{w_{k,l,m}, 1 \leq k \leq K, 1 \leq l \leq L, 1 \leq m \leq M\}$ is the set that contains the ensemble of contract bundles. Motivated by [137], in the following we consider the function $h(x_{k,l,m}) = \frac{c}{1-\lambda} x_{k,l,m}^{1-\lambda}$ to capture the sharp increase of the edge server's marginal rate of satisfaction with the user's effort increase, by intelligently controlling $c \in [0, 1]$ and $\lambda \in (0, 1)$.

5.5.2 Contract Formulation

Considering the realistic scenario of the incompleteness of information from the edge server's perspective, the designed contract bundles should bear specific properties to promote the users' participation in the contract. In particular, the edge server should ensure that each user experiences a non-negative utility, while its utility is, also, maximized when selecting the contract bundle designated for its specific type. These two conditions are summarized under the notions of Individual Rationality (IR) and Incentive Compatibility (IC), which are formally defined below.

Definition 5.1. ***(Individual Rationality (IR))*** *A contract bundle $w_{k,l,m} = \{x_{k,l,m}, r_{k,l,m}\}$ satisfies the individual rationality condition if each (k, l, m)-type user for all $1 \leq k \leq K, 1 \leq l \leq L, 1 \leq m \leq M$ receives a non-negative utility, i.e.,*

$$U_{k,l,m}(w_{k,l,m}) \geq 0, \forall k, l, m. \tag{5.13}$$

Definition 5.2. ***(Incentive Compatibility (IC))*** *Each (k, l, m)-type user for all $1 \leq k \leq K, 1 \leq l \leq L, 1 \leq m \leq M$ receives the maximum utility, when selecting the contract bundle $w_{k,l,m} = \{x_{k,l,m}, r_{k,l,m}\}$ that is intended for its own type, i.e.,*

$$U_{k,l,m}(w_{k,l,m}) \geq U_{k,l,m}(w_{k',l',m'}), \forall k, l, m, k \neq k', l \neq l', m \neq m'. \tag{5.14}$$

Hence, the multi-dimensional contract problem to be solved by the edge server can be formally written as:

$$\max_{W} \quad V(W) \tag{5.15a}$$

$$\textbf{s.t.} \quad (5.13), (5.14). \tag{5.15b}$$

The resulting optimization problem in Eq. (5.15) includes KLM IR and $KLM(KLM-1)$ IC constraints, which fully interconnect the contract bundle design between the different user types. To derive a tractable solution, an appropriate procedure should take place to reduce its constraints, which primarily differs from the standard method used in the one-dimensional contract problems (e.g., [75, 131, 132, 133, 134, 135, 136]) and is comprehensively presented in Section 5.5.3 and Section 5.5.4.

5.5.3 Contract Feasibility

In this section, we study the necessary conditions that must be satisfied to render the formulated contract problem feasible. To facilitate this analysis, we first transform the three-dimensional contract problem to a single-dimensional one, by introducing a single "virtual" user type that bears all three-dimensional private information of the users. To this end, we resort to some useful properties of the theory of economics.

We consider a (k, l, m)-type user's indifference curve in the contract plane $\{x_{k,l,m}, r_{k,l,m}\}$ between its effort and reward, which under a fixed utility value $U(w) = \bar{U}$ satisfies:

$$\begin{aligned} \bar{U} &= r_{k,l,m} - (1.5 + \delta_m - \beta_k \gamma_l) q(x_{k,l,m}) \\ &= Q_{k,l,m}(x_{k,l,m}) + r_{k,l,m}, \end{aligned} \tag{5.16}$$

which actually yields all combinations of $\{x_{k,l,m}, r_{k,l,m}\}$ that result in the same utility to the users.

The slope s of the indifference curve is calculated by taking the partial derivatives of both sides in Eq. (5.16) as:

$$\begin{aligned} s_{k,l,m}(x_{k,l,m}) &= -\frac{\partial Q_{k,l,m}}{\partial x_{k,l,m}} = \frac{\partial r_{k,l,m}}{\partial x_{k,l,m}} \\ &= (1.5 + \delta_m - \beta_k \gamma_l) q'(x_{k,l,m}), \end{aligned} \tag{5.17}$$

which is referred to as "marginal rate of substitution", implying the rate at which a user is expected to abandon a $\{x_{k,l,m}, r_{k,l,m}\}$ combination in exchange for another while maintaining the same utility value. Apparently, Eq. (5.17) depends on the three-dimensional (k,l,m)-type in a combined manner, and the effort $x_{k,l,m}$. By scrutinizing the definition of parameter s, we can easily deduce that the lower the value of s, the lower the delay sensitivity evaluation type δ and the higher the application size and intensity evaluation types β and γ, respectively. This leads to a higher user's willingness to participate in the contract. On the contrary, the opposite holds under a higher value of s, which increases the user's unwillingness to participate. Hence, as the value of the marginal rate of substitution s in Eq. (5.17) increases, the user's overall willingness decreases. Therefore, we may additionally refer to s as the "unwillingness-to-participate" parameter.

Without loss of generality, we sort the $K \times L \times M$ user types in ascending order with respect to the unwillingness-to-participate parameter s as follows:

$$Z_1(x), \ldots, Z_i(x), \ldots, Z_{KLM}(x), \tag{5.18}$$

where $Z_i(x) \triangleq (\beta_i, \gamma_i, \delta_i), 1 \leq i \leq KLM$ denotes a user type under the new formulation, which is actually the virtual user type we are seeking. Thus, considering an effort x and under the ordering in Eq. (5.18), it holds that:

$$s(Z_1, x) \leq \cdots \leq s(Z_i, x) \leq \cdots \leq s(Z_{KLM}, x). \tag{5.19}$$

It is interesting that although the value of $s(Z_i, x)$ changes for different efforts x, the virtual user type ordering in Eq. (5.18) remains unchanged, which we elaborate on Lemma 5.1 below.

Lemma 5.1. *The new user type ordering in Eq. (5.19) is independent of the effort x, i.e., $Z_i(x) = Z_i(x'), x \neq x', 1 \leq i \leq KLM$.*

Proof. The proof of this lemma stems intuitively from the fact that the unwillingness-to-participate parameter $s(\beta, \gamma, \delta, x)$ has a separable structure concerning the three-dimensional types (β, γ, δ) and the effort x, as can be easily observed by its definition in Eq. (5.17). □

In the remainder of this work, we directly use Z_i to refer to the virtual user type, referred to as unwillingness-to-participate user type. Also, the contract bundle intended for Z_i is denoted as $w_i = \{x_i, r_i\}$, while this notation applies to all other considered variables. Consequently, the utility function of a user type Z_i is written as $U_i = Q(Z_i, x_i) + r_i$, where $Q(Z_i, x_i)$ is the equivalent of $Q_{k,l,m}(x_{k,l,m})$.

Given the outcome of Lemma 5.1, we conclude that whatever the value of x is, the minimum unwillingness-to-participate user type is $Z_1 = (\beta_K, \gamma_L, \delta_1)$, whose application size and intensity is the highest, while its delay sensitivity is the lowest. Conversely, the maximum unwillingness-to-participate user type is $Z_{KLM} = (\beta_1, \gamma_1, \delta_M)$, which, also, attains the minimum utility based on the definition of utility in Eq. (5.11).

Next, we derive the necessary conditions that render a contract $W = \{w_i, 1 \leq i \leq KLM\}$ feasible, meaning that the IR and IC conditions defined in Eq. (5.13) and Eq. (5.14), respectively, are successfully met.

Lemma 5.2. *For any feasible contract* $W = \{w_i, 1 \leq i \leq KLM\}$*, it holds true that* $x_i > x_j \Leftrightarrow r_i > r_j$*.*

Proof. First, we prove that $r_i > r_j \Rightarrow x_i > x_j$, by utilizing the IC condition that holds for user type Z_j, which gives $Q(Z_j, x_j) + r_j \geq Q(Z_j, x_i) + r_i \Leftrightarrow Q(Z_j, x_j) - Q(Z_j, x_i) \geq r_i - r_j$. Thus, if $r_i > r_j$ then $Q(Z_j, x_j) > Q(Z_j, x_i)$ and considering that function Q is decreasing with respect to x, we get $x_i > x_j$.

To prove that $x_i > x_j \Rightarrow r_i > r_j$, we follow a similar procedure and we elaborate on the IC condition that holds for user type Z_i as $Q(Z_i, x_i) + r_i \geq Q(Z_i, x_j) + r_j \Leftrightarrow Q(Z_i, x_i) - Q(Z_i, x_j) \geq r_j - r_i$. Then, if $x_i > x_j \overset{Q\searrow}{\Longleftrightarrow} Q(Z_i, x_i) < Q(Z_i, x_j)$ and thus, it can be easily concluded that $r_i > r_j$. This completes the proof. □

The rationale behind Lemma 5.2 is that a user receives a higher reward when providing a higher effort to the edge server, to be properly incentivized to participate in the contract.

Lemma 5.3. ***(Monotonicity)*** *For any feasible contract* $W = \{w_i, 1 \leq i \leq KLM\}$*, it holds true that* $s(Z_i, x) > s(Z_j, x) \Rightarrow x_i \leq x_j$*, for any* x*.*

Proof. We prove this lemma by contradiction, assuming that there exists x_i and x_j, such that $x_i > x_j$, which gives $s(Z_i, x) > s(Z_j, x)$, for any x.

We write the IC conditions that hold for the user types Z_i and Z_j, respectively, as $Q(Z_i, x_i) + r_i \geq Q(Z_i, x_j) + r_j$ and $Q(Z_j, x_j) + r_j \geq Q(Z_j, x_i) + r_i$. By adding these two IC condition inequalities by parts, we get $Q(Z_i, x_i) + Q(Z_j, x_j) \geq Q(Z_i, x_j) + Q(Z_j, x_i)$, which is equivalently written as:

$$\big[Q(Z_i, x_i) + Q(Z_j, x_j)\big] - \big[Q(Z_i, x_j) + Q(Z_j, x_i)\big] \geq 0. \tag{5.20}$$

Elaborating on Eq. (5.20) via the fundamental theorem of calculus, we obtain:

$$\begin{aligned} &\big[Q(Z_i, x_i) + Q(Z_j, x_j)\big] - \big[Q(Z_i, x_j) + Q(Z_j, x_i)\big] \\ &= \int_{x_j}^{x_i} \frac{\partial Q(Z_i, x)}{\partial x} dx - \int_{x_j}^{x_i} \frac{\partial Q(Z_j, x)}{\partial x} dx \\ &= \int_{x_j}^{x_i} - \big[s(Z_i, x) - s(Z_j, x)\big]\, dx. \end{aligned} \tag{5.21}$$

Since $x_i > x_j$, Eq. (5.21) gives $s(Z_i, x) < s(Z_j, x)$, which contradicts with our initial assumption. In this way, we have proved that there does not exist $x_i > x_j$ such that $s(Z_i, x) > s(Z_j, x)$, which confirms the soundness of this lemma. □

The reasoning behind the monotonicity condition in Lemma 5.3 is that a higher unwillingness-to-participate user type provides a lower effort to the edge server and, thus, is rewarded less, taking also into account Lemma 5.2.

Based on the above analysis, we can summarize the necessary conditions of a feasible contract in the following theorem.

Theorem 5.1. ***(Necessary Conditions)*** *A feasible contract* $W = \{w_i, 1 \leq i \leq KLM\}$ *must meet the following two conditions concurrently:* $x_1 \geq \cdots \geq x_i \geq \cdots \geq x_{KLM}$ *and* $r_1 \geq \cdots \geq r_i \geq \cdots \geq r_{KLM}$*.*

5.5.4 Contract Sufficiency

In this section, we resolve the problem of reducing the IR and IC conditions, defined in Eq. (5.13) and Eq. (5.14), respectively, as a means of obtaining an optimal solution for the contract problem designed in Eq. (5.15) in Section 5.5.3. The outcome of this analysis is the definition of the sufficient conditions of a feasible contract under the realistic scenario of incompleteness of information.

Lemma 5.4. ***(IR Conditions Reduction)*** *Under a feasible contract, if the IR condition of the lowest utility user type, i.e., the highest unwillingness-to-participate user type Z_{KLM}, holds, then the IR conditions of all other user types are automatically satisfied:*

$$U_{KLM}(w_{KLM}) \geq 0 \Leftrightarrow U_i(w_i) \geq 0, 1 \leq i \leq KLM. \tag{5.22}$$

Proof. The IC condition that holds between a user type $Z_i, 1 \leq i \leq KLM$ and the lowest utility user type Z_{KLM} is $U_i(w_i) \geq U_i(w_{KLM})$. Furthermore, for the minimum utility user type, it holds that $U_{KLM}(w_{KLM}) \leq U_i(w_{KLM}), 1 \leq i \leq KLM$. Thus, if $U_{KLM}(w_{KLM}) \geq 0$, then $U_i(w_i) \geq 0, 1 \leq i \leq KLM$. This completes the proof. □

The Lemma 5.4 allows the reduction of the KLM IR constraints of the optimization problem in Eq. (5.15) to a single IR constraint, i.e., $U_{KLM}(w_{KLM}) \geq 0$.

Next, we introduce the Pairwise Incentive Compatibility (PIC) condition to facilitate the IC conditions reduction process later in this section.

Lemma 5.5. ***(Pairwise Incentive Compatibility (PIC))*** *The contract bundles $w_i, w_j \in W, 1 \leq i, j \leq KLM, i \neq j$ are pairwise incentive compatible, denoted as $w_i \overset{PIC}{\Longleftrightarrow} w_j$, if the following two conditions are concurrently satisfied: $U_i(w_i) \geq U_i(w_j)$ and $U_j(w_j) \geq U_j(w_i)$.*

Lemma 5.6. ***(IC Conditions Reduction)*** *Under a feasible contract, the following condition holds for any $i_1 < i_2 < i_3$:*

$$\textit{If } w_1 \overset{PIC}{\Longleftrightarrow} w_2 \textit{ and } w_2 \overset{PIC}{\Longleftrightarrow} w_3, \textit{ then } w_1 \overset{PIC}{\Longleftrightarrow} w_3. \tag{5.23}$$

Proof. To prove this lemma, we write the IC conditions that are satisfied for the user types Z_{i1} and Z_{i2}, respectively, as:

$$Q(Z_{i_1}, x_{i_1}) + r_{i_1} \geq Q(Z_{i_1}, x_{i_2}) + r_{i_2}, \tag{5.24}$$

and

$$Q(Z_{i_2}, x_{i_2}) + r_{i_2} \geq Q(Z_{i_2}, x_{i_3}) + r_{i_3}. \tag{5.25}$$

Since $i_1 < i_2 < i_3$, from Theorem 5.1 we have $x_{i_1} > x_{i_2} > x_{i_3}$ and $s(Z_{i_1}, x) < s(Z_{i_2}, x) < s(Z_{i_3}, x)$. Founded upon this, it holds that $\int_{x_{i_3}}^{x_{i_2}} [s(Z_{i_2}, x) - s(Z_{i_1}, x)]dx \geq 0$, on which we subsequently elaborate according to the fundamental theorem of calculus as:

$$\begin{aligned}
&\int_{x_{i_3}}^{x_{i_2}} \left[s(Z_{i_2}, x) - s(Z_{i_1}, x)\right] dx \\
&= \int_{x_{i_2}}^{x_{i_3}} \frac{\partial Q(Z_{i_2}, x)}{\partial x} dx - \int_{x_{i_2}}^{x_{i_3}} \frac{\partial Q(Z_{i_1}, x)}{\partial x} dx \\
&= \left[Q(Z_{i_2}, x_{i_3}) - Q(Z_{i_2}, x_{i_2})\right] - \left[Q(Z_{i_1}, x_{i_3}) - Q(Z_{i_1}, x_{i_2})\right].
\end{aligned} \tag{5.26}$$

Therefore, the following condition holds, also, true:

$$Q(Z_{i_2}, x_{i_3}) - Q(Z_{i_2}, x_{i_2}) \geq Q(Z_{i_1}, x_{i_3}) - Q(Z_{i_1}, x_{i_2}). \tag{5.27}$$

By adding the three inequalities in Eq. (5.24), Eq. (5.25) and Eq. (5.27) by parts, we get:

$$Q(Z_{i_1}, x_{i_1}) + r_{i_1} \geq Q(Z_{i_3}, x_{i_3}) + r_{i_3}. \tag{5.28}$$

Another set of IC conditions that can be written for the user types Z_{i_3} and Z_{i_2}, is:

$$Q(Z_{i_3}, x_{i_3}) + r_{i_3} \geq Q(Z_{i_3}, x_{i_2}) + r_{i_2}, \tag{5.29}$$

and

$$Q(Z_{i_2}, x_{i_2}) + r_{i_2} \geq Q(Z_{i_2}, x_{i_1}) + r_{i_1}. \tag{5.30}$$

By applying similar steps to Eq. (5.26) via the use of the fundamental theorem of calculus, we can easily conclude the next condition:

$$Q(Z_{i_3}, x_{i_2}) - Q(Z_{i_3}, x_{i_1}) \geq Q(Z_{i_2}, x_{i_2}) - Q(Z_{i_2}, x_{i_1}). \tag{5.31}$$

We add Eq. (5.29)-(5.31) by parts and we obtain:

$$Q(Z_{i_3}, x_{i_3}) + r_{i_3} \geq Q(Z_{i_3}, x_{i_1}) + r_{i_1}. \tag{5.32}$$

The combination of Eq. (5.28) and Eq. (5.32) proves that $w_1 \overset{PIC}{\Longleftrightarrow} w_3$, confirming the lemma. □

The Lemma 5.6 enables the reduction of the $KLM(KLM-1)$ IC constraints of the optimization problem in Eq. (5.15) into a set of $2(KLM-1)$ PIC constraints between the adjacent user types Z_i and $Z_{i+1}, 1 \leq i \leq KLM-1$.

By combining our findings in Section 5.5.3 and Section 5.5.4 so far, we can summarize the sufficient conditions for a feasible contract in the Theorem 5.2, below.

Theorem 5.2. ***(Sufficient Conditions)*** *Under a feasible contract, the IR and IC conditions can be reduced as:*

1. $x_1 \geq \cdots \geq x_i \geq \cdots \geq x_{KLM}$,
2. $U_{KLM}(w_{KLM}) \geq 0$,
3. $r_{i+1} - Q(Z_{i+1}, x_i) + Q(Z_{i+1}, x_{i+1}) \leq r_i \leq r_{i+1} + Q(Z_i, x_{i+1}) - Q(Z_i, x_i), 1 \leq i \leq KLM-1$.

The first condition in Theorem 5.2 derives from the necessary conditions in Theorem 5.1, while the second condition stems from the findings in Lemma 5.4 and pertains to the IR conditions reduction. Concerning the third condition in Theorem 5.2, this represents the PIC conditions, as defined in Lemma 5.5, between two adjacent user types i and $i+1$, which constitutes the sufficient condition that should be met as a result of the IC conditions reduction procedure described in Lemma 5.6.

Based on the preceding analysis and the reduced IR and IC conditions listed in Theorem 5.2, the optimization problem in Eq. (5.15) is equivalently transformed as follows:

$$\max_{W} \quad V(W) = \sum_{i=1}^{KLM} Pr_i \left(h(x_i) - \xi r_i\right) \tag{5.33a}$$

$$\textbf{s.t.} \quad \text{Conditions in Theorem 5.2.} \tag{5.33b}$$

Without loss of generality and for ease in the optimal contract bundles' derivation, we consider the users' rewards as strictly increasing functions with their efforts in respect to

the fact that the edge server acts fairly and rewards more the users that provide a higher effort, as described in Theorem 5.1, and we define $r_i(x_i) = \sqrt{Z_i}x_i$. Hence, the edge server's utility function $V(W)$, as described in Eq. (5.12), is concave as the sum of concave functions on $x_i, 1 \leq i \leq KLM$, while the reduced constraints form a convex set. Thus, by applying standard optimization methods and utilizing existing concave/convex optimization tools [88], the optimal contract bundles $w_i^* = \{x_i^*, r_i^*\}, 1 \leq i \leq KLM$.

5.5.5 Benchmark Contract under Complete Information

In this section, a benchmark contract-based incentive mechanism is introduced, which is related to the case of complete information, in the sense that the edge server is a priori aware of the users' private information, i.e., their unwillingness-to-participate user types. Under this ideal case, the edge server can fully exploit the users' efforts and marginally satisfy their IR conditions to ensure their participation in the contract. Hence, the optimization problem to be solved by the edge server for each user type $1 \leq i \leq KLM$ is written as follows:

$$\max_{w_i} \quad v_i = h(x_i) - \xi r_i, 1 \leq i \leq KLM, \tag{5.34a}$$

$$\textbf{s.t.} \quad Q(Z_i, x_i) + r_i = 0. \tag{5.34b}$$

From Eq. (5.34b) we get $r_i^* = -Q(Z_i, x_i) = Z_i x_i^2$, while Eq. (5.34a) is written as $v_i = h(x_i) - \xi r_i = \frac{c}{1-\lambda} x^{1-\lambda} - \xi r_i$, based on the provided definitions of the functions $Q(\cdot)$, $q(\cdot)$, $h(\cdot)$ earlier in this section. By substituting r_i^* back to v_i and calculating the first order derivative of v_i with respect to x_i, we get $\frac{\partial v_i}{\partial x_i} = \frac{c}{x_i^\lambda} - 2\xi Z_i x_i$. By solving the equation $\frac{\partial v_i}{\partial x_i} = 0$ with respect to x_i we obtain the optimal solution of the optimization problem, which is expressed as $x_i^* = \left(\frac{c}{2\xi Z_i}\right)^{\frac{1}{1+\lambda}}$.

Concerning the feasibility of the optimization problem in Eq. (5.34a)-(5.34b), by taking into account that $\xi \geq 1$, $c \in [0, 1]$, $\lambda \in (0, 1)$ and $Z_i \in [0.5, 2.5], 1 \leq i \leq KLM$, the latter of which is determined by calculating the extreme values of the term $Z_i = 1.5 + \delta_i - \beta_i \gamma_i$, it holds that $x_i^* \geq 0, 1 \leq i \leq KLM$. Additionally, considering the extreme case that $c = \xi = 1$ and $Z_i = 0.5$, under which the term $\frac{c}{2\xi Z_i}$ takes its highest value that is equal to $\frac{c}{2\xi Z_i} = 1$, it is verified that $x_i^* \leq 1, 1 \leq i \leq KLM$. Hence, the optimal solution x_i^* is within the required range $[0, 1]$, yielding a feasible solution to the problem.

5.6 Stackelberg Game-based Resource Allocation

After the completion of the multi-dimensional contract-based incentive mechanism, each user n has autonomously - and via the interaction with the edge server - determined its optimal amount of effort, i.e., the percentage x_n^* of the task $\phi_n d_n$ that is offloaded to the edge, which is allowed to be further transmitted and processed at the fog. Depending on the user's n application's A_n characteristics, each user n is represented by an unwillingness-to-participate user type Z_i and, thus, the optimal contract bundle for this user is $w_n^* = \{x_n^*, r_n^*\} \leftrightarrow w_i^* \in W = \{w_i^*, 1 \leq i \leq KLM\}$.

At this second stage, the joint communications and computing resource allocation is pursued under a Stackelberg game-theoretic approach, in which the edge server (i.e., the leader) determines each user's n optimal offloaded task $\phi_n d_n^*$ and the users (i.e., the followers) decide on their optimal uplink transmission power p_n^* iteratively, by exchanging information between each other. Specifically, with the term "task offloading optimization" we refer to the optimal amount of bytes d_n^* offloaded by each user n that determine the whole optimal amount of offloaded task $\phi_n d_n^*$. It should be noted that the joint computation task offloading

and uplink transmission power allocation problem in NOMA-enabled computing environments, under both the energy efficiency maximization and the delay/time minimization objectives, as adopted in this work and presented later in this section, is generally non-convex and NP-hard [156, 157, 141]. As a result, there does not exist any algorithm that provides an optimal solution to this joint problem in polynomial time. For this reason, either approximation or alternating [158] optimization algorithms are proposed in the literature to deal with it. Indeed, the proposed Stackelberg game-theoretic approach is aligned with both the decentralized and iterative optimization needs of the considered two-variable problem. Next, the optimization problems of the leader and followers are presented, while the overall incentive mechanism and resource allocation framework is summarized in Algorithm 5.1.

5.6.1 Leader's Optimization

Given the users' uplink transmission power vector $\mathbf{p} = [p_1, \ldots, p_n, \ldots, p_N]$, the edge server seeks to maximize its perceived satisfaction minus the end-to-end edge-fog computing environment's incurred energy overhead. To this end, the edge server determines the vector of the optimal amount of offloaded bytes $\mathbf{d}^* = [d_1^*, \ldots, d_n^*, \ldots, d_N^*]$, while meeting the users' end-to-end completion time and energy constraints, and its personal energy constraint that stems from its inherent limitation on its available energy. Therefore, the corresponding optimization problem that is treated by the edge server is formulated as follows:

$$\max_{\mathbf{d}} \quad \sum_{n=1}^{|N|} \left[1 - e^{\frac{2d_n}{D_n}} - \mathcal{C} \left(E_n^{off} + E_n^{exec} + E_e^{n,off} + E_e^{n,exec} \right) \right] \tag{5.35a}$$

$$\textbf{s.t.} \quad 0 \leq d_n \leq D_n, \forall n \in \mathcal{N}, \tag{5.35b}$$

$$\max\{T_n^{off}, T_n^{exec}\} + \max\{T_e^{n,off}, T_e^{n,exec}\} \leq T_n, \forall n \in \mathcal{N}, \tag{5.35c}$$

$$E_n^{off} + E_n^{exec} \leq E_n, \forall n \in \mathcal{N}, \tag{5.35d}$$

$$\sum_{n=1}^{N} \left(E_e^{n,off} + E_e^{n,exec} \right) \leq E_e. \tag{5.35e}$$

Regarding the physical meaning and interpretation of the edge server's utility function in Eq. (5.35a), the term $1 - e^{\frac{2d_n}{D_n}}$ constitutes a strictly increasing and concave function with respect to each user's n amount of offloaded bytes d_n, expressing the edge server's satisfaction, which saturates as its computational burden increases. The remainder of Eq. (5.35a) constitutes the end-to-end edge-fog computing environment's total energy consumption (overhead), while $\mathcal{C} \in \mathbb{R}^+$ is a cost-of-energy constant factor measured in [1/J]. Concerning the optimization problem's constraints, Eq. (5.35b) indicates the feasible range of values of each user's amount of offloaded bytes d_n. Eq. (5.35c) represents each user's n end-to-end completion time requirement, which is calculated as the sum of the maximum time overheads from the transmission and the execution at the user and the edge server layers, assuming that the wireless transmission and computation processes can be performed concurrently. Last, Eq. (5.35d) and Eq. (5.35e) guarantee each user device's and the edge server's energy consumption constraint, respectively, where E_e [J] is the edge server's maximum energy constraint.

The optimization problem in Eq. (5.35a)-(5.35e) is concave, since the utility function is a sum of concave functions on $d_n, \forall n \in \mathcal{N}$ and the constraints form a compact, i.e., closed and bounded, and convex set. Therefore, to derive the optimal solution, which is the vector of the optimal amount of offloaded bytes $\mathbf{d}^* = [d_1^*, \ldots, d_n^*, \ldots, d_N^*]$, existing concave/convex optimization tools can be utilized [88].

5.6.2 Followers' Optimization

Given the amount of offloaded bytes d_n for each user n, after broadcasting by the edge server to the users, the users' uplink transmission power control takes place. Specifically, each user aims to distributively maximize its transmission-based energy efficiency, by optimizing its uplink transmission power to the edge server, while satisfying its personal transmission time requirement. As a result, the optimization problem to be solved by each user n is given by:

$$\max_{p_n} \quad EE_n(p_n, \mathbf{p}_{-n}) = \frac{R_n}{p_n}, \forall n \in \mathcal{N} \tag{5.36a}$$

$$\textbf{s.t.} \quad 0 \leq p_n \leq p_n^{max}, \forall n \in \mathcal{N}, \tag{5.36b}$$

$$G_n p_n - \sum_{n'=1}^{n-1} G_{n'} p_{n'} \geq p_{tol}, n = 2, \ldots, N, \tag{5.36c}$$

$$T_n^{off} \leq T_n^{off,max}, \forall n \in \mathcal{N}. \tag{5.36d}$$

In the above optimization problem, Eq. (5.36a) represents the user's n energy efficiency utility function, where $\mathbf{p}_{-n} = [p_1, \ldots, p_{n-1}, p_{n+1}, \ldots, p_N]$ is the vector of uplink transmission powers of all users except for user n. The constraint in Eq. (5.36b) guarantees the user's satisfaction of its maximum uplink transmission power budget p_n^{max}, while Eq. (5.36c) guarantees the successful decoding of the user's signal via the SIC technique at the edge server's receiver, according to the receiver's sensitivity/tolerance p_{tol}. Eq. (5.36d) refers to the user's personal transmission time constraint $T_n^{off,max}$ [s].

To capture the interplay among the different users' power control procedure, a non-cooperative game is formulated among them, denoted as $\Pi = [\mathcal{N}, \{\Sigma_n\}_{\forall n \in \mathcal{N}}, \{EE_n\}_{\forall n \in \mathcal{N}}]$, where $\mathcal{N}$ is the set of players, i.e., the users, Σ_n is each user's strategy set of feasible power levels, as imposed by the constraints in Eq. (5.36b)-(5.36d), and EE_n is each user's utility function. The non-cooperative game Π is treated as a distributed utility maximization problem, in which each user n updates its uplink transmission power p_n autonomously, by possessing prior information about the other users' transmission power levels $\mathbf{p}_{-n}$, as broadcasted by the edge server.

Towards solving the non-cooperative game Π, the concept of Nash equilibrium is adopted, and the optimal users' strategy vector $\mathbf{p}^* = [p_1^*, \ldots, p_n^*, \ldots, p_N^*]$, from which no user has the incentive to deviate given the strategies of the rest of the users, is determined via a Best Response Dynamics (BRD) algorithm. The interested reader may refer to [159] regarding the definition of the Nash equilibrium, as well as the description of the BRD algorithm. To ensure the existence of at least one Nash equilibrium point for the non-cooperative game Π and thus, the convergence of the users' strategies to the Nash equilibrium , we adopt the theory of the n-person generalized concave games [121].

Theorem 5.3. ***(Existence of Nash Equilibrium)*** *The non-cooperative game Π is a n-person generalized concave game and admits at least one Nash equilibrium point if the following conditions hold true [121]:*

1. *the strategy sets $\Sigma_1, \ldots, \Sigma_N$ are non-empty, compact, convex subsets of finite dimensional Euclidean spaces,*

2. *all utility functions $EE_1, \ldots, EE_N$ are continuous on $\Sigma = \Sigma_1 \times \cdots \times \Sigma_N$,*

3. *every utility EE_n is a quasi-concave function of p_n over Σ_n if all the other strategies are held fixed.*

The energy efficiency problem under consideration has been extensively studied in the literature and it is well known that bears the properties that are summarized in Theorem 5.3 [160, 32], while an extensive proof of Theorem 5.3 can be found in Chapter 4 and Section 4.5.3. Given that each follower's, i.e., user's, distributed optimization problem in Eq. (5.36a)-(5.36d) is quasi-concave due to the quasi-concave energy efficiency function, this can be effectively treated by applying the Dinkelbach's algorithm [119, 32] , which transforms the quasi-concave problem into a series of concave problems that are iteratively solved until convergence. Accordingly, each concave problem can be solved based on existing optimization tools [88].

After the convergence of the non-cooperative game, the users' optimal uplink transmission powers $\mathbf{p}^*$ are fed back to the edge server, and the next iteration of the Stackelberg game is established. This procedure is repeated until convergence of the overall Stackelberg game is reached and the Stackelberg equilibrium point $(\mathbf{d}^*, \mathbf{p}^*)$ is found, according to which neither the edge server nor the users have any incentive to deviate from, as shown in Algorithm 5.1.

Algorithm 5.1 Incentive and resource allocation framework.

Initialize the discrete sets $\mathcal{D}$, Φ, $\mathcal{T}$, B, Γ, Δ.
Calculate the unwillingness-to-participate user types $Z_i, 1 \leq i \leq KLM$ and sort them in ascending order.
Initialize ξ, c, λ, $r(\cdot)$, $q(\cdot)$, $h(\cdot)$.
Design the optimal contract bundles $w_i^* = \{x_i^*, r_i^*\}, 1 \leq i \leq KML$ by solving Eq. (5.33).

Initialize the set $\mathcal{N}$ and the edge-fog computing environment, including users', edge, and fog servers' locations.
Initialize D_n, ϕ_n, T_n, E_n, G_n, p_n^{max}, $T_n^{off,max}$, F_n, σ_n, E_e, G_e, p_e, W_e, a_e, F_e, σ_e, W_f, a_f, ρ, I_0, p_{tol}, $\mathcal{C}$.
Map each user to its optimal contract bundle $w_n^* = \{x_n^*, r_n^*\} \leftrightarrow w_i^* \in W = \{w_i^*, 1 \leq i \leq KLM\}$.
Sort the users in ascending order according to G_n.
Initialize randomly $p_n \in [0, p_n^{max}], \forall n \in \mathcal{N}$.
Set $i = 0$.
repeat
  Set $i = i + 1$.
  Determine the optimal amount of offloaded bytes $d_n^{*(i)}, \forall n \in \mathcal{N}$ by solving Eq. (5.35a)-(5.35e).
  Set $j = 0$.
  repeat
    Set $j = j + 1$.
    for $n \in \mathcal{N}$ **do**
      Determine the optimal uplink transmission power $p_n^{*(j)}$ by solving Eq. (5.36a)-(5.36d).
    end for
  until $|p_n^{*(j)} - p_n^{*(j-1)}| \leq \epsilon, \forall n \in \mathcal{N}$, where $\epsilon \approx 10^{-5}$.
until $|d_n^{*(i)} - d_n^{*(i-1)}| \leq \epsilon, \forall n \in \mathcal{N}$, where $\epsilon \approx 10^{-5}$.

5.6.3 Computation Complexity

To facilitate the derivation of the overall proposed incentive mechanism and resource allocation algorithm's computation complexity, as presented in Algorithm 5.1, the following

algorithmic complexities are considered alone. First, the asymptotic complexity of a convex optimization problem is polynomial in the number of the optimization variables [111, 32], which applies to the optimization problems in Eq. (5.33), Eq. (5.35a)-(5.35e) and Eq. (5.36a)-(5.36d), while the Dinkelbach's algorithm has super-linear convergence rate [119, 120]. The users' sorting concerning their channel gain can be performed with $\mathcal{O}(N^2)$ complexity via the Quicksort algorithm, while for the mapping of each user to its optimal contract bundle a searching algorithm can be employed, e.g., the Binary Search Algorithm, whose algorithmic complexity is $\mathcal{O}(log(KLM))$ in our case, due to the KLM existing contract bundles. The rest of typical mathematical manipulations are of $\mathcal{O}(1)$ complexity.

We indicate as I and J the total number of iterations required for the Stackelberg and the non-cooperative game among the users to converge, respectively. Also, following commonly used practices, we denote as I_D the total number of iterations required for the Dinkelbach algorithm to converge when solving a single user's optimization problem in Eq. (5.36a)-(5.36d). As a result, considering that the distributed non-cooperative game among the users is performed in parallel, the overall computation complexity of Algorithm 5.1 is calculated as $\mathcal{O}\left(2 \cdot KLM + N \cdot log(KLM) + N^2 + I \cdot (N + J \cdot I_D \cdot 1)\right)$. Indicative numerical results that depict the actual number of Stackelberg game iterations, which are required until convergence is met, are enclosed in Section 5.7.2 below.

5.7 Performance Evaluation

This section is devoted to the performance evaluation of the proposed incentive mechanism and the joint task offloading and uplink power control procedure, via modeling and simulation. First, we examine the operational characteristics of the multi-dimensional contract-based incentive mechanism, considering, also, the benchmark contract under complete information (as described in Section 5.5). Subsequently, we focus on validating the operation and performance of the Stackelberg game-based joint task offloading and power control problem, accounting for its convergence behavior, as well as comparing it against various alternative baseline offloading approaches. It should be noted that NOMA has been adopted as an underlying technique to facilitate the users' multiplexing and transmissions to the edge. The results of this work are also presented in [161].

The simulation setting and the parameters that were used throughout the numerical evaluation enclosed in the remainder of this section are initialized as follows. We consider a two-layer edge-fog computing environment, consisting of an edge server, which lies 200 m away from a fog server, and N users deployed with 20-meter increasing distance from the edge server that form a NOMA cluster. Each user has a computing application A_n, whose characteristics can be derived from the following sets: $\mathcal{D} = \{1, 1.2, 1.4\}$ Mbits, $\Phi = \{20, 30, 40\}$ CPU cycles/bit, $\mathcal{T} = \{0.08, 0.1, 0.12\}$ s and $\mathcal{E} = \{1\}$ J. As a result, we assume that there exist $K \times L \times M = 3 \times 3 \times 3$ different combinations of user application characteristics. The users offload part of their computation tasks to the edge server, while a part of them can be further forwarded by the edge server to the fog, if beneficial. Both the users-to-edge server and edge-to-fog server transmissions are performed wirelessly, while the corresponding bandwidth in the two transmission levels is defined as $W_e = 5$ MHz and $W_f = 1$ MHz, accordingly. Other communications-related parameters are set as: $p_n^{max} = 24$ dBm, $T_n^{off,max} = 0.05$ s, $p_e = 24$ dBm, $a_e = 3.5$, $a_f = 2$, $E_e = 200$ J, $\rho = -20$ dB, $I_0 = -174$ dBm/Hz, $p_{tol} = -114$ dBm. Considering the computing-related parameters, we consider $F_n = 10^9$ CPU cycles/s and $\sigma_n = 10^{-27}$ J/CPU cycle for each user, and $F_e = 5 \times 10^{11}$ CPU cycles/s and $\sigma_e = 10^{-29}$ J/CPU cycle for the edge server [142]. Last, regarding the multi-dimensional contract we define the parameters $c = 0.5$, $\lambda = 0.8$, $\xi = 1$, while we set $\mathcal{C} = 10^4$ in the Stackelberg game, subsequently. Finally, for statistical purposes, the numerical results enclosed in Section 5.7.2, below, which pertain to the

Stackelberg game-based resource allocation procedure, have been averaged over 100 different users' computing application characteristics' realizations.

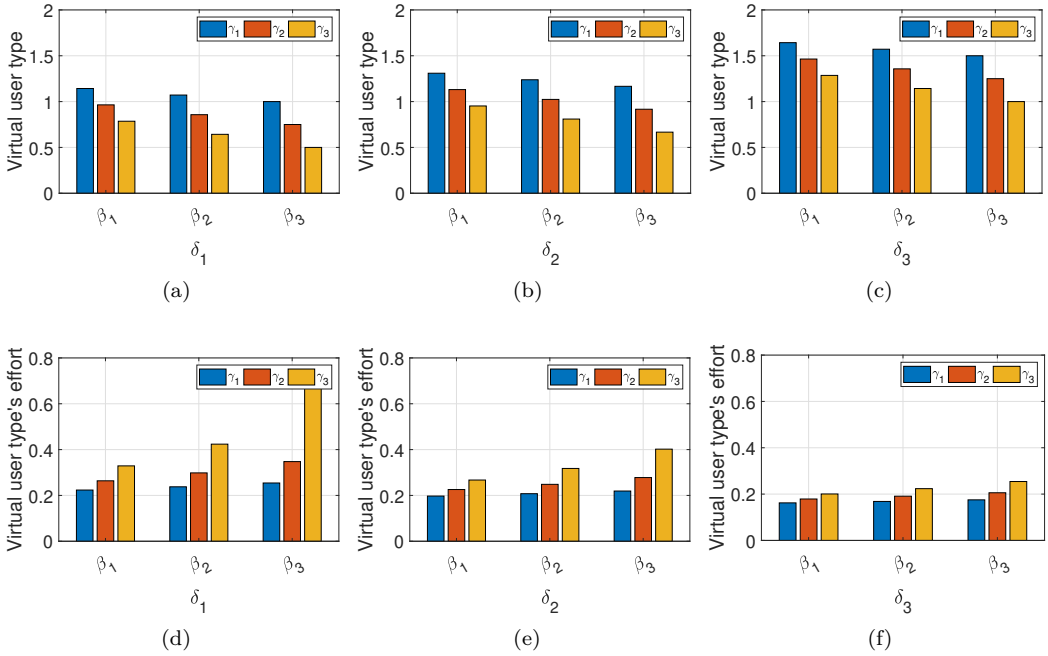

Figure 5.3: Pure evaluation of multi-dimensional contract under different values of the three-dimensional user types (β, γ, δ).

5.7.1 Evaluation of Multi-dimensional Contract-based Incentive Mechanism

Given that there exist $K \times L \times M = 3 \times 3 \times 3$ different combinations of user application characteristics, then, $3 \times 3 \times 3$ different unwillingness-to-participate user types are formed, capturing the (un)willingness to allow part of their initially offloaded tasks to the edge to be further forwarded and processed at the fog. In this section, we first scrutinize the pure operation of the designed multi-dimensional contract, by analyzing the behavior and trend of the resulting $3 \times 3 \times 3$ unwillingness-to-participate (or virtual) user types and their suited optimal efforts, under different values of the three-dimensional private information (β, γ, δ). In particular, in Fig. 5.3, the values of the virtual user types and their optimal efforts are depicted as a function of the different values of (β, γ, δ), assuming that are sorted in ascending order as $\beta_1 \leq \beta_2 \leq \beta_3$, $\gamma_1 \leq \gamma_2 \leq \gamma_3$ and $\delta_1 \leq \delta_2 \leq \delta_3$. From Fig. 5.3a-5.3c, we observe that as the delay sensitivity evaluation type δ increases, then the values of the virtual user types increase, resulting in lower provided efforts to the edge server in Fig. 5.3d-5.3f, which in turn, verify the monotonicity condition of the contract in Lemma 5.3. Focusing on a single value of δ, e.g., δ_1 in Fig. 5.3a, then it can be easily deduced that a low value of either parameter β or γ results in a higher value of the virtual user type, according to the definition of the unwillingness-to-participate parameter in Eq. (5.17). As a result of the higher unwillingness to participate in the contract, the users' efforts decrease, as shown in Fig. 5.3d. The same observation holds for the instances δ_2 and δ_3 regarding the values of the virtual user types in Fig. 5.3b-5.3c and their optimal efforts in Fig. 5.3e-5.3f, respectively.

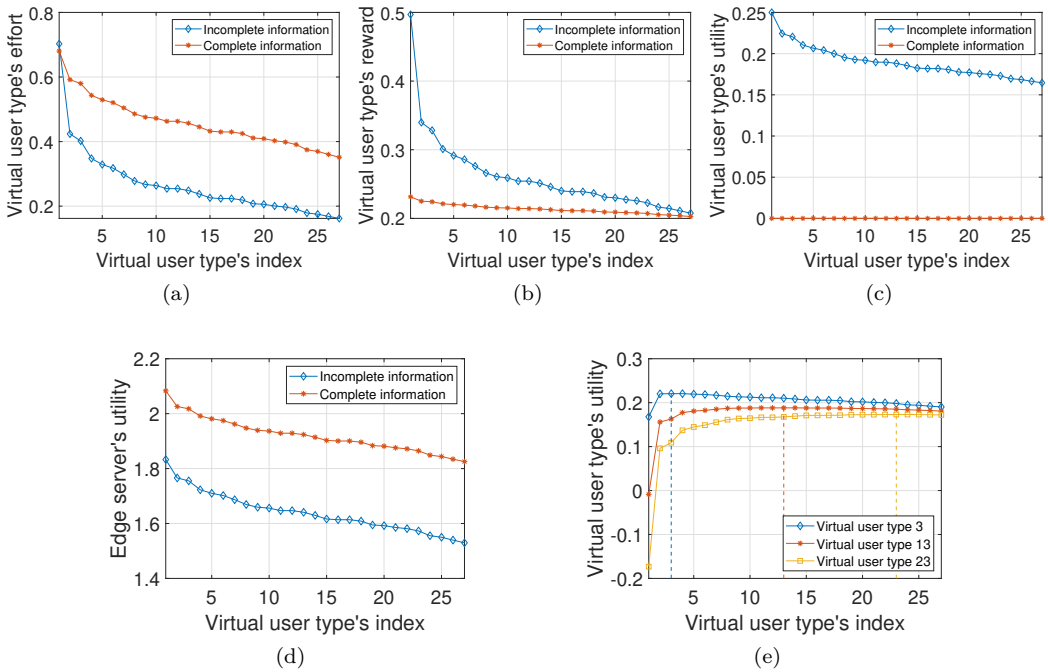

Figure 5.4: Comparative evaluation of multi-dimensional contract under incomplete and complete information cases.

This is quite intuitive, since β and γ represent an evaluation of the application size and intensity, higher values of which show the "need" to participate in the contract to offload as many bytes as possible.

Next, we proceed to the comparative evaluation of the proposed multi-dimensional contract, taking into account the benchmark complete information contract case. To this end, in Fig. 5.4, we consider the $K \times L \times M$ virtual user types sorted in ascending order as $Z_1(x) \leq \cdots \leq Z_i(x) \leq \cdots \leq Z_{KLM}(x), 1 \leq i \leq KLM$, indicating them by their sorted index (horizontal axis), and we examine the values of different metrics, such as their efforts, rewards or utilities (vertical axis), under both the incomplete and complete information cases. All graphs in Fig. 5.4a-5.4d validate the monotonic behavior of the designed contract, according to which a higher unwillingness-to-participate/virtual user type provides a lower effort to the edge server, and, hence, is rewarded less, yielding at lower utilities for both itself and the edge server. Evidently, in the complete information case, the edge server designs contract bundles that require higher efforts to be provided by the users in exchange for lower rewards compared to the incomplete information case. This naturally stems from the fact that the edge server knows a priori the users' types and fully exploits their efforts, by marginally ensuring their participation in the contract, i.e., the satisfaction of their Individual Rationality (IR) conditions, as expressed in Eq. (5.34b). Accordingly, in the complete information case, each virtual user type perceives a zero utility, as illustrated in Fig. 5.4c, while the edge server achieves a higher utility per user type under such an ideal complete information availability case compared to the incomplete information one (Fig. 5.4d). To complement our evaluation of the multi-dimensional contract-based incentive mechanism, we investigate the derived optimal contract bundles' compliance to the Incentive Compatibility (IC) condition in Definition 5.2. For this reason, the virtual user types of index 3, 13,

and 23 are indicatively selected and their utility values are plotted over all the $K \times L \times M$ contract bundles that have been designed by the edge server (horizontal axis), as shown in Fig. 5.4e. Indeed, it can be easily observed that the utility of either virtual user type from the 3, 13, and 23 is maximized when selecting the contract bundle that is tailored to this specific type, verifying the incentive compatibility of the designed contract.

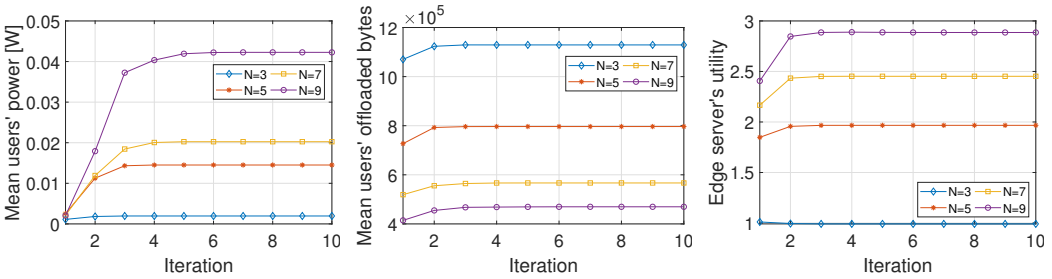

(a) (b) (c)

Figure 5.5: Convergence evaluation of Stackelberg game-based resource allocation under different numbers of users N.

5.7.2 Evaluation of Non-Cooperative Game-based Offloading Mechanism

In this section, we aim to elucidate the operational characteristics of the proposed Stackelberg game-based overall task offloading and power control procedure. To this end, we initially study the pure performance and convergence behavior of the proposed Stackelberg game, by examining the progression in the values of different metrics as a function of the different iterations that are required for the game to converge. In particular, Fig. 5.5a-5.5b presents the mean users' transmission power levels and amount of offloaded bytes, accordingly, concerning the corresponding Stackelberg game iteration index. The different curves that are incorporated in Fig. 5.5a-5.5b, correspond to different scenarios with respect to the number of users existing in the system, i.e., $N = \{3, 5, 7, 9\}$, that share the same wireless access bandwidth and are multiplexed via the NOMA technique. Additionally, Fig. 5.5c depicts the edge server's utility, as defined in Eq. (5.35a) in the leader's optimization problem in Section 5.6.1, as a function of the Stackelberg game iteration index.

The results reveal that the overall interaction between the leader and the followers, via the Stackelberg game, is completed after a small number of iterations (i.e., approximately $I = 6$ iterations for practical purposes), while the number of iterations required increases with the number of the users existing in the NOMA cluster. This can be easily noticed and verified by comparing the curves that regard $N = 3$ and $N = 9$ number of users in Fig. 5.5a-5.5c. Furthermore, it is confirmed that as the number of users increases, then their mean consumed uplink transmission power, as derived from the non-cooperative game among them in Section 5.6.2, increases as well, whereas their mean offloaded bytes to the edge server decrease, as calculated by the leader's optimization problem in Section 5.6.1. On the one hand, the latter originates from the fact that the overall sensed interference by the users within the NOMA cluster increases, affecting, i.e., reducing, their achieved data rate and, hence, increasing the required time to transmit their data. On the other hand, this behavior is, also, encouraged by the edge server's, i.e., the leader's, utility function, which expresses the edge server's dissatisfaction and disutility from the increase in the amount of offloaded bytes by each user and is denoted by the term $1 - e^{\frac{2d_n}{D_n}}$ in Eq. (5.35a). On the

contrary, considering the absolute increase in the sum of users' offloaded bytes due to the increase in the number of users in the system, the edge server's utility increases, as can be seen in Fig. 5.5c.

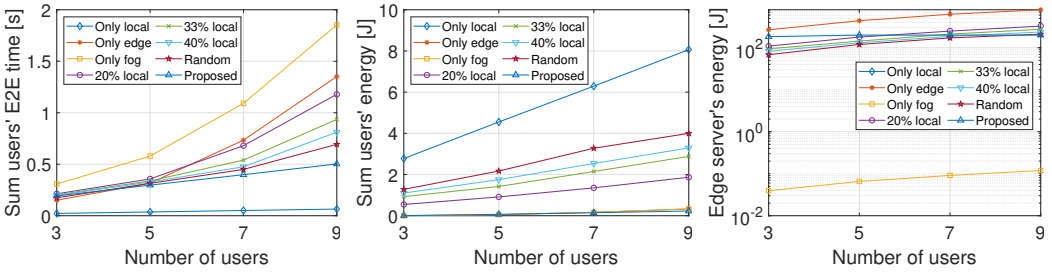

(a) (b) (c)

Figure 5.6: Comparative evaluation of Stackelberg game-based resource allocation under different offloading approaches and number of users N.

Subsequently, we aim to investigate the effectiveness and efficiency of the proposed Stackelberg game-based resource allocation, by comparing it against various alternative baseline offloading approaches. Specifically, in our comparative analysis we consider the cases in which the users' tasks are computed: exclusively locally ("Only local"), at the edge ("Only edge"), or at the fog ("Only fog"), as well as indicative intermediate cases that 20%, 33% or 40% of the users' total bytes are computed locally, denoted as "20% local", "33% local" and "40% local", respectively, are also taken into account. In these latter cases the rest offloaded amount of bytes, i.e., 80%, 67%, and 60% of the overall user application bytes, is equally split between the edge and fog server layers. Last, we, also, invoke the "Random" offloading baseline case, under which a random amount of bytes is offloaded to the edge and fog server layers. At this point, it should be noted that for fairness purposes in all of the aforementioned offloading approaches that require users-to-edge server wireless transmissions, the non-cooperative game among the users that determines their optimal uplink transmission powers to the edge, is performed without exception.

Fig. 5.6a presents the sum of users' end-to-end time overhead, which is calculated based on Eq. (5.35c), concerning the different offloading approaches and different numbers of users existing in the system. Apparently, our proposed approach exhibits the lowest sum users' end-to-end time overhead, with the lowest marginal increase with the number of users, except for the "Only local" case, which benefited in terms of time by the zero users-to-edge server and edge-to-fog server wireless transmissions. However, as clearly shown in Fig. 5.6b, this latter behavior of the "Only local" case occurs at the cost of much higher energy consumption (i.e., the worst performance among all alternatives) for the energy-constrained user devices due to local execution, as is discussed later in this section.

To better visualize the effect of the increased users' end-to-end time overhead on the satisfaction of their completion time requirement $T_n, \forall n \in \mathcal{N}$, we summarize the percentages of the users that successfully met their time constraints in Table 5.1, considering all the aforementioned offloading alternatives for different number of users in the system. It should be noted that in the designed simulation setup, the "Only local" case provides always a feasible solution in terms of user time satisfaction, though at the cost of high energy consumption from the users' perspective. As demonstrated by the provided results in Table 5.1, the proposed approach proves to be the only one among the rest of the examined offloading alternatives that allows for the satisfaction of the users' completion time constraints under varying numbers of users. Especially, as the number of users increases, e.g., $N = 9$, the

majority of the baseline offloading approaches fail to satisfy the users' requirements, while in most cases the percentage of satisfied users drops significantly below 50%. Therefore, it becomes apparent, that the dynamic and adaptive features of our proposed optimization-driven approach, achieve the 100% assurance of each user's end-to-end completion time requirement in all considered settings.

Table 5.1: Percentage of users that satisfy their end-to-end time requirement under different offloading approaches.

Approach	$N = 3$	$N = 5$	$N = 7$	$N = 9$
Only local	100%	100%	100%	100%
Only edge	100%	90.8%	50%	34.89%
Only fog	44.67%	32%	15.43%	10.67%
20% local	100%	98.8%	61.14%	36.45%
33% local	100%	100%	86.29%	53.33%
40% local	100%	100%	97.43%	66.89%
Random	97.33%	95.6%	93.71%	81.11%
Proposed	100%	100%	100%	100%

Continuing, in Fig. 5.6b, the sum users' energy overhead, which accounts for both the wireless transmissions to the edge and their local computation energy consumption, according to Eq. (5.35d), is depicted, verifying that the proposed approach yields the lowest sum users' energy consumption along with the "Only edge" and "Only fog" baseline cases. However, it is reminded that these other two alternatives, as shown in Table 5.1, fail to meet the user time constraints for most of the users in most of the different numbers of user cases, thus resulting in lower user satisfaction percentages compared to the proposed one. Concerning the edge server's energy consumption, which is derived following Eq. (5.35e) and accounts, also, for both the wireless transmission and the computation energy overheads, Fig. 5.6c demonstrates that in our proposed approach, the edge server operates at its maximum allowed energy consumption point, as denoted by the E_e constraint, while the "Only fog" case intuitively incurs significantly low energy consumption to the edge, at the excessive cost of increased users' energy consumption. It is noteworthy that in Fig. 5.6c, the "Only local" case that results in zero edge server's energy consumption is omitted due to the inherent limitation of the logarithmic scale used. Regarding the rest of the alternative scenarios, i.e., "20% local", "33% local", "40% local" and "Random", they appear to yield similar edge server energy consumption, slightly exceeding the edge server's upper energy consumption point E_e as the number of users increases, in contrast to the "Only edge" scenario, which steadily exceeds the edge server's upper energy consumption bound, having to deal with the whole system's computation burden.

Chapter 6

Resource Allocation in RSMA Multi-server Multi-access Edge Computing Networks

6.1 General Setting

In this chapter, we delve into the distribution of the users' offloaded computation tasks horizontally (i.e., within the same computing tier) to multiple servers. Specifically, motivated by the distributed deployment of Multi-Access Edge Computing (MEC) servers within the Radio Access Network (RAN) and the advancements in next-generation non-orthogonal multiple access techniques, we suggest that the users utilize the different available RANs nearby and offload computation tasks of their compute-intensive and latency-critical applications to multiple MEC servers simultaneously. To tackle the critical problem of inter-server interference management stemming from the concurrent transmissions of a user to multiple servers, we examine the application of the Rate-Splitting Multiple Access (RSMA) technique, which is considered a key enabler of the upcoming 6G wireless networks. The rate-splitting lies in splitting a user's message into two or more parts that can be flexibly decoded at one or more receivers, respectively. The common message – as it is called – is intended for and decoded by all the involved servers in the transmission, contrary to a private message intended for each MEC server separately. As a result, when decoding the private message, the interference originating from the other servers' private messages is treated as noise. By smartly controlling the split among the common and private messages, an acceptable tradeoff between efficient spectrum usage, multi-server interference management, and signal processing complexity at the receivers is achieved.

Apparently, the MEC network's performance is majorly interwoven with the radio resource allocation under the RSMA technique to achieve the user application's targeted latency requirement and thus should be studied jointly. Consequently, the challenging problem of joint computation task offloading and radio and computing resource allocation among the users and the multiple MEC servers arises, which remains mainly unsolved in the literature, and we strive to address it. Specifically, in this chapter, we introduce a holistic solution to minimize the sum of users' maximum experienced delay among the different MEC servers, stemming from both the computation task offloading and processing. To this end, the users' computation task assignment ratios to the different MEC servers, and their allocated rates, uplink transmission powers, and computing resources with reference to the corresponding MEC server are jointly optimized. The formulated min-max-sum problem

is equivalently transformed and decomposed into two independent sub-problems, namely the rate and power allocation and the computing resource allocation problems, while the optimal solution of computation task assignment naturally derives from the aforementioned transformation and decomposition procedure. In this way, a near-optimal solution to the initial problem is concluded that is proved to be highly efficient in terms of complexity and experienced delay by the users compared to conventional non-linear optimization algorithms.

6.2 Related Work

The problem of joint task offloading and resource allocation in MEC networks is well-established in the literature and has been extensively studied under different network settings and objectives over the years. Preliminary works focused on single-server network topologies, and can be further distinguished according to the adopted wireless access technique, i.e., Orthogonal Frequency Division Multiple Access (OFDMA) [162], power-domain NOMA [141], and Multi-Carrier (MC)-NOMA [163]. In [162], the joint problem of computation task assignment, computing resource allocation, and subcarrier allocation is treated via an iterative algorithm, to minimize the total MEC system's energy consumption. In [141], the authors consider a pure NOMA case and perform computation task assignment and uplink power control to minimize the maximum task completion time among the users. The formulated minimax optimization problem is then solved via a bisection search iterative algorithm. Complementary to the above, the work in [163] considers MC-NOMA and jointly optimizes the users' task offloading decision, subchannel assignment, uplink transmission power, and allocated computing resource to minimize the weighted sum of the system's computation time and energy overhead. Last, a comparative analysis over Orthogonal Multiple Access (OMA)-based and NOMA-based MEC systems is presented in [164] regarding the problem of minimizing the total system's energy consumption.

However, a remarkable amount of work can also be found on multi-server MEC network topologies, employing both OMA [165, 166] and power-domain NOMA [167, 168, 169, 170]. Both works in [165, 166] account concurrently for multiple optimization objectives (e.g., minimization of MEC system's total time and energy overhead, users' subscription cost) and derive the task offloading decision and the power and computing resource allocation of the users. Considering the NOMA-based MEC topologies, the works in [167, 168, 169] target the MEC system's energy consumption minimization, whereas [170] pursues each user's maximum task completion time minimization among the different MEC servers. All of them optimize quite similar sets of variables but differ in the optimization techniques used such as Reinforcement Learning (RL) algorithms apart from conventional optimization [167], the underlying network setting in terms of perfect or imperfect Channel State Information (CSI) [168], and the consideration of the additional problem of Central Processing Unit (CPU) frequency scheduling along [169]. Although multi-server MEC topologies are considered, the concurrent task offloading to multiple MEC servers is exclusively studied in [167, 168, 170], the former two of which focus on the sum system's energy consumption minimization. As a result, the problem of minimizing the sum of users' maximum experienced delay among multiple MEC servers that results in a min-max-sum problem formulation remains notably unexplored.

Regarding the literature around the RSMA technique, several works have been recently published dealing with fundamental problems related to resource allocation in pure wireless communication scenarios. Indicative examples constitute the works in [27, 171, 172, 173, 174], where the joint rate and power control are performed under different performance metrics. In [27] and [171], the sum-rate and weighted sum-rate maximization in downlink multi-user Sinlge-Input Single-Output (SISO) and Multiple-Input Single-Output (MISO) systems are studied, respectively, and two different iterative algorithms are proposed to ob-

tain solutions to the formulated non-convex problems. The energy efficiency of a two-user downlink RSMA MISO system is pursued in [172], while another interesting approach towards controlling the spectral and energy efficiency tradeoff in a multi-user downlink RSMA Multiple-Input Multiple-Output (MIMO) system appears in [173]. Considering learning-based optimization frameworks, the authors in [174] design and propose the application of Deep Reinforcement Learning (DRL) algorithms to target both the sum-rate and energy efficiency maximization in downlink multi-user RSMA networks. Moving one step further, the authors in [175] introduce the model of RSMA-based Simultaneous Wireless Information and Power Transfer (SWIPT) in MISO Broadcast Channels (BC) and study the precoder design of the Information Receivers (IRs) and the Energy Receivers (ERs) along with the common-message rate control problem to maximize the system's weighted sum rate.

Other attempts are gradually being made in the direction of exploiting the benefits of RSMA and supporting specific types of applications and services. For instance, in [176], the idea of integrating RSMA with Time Division Duplex (TDD) cell-free massive MIMO to support massive machine-type communications is investigated. Other applications of RSMA to a bistatic Dual-Functional Radar-Communication (DFRC) satellite system and a vehicular communication network aided by Unmanned Aerial Vehicles (UAVs) and Reconfigurable Intelligent Surfaces (RISs) can be found in [177] and [178], respectively. Regarding the utilization of RSMA as a means of enabling the users' computation task offloading in MEC applications, only a limited number of works exists, i.e., [179, 180]. In [179], RSMA is used to assist MEC in a Cognitive Radio (CR) network, such that the secondary user avoids deteriorating the primary user's offloading by dynamically adjusting the rate-splitting parameters related to its transmission. In [180], a single-server MEC network is considered, where aerial users offload their tasks via RSMA, and the joint problem of offloading decision, rate, and uplink power control, and decoding order optimization is solved via a Deep Deterministic Policy Gradient (DDPG) method.

6.3 Contributions & Outline

In this chapter, we capitalize on the ability to simultaneously access multiple servers in a multi-server MEC system and suggest the application of the novel RSMA technique, which is considered a key multiple access technique in the upcoming 6G wireless networks. Consequently, the challenging problem of joint computation task offloading and radio and computing resource allocation among the users and the multiple MEC servers arises, which remains mainly unsolved in the literature, and we strive to address it. The main contributions of this work are summarized as follows.

1. The problem of minimizing the sum of users' maximum experienced delay stemming from their task's offloading and processing among the different MEC servers is formulated. The aim is to jointly optimize the users' computation task offloading assignment ratios to the different MEC servers and their allocated rates, uplink transmission powers, and computing resources related to the corresponding MEC server.

2. The equivalent transformation of the initially formulated min-max-sum problem is analyzed to lead to an objective function of continuous form and derive the optimal conditions holding for the problem.

3. The Karush-Kuhn-Tucker (KKT) conditions are employed to decompose the transformed problem into two independent sub-problems, the solutions of which separately provide suboptimal values for the radio (i.e., uplink transmission power and rate) and optimal values for the computing resource allocation. The optimal computation task

assignment to the different MEC servers is also directly derived from the equivalent problem transformation and decomposition analysis.

4. Numerical results are obtained via modeling and simulation to demonstrate the efficiency of the proposed solution in terms of complexity and experienced delay by the users and to showcase the overall system's effectiveness against other traditional multiple access techniques.

6.4 System Model

We consider an RSMA-based multi-server MEC system, as illustrated in Fig. 6.1, which consists of multiple MEC servers of potentially different computing capabilities that reside at the Base Stations (BSs) or the Access Points (APs) of the mobile network infrastructure. The MEC servers serve the purpose of offering computing services to the mobile users existing in the system. We assume that each user fully offloads its computation task, due to the limited energy availability of the user device, while a combination of different available MEC servers can be chosen to process different parts of its computation task. Specifically, heavy Machine Learning (ML) tasks, e.g., image processing, can benefit from multi-server MEC offloading. Different video feeds generated from vehicular, healthcare, or security applications - to name a few - can be offloaded to different MEC servers for processing [181, 182, 183]. In this way, the total task complexity is reduced, and various levels of processing accuracy can be targeted for each part of the task based on each MEC server's computing capability.

Both the BSs or APs that host the MEC servers and the users are equipped with a single antenna. The overall system bandwidth is B Hz. To eliminate the inter-user interference in such a multi-user multi-server communication scenario, it is assumed that the users utilize separate frequency bands of bandwidth $B_n = \frac{B}{N}$ Hz to accommodate their computation task offloading, while a single user's transmissions to multiple MEC servers are performed concurrently and under the same frequency band, via the application of the RSMA technique.

We denote the set of MEC servers by $\mathcal{M} = \{1, \ldots, M\}$ and the set of offloading users by $\mathcal{N} = \{1, \ldots, N\}$. A user's n computation task is defined as $C_n = \phi_n D_n$ [CPU cycles], where D_n [bits] and ϕ_n [CPU cycles/bit] denote the task's input data and intensity, respectively. It is considered that a task C_n can be arbitrarily partitioned into subsets of any size that, in turn, can be computed at different MEC servers. Specifically, we indicate as $\beta_{n,m} \in [0, 1]$ the user's n computation task assignment ratio to MEC server m, such that $\sum_{m=1}^{M} \beta_{n,m} = 1, \forall n \in \mathcal{N}$.

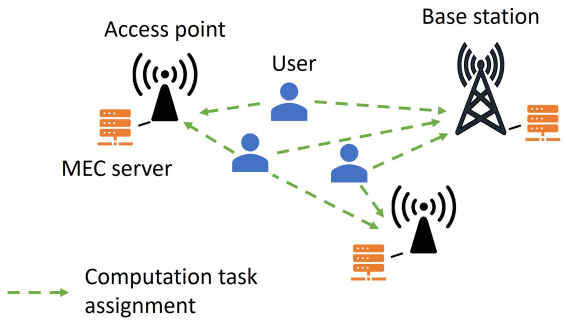

Figure 6.1: High-level overview of the multi-server MEC system.

6.4.1 Communication Model

Concerning the RSMA-based communication model, we denote as $W_{n,m}$ the message of user n intended for MEC server m, containing the corresponding offloaded computation task $\beta_{n,m}C_n$. Each message $W_{n,m}$ is split into a common and a private part, i.e., $W^c_{n,m}$ and $W^p_{n,m}$, respectively. The common parts intended for all MEC servers from user n, i.e., $W^c_{n,1}, \ldots, W^c_{n,m}, \ldots, W^c_{n,M}$, are combined and encoded into a single common stream $s_{n,0}$ that is transmitted to all MEC servers with uplink transmission power $p_{n,0}$ [Watt]. The remaining private messages $W^p_{n,m}, \forall m \in M$ are encoded into different private streams $s_{n,m}$ and are separately transmitted to the MEC servers with uplink transmission power $p_{n,m}$ [Watt]. Hence, the transmitted signal of user n is defined as:

$$x_n = \sqrt{p_{n,0}} s_{n,0} + \sum_{m=1}^{M} \sqrt{p_{n,m}} s_{n,m}. \tag{6.1}$$

The received signal at each MEC server m that is transmitted by user n is given by:

$$y_{n,m} = \sqrt{G_{n,m} p_{n,0}} s_{n,0} + \sum_{j=1}^{M} \sqrt{G_{n,m} p_{n,j}} s_{n,j} + z_{n,m}, \tag{6.2}$$

where $G_{n,m}$ denotes the channel gain between user n and MEC server m and $z_{n,m}$ is the corresponding Additive White Gaussian Noise (AWGN) with zero mean and variance σ^2.

Accordingly, the achievable rate of decoding the common stream $s_{n,0}$ transmitted by user n to each MEC server m is:

$$c_{n,m} = B_n \log_2 \left(1 + \frac{G_{n,m} p_{n,0}}{G_{n,m} \sum_{j=1}^{M} p_{n,j} + \sigma^2} \right) [bps]. \tag{6.3}$$

Without loss of generality, we consider that the channel gains between a user n and the offloading MEC servers are sorted in ascending manner, i.e., $G_{n,1} \leq \cdots \leq G_{n,m} \leq \cdots \leq G_{n,M}$. We denote as $a_{n,m}$ [bps] the allocated rate of the common stream $s_{n,0}$ transmitted by user n to each MEC server m. Then, in order to ensure that all MEC servers $m \in \mathcal{M}$ can successfully decode the user's n common stream $s_{n,0}$, the allocated rates $a_{n,m}$ should satisfy the following condition:

$$\begin{aligned} \sum_{m=1}^{M} a_{n,m} &\leq \min_{m \in \mathcal{M}} c_{n,m} \\ &= B_n \log_2 \left(1 + \frac{G_{n,1} p_{n,0}}{G_{n,1} \sum_{m=1}^{M} p_{n,m} + \sigma^2} \right) = c_{n,1}, \end{aligned} \tag{6.4}$$

where the equality follows from the channel gains' ordering.

Additionally, for the Successive Interference Cancellation (SIC) to be successfully implemented at the receiver of each MEC server m, the following condition should be satisfied for each user n:

$$G_{n,m} p_{n,0} - G_{n,m} \sum_{j=1}^{M} p_{n,j} \geq P_n^{tol}, \tag{6.5}$$

where P_n^{tol} [Watt] is the corresponding receiver's SIC decoding tolerance/sensitivity. Following the ordering of the channel gains, Eq. (2.4) can be reduced as:

$$G_{n,1} p_{n,0} - G_{n,1} \sum_{m=1}^{M} p_{n,m} \geq P_n^{tol}. \tag{6.6}$$

After the decoding of the user's n common stream at each MEC server, the decoding of the corresponding private stream $s_{n,m}$ takes place at each MEC server, the achievable rate of which is calculated as:

$$r_{n,m} = B_n \log_2 \left(1 + \frac{G_{n,m} p_{n,m}}{G_{n,m} \sum_{j=1, j \neq m}^{M} p_{n,j} + \sigma^2} \right) [bps]. \tag{6.7}$$

The total achievable offloading rate from user n to MEC server m is:

$$\begin{aligned} r_{n,m}^{tot} &= a_{n,m} + r_{n,m} \\ &= a_{n,m} + B_n \log_2 \left(1 + \frac{G_{n,m} p_{n,m}}{G_{n,m} \sum_{j=1, j \neq m}^{M} p_{n,j} + \sigma^2} \right). \end{aligned} \tag{6.8}$$

Therefore, given that $\beta_{n,m} D_n$ [bits] are transmitted by user n to each MEC server m, then the corresponding transmission/offloading delay is defined as follows:

$$T_{n,m}^{off} = \frac{\beta_{n,m} D_n}{r_{n,m}^{tot}} [s]. \tag{6.9}$$

6.4.2 Computing Model

The computing model regards the remote processing of different parts of each user's n computation task at the different available MEC servers. Specifically, we denote as $f_{n,m}$ [CPU cycles/s] the computing resource that the MEC server m allocates to user n for the processing of its task, for which it holds that $\sum_{n=1}^{N} f_{n,m} = F_m, \forall m$, where F_m [CPU cycles/s] is the total computing resource owned by MEC server m. Given that $\beta_{n,m} \phi_n D_n$ [CPU cycles] are processed by MEC server m for user n, then the corresponding processing delay is given by:

$$T_{n,m}^{proc} = \frac{\beta_{n,m} D_n \phi_n}{f_{n,m}} [s]. \tag{6.10}$$

As a result, the overall experienced delay by a user n from the computation task offloading and processing at an MEC server m is:

$$T_{n,m} = T_{n,m}^{off} + T_{n,m}^{proc}. \tag{6.11}$$

It should be noted that, in this work, the delay incurred by the downlink transmission of the computed output from the MEC servers to the corresponding users is omitted since its impact on the overall delay experienced by the users is negligible [168, 165, 170]. On the one hand, the size of the computed output is usually much smaller than the input while on the other hand, the downlink transmission is subjected to less interference and is performed with significantly higher power than the uplink transmission/offloading performed by the user devices.

6.5 Problem Formulation, Transformation & Decomposition

6.5.1 Problem Formulation

In this work, our objective is to minimize the sum of the users' maximum experienced delay stemming from their computation task offloading and processing among the different MEC servers, as defined in Eq. (6.11). To achieve this, we jointly optimize each

user's n vectors of allocated common-message rates $\mathbf{a}_n = [a_{n,1}, \ldots, a_{n,m}, \ldots, a_{n,M}]^T$, uplink transmission powers $\mathbf{p}_n = [p_{n,0}, p_{n,1}, \ldots, p_{n,m}, \ldots, p_{n,m}]^T$, computing resources $\mathbf{f}_n = [f_{n,1}, \ldots, f_{n,m}, \ldots, f_{n,M}]^T$, and computation task assignment ratios $\boldsymbol{\beta}_n = [\beta_{n,1}, \ldots, \beta_{n,m}, \ldots, \beta_{n,M}]^T$ to the MEC servers. The corresponding maximum delay minimization problem to be solved is formally written as follows:

$$\min_{\mathbf{a}_n, \mathbf{p}_n, \mathbf{f}_n, \boldsymbol{\beta}_n, \forall n} \quad \sum_{n=1}^{N} \max_{m \in \mathcal{M}} \left\{ T_{n,m} \right\} \tag{6.12a}$$

$$\textbf{s.t.} \quad \sum_{m=1}^{M} a_{n,m} \leq B_n \log_2 \left(1 + \frac{G_{n,1} p_{n,0}}{G_{n,1} \sum_{m=1}^{M} p_{n,m} + \sigma^2} \right), \forall n, \tag{6.12b}$$

$$G_{n,1} p_{n,0} - G_{n,1} \sum_{m=1}^{M} p_{n,m} \geq P_n^{tol}, \forall n, \tag{6.12c}$$

$$p_{n,0} + \sum_{m=1}^{M} p_{n,m} \leq P_n^{max}, \forall n, \tag{6.12d}$$

$$\sum_{n=1}^{N} f_{n,m} \leq F_m, \forall m, \tag{6.12e}$$

$$\sum_{m=1}^{M} \beta_{n,m} = 1, \forall n, \tag{6.12f}$$

$$r_{n,m}^{tot} \geq R_n^{min}, \forall n, m, \tag{6.12g}$$

$$a_{n,m}, p_{n,0}, p_{n,m}, f_{n,m} \geq 0, \; \beta_{n,m} \in [0,1], \forall n, m, \tag{6.12h}$$

where P_n^{max} [Watt] and R_n^{min} [bps] are the user's n maximum power budget and minimum allowable uplink transmission/offloading rate requirement, respectively. The constraints of the formulated optimization problem are explained as follows. Eq. (6.12b) and (6.12c) represent the required constraints over each user's n allocated common-message rates $\mathbf{a}_n$ and powers $\mathbf{p}_n$, respectively, for the successful decoding and implementation of the SIC technique at the receivers of the MEC servers, as analytically described earlier in Section 6.4. Also, Eq. (6.12d) constitutes each user's n maximum transmission power constraint. Eq. (6.12e) guarantees that the allocated computing resources by each MEC server m to the users do not exceed the corresponding MEC server's maximum computing resource availability F_m [CPU cycles/s] while Eq. (6.12f) ensures that each user's n computation task is fully offloaded to the available MEC servers. Eq. (6.12g) captures each user's n minimum acceptable offloading data rate to each MEC server m. Last, Eq. (6.12h) defines the feasible range of values of the optimization variables.

The optimization problem (6.12) is non-convex, due to the non-convexity of the objective function, while the rate $\mathbf{a}_n$, power $\mathbf{p}_n$, computing resource $\mathbf{f}_n$, and task offloading $\boldsymbol{\beta}_n$ vectors are highly coupled, complicating the derivation of a tractable solution. Thus, it is challenging to obtain a global optimum within polynomial time. In the following, we outline the procedures of equivalent transformation and decomposition of problem (6.12) that allow the derivation of a local minimum.

6.5.2 Problem Transformation & Optimal Conditions

Our first result allows reducing the objective function (6.12a) to a differentiable expression.

Lemma 6.1. *Let* $\left\{\{a_{n,m}, p_{n,m}, f_{n,m}, \beta_{n,m}\}_m, p_{n,0}\right\}_n$ *be an optimal solution to problem (6.12). Then, it holds*

$$T_{n,1} = T_{n,2} = \cdots = T_{n,M}, \forall n, \tag{6.13}$$

where $T_{n,m} = T_{n,m}(a_{n,m}, p_{n,0}, p_{n,m}, f_{n,m}, \beta_{n,m}) = \frac{\beta_{n,m} D_n}{r^{tot}_{n,m}} + \frac{\beta_{n,m} D_n \phi_n}{f_{n,m}}$.

Proof. Lemma 6.1 is proved by contradiction. Let $\left\{\{a_{n,m}, p_{n,m}, f_{n,m}, \beta_{n,m}\}_m, p_{n,0}\right\}_n$ be an optimal solution of problem (6.12), for which, without loss of generality, it holds

$$T_{n,1}(a_{n,1}, p_{n,1}, f_{n,1}, \beta_{n,1}) > T_{n,2}(a_{n,2}, p_{n,2}, f_{n,2}, \beta_{n,2}), \tag{6.14}$$

for some $n \in \mathcal{N}$. This implies that there exists $\varepsilon > 0$ such that

$$T_{n,1}(a_{n,1}, p_{n,1}, f_{n,1}, \beta_{n,1} - \varepsilon) > T_{n,2}(a_{n,2}, p_{n,2}, f_{n,2}, \beta_{n,2} + \varepsilon), \tag{6.15}$$

and thus we conclude that

$$\begin{aligned} T_{n,1}(a_{n,1}, p_{n,1}, f_{n,1}, \beta_{n,1}) &> T_{n,1}(a_{n,1}, p_{n,1}, f_{n,1}, \beta_{n,1} - \varepsilon) \\ &> T_{n,2}(a_{n,2}, p_{n,2}, f_{n,2}, \beta_{n,2} + \varepsilon). \end{aligned} \tag{6.16}$$

In particular, we conclude that if we replace the points $\beta_{n,1}, \beta_{n,2}$ with the points $\beta_{n,1} - \varepsilon, \beta_{n,2} + \varepsilon$, we then obtain a point belonging to the feasible region for which the objective function decreases, contrariwise to the assumption that the points $\beta_{n,1}, \beta_{n,2}$ are optimal. □

According to the Lemma 6.1, the users' overall experienced delays $T_{n,m}$ at the different MEC servers $m \in \mathcal{M}$ are equal to each other at the optimal solution point. This observation is subsequently utilized to equivalently transform the problem's objective function, as described in Lemma 6.2, below.

Lemma 6.2. *Let* $\left\{\{a_{n,m}, p_{n,m}, f_{n,m}, \beta_{n,m}\}_m, p_{n,0}\right\}_n$ *be an optimal solution of problem (6.12). Then, it holds*

$$T_{n,m} = D_n \frac{1 + \sum_{m=1}^{M} \beta_{n,m} \frac{\phi_n}{f_{n,m}} r^{tot}_{n,m}}{\sum_{m=1}^{M} r^{tot}_{n,m}}, \forall n, m. \tag{6.17}$$

Proof. From Lemma 6.1, we have proved that at the optimal solution point, it holds that $T_{n,1} = \cdots = T_{n,M}, \forall n$, which may equivalently be written as:

$$\frac{\beta_{n,1} D_n + \frac{\beta_{n,1} D_n \phi_n}{f_{n,1}} r^{tot}_{n,1}}{r^{tot}_{n,1}} = \cdots = \frac{\beta_{n,M} D_n + \frac{\beta_{n,M} D_n \phi_n}{f_{n,M}} r^{tot}_{n,M}}{r^{tot}_{n,M}}. \tag{6.18}$$

Now observe that for each $m \in \{2, \ldots, M\}$ it holds

$$t_m = \frac{\beta_{n,m} D_n + \frac{\beta_{n,m} D_n \phi_n}{f_{n,m}} r^{tot}_{n,m}}{\beta_{n,1} D_n + \frac{\beta_{n,1} D_n \phi_n}{f_{n,1}} r^{tot}_{n,1}} = \frac{r^{tot}_{n,m}}{r^{tot}_{n,1}}, \tag{6.19}$$

which, in turn, implies that

$$\begin{aligned} T_{n,1} &= D_n \frac{\beta_{n,1} + \beta_{n,1}\frac{\phi_n}{f_{n,1}} r_{n,1}^{tot}}{r_{n,1}^{tot}} \\ &= D_n \frac{\left(\beta_{n,1} + \beta_{n,1}\frac{\phi_n}{f_{n,1}} r_{n,1}^{tot}\right) \cdot (1 + t_2 + \cdots + t_M)}{r_{n,1}^{tot} \cdot (1 + t_2 + \cdots + t_M)} \\ &= D_n \frac{\sum_{m=1}^{M} \left(\beta_{n,m} + \beta_{n,m}\frac{\phi_n}{f_{n,m}} r_{n,m}^{tot}\right)}{\sum_{m=1}^{M} r_{n,m}^{tot}} \\ &= D_n \frac{1 + \sum_{m=1}^{M} \beta_{n,m}\frac{\phi_n}{f_{n,m}} r_{n,m}^{tot}}{\sum_{m=1}^{M} r_{n,m}^{tot}}, \end{aligned} \tag{6.20}$$

where the last equality follows from $\sum_{m=1}^{M} \beta_{n,m} = 1$. Since $T_{n,1} = \cdots = T_{n,M}$ the result follows. □

Therefore, the outcome of Lemma 6.2 is the transformation of the problem's objective function into a continuously differentiable function, which allows further mathematical manipulations toward obtaining a solution to the overall problem. Next, we proceed to the analysis of the optimal conditions that further simplify the initially formulated problem.

Lemma 6.3. *At the optimal solution of problem (6.12), the constraint (6.12b) over the common-message rate holds with equality:* $\sum_{m=1}^{M} a_{n,m} = B_n \log_2\left(1 + \frac{G_{n,1}p_{n,0}}{G_{n,1}\sum_{m=1}^{M} p_{n,m} + \sigma^2}\right), \forall n.$

Proof. Lemma 6.3 can be easily proved by contradiction. □

In particular, Lemma 6.3 implies that for an optimal choice of $a_{n,m}, \forall n, m$, the sum of total achievable offloading rates from user n to the different MEC servers is:

$$\begin{aligned} \sum_{m=1}^{M} r_{n,m}^{tot} &= B_n \log_2\left(1 + \frac{G_{n,1}p_{n,0}}{G_{n,1}\sum_{m=1}^{M} p_{n,m} + \sigma^2}\right) \\ &\quad + \sum_{m=1}^{M} B_n \log_2\left(1 + \frac{G_{n,m}p_{n,m}}{G_{n,m}\sum_{j=1,j\neq m}^{M} p_{n,j} + \sigma^2}\right), \end{aligned} \tag{6.21}$$

which should be noted that does not depend on $a_{n,m}, \forall m$.

Lemma 6.4. *At the optimal solution of problem (6.12), the constraint (6.12d) over the uplink transmission powers of the private messages holds with equality:* $\sum_{m=1}^{M} p_{n,m} = P_n^{max} - p_{n,0}, \forall n.$

Proof. Let $p_{n,i}, i \in \mathcal{M}$, be an optimal solution of problem (6.12). Suppose, towards arriving at a contradiction, that $\sum_{m=1}^{M} p_{n,m} < P_n^{\max} - p_{n,0}$. Set $\alpha = \frac{P_n^{\max}}{p_{n,0} + \sum_{m=1}^{M} p_{n,m}}$, and note that $\alpha > 1$. Now, define $p_{n,i}^* = \alpha p_{n,i}$, for $i \in \mathcal{M}$. It can be easily noticed if we replace the values $p_{n,i}, i \in \mathcal{M}$ in the optimal solution with the values $p_{n,i}^*, i \in \mathcal{M}$, then the objective function decreases. Furthermore, since it holds that

$$p_{n,0}^* - \sum_{m=1}^{M} p_{n,m}^* = \alpha \cdot \left(p_{n,0} - \sum_{m=1}^{M} p_{n,m}\right) > p_{n,0} - \sum_{m=1}^{M} p_{n,m} \geq \frac{P_n^{tol}}{G_{n,1}}, \tag{6.22}$$

the points $p^*_{n,i}, i \in \{0, 1, \ldots, M\}$, belong to the feasible region of problem (6.12), thus contradicting the assumption that $p_{n,i}, i \in \{0, 1, \ldots, M\}$, is optimal. □

Lemmas 6.3 and 6.4, so far, provided the optimal conditions that hold with respect to the users' allocated common-message rates and private-message uplink transmission powers. Lemma 6.5, below, focuses on the optimal condition that holds for the allocated computing resources to the users.

Lemma 6.5. *At the optimal solution of problem (6.12), the constraint (6.12e) over the allocated computing resources holds with equality:* $\sum_{n=1}^{N} f_{n,m} = F_m, \forall m$.

Proof. Lemma 6.5 can be easily proved by contradiction. □

Owing to the preceding analysis, the initially formulated maximum delay minimization problem (6.12) is reformulated as follows:

$$\min_{\mathbf{a}_n, \mathbf{p}_n, \mathbf{f}_n, \boldsymbol{\beta}_n, \forall n} \quad \sum_{n=1}^{N} D_n \frac{1 + \sum_{m=1}^{M} \beta_{n,m} \frac{\phi_n}{f_{n,m}} r^{tot}_{n,m}}{\sum_{m=1}^{M} r^{tot}_{n,m}} \tag{6.23a}$$

$$\textbf{s.t.} \quad \sum_{m=1}^{M} a_{n,m} = B_n \log_2 \left(1 + \frac{G_{n,1} p_{n,0}}{G_{n,1} \sum_{m=1}^{M} p_{n,m} + \sigma^2} \right), \forall n, \tag{6.23b}$$

$$p_{n,0} \geq \frac{1}{2} P^{max}_n + \frac{1}{2} \frac{P^{tol}_n}{G_{n,1}}, \forall n, \tag{6.23c}$$

$$\sum_{m=1}^{M} p_{n,m} = P^{max}_n - p_{n,0}, \forall n, \tag{6.23d}$$

$$\sum_{n=1}^{N} f_{n,m} = F_m, \forall m, \tag{6.23e}$$

$$\sum_{m=1}^{M} \beta_{n,m} = 1, \forall n, \tag{6.23f}$$

$$r^{tot}_{n,m} \geq R^{min}_n, \forall n, m, \tag{6.23g}$$

$$a_{n,m}, p_{n,0}, p_{n,m}, f_{n,m} \geq 0, \; \beta_{n,m} \in [0, 1], \forall n, m, \tag{6.23h}$$

where constraint (6.23c) derives from (6.12c) following Lemma 6.4 and by setting $\sum_{m=1}^{M} p_{n,m} = P^{max}_n - p_{n,0}$.

6.5.3 Problem Decomposition

In this section, we exploit the structure of the equivalently transformed problem (6.23), which, upon combination with the KKT conditions, allows the decomposition of the problem into two independent sub-problems that can separately provide suboptimal solutions to the radio and optimal solutions to the computing resource allocation. We begin by first describing the KKT conditions corresponding to problem (6.23).

The Lagrangian function (see [184, Theorem 2.1]) of problem (6.23) can be written as:

$$\begin{aligned}\mathcal{L} = \sum_{n=1}^{N} \Bigg\{ & D_n \frac{1+\sum_{m=1}^{M} \beta_{n,m} \frac{\phi_n}{f_{n,m}} r_{n,m}^{tot}}{\sum_{m=1}^{M} r_{n,m}^{tot}} \\ & + \lambda_n^a \left(\sum_{m=1}^{M} a_{n,m} - B_n \log_2 \left(1 + \frac{G_{n,1} p_{n,0}}{G_{n,1} \sum_{m=1}^{M} p_{n,m} + \sigma^2} \right) \right) \\ & + \lambda_n^0 \left(\frac{1}{2} P_n^{max} + \frac{1}{2} \frac{P_n^{tol}}{G_{n,1}} - p_{n,0} \right) + \sum_{m=1}^{M} \lambda_{n,m}^r \left(R_n^{min} - r_{n,m}^{tot} \right) \\ & + \lambda_n^p \left(\sum_{m=1}^{M} p_{n,m} - P_n^{max} + p_{n,0} \right) + \lambda_n^\beta \left(\sum_{m=1}^{M} \beta_{n,m} - 1 \right) \Bigg\} \\ & + \sum_{m=1}^{M} \lambda_m^f \left(\sum_{n=1}^{N} f_{n,m} - F_m \right), \end{aligned} \tag{6.24}$$

where for each n and m, $\lambda_n^a, \lambda_n^0, \lambda_{n,m}^r, \lambda_n^p, \lambda_n^\beta, \lambda_m^f \geq 0$ are the, so-called, Lagrange multipliers that correspond to the constraints of problem (6.23).

It follows from the KKT theorem (see [184, Theorem 2.1]) that if $\left\{ a_{n,m}, p_{n,m}, f_{n,m}, \beta_{n,m} \right\}_m, p_{n,0} \Big\}_n$ is a local minimum of problem (6.23), then there exist Lagrange multipliers $\lambda_n^a, \lambda_n^0, \lambda_{n,m}^r, \lambda_n^p, \lambda_n^\beta, \lambda_m^f$ such that

$$\frac{\partial \mathcal{L}}{\partial a_{n,m}} = \frac{\partial \mathcal{L}}{\partial p_{n,0}} = \frac{\partial \mathcal{L}}{\partial p_{n,m}} = \frac{\partial \mathcal{L}}{\partial f_{n,m}} = \frac{\partial \mathcal{L}}{\partial \beta_{n,m}} = 0, \tag{6.25}$$

which is the stationary condition of the KKT conditions.

Lemma 6.6. *Let* $\left\{ \{ a_{n,m}, p_{n,m}, f_{n,m}, \beta_{n,m} \}_m, p_{n,0} \right\}_n$ *be a local minimum of problem* (6.23). *Then, it holds*

$$\frac{r_{n,m}^{tot}}{f_{n,m}} = \frac{\sum_{j=1}^{M} r_{n,j}^{tot}}{\sum_{j=1}^{M} f_{n,j}}. \tag{6.26}$$

Proof. Note that Eq. (6.25) and the partial derivative with respect to $\beta_{n,m}$ imply that for each $m \in \mathcal{M}$ it holds $\frac{\partial \mathcal{L}}{\partial \beta_{n,m}} = 0$, which in turn yields:

$$\frac{r_{n,1}^{tot}}{f_{n,1}} = \cdots \frac{r_{n,M}^{tot}}{f_{n,M}} = -\lambda_n^\beta. \tag{6.27}$$

Let m be fixed and for each $j \neq m$ let $t_j = \frac{r_{n,j}^{tot}}{r_{n,m}^{tot}} = \frac{f_{n,j}}{f_{n,m}}$. Then, Eq. (6.27) implies that

$$\frac{r_{n,m}^{tot}}{f_{n,m}} = \frac{r_{n,m}^{tot} \cdot (1 + \sum_{j \neq m} t_j)}{f_{n,m} \cdot (1 + \sum_{j \neq m} t_j)} = \frac{\sum_{j=1}^{M} r_{n,j}^{tot}}{\sum_{j=1}^{M} f_{n,j}}, \tag{6.28}$$

completing the proof. □

Now, using Eq. (6.26) and the fact that $\sum_{m=1}^{M} \beta_{n,m} = 1$, we may write each addend in

the objective function (6.23a) as:

$$
\begin{aligned}
T_{n,m} &= D_n \frac{1 + \sum_{m=1}^{M} \beta_{n,m} \frac{\phi_n}{f_{n,m}} r_{n,m}^{tot}}{\sum_{m=1}^{M} r_{n,m}^{tot}} \\
&= \frac{D_n}{\sum_{m=1}^{M} r_{n,m}^{tot}} + \frac{\sum_{m=1}^{M} \beta_{n,m} D_n \phi_n \frac{\sum_{j=1}^{M} r_{n,j}^{tot}}{\sum_{j=1}^{M} f_{n,j}^{tot}}}{\sum_{m=1}^{M} r_{n,m}^{tot}} \\
&= \frac{D_n}{\sum_{m=1}^{M} r_{n,m}^{tot}} + \frac{D_n \phi_n}{\sum_{m=1}^{M} f_{n,m}}. \qquad (6.29)
\end{aligned}
$$

Observe that the first term of Eq. (6.29) depends only on $\{p_{n,0}, \{p_{n,m}\}_m\}_n$ and thus, indirectly on $\{a_{n,m}\}_{n,m}$, whereas the second term depends only on $\{f_{n,m}\}_{n,m}$. Consequently, the transformed problem (6.23) is further decomposed into two independent optimization problems.

First, given the assumption that different users utilize different frequency bands to accommodate their computation task offloading and thus, their transmissions do not interfere with each other, it suffices to solve N independent problems to derive each user's n optimal common-message rate $\mathbf{a}_n^*$ and uplink transmission power $\mathbf{p}_n^*$ vectors. Based on the first term of Eq. (6.29), the corresponding optimization problem may be written as the maximization of each user's n sum of total achievable offloading rates to the different MEC servers. The solution to this problem will be discussed later in Section 6.6.3, while its formal description is as follows:

$$
\max_{\substack{a_{n,m}, p_{n,0}, \\ p_{n,m} \geq 0, \forall m}} \quad \sum_{m=1}^{M} r_{n,m}^{tot} \qquad (6.30a)
$$

$$
\textbf{s.t.} \qquad \text{(6.23b), (6.23c), (6.23d), (6.23g).} \qquad (6.30b)
$$

Regarding the derivation of each user's n optimal computing resource allocation $\mathbf{f}_n^*$ vector, it suffices to solve the following problem:

$$
\min_{f_{n,m} \geq 0, \forall n,m} \quad \sum_{n=1}^{N} \frac{D_n \phi_n}{\sum_{m=1}^{M} f_{n,m}} \qquad (6.31a)
$$

$$
\textbf{s.t.} \quad \sum_{n=1}^{N} f_{n,m} = F_m, \forall m. \qquad (6.31b)
$$

The closed-form solution of problem (6.31) and the procedure that results in this solution are detailed later in Section 6.6.2.

6.6 Delay Minimization Solution for RSMA-based Multi-server MEC Systems

In this section, we present the proposed solution to the joint computation task offloading and radio and computing resource allocation problem. First, in Section 6.6.1, the users' optimal computation task assignment ratios to the different MEC servers are determined, based on the preceding analysis of equivalent problem transformation and decomposition. Then, the optimal solution to the computing resource allocation problem (6.31) is derived using the KKT conditions (Section 6.6.2), while an iterative algorithm is utilized to lead

to a suboptimal solution for the joint rate and uplink transmission power problem (6.30) (Section 6.6.3). The section concludes with the algorithm description of the overall proposed solution and its complexity analysis (Section 6.6.4).

6.6.1 Computation Task Assignment

The overall problem transformation and decomposition analysis presented in the previous section is founded on the basis that, in the optimal solution, the users' experienced delays related to different MEC servers are equal to each other, i.e., $T_{n,1} = T_{n,2} = \cdots = T_{n,M}, \forall n, m$. Particularly, in Lemma 6.1, it has been proved that to minimize each user's n maximum experienced delay among the different MEC servers, each user's vector of computation task offloading assignment ratios $\boldsymbol{\beta}^*$ will be optimized such that the equalization of the experienced delays related to different MEC servers is achieved. Lemma 6.7, below, provides the optimal solution to this problem along with insights on how to obtain this solution.

Lemma 6.7. *Let* $\left\{\{a_{n,m}, p_{n,m}, f_{n,m}, \beta^*_{n,m}\}_m, p_{n,0}\right\}_n$ *be a local minimum of problem* (6.23). *Then, each user's* n *optimal computation task assignment ratio to MEC server* m *is:*

$$\beta^*_{n,m} = \frac{\frac{r^{tot}_{n,m} \cdot f_{n,m}}{f_{n,m} + \phi_n r^{tot}_{n,m}}}{\sum_{m=1}^{M} \frac{r^{tot}_{n,m} \cdot f_{n,m}}{f_{n,m} + \phi_n r^{tot}_{n,m}}}, \forall n, m, \tag{6.32}$$

satisfying the conditions $\beta^*_{n,m} \in [0, 1]$ *and* $\sum_{m=1}^{M} \beta^*_{n,m} = 1$.

Proof. From the general definition of each user's n overall experienced delay $T_{n,m}$, we have

$$\begin{aligned} T_{n,m} &= \frac{\beta_{n,m} D_n}{r^{tot}_{n,m}} + \frac{\beta_{n,m} D_n \phi_n}{f_{n,m}} \\ &= D_n \beta_{n,m} \frac{f_{n,m} + \phi_n r^{tot}_{n,m}}{r^{tot}_{n,m} \cdot f_{n,m}}. \end{aligned} \tag{6.33}$$

Furthermore, Eq. (6.29) implies that

$$\begin{aligned} T_{n,m} &= \frac{D_n}{\sum_{m=1}^{M} r^{tot}_{n,m}} + \frac{D_n \phi_n}{\sum_{m=1}^{M} f_{n,m}} \\ &= \frac{D_n}{\sum_{m=1}^{M} \frac{r^{tot}_{n,m}}{1 + \phi_n \frac{\sum_{j=1}^{M} r^{tot}_{n,j}}{\sum_{j=1}^{M} f_{n,j}}}} \\ &\overset{\text{Eq. (19)}}{=} \frac{D_n}{\sum_{m=1}^{M} \frac{r^{tot}_{n,m}}{1 + \phi_n \frac{r^{tot}_{n,m}}{f_{n,m}}}} \\ &= \frac{D_n}{\sum_{m=1}^{M} \frac{r^{tot}_{n,m} \cdot f_{n,m}}{f_{n,m} + \phi_n r^{tot}_{n,m}}}. \end{aligned} \tag{6.34}$$

By setting Eq. (6.33) and (6.34) equal to each other and solving with respect to $\beta_{n,m}$, the result of Lemma 6.7 follows. □

6.6.2 Computing Resource Allocation

In the following, the solution to problem (6.31) is derived, which provides the optimal computing resource allocation vectors $\mathbf{f}^*_n$ for all users $n \in \mathcal{N}$ in the system.

Lemma 6.8. *Let $\{f^*_{n,m}\}_{n,m}$ be a global minimum of problem (6.31). Then, each user's n optimal computing resource allocation by each MEC server m is:*

$$f^*_{n,m} = F_m \frac{\sqrt{D_n \phi_n}}{\sum_{j=1}^{N} \sqrt{D_j \phi_j}}, \forall n, m. \tag{6.35}$$

Proof. We begin by considering the following more general problem:

$$\min_{z_n \geq 0, \forall n} \quad \sum_{n=1}^{N} \frac{D_n \phi_n}{z_n} \tag{6.36a}$$

$$\textbf{s.t.} \quad \sum_{n=1}^{N} z_n = \sum_{m=1}^{M} F_m, \tag{6.36b}$$

which is obtained by setting $z_n = \sum_{m=1}^{M} f_{n,m}, \forall n$, in problem (6.31). The constraints of problem (6.36) are convex, while it can be easily found that the objective function (6.36a) is also convex by verifying that the corresponding Hessian is positive definite. As a result, problem (6.36) is convex and a globally optimal solution can be obtained using the KKT conditions (see [184, Theorem 3.8]). The Lagrange function of problem (6.36) is given by:

$$\Lambda = \sum_{n=1}^{N} \frac{D_n \phi_n}{z_n} + \lambda \left(\sum_{n=1}^{N} z_n - \sum_{m=1}^{M} F_m \right), \tag{6.37}$$

where $\lambda \geq 0$ is the corresponding Lagrange multiplier of constraint (6.36b). From the stationary condition $\frac{\partial \Lambda}{\partial z_n} = 0, \forall n$, we get that $\frac{D_n \phi_n}{z_n^2} = \lambda, \forall n$, and therefore it holds

$$z_n = \sqrt{\frac{D_n \phi_n}{\lambda}}, \forall n. \tag{6.38}$$

In particular, considering Eq. (6.36b), this implies that

$$\sum_{m=1}^{M} F_m = \sum_{n=1}^{N} z_n = \frac{1}{\sqrt{\lambda}} \sum_{n=1}^{N} \sqrt{D_n \phi_n}, \tag{6.39}$$

and a global optimal solution of problem (6.36) follows as:

$$z^*_n = \left(\sum_{m=1}^{M} F_m \right) \frac{\sqrt{D_n \phi_n}}{\sum_{j=1}^{N} \sqrt{D_j \phi_j}}, \forall n. \tag{6.40}$$

Now, set $f^*_{n,m} = F_m \frac{\sqrt{D_n \phi_n}}{\sum_{j=1}^{N} \sqrt{D_j \phi_j}}, \forall n, m$ and obtain each user's n optimal computing resource allocation by the different MEC servers.

It is straightforward to verify that the points $\{f^*_{n,m}\}_{n,m}$ belong to the feasible region of problem (6.31), and that the objective function (6.31a) evaluated at the points given by Eq. (6.35) is equal to the function (6.36a) evaluated at the points given by Eq. (6.40). Summarizing the above, we conclude that the points defined in Eq. (6.35) constitute a global minimum of problem (6.31). □

6.6.3 Rate & Uplink Transmission Power Allocation

Considering each user's n optimal common-message rate $\mathbf{a}_n^*$ and uplink transmission power $\mathbf{p}_n^*$ vectors, these are determined by solving problem (6.30), independently for each user. The analytic formal presentation of the corresponding optimization problem to be solved for each user is written as:

$$\max_{\substack{a_{n,m},p_{n,0},\\ p_{n,m}\geq 0,\forall m}} \quad \sum_{m=1}^{M} r_{n,m}^{tot} \tag{6.41a}$$

$$\textbf{s.t.} \quad \sum_{m=1}^{M} a_{n,m} = B_n \log_2\left(1+\frac{G_{n,1}p_{n,0}}{G_{n,1}\sum_{m=1}^{M} p_{n,m}+\sigma^2}\right), \tag{6.41b}$$

$$p_{n,0} \geq \frac{1}{2}P_n^{max} + \frac{1}{2}\frac{P_n^{tol}}{G_{n,1}}, \tag{6.41c}$$

$$\sum_{m=1}^{M} p_{n,m} = P_n^{max} - p_{n,0}, \tag{6.41d}$$

$$r_{n,m}^{tot} \geq R_n^{min}, \forall m. \tag{6.41e}$$

From the definition of problem (6.41), it can be easily concluded that it resembles the typical sum rate maximization problem in the downlink communication scenario between a single BS and multiple users, where the transmissions from the BS to the different users are multiplexed via the RSMA technique. Therefore, given the intensive efforts in the literature so far in the domain of RSMA-based wireless communications, an analytic solution to the latter problem exists and can be found in [27]. In this work, we capitalize on the analogy between the single-user multi-server MEC system and the single-BS multi-user communications system and borrow the common rate and uplink transmission power allocation solution introduced in [27]. In the following, we summarize the respective solution as applied in our RSMA-based multi-server MEC system, while the interested reader may refer to [27] for the details.

In detail, owing to problem's (6.41) non-convexity, it is generally hard to directly optimize the parameters $a_{n,m}, p_{n,m}, \forall m$ and $p_{n,0}$ of each user n, and for this reason, an iterative optimization procedure is followed. First, considering that each user's n common-message rates $a_{n,m}, \forall m$ and uplink transmission power $p_{n,0}$ are fixed, its optimal uplink transmission powers $p_{n,m}^*$ of the private messages to the different MEC servers are determined according to Lemma 6.9 below.

Lemma 6.9 (see [27], Theorems 1 and 2)**.** *Let $\{\{a_{n,m}, p_{n,m}^*\}_m, p_{n,0}\}_n$ be a local maximum of problem* (6.41)*. Then, there exists $m_0 \in \mathcal{M}$ such that each user's n optimal uplink transmission power of the private message to each MEC server m is:*

$$p_{n,m}^* = \begin{cases} p_{n,m}^{min}, & \text{if } m \neq m_0, \\ P_n^{max} - p_{n,0} - \sum_{m\neq m_0} p_{n,m}^{min}, & \text{if } m = m_0, \end{cases} \tag{6.42}$$

where

$$p_{n,m}^{min} = \left(1 - 2^{\frac{a_{n,m}-R_n^{min}}{B_n}}\right) \cdot \left(P_n^{max} - p_{n,0} + \frac{\sigma^2}{G_{n,m}}\right) \tag{6.43}$$

and

$$m_0 = \underset{m\in\mathcal{M}}{\operatorname{argmin}}\, 2^{\frac{a_{n,m}-R_n^{min}}{B_n}} \left(P_n^{max} - p_{n,0} + \frac{\sigma^2}{G_{n,m}}\right). \tag{6.44}$$

From Lemma 6.9, it can be deduced that each user's n optimal solutions $p^*_{n,m}, \forall m$ are equal to the minimum acceptable uplink transmission powers $p^{min}_{n,m}$ that meet the user's minimum offloading rate requirement in Eq. (6.41e), except for one MEC server $m_0 \in \mathcal{M}$, the wireless link between which and the user n is allocated the whole amount of the remaining power of the user n from P^{max}_n. The purpose of the latter is to allow the maximization of the user's n sum of total offloading rates to the different MEC servers. Consequently, the MEC server m_0 that is specifically selected for this purpose is determined as $m_0 = \underset{m \in \mathcal{M}}{\operatorname{argmax}}\, r^{tot}_{n,m}$, which by substitution of Eq. (6.42) gives $m_0 = \underset{m \in \mathcal{M}}{\operatorname{argmin}}\, 2^{\frac{a_{n,m} - R^{min}_n}{B_n}} \left(P^{max}_n - p_{n,0} + \frac{\sigma^2}{G_{n,m}} \right)$.

Given each user's n optimal uplink transmission powers $p^*_{n,m}, \forall m$ of the private messages and considering the corresponding common-message power $p_{n,0}$ as fixed, the user's n optimal common-message rates $a^*_{n,m}$ to the different MEC servers are obtained as described in Lemma 6.10, below.

Lemma 6.10 (see [27], Theorem 3)**.** *Let $\{\{a^*_{n,m}, p_{n,m}\}_m, p_{n,0}\}_n$ be local maximum of problem* (6.41)*. Considering the different MEC servers sorted in ascending order as per the channel gains between them and the user n, i.e., $G_{n,1} \leq \cdots \leq G_{n,m} \leq \cdots \leq G_{n,M}$, each user's n optimal common-message rate to each MEC server m is:*

i) if $c_1 < M \cdot R^{min}_n$:

$$a^*_{n,m} = \begin{cases} R^{min}_n, & \text{if } m < l, \\ c_1 - (l-1) \cdot R^{min}_n, & \text{if } m = l, \\ 0, & \text{otherwise}, \end{cases} \tag{6.45}$$

where l satisfies $(l-1) \cdot R^{min}_n \leq c_1 \leq l \cdot R^{min}_n$ with $0 \leq l < M$, and c_1 is as defined in Eq. (6.4).

ii) if $c_1 \geq M \cdot R^{min}_n$:

$$a^*_{n,m} = R^{min}_n, \forall m. \tag{6.46}$$

Lemma 6.10 indicates that it is optimal to allocate more rate to the wireless links between the user and the MEC servers of lower channel gains, and equal in amount to the user's minimum offloading rate requirement R^{min}_n, enabling in this way the maximization of the user's n sum of total offloading rates to the different MEC servers. Also, given the obtained solution $a^*_{n,m}$, we can return to Lemma 6.9 and observe that the specific m_0 that should be selected is equal to $m_0 = M$. In other words, the wireless link between user n and MEC server M that is characterized by the maximum channel gain $G_{n,M}$ is optimal to be allocated more power.

Given the solution $a^*_{n,m}, \forall m$, the user's n optimal uplink transmission power $p^*_{n,0}$ of the common message to the different MEC servers is, then, calculated as follows.

Lemma 6.11 (see [27], Theorem 5)**.** *Let $\{\{a_{n,m}, p_{n,m}\}_m, p^*_{n,0}\}_n$ be a local maximum of problem* (6.41)*. Then, each user's n optimal uplink transmission power of the common message to the MEC servers is:*

$$p^*_{n,0} \in \left\{ \frac{1}{2} P^{max}_n + \frac{1}{2} \frac{P^{tol}_n}{G_{n,1}}, \left(1 - 2^{-\sum_{m=1}^{M} a_{n,m}} \right) \cdot \left(P^{max}_n + \frac{\sigma^2}{G_{n,1}} \right), P_{n,0} \right\} \tag{6.47}$$

where $P_{n,0}$ satisfies the following condition:

$$\sum_{m=1}^{M}\left(1-2^{\frac{a_{n,m}-R_n^{min}}{B_n}}\right)\cdot\left(P_n^{max}-P_{n,0}+\frac{\sigma^2}{G_{n,m}}\right)=P_n^{max}-P_{n,0}. \tag{6.48}$$

Practically, Lemma 6.11 implies that the user's n optimal uplink transmission power $p_{n,0}^*$ of its common message to the different MEC servers is equal to one out of the candidate values defined in the discrete set of Eq. (6.47), which results in the maximum sum of the total offloading rates, i.e., the maximum value of the objective function (6.41a).

6.6.4 Algorithm Overview

The overall solution to the joint task offloading and radio and computing resource allocation problem scrutinized in this work under the RSMA-based multi-server MEC system, while targeting the sum of users' maximum experienced delay minimization, is analytically presented in Algorithm 6.1. Especially, lines 6-10 of Algorithm 6.1, illustrate the iterative procedure that is followed to obtain the optimal common-message rate and uplink transmission power for each user. Considering that the solutions of all optimized parameters are given in closed forms, the complexity of the overall Algorithm 6.1 is $\mathcal{O}(NMT)$, where T denotes the number of iterations required for the iterative procedure in lines 6-10 to converge. Indicative numerical results regarding the real execution time required for Algorithm 6.1 to converge are presented in Section 6.7.

Algorithm 6.1 Joint Task Offloading, and Radio and Computing Resource Allocation in RSMA-based multi-server MEC systems

1: Initialize σ^2, $B_n, P_n^{tol}, P_n^{max}, R_n^{min}, D_n, \phi_n, G_{n,m}, F_m$, $\forall n, m$.
2: Determine $f_{n,m}^*, \forall n, m$ based on Lemma 6.8 and Eq. (6.35).
3: Determine $\beta_{n,m}^*, \forall n, m$ based on Lemma 6.7 and Eq. (6.32).
4: **for** $n \in \mathcal{N}$ **do**
5: Initialize $a_{n,m}^{(0)}, \forall m$, $p_{n,0}^{(0)}$ and set $t = 1$.
6: **repeat**
7: Given $p_{n,0}^{(t-1)}$, determine $a_{n,m}^{(t)}, \forall m$ based on Lemma 6.10 and Eq. (6.45)-(6.46).
8: Given $a_{n,m}^{(t)}, \forall m$, determine $p_{n,0}^{(t)}$ based on Lemma 6.11 and Eq. (6.47).
9: Set $t = t + 1$.
10: **until** the objective value (6.41a) converges.
11: Set $a_{n,m}^* = a_{n,m}^{(t)}, \forall m$ and $p_{n,0}^* = p_{n,0}^{(t)}, \forall m$.
12: Derive $p_{n,m}^*, \forall m$ based on Lemma 6.9 and Eq. (6.42).
13: **end for**

6.7 Performance Evaluation

In this section, the performance of the proposed solution for the joint task offloading and radio and computing resource allocation in RSMA-based multi-server MEC systems is evaluated via modeling and simulation. Throughout our simulation experiments, we consider N users randomly and uniformly distributed in a square area of size 150×150 m. The users concurrently offload part of their computation tasks to M MEC servers spatially uniformly located within this area. The channel gain between user n and MEC server m is calculated

based on the distance-based path loss model $PL = 128.1 + 37.6 \log_{10}(d)$, with d measured in km, while the standard deviation of the shadow fading is 4 dB [165, 27]. Depending on the simulation setup, different values of the overall system bandwidth B [Hz] are considered, while the rest of the communication-related parameters are set as $\sigma^2 = -104$ dB, $P_n^{max} = 24$ dBm, $R_n^{min} = 1$ Mbps and $P_n^{tol} = -94$ dBm, $\forall n \in \mathcal{N}$, unless otherwise explicitly stated. The input data size of each user is $D_n = 2$ Mbits, while the value of its computation task size C_n [CPU cycles] varies depending on the simulation setup and the system density. The computing resource availability of the MEC servers is considered as $F_m = 5$ GHz, $\forall m \in \mathcal{M}$. The simulation results have been averaged over 3000 different channel realizations. The results of this work are also presented in [185].

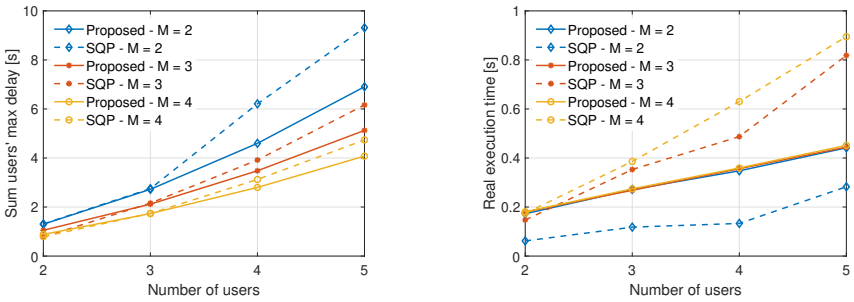

(a) (b)

Figure 6.2: Comparison between the proposed and SQP algorithms' solutions in terms of the (a) sum of users' maximum experienced delay, and (b) real execution time.

First, to characterize and evaluate the effectiveness of the proposed solution, we compare its performance against the solution of the Sequential Quadratic Programming (SQP) iterative algorithm used in constrained non-linear optimization [87]. SQP algorithm is widely implemented as part of the optimization toolbox of different programming platforms, such as MATLAB [88], and, in this evaluation scenario, is used to solve the initially formulated min-max-sum problem (6.12). Due to the high complexity of the original problem (6.12) and the inability of the SQP algorithm to result in a stable and feasible solution as the number of users and MEC servers increases, the comparison is carried out in a small system of $B = 5$ MHz overall bandwidth with $N = [2, 5]$ users, the computation task size of which is set equal to $C_n = 2000$ Mega-CPU cycles. The outcome of the comparison between the SQP algorithm (labeled as "SQP") and Algorithm 6.1 (labeled as "Proposed") is reported in Fig. 6.2. In particular, Fig. 6.2a illustrates the sum of the users' maximum experienced delay among the different MEC servers (vertical axis) that is defined in Eq. (6.12a), as a function of the number of users (horizontal axis) and MEC servers (different graph coloring), whereas Fig. 6.2b examines the real execution time in seconds required for each one of the proposed and SQP algorithms to obtain a solution (vertical axis) under different user and MEC server numbers.

The numerical results reveal that for particularly small systems with $N = 2$ or $N = 3$ users, the two algorithms present comparable performance regarding the minimum achievable value of the optimization objective (Fig. 6.2a). On the contrary, as the number of users increases, the proposed algorithm manages to conclude at lower sums of the users' maximum experienced delay among the different MEC servers than the SQP, while this performance gap between the two algorithms diminishes as the number of MEC servers increases. This is owed to the fact that for a small number of MEC servers, the SQP algorithm can quickly pinpoint a local minimum of the problem by potentially sacrificing the minimization proce-

dure's performance. The latter is further corroborated in Fig. 6.2b, where it is demonstrated that the real execution time required for the SQP algorithm to lead to a solution is increasing proportionally to both the number of users and MEC servers in the system, being faster than the proposed algorithm for $M = 2$ and slower for $M = 3$ or $M = 4$. At this point, it is quite interesting to observe that although the proposed algorithm's complexity is a function of both N and M (see Section 6.6.4), its real execution time is steered by the for loop initiated in line 4 of Algorithm 6.1, and thus is mainly affected by the number of users existing in the system. Consequently, its real execution time gets gradually higher for more users in the system but remains unchanged as the number of servers increases. Concluding, the proposed algorithm strikes a good balance between the users' achieved maximum experienced delay and the real execution time.

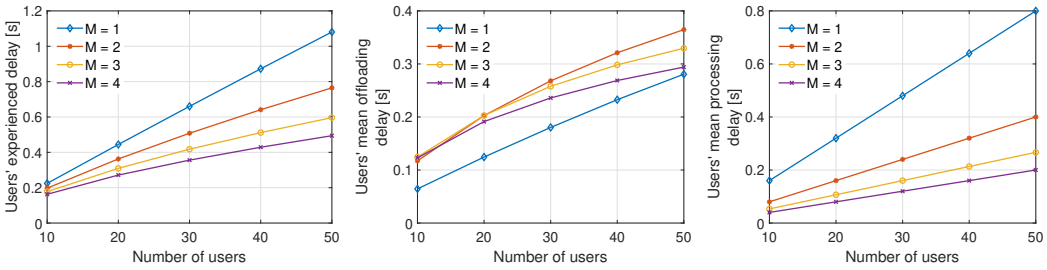

Figure 6.3: Pure performance evaluation of the proposed solution in terms of the users' (a) overall experienced delay, (b) mean offloading delay, and (c) mean processing delay.

Subsequently, we aim to evaluate the pure performance of the proposed solution under a large-scale system and interpret the operation of this multi-server MEC system in terms of the individual offloading and processing delays as the number of users and MEC servers increases. In this simulation setup, the overall system bandwidth is set equal to $B = 20$ MHz, and the number of users and servers varies in the intervals $N = [10, 50]$ and $M = [1, 4]$, while each user's computation task size is set as $C_n = 80$ Mega-CPU cycles. Fig. 6.3 depicts the mean values of the users' (a) overall experienced delays as defined in Eq. (6.17), (b) mean offloading delays to the different MEC servers, and (c) mean processing delays at the different MEC servers. Apparently, considering a fixed number of MEC servers, the higher the number of users existing in the system, then the higher their overall experienced delay is. The inverse behavior is observed as the number of MEC servers increases, given a fixed number of users. The rationale behind this operation is as follows. Considering that the MEC servers are spatially uniformly distributed within the square area, the denser this area becomes with the number of MEC servers increasing from $M = 2$ to $M = 4$, the users are getting closer to the MEC servers and achieve higher data rates (see Fig. 6.4), while the overall system's computing capacity increases at the same time. For this reason, both the users' mean offloading and processing delay at the different MEC servers decrease. Concerning the special case, when a single MEC server exists in the system (i.e., $M = 1$), Fig. 6.3b shows that a lower offloading delay is achieved compared to the multi-server MEC case since the users utilize the whole available bandwidth $B_n = \frac{B}{N}$ [Hz] to them without splitting it to accommodate multiple concurrent transmissions. This behavior is further corroborated by the results in Fig. 6.4 where it is implied that a higher offloading data rate per server is achieved by the users under the single-MEC server case. Nevertheless, given the high computing demands of the users, a significantly higher processing delay is caused in the single-server case than the multi-server case, which dominates and results in low

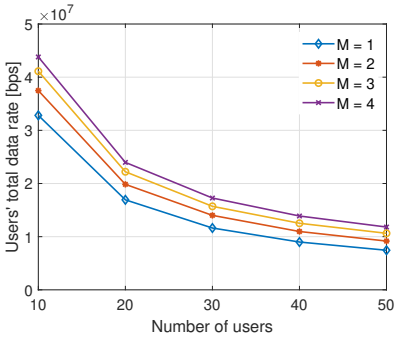

Figure 6.4: Pure performance evaluation of the proposed solution in terms of the users' total data rate.

overall experienced delays on the users' side for the latter. This highlights the superiority and benefits of multi-server to single-server MEC offloading in dense and high-computing demands systems.

To further identify the performance gains of an RSMA-based multi-server MEC system regarding the users' experienced delay, we compare its performance against the equivalent NOMA-based implementation in [170] and an OFDMA-based implementation, whose solution of problem (6.30) follows the work in [186]. The comparison is performed considering the same simulation setup as in Fig. 6.3, while an indicative number of $N = 40$ users and $M = 3$ MEC servers is selected. In Table 6.1, the mean values of the users' overall experienced delays (as defined in Eq. (6.17)) are summarized, considering different values of the minimum acceptable offloading data rate R_n^{min} to the MEC servers. As the minimum data rate demand R_n^{min} increases, the users' experienced delay ameliorates both in the RSMA and NOMA-based MEC systems, while the RSMA-based MEC system yields at average 28 ms lower experienced delays to the users compared to the NOMA-based one in all examined R_n^{min} cases. The OFDMA-based MEC system operates only under very low R_n^{min} demands, i.e., $R_n^{min} = 0.5$ Mbps, for the given available bandwidth, number of users and servers, where its performance surpasses the RSMA and NOMA-based systems. The latter is justified by the fact that, in OFDMA, each separate transmission/offloading is performed over a distinct frequency band that does not interfere with any other, resulting in a higher data rate and thus, lower users' experienced delay.

Table 6.1: Comparison among RSMA, NOMA, and OFDMA-based schemes in terms of the users' overall experienced delay, under different values of R_n^{min}.

	R_n^{min}			
Technique	0.5 Mbps	0.75 Mbps	1 Mbps	1.25 Mbps
RSMA	0.6194	0.5570	0.5117	0.4777
NOMA	0.6398	0.5827	0.5404	0.5082
OFDMA	0.5143	-	-	-
	1.5 Mbps	1.75 Mbps	2 Mbps	
RSMA	0.4521	0.4333	0.4229	
NOMA	0.4852	-	-	
OFDMA	-	-	-	

The results indicate that the RSMA-based system proves to be the only one among the rest of the alternatives that can provide a solution to the sum rate maximization problem (6.30) for increasing values of R_n^{min} up to 2 Mbps which is attributed to the intelligent control between decoding interference and treating interference as noise. Specifically, when employing power-domain NOMA, each transmission of a user to a MEC server senses the interference that stems from all other transmissions to the MEC servers for which the user-to-MEC-server channel gain is higher, making it hard to reach the minimum acceptable data rate requirement R_n^{min}. On the other hand, the inability of the implementation under the OFDMA technique to achieve a high value for the minimum acceptable data rate lies in the total available bandwidth fragmentation to N equal portions allocated to each user individually, each of which is then divided into M portions to facilitate the computation task offloading to the M different MEC servers.

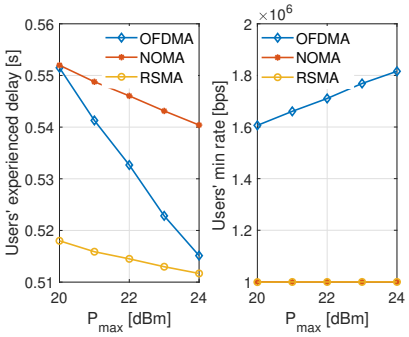

Figure 6.5: Comparison between RSMA, NOMA, and OFDMA-based schemes in terms of the users' (a) overall experienced delay, and (b) min data rate, under different values of P_n^{max}.

Fig. 6.5 illustrates the mean values of the users' experienced delays under the RSMA, NOMA, and OFDMA techniques, but this time considering different values of the users' maximum power budget P_n^{max}. As the users' power budget P_n^{max} increases, they can achieve higher offloading rates and thus, experience lower delays (left sub-figure) under all comparative multiple access techniques, while the RSMA-based solution provides constantly better performance. Fig. 6.5, also, reveals the significant impact that the maximum power budget P_n^{max} has on the performance of the OFDMA-based system, where the optimal solution for each user is to equally allocate its power to the different offloading MEC servers, i.e., $\frac{P_n^{max}}{M}$, and maximize the individual data rates to the servers since no interference exists between them. This effect is claimed by the sharp decrease in the users' experienced delays as their power budget gets higher (left sub-figure), which is further justified by the behavior of the users' minimum achievable data rate among the different MEC servers at the right sub-figure.

Chapter 7

Conclusions & Future Work

In this chapter, the main outcomes of this thesis are discussed (Section 7.1). Also, interesting directions for further research in the future are identified. Appendix A lists the publications that the author contributed to this thesis.

7.1 Conclusions

The advancements in NextG 5G wireless networks enable and are particularly enabled by the exaggerated data traffic demands and congestion, creating a never-ending cycle of fundamental and disruptive changes in the underlying wireless network architecture, infrastructure, and operation in general. Besides, the stringent and diversified user-application requirements hinder seamless service provisioning from the network operators' and providers' perspective, bringing the existing networks to their operational and capacity limits. Although various technologies have emerged lately in the direction of increasing spectrum capacity and expanding mobile computing service delivery, their plain and simplistic adoption is insufficient to address the resource-sharing problem. Apparently, a structural redesign of the resource management and optimization approaches is needed to be aligned with the evolution of the rest of the network.

In this thesis, we aimed to fill this gap by designing and developing resource management and optimization solutions that are compatible with and account for the emerging NextG 5G network's technologies and architectural paradigms while providing a more pragmatic and real-life spirit in the modeling and the derivation of the respective solutions. The specific common assumptions and practices of traditional resource management frameworks that we aimed to reduce are mainly: (i) the ability of the network to perform decision-making in a centralized manner, (ii) the existence of complete/full information at the different network entities, (iii) the altruistic and unselfish behavior of the network entities towards common pool resource sharing, (iv) the unilateral treatment of radio and computing resource management problems. To deal with the aforementioned challenges, different economic-theoretic models from the fields of Game Theory and Contract Theory were adopted to formulate and solve novel use case scenarios while considering multiple resources to be allocated, several network entities, and, thus, heterogeneous optimization objectives simultaneously. Thorough experimentation and simulation of the designed and proposed resource management solutions complemented our work to evaluate their operational characteristics and behavior under varying scenarios and against other state-of-the-art frameworks in the literature. Apart from the inherent benefits of the proposed frameworks owing to their distributed nature and flexibility, notable performance advantages were also identified in terms of spectral and energy efficiency, resource fairness, and response time minimization, to name a few.

The conclusions to which we arrived are the following:

- **Contract Theory can provide a powerful tool to enable decentralized decision-making under incompleteness of information.**
  Generally, Contract Theory provides the principles and mathematical foundations for how to regulate a market under the existence of incompleteness of information, e.g., the employment contract between employer and employees. Capitalizing on its statistical knowledge about the employees' (named as agents) private information, the employer (known as the principal) creates a menu of contractual arrangements, and each agent autonomously selects the one arrangement out of the menu that best fits its private information. The specific model has been successfully used in this thesis to formulate and solve the typical uplink power control problem in a NOMA-based heterogeneous multi-BS wireless network under the case of incomplete CSI on the BSs' behalf. The users, from their side, having potentially a better estimation regarding their experienced wireless channel conditions, are allowed to self-adapt and autonomously select the uplink transmission power level that best fits them out of the different contracts designed by the BSs. In this way, it is concurrently guaranteed that the selected contract meets the BSs' requirement for successful implementation of the SIC technique and signal decoding.

- **Contract Theory can be successfully used to reconcile conflicting goals of the network entities.**
  By designing mutually beneficial contractual arrangements, the principal can reconcile its conflicting goal with the agents that participate in the contract. To this end, a sort of reward is offered to the corresponding agents proportional to their private information and their autonomously selected effort for compensating their effort or even motivating them to provide a higher effort than they can afford. This concept of reconciling conflicting goals between the users and the computing service providers has been successfully applied within a multi-tier mobile computing network. Specifically, the novel idea presented in this thesis is to adequately motivate the selfish and greedily-acting users to utilize the whole spectrum of the computing continuum (including the edge and fog service layers in our work). Due to its appealing properties concerning its proximity to the users and the adequate computing capacity, the users tend to prefer more edge computing services to fog ones, gradually leading to the edge service layer's congestion and performance degradation. By properly designing contractual agreements, e.g., subscription packages, that provide a good tradeoff between monetary cost and QoS satisfaction, the computing service providers can shift the users' preferences and increase the network's capacity and efficiency.

- **Game Theory is another powerful tool to enable distributed decision-making between multiple heterogeneous network entities.**
  Given the already distributed nature of NextG 5G wireless networks and the inherent competition for sharing a common pool of resources such as spectrum or computing power of a remote server, we have extensively applied the principles of Game Theory in our works and our proposed frameworks. The specific application of this modeling has been used to allow for the users' distributed uplink power control in pure wireless communication networks while competing for the shared spectrum through which their transmissions are performed. Other game-theoretic models enable the hierarchical modeling of the players in the game in the form of leader(s) and follower(s). In this type of game, the leader makes a decision that is observable to the followers, who subsequently make their personal decisions. This game-theoretic model has also been widely applied to capture the hierarchy between the decisions of the BS or remote

server and the users lying in the user plane. Each distributively formulated and solved problem by the network entities becomes a maximization/minimization problem over a well-defined function. Then, Game Theory offers the tools for concrete mathematical formulations and provides interesting solution concepts leading to stable game outcomes, such as the Nash Equilibrium point that provides a common way to measure the effectiveness of the proposed framework.

- **Real-life modeling of network's behavior is complex, but the proposed frameworks and solutions need to be of low complexity.**
  Real-life applications on the NextG 5G environment require instantaneous transmissions and offloading, as well as real-time computations and decision-making to meet the ultra-low-latency and high-reliability QoS requirements. Furthermore, from a scalability perspective, a high-complexity centralized algorithm can rapidly become a bottleneck for the network from the viewpoints of execution and information transmission signaling overhead towards the centralized entity. In this context, effective and efficient algorithms of low complexity are required. Economic-theoretic and reinforcement learning algorithms tend to fit the above description by distributing the process and allowing each individual to perform the corresponding calculations. In this thesis, we designed and proposed relatively complex models that capture the participants' behavior, interdependent interactions, and decisions in a realistic manner but require low-complexity computations to converge to the optimum outcome.

- **Reconfigurable Intelligent Surfaces (RISs) can ameliorate both the spectral and the energy efficiency of the network.**
  Reconfigurable Intelligent Surfaces (RISs) consist of several reflecting elements constructed by engineered meta-materials, which can reflect the impinging electromagnetic waves by specifying their phase shift via a controller. The controller can be dynamically configured in a software-defined manner to adjust the placement of the elements to provide programmable properties to the radio propagation environment. This property is aligned with the broader vision of NextG 5G networks for instantaneous reconfigurability and adaptability, depending on the network's needs. At the same time, however, the employment of RISs has been verified - within the context of this thesis - that achieves its ultimate goal of combating the unfavorable propagation conditions due to the wireless channels' fading. Specifically, the prospect of RISs to enhance the energy and spectral efficiency along both the wireless access and the wireless backhaul of the network has been investigated, demonstrating the superior achieved performance compared to the benchmarking scenario where no RISs are deployed within the network topology. In this way, the network connectivity and the individual network entities' battery lifetime can be extended.

- **Using the whole spectrum of computing continuum leads to superior performance in terms of both energy and response time.**
  Apart from the QoS requirements of the user applications that steer the users' preferences and decisions towards a computing service provider (i.e., edge, fog, cloud), their inherent selfish and greedy behavioral characteristics play an important role when competing for a common pool of resources. Modeling the behavioral and economic interplay between the users and the competitive computing service providers is imperative to provide real-life spirit during the computing request scheduling and computing resource allocation procedure across the different computing service layers. This is the key idea upon which our proposed framework has been built towards utilizing the whole spectrum of the computing continuum, using Contract and Game Theories. The main findings of our work are that the proper utilization of multiple

tiers of computing capabilities allows for 100% satisfaction of the users' computing response time requirements while maintaining low energy consumption levels at the different computing layers when compared to different offloading alternatives, e.g., only local on users' devices, only edge, only fog.

- **Concurrent computation offloading to multiple servers reduces response times while allowing for customization and security.**
  Multi-server MEC offloading is another valuable strategy for various computing applications. This strategy takes advantage of the geographically distributed servers within the RAN of the NextG 5G networks to reduce the latency for users in different regions. The users of limited computation or energy availability can offload parts of their computation task to a combination of available MEC servers. Given that each MEC server is characterized by a different configuration, e.g., computing power and integrity in the calculations, this strategy allows for customization and flexibility from the user side depending on the needs of each part of the offloaded task. Specifically, heavy Machine Learning (ML) tasks, e.g., image processing, can benefit from multi-server MEC offloading. Different video feeds generated from vehicular, healthcare, or security applications - to name a few - can be offloaded to different MEC servers for processing. In this way, the total task complexity is reduced, and various levels of processing accuracy can be targeted for each part of the task based on each MEC server's computing capability. At the same time, distributing computations across multiple servers can improve security in the event of a security breach on one server. Specifically, regarding the reduced latency, this benefit has been practically identified and measured in this thesis while experimenting with different multiple access techniques during the users' radio transmission.

- **Designing holistic solutions is of utmost importance to exploit the full potential of the network architecture, infrastructure, and technology.**
  The NextG 5G wireless communication and mobile computing networks comprise an ever-rising number of degrees of freedom concerning the resources that need to be concurrently managed, stemming from the various enabling architectural paradigms and technologies adopted. The spectrum, transmission power, data rate, association to BSs, association to remote servers, RISs' elements' phase shifts, computation offloading, and computing power constitute only a few of the different parameters and resources that need to be considered at each time while a different subset of them has been jointly optimized in the context of this thesis. The specific outcomes of this thesis have verified the dominance of holistic optimization frameworks when compared against benchmarking solutions that unilaterally treat the optimization of different types of resources, resulting in more spectral, energy, and response-time efficient solutions. Low-complexity frameworks to address such combinatorial problems that most likely do not bear either linear or convex properties within polynomial time (i.e., milliseconds) are of significant and practical importance, further revealing the effectiveness of economic-theoretic modeling and solution frameworks.

7.2 Future Work

The work summarized in this thesis proposes a realistic, though, generic framework for resource management and optimization, where the control intelligence and decision-making process lie at the distributed network entities of the multi-tier and highly heterogeneous network topology. By either modeling the competitive interactions between them (game-theoretic modeling) or seeking to introduce their cooperation via contractual arrangements

(contract-theoretic modeling), the self-adaptation and optimization of the different network entities are encouraged, while providing a realistic flavor by reducing common assumptions, such as the existence of complete/full knowledge or the altruistic acting towards a common goal. Of course, interesting extensions of this theoretical framework can arise, and novel applications under the emerging 6G networks can be explored.

First, building upon the competitiveness of the underlying wireless communication and mobile computing network, new solution concepts based on the Market Equilibrium (ME) - or Economic Equilibrium as it is also called - can be explored. The ME is a fundamental concept in economics, describing the case in which the supply of a good or service matches the demand for that good or service in the market [187]. In other words, it is the point at which the quantity of a product that producers are willing to supply is equal to the quantity that consumers are willing to buy. The ME ensures that the resources are allocated efficiently, are not wasted, and the prices of the goods or services cover the producer costs. As a result, understanding the ME is critical for determining the prices and the quantities in a market economy, while it can also provide insights and predict how changes in various factors can impact the market. Market equilibrium concepts apply to wireless networks as well. In the context of wireless communication, market equilibrium helps optimize the allocation of limited resources such as radio spectrum and network capacity [188]. When supply (network capacity) aligns with demand (user data traffic), it results in efficient resource utilization. If the network capacity exceeds demand, it represents an underutilization of resources, whereas excess demand without sufficient capacity leads to congestion and a degraded user experience. Wireless providers constantly strive to find the equilibrium point where they can efficiently meet user demand while managing network investments. Market equilibrium principles guide decisions on pricing, capacity expansion, and quality of service to ensure the smooth operation of wireless networks while meeting consumer needs. Similar analogies can be made for the mobile computing market, offering computation offloading as a service, or any other service provided inherently by the network to the subscribed users.

Another interesting extension more related to the users' perspective when subscribing to a communication or computing service is their QoS satisfaction instead of the myopic QoS maximization. In this thesis - and in the majority of the literature on wireless networks - the user-centric solution concepts based on Game Theory concentrate on the users' total QoS maximization captured by their utility function. Such a strategy, however, results in unjustified network resource drainage or unfair resource allocation among the users. Instead of targeting optimality, the philosophy of aiming at a satisfactory QoS can be adopted. There are naturally several types of services that users are either simply interested in achieving a minimum QoS level, or they are insensitive to small QoS changes, such that there is no point in consuming additional resources or paying higher subscription fees for a better QoS level. This allows for remarkable savings in terms of power, cost, and signal processing complexity from the users' side, as well as contributes to increasing network capacity in the number of satisfied users while offering more personalized user satisfaction treatment. Given the need for sustainability in the designed and proposed resource allocation frameworks for future wireless networks, the concept of QoS satisfaction can ameliorate energy efficiency and overall resource utilization. This solution concept can be realized by following problem formulations based on Games in Satisfaction Form [189].

Considering the extension of the application of the proposed theoretical frameworks, an intriguing example constitutes Federated Learning (FL) over wireless networks. Federated learning is a distributed machine learning method that enables mobile users to collaboratively learn a shared prediction model while keeping their collected data on their devices [190, 191]. To train an FL algorithm over a wireless network, the users must transmit the training parameters over wireless links to the responsible network entity that controls the federated learning procedure (e.g., edge server), which in turn can introduce training

errors due to the limited and shared wireless resources between them, as well as the inherent unreliability of the wireless propagation environment. First, as implied by its operation, FL provides a distributed communication and computing architectural paradigm perfectly aligned with the ones studied in this thesis. Secondly, the incompleteness of information between the users and their communication with the controlling network entity worsens the training procedure and results in the users' unnecessary energy consumption for both transmission and local model training/computation task execution. The latter has as a consequence limited motivation from the users' perspective to participate in a federated learning procedure, calling for appropriate mutually beneficial arrangements between them and the controlling entity. Last, holistic solutions that jointly treat the problem of radio and computing resource allocation at the user devices' side should be implemented to unleash this architectural paradigm's benefits. Therefore, the problem of federated learning over wireless networks provides a perfect application that naturally extends our work along the different research directions that we tackle [192].

Last, apart from the different theoretical frameworks and emerging application examples where our proposed resource management solutions could provide a good fit, the evolution of the resource management algorithms is also possible and even necessary. Continuing on the wide topic and research area of machine learning while placing our focus on Reinforcement Learning (RL) and Deep Reinforcement Learning (DRL) [193], several practices and algorithms from the latter field can be utilized and contribute to the excellence of our proposed frameworks. Indeed, RL/DRL is another powerful tool that enables decision-making in situations where perfect information on the system is impossible, by simply relying on the corresponding agent's past actions and the observation of its effects on them and the environment, possibly ignoring the effect on other agents or more precise network information. RL/DRL can also model both single-agent and multi-agent systems and distributively solve resource management problems when the second case applies, allowing at the same time more complex modeling in general compared to the meticulously hand-crafted economic-theoretic utility functions [194]. As a consequence, more complex behaviors, interactions and decisions can be captured, leading to even more realistic solutions to the resource management and optimization problem, with the cost, however, of potentially higher execution and training times.

Appendix A

Author's Publications

International Peer Reviewed Journals

- **M. Diamanti**, N. Fryganiotis, S. Papavassiliou, C. Pelekis, E. E. Tsiropoulou, "Minimum Collisions Assignment in Interdependent Networked Systems via Defective Colorings," in ITU Journal on Future and Evolving Technologies. (Under review)

- P. Charatsaris, **M. Diamanti**, S. Papavassiliou, "Joint User Association and Resource Allocation for Hierarchical Federated Learning based on Games in Satisfaction Form," in IEEE Open Journal of the Communications Society. (Revision submitted)

- G. Kakkavas, **M. Diamanti**, V. Karyotis, K. N. Nyarko, M. Gabriel, A. Zafeiropoulos, S. Papavassiliou, K. Moessner, "5G Perspective of Connected Autonomous Vehicles: Current Landscape and Challenges Toward 6G," in IEEE Wireless Communications Magazine. (Revision submitted)

- **M. Diamanti**, G. Kapsalis, E. E. Tsiropoulou and S. Papavassiliou, "Energy-Efficient Rate-Splitting Multiple Access: A Deep Reinforcement Learning-Based Framework," in IEEE Open Journal of the Communications Society, doi: 10.1109/OJCOMS.2023.3322047.

- **M. Diamanti**, C. Pelekis, E. E. Tsiropoulou and S. Papavassiliou, "Delay Minimization for Rate-Splitting Multiple Access-Based Multi-Server MEC Offloading," in IEEE/ACM Transactions on Networking, doi: 10.1109/ TNET.2023.3311131.

- M. S. Siraj, A. B. Rahman, **M. Diamanti**, E. E. Tsiropoulou and S. Papavassiliou, "Alternative Positioning, Navigation, and Timing Enabled by Games in Satisfaction Form and Reconfigurable Intelligent Surfaces," in IEEE Systems Journal, vol. 17, no. 3, pp. 5035-5046, Sept. 2023, doi: 10.1109/JSYST.2023.3268989.

- S. Hossain, N. Irtija, **M. Diamanti**, F. Sangoleye, E. E. Tsiropoulou, S. Papavassiliou, "Reconfigurable Intelligent Surfaces-enabled Edge Computing: A Location-aware Task Offloading Framework," in ITU Journal on Future and Evolving Technologies, vol. 3, no. 3, pp. 830-843, 2022, doi: 10.52953/FLTJ9889.

- **M. Diamanti**, P. Charatsaris, E. E. Tsiropoulou and S. Papavassiliou, "Incentive Mechanism and Resource Allocation for Edge-Fog Networks Driven by Multi-Dimensional Contract and Game Theories," in IEEE Open Journal of the Communications Society, vol. 3, pp. 435-452, 2022, doi: 10.1109/OJCOMS.2022.3154536.

- G. Kakkavas, **M. Diamanti**, A. Stamou, V. Karyotis, F. Bouali, J. Pinola, O. Apilo, S. Papavassiliou, K. Moessner, "Design, Development, and Evaluation of 5G-Enabled Vehicular Services: The 5G-HEART Perspective," Sensors, vol. 22, no. 2, p. 426, Jan. 2022, doi: 10.3390/s22020426.

- **M. Diamanti**, P. Charatsaris, E. E. Tsiropoulou and S. Papavassiliou, "The Prospect of Reconfigurable Intelligent Surfaces in Integrated Access and Backhaul Networks," in IEEE Transactions on Green Communications and Networking, vol. 6, no. 2, pp. 859-872, June 2022, doi: 10.1109/TGCN.2021.3126784.

- **M. Diamanti**, G. Fragkos, E. E. Tsiropoulou and S. Papavassiliou, "Unified User Association and Contract-Theoretic Resource Orchestration in NOMA Heterogeneous Wireless Networks," in IEEE Open Journal of the Communications Society, vol. 1, pp. 1485-1502, 2020, doi: 10.1109/OJCOMS.2020.3024778.

International Conferences

- **M. Diamanti**, G. Kapsalis, E. E. Tsiropoulou, S. Papavassiliou, "Energy-Efficient Power and Rate Allocation for Rate-Splitting Multiple Access via Deep Q-Learning," in GLOBECOM Workshops 2023 - 2023 IEEE Global Communications Conference Workshops. (Accepted)

- P. Charatsaris, **M. Diamanti**, E. E. Tsiropoulou and S. Papavassiliou, "Efficient Power Control for Integrated Sensing and Communication Networks with Dual Connectivity," ICC 2023 - IEEE International Conference on Communications, Rome, Italy, 2023, pp. 5910-5915, doi: 10.1109/ICC45041.2023.10279737.

- P. Charatsaris, **M. Diamanti** and S. Papavassiliou, "On the Accuracy-Energy Tradeoff for Hierarchical Federated Learning via Satisfaction Equilibrium," 2023 19th International Conference on Distributed Computing in Smart Systems and the Internet of Things (DCOSS-IoT), Pafos, Cyprus, 2023, pp. 422-428, doi: 10.1109/DCOSS-IoT58021.2023.00073.

- G. Kakkavas, K. N. Nyarko, C. Lahoud, D. Kuehnert, P. Kueffner, M. Gabriel, S. Ehsanfar, **M. Diamanti**, V. Karyotis, K. Moessner, S. Papavassiliou, "Demo Proposal: Tele-Operated Support over 4G/5G Mobile Communications," 2021 IEEE International Mediterranean Conference on Communications and Networking (MeditCom), Athens, Greece, 2021, pp. 1-2, doi: 10.1109/MeditCom49071.2021.9647643.

- M. S. Siraj, A. B. Rahman, **M. Diamanti**, E. E. Tsiropoulou, S. Papavassiliou and J. Plusquellic, "Orchestration of Reconfigurable Intelligent Surfaces for Positioning, Navigation, and Timing," MILCOM 2022 - 2022 IEEE Military Communications Conference (MILCOM), Rockville, MD, USA, 2022, pp. 148-153, doi: 10.1109/MILCOM55135.2022.10017665.

- P. Charatsaris, **M. Diamanti**, E. E. Tsiropoulou and S. Papavassiliou, "Competitive Energy Allocation for Aerial Computation Offloading: A Colonel Blotto Game," GLOBECOM 2022 - 2022 IEEE Global Communications Conference, Rio de Janeiro, Brazil, 2022, pp. 970-975, doi: 10.1109/GLOBECOM48099.2022.10001655.

- **M. Diamanti**, N. Fryganiotis, S. Papavassiliou, C. Pelekis and E. E. Tsiropoulou, "On the Minimum Collisions Assignment Problem in Interdependent Networked Systems," 2022 IEEE Symposium on Computers and Communications (ISCC), 2022, pp. 1-6, doi: 10.1109/ISCC55528.2022.9912969.

- **M. Diamanti** and S. Papavassiliou, "Trading in Collaborative Mobile Edge Computing Networks: A Contract Theory-based Auction Model," 2022 IEEE 18th International Conference on Distributed Computing in Sensor Systems (DCOSS), 2022, pp. 387-393, doi: 10.1109/DCOSS54816.2022.00068.

- **M. Diamanti**, E. E. Tsiropoulou and S. Papavassiliou, "An Incentivization Mechanism for Green Computing Continuum of Delay-Tolerant Tasks," ICC 2022 - IEEE International Conference on Communications, 2022, pp. 3538-3543, doi: 10.1109/ICC45855.2022.9838752.

- G. Kakkavas, **M. Diamanti**, M. Gabriel, C. Lahoud, P. Akula, V. Karyotis, K. Moessner, S. Papavassiliou, "Demo Proposal: Tele-Operated Support over 4G/5G Mobile Communications," 2021 IEEE International Mediterranean Conference on Communications and Networking (MeditCom), 2021, pp. 1-2, doi: 10.1109/MeditCom49071.2021.9647643.

- G. Kakkavas, **M. Diamanti**, A. Stamou, V. Karyotis, S. Papavassiliou, F. Bouali, K. Moessner, "5G Network Requirement Analysis and Slice Dimensioning for Sustainable Vehicular Services," 2021 17th International Conference on Distributed Computing in Sensor Systems (DCOSS), 2021, pp. 495-502, doi: 10.1109/DCOSS52077.2021.00082.

- **M. Diamanti**, E. E. Tsiropoulou and S. Papavassiliou, "The Joint Power of NOMA and Reconfigurable Intelligent Surfaces in SWIPT Networks," 2021 IEEE 22nd International Workshop on Signal Processing Advances in Wireless Communications (SPAWC), 2021, pp. 621-625, doi: 10.1109/SPAWC51858.2021.9593111.

- **M. Diamanti**, M. Tsampazi, E. E. Tsiropoulou and S. Papavassiliou, "Energy Efficient Multi-User Communications Aided by Reconfigurable Intelligent Surfaces and UAVs," 2021 IEEE International Conference on Smart Computing (SMARTCOMP), 2021, pp. 371-376, doi: 10.1109/SMARTCOMP52413.2021.00075.

- **M. Diamanti**, E. E. Tsiropoulou and S. Papavassiliou, "Resource Orchestration in UAV-assisted NOMA Wireless Networks: A Labor Economics Perspective," ICC 2021 - IEEE International Conference on Communications, 2021, pp. 1-6, doi: 10.1109/ICC42927.2021.9500715.

- **M. Diamanti**, G. Fragkos, E. E. Tsiropoulou, S. Papavassiliou, "Resource Orchestration in Interference-Limited Small Cell Networks: A Contract-Theoretic Approach," International Conference on Network Games, Control and Optimization (NETGCOOP), Springer, Cham, 2021, pp. 101-109, doi: 10.1007/978-3-030-87473-5_10.

Εκτεταμένη Περίληψη

Υπό το πρίσμα του ευρύτερου οράματος για ψηφιοποίηση και μετασχηματισμό των κάθετων βιομηχανιών (π.χ. έξυπνες πόλεις, έξυπνο σύστημα υγείας, έξυπνα εργοστάσια), σημειώνεται μια άνευ προηγουμένου αύξηση των εφαρμογών με εντατικές απαιτήσεις ως προς τον όγκο των δεδομένων που διαχειρίζονται και την αναγκαία υπολογιστική ισχύ για την επεξεργασία αυτών. Αυτό έχει ως αποτέλεσμα την επιβολή αυστηρών απαιτήσεων που αφορούν το ασύρματο δίκτυο επικοινωνιών και υπολογισμών. Ως μέσο επέκτασης της συνδεσιμότητας, αύξησης της φασματικής και ενεργειακής απόδοσης και μείωσης της χρονικής καθυστέρησης, μια πληθώρα τεχνολογιών και αρχιτεκτονικών παραδειγμάτων αναδεικνύονται ως βασικά μέσα ενεργοποίησης και ενδυνάμωσης των ασύρματων δικτύων 5G επόμενης γενιάς. Σε αυτό το πλαίσιο, η απλοϊκή υιοθέτηση υφιστάμενων λύσεων σε παραδοσιακά προβλήματα κατανομής πόρων είναι αναποτελεσματική για την εξερεύνηση και την εκμετάλλευση των δυνατοτήτων του δικτύου. Αντίθετα, αρκετοί βαθμοί ελευθερίας πρέπει να καθορίζονται ταυτόχρονα σχετικά με τη φύση και το είδος των πόρων που κατανέμονται στο δίκτυο, λαμβάνοντας ταυτόχρονα υπόψιν τον πολύπλευρο ανταγωνισμό μεταξύ των διαφορετικών ενδιαφερόμενων μερών (π.χ. συνδρομητές, πάροχοι).

Στη διατριβή αυτή αναλύονται οι συγκεκριμένες τεχνολογίες που λειτουργούν ως βασικά μέσα ενεργοποίησης των εξεταζόμενων ασύρματων δικτύων επόμενης γενιάς σε συνδυασμό με τα προβλήματα διαχείρισης πόρων που αυτές αναδεικνύουν και τα οποία λαμβάνονται υπόψιν. Ειδικότερα, παρακάτω μελετώνται εξελίξεις στην ασύρματη διεπαφή (air interface), όπως νέες τεχνικές πολλαπλής πρόσβασης ή άλλες τεχνολογίες επεμβατικές προς το ασύρματο περιβάλλον διάδοσης, εξελίξεις που αφορούν στην αρχιτεκτονική του δικτύου, αλλά και στη μορφή της ευφυίας που αυτό πρέπει να φέρει.

1. Εξελίξεις στην ασύρματη διεπαφή

1.Α. Νέες τεχνικές πολλαπλής πρόσβασης

Μέσα σε αυτό το συμφορημένο και απαιτητικό περιβάλλον ασύρματων επικοινωνιών, το πρόβλημα της αποτελεσματικής, συνετής και φειδωλής χρήσης των πόρων και των δυνατοτήτων του συστήματος και των χρηστών γίνεται ακόμη πιο επείγον. Από την πλευρά του ασύρματου δικτύου, αυτή η ανάγκη αντικατοπτρίζεται στην αποτελεσματική χρήση των διαθέσιμων πόρων φάσματος. Από την πλευρά των χρηστών, αυτοί πρέπει να διαχειρίζονται έξυπνα την επένδυση ισχύος των φορητών συσκευών τους για την εκτέλεση διαφορετικών εργασιών επικοινωνίας και υπολογισμού. Πράγματι, η τεχνική πολλαπλής πρόσβασης που χρησιμοποιείται για την πολυπλεξία των διαφορετικών μεταδόσεων που πραγματοποιούνται είτε στην ζεύξη ανόδου ή καθόδου είναι κρίσιμη για τη φασματική και την ενεργειακή απόδοση του δικτύου.

Προηγούμενες γενιές ασύρματων δικτύων, π.χ., 1G, 2G, 3G, βασίζονταν αποκλειστικά σε τεχνικές Ορθογωνικής Πολλαπλής Πρόσβασης (Orthogonal Multiple Access - OMA) [19], σύμφωνα με τις οποίες τα διαθέσιμα Μπλοκ Πόρων (Resource Blocks - RB) σε κάθε κυψέλη χωρίζονται ορθογώνια είτε στο πεδίο του χρόνου, της συχνότητας ή του κώδικα και κατανέμονται κατάλληλα έτσι ώστε να καταστέλλεται η παρεμβολή μεταξύ γειτονικών RBs. Αν και οι τεχνικές OMA επιτρέπουν την απλή ανίχνευση σήματος στον δέκτη, είναι σημαντικά περιοριστικές στον αριθμό των ταυτόχρονων μεταδόσεων που μπορούν να υποστηρίξουν λόγω του πεπερασμένου αριθμού των διαθέσιμων RBs και, ως εκ τούτου, οδηγούν σε κακή χρήση του φάσματος. Επιπλέον, η πιθανή κακή ποιότητα του καναλιού των χρηστών σε συνδυασμό με την τυχαία φύση του ασύρματου περιβάλλοντος διάδοσης δεν μπορούν να εγγυηθούν την επιτυχία της μετάδοσης δεδομένων ακόμη και υπό ορθογώνια κατανομή πόρων φάσματος. Ως εκ τούτου, ο σχεδιασμός και η ανάπτυξη προηγμένων και ισχυρών τεχνικών πολλαπλής πρόσβασης διερευνάται συνεχώς τα

τελευταία χρόνια, με αποτέλεσμα την εισαγωγή της Μη Ορθογωνικής Πολλαπλής Πρόσβασης (Non-Orthogonal Multiple Access - NOMA) [21].

1.Α.1. Μη Ορθογωνική Πολλαπλή Πρόσβαση (Non-Orthogonal Multiple Access - NOMA): Το NOMA είναι μια βασική τεχνική που επιτρέπει την αποτελεσματική εκμετάλλευση των διαθέσιμων ραδιοπόρων και την εξυπηρέτηση πολλών χρηστών ταυτόχρονα στο ίδιο RB, πολυπλέκοντας τα σήματά τους στο πεδίο της ισχύος [22] ή στο πεδίο του κώδικα [23]. Για παράδειγμα, θεωρώντας τη ζεύξη καθόδου και εφαρμόζοντας το NOMA στο πεδίο της ισχύος [24], τα σήματα προς μετάδοση από το σταθμό βάσης υφίστανται υπέρθεση και έπειτα μεταδίδονται σε πολλούς χρήστες χρησιμοποιώντας διαφορετικά επίπεδα ισχύος. Οι χρήστες με σχετικά υψηλό κέρδος καναλιού αποκωδικοποιούν τα σήματα παρεμβολής πριν αποκωδικοποιήσουν το σήμα που προορίζεται για αυτούς χρησιμοποιώντας την τεχνική Διαδοχικής Ακύρωσης Παρεμβολών (Successive Interference Cancellation - SIC), ενώ οι χρήστες χαμηλού κέρδους καναλιού αντιμετωπίζουν την παρεμβολή ως θόρυβο. Από την άλλη πλευρά, κατά την εφαρμογή του NOMA στο πεδίο της ισχύος στη ζεύξη ανόδου [24], η αποκωδικοποίηση του υπερτιθέμενου σήματος που λαμβάνεται από το σταθμό βάσης ξεκινά από το σήμα του χρήστη με το υψηλότερο κέρδος καναλιού, καθώς το σήμα του είναι πιο πιθανό το ισχυρότερο. Οι χρήστες με υψηλό κέρδος καναλιού υπόκεινται σε παρεμβολές από όλους τους άλλους χρήστες του συστήματος, ενώ οι χρήστες χαμηλού κέρδους καναλιού απολαμβάνουν μετάδοση χωρίς παρεμβολές. Δεδομένου ότι οι χρήστες διακρίνονται με βάση την ποιότητα της ασύρματης σύνδεσής τους και την αντίστοιχη επένδυση ισχύος κατά τη μετάδοση που, με τη σειρά της, καθορίζεται βάσει της επιδιωκόμενης ποιότητας υπηρεσίας, το NOMA παρέχει μια αποτελεσματική μέθοδο για την επίτευξη δικαιοσύνης μεταξύ των διαφορετικών χρηστών. Ωστόσο, τα επιτεύγματα του NOMA όσον αφορά τη φασματική και ενεργειακή απόδοση, καθώς και τη δικαιοσύνη μεταξύ των χρηστών, συνοδεύονται από το κόστος της αυξημένης πολυπλοκότητας αποκωδικοποίησης σήματος στους δέκτες σε αντίθεση με τις παραδοσιακές τεχνικές OMA.

1.Α.2. Πολλαπλή Πρόσβαση Διαίρεσης Ρυθμού (Rate-Splitting Multiple Access - RSMA): Το RSMA ανήκει στην ευρύτερη κατηγορία των μη ορθογωνικών τεχνικών πολλαπλής πρόσβασης και θεωρείται πρακτικά ως ο διάδοχος του NOMA, παρέχοντας ένα γενικότερο και ισχυρότερο πλαίσιο μετάδοσης από τον προκάτοχό του [25, 26]. Ακολουθώντας αυτή την τεχνική, τα μηνύματα καθενός χρήστη χωρίζονται σε κοινά (common parts) και ιδιωτικά (private parts) μέρη στον πομπό, έτσι ώστε μέρος της παρεμβολής να αποκωδικοποιείται στον δέκτη ενώ το υπόλοιπο να αντιμετωπίζεται ως θόρυβος. Με αυτόν τον τρόπο, το RSMA επιτρέπει την ομαλή γεφύρωση και, επομένως, τον συμβιβασμό των δύο ακραίων στρατηγικών διαχείρισης παρεμβολών, δηλαδή αυτών της αντιμετώπισης των παρεμβολών ως θορύβου και της πλήρους αποκωδικοποίησης παρεμβολών. Η πρώτη ακραία περίπτωση είναι χαρακτηριστική των συστημάτων Πολλαπλής Πρόσβασης Διαίρεσης Χώρου (Space Division Multiple Access - SDMA) και Πολλαπλής Εισόδου Πολλαπλής Εξόδου (Multiple Input Multiple Output - MIMO), ενώ η δεύτερη προετείνεται από το NOMA. Για παράδειγμα, κατά το RSMA στη ζεύξη καθόδου [27], το υπερτιθέμενο μήνυμα που μεταδίδεται από το σταθμό βάσης προς πολλούς χρήστες χωρίζεται σε ένα κοινό μήνυμα (common message) και ένα ιδιωτικό μήνυμα (private message). Το κοινό μήνυμα προορίζεται και αποκωδικοποιείται από όλους τους εμπλεκόμενους χρήστες στη μετάδοση, ενώ το ιδιωτικό μήνυμα αφορά κάθε χρήστη ξεχωριστά. Ως αποτέλεσμα, κατά την αποκωδικοποίηση του ιδιωτικού μηνύματος, οι παρεμβολές που προέρχονται από τα ιδιωτικά μηνύματα των άλλων χρηστών αντιμετωπίζονται ως θόρυβος. Με αυτόν τον τρόπο, μπορεί να επιτευχθεί μια καλή ισορροπία μεταξύ αποτελεσματικής χρήσης φάσματος, διαχείρισης παρεμβολών και πολυπλοκότητας επεξεργασίας σήματος, βελτιώνοντας την απόδοση του ασύρματου δικτύου.

1.Β. Αναδιαμορφώσιμες Έξυπνες Επιφάνειες (Reconfigurable Intelligent Surfaces - RIS)

Με στόχο την αντιμετώπιση του προβλήματος της επέκτασης της κάλυψης του δικτύου, η τεχνολογία των Αναδιαμορφώσιμων Έξυπνων Επιφανειών (Reconfigurable Intelligent Surfaces

- RIS) αναδείχθηκε ως ένας άλλος βασικός ενεργοποιητής των ασύρματων δικτύων επόμενης γενιάς 5G. Η εισαγωγή των RIS ως τρόπου χειρισμού του περιβάλλοντος ασύρματης διάδοσης αποτελεί ένα προκαταρκτικό βήμα προς το ευρύτερο όραμα των Δικτύων Καθοριζόμενων από Λογισμικό (Software-Defined Networking - SDN), σύμφωνα με το οποίο τα δίκτυα μπορούν να ελέγχονται εξ αποστάσεως μέσω της χρήσης προγραμματιζόμενου λογισμικού [28]. Επιπλέον, ο σχεδιασμός των RIS ικανοποιεί τη βασική απαίτηση για ευέλικτες, εφικτές και οικονομικά αποδοτικές λύσεις όσον αφορά την ανάπτυξη, τη συντήρηση και τον έλεγχο. Ως εκ τούτου, πολλές ερευνητικές εργασίες μπορούν να βρεθούν στη βιβλιογραφία που μελετούν διαφορετικές πτυχές του σχεδιασμού, της ανάπτυξης και της βελτιστοποίησής τους, κάνοντας χρήση και άλλων όρων, όπως Έξυπνες Ανακλαστικές Επιφάνειες (Intelligent Reflecting Surfaces - IRS) [29] και Μεγάλες Ευφυείς Επιφάνειες (Large Intelligent Surfaces - LIS) [30]. Πρακτικά, ένα RIS είναι μια ελεγχόμενη από λογισμικό μεταεπιφάνεια χαμηλού πάχους και σχήματος μιας δισδιάστατης επίπεδης διάταξης που αποτελείται από έναν αριθμό παθητικών ανακλαστικών στοιχείων χαμηλού κόστους. Κάθε μεμονωμένο ανακλαστικό στοιχείο μπορεί ανεξάρτητα να αντανακλά τα προσπίπτοντα σήματα προς έναν επιθυμητό προορισμό, ο οποίος καθορίζεται με ψηφιακό έλεγχο του ρυθμιζόμενου πλάτους και των μετατοπίσεων φάσης των στοιχείων του RIS μέσω ενός έξυπνου ελεγκτή. Ο αθροιστικός στόχος πίσω από τον έλεγχο των ανακλαστικών στοιχείων μπορεί να αφορά τη μεγιστοποίηση της φασματικής απόδοσης [31], την ελαχιστοποίηση κατανάλωσης ενέργειας [32] ή την παροχή Εξαιρετικά Αξιόπιστων υπηρεσιών Χαμηλής Χρονικής Απόκρισης (Ultra Reliable Low Latency - URLL) [33]. Εν τω μεταξύ, τα RIS μπορούν να εγκατασταθούν οπουδήποτε, επικαλύπτοντας επιφάνειες εδάφους [34] ή ακόμα και αερομεταφερόμενες πλατφόρμες [35].

2. Εξελίξεις στην αρχιτεκτονική δικτύου

Μέχρι στιγμής, τα υπάρχοντα ασύρματα δίκτυα έχουν σχεδιαστεί για να εξυπηρετούν ουσιαστικά επικοινωνίες προσανατολισμένες στα bit, σε αντίθεση με την προσανατολισμένη στην εκτέλεση εργασιών υπολογισμού φύση των ασύρματων επικοινωνιών επόμενης γενιάς. Τα δίκτυα επόμενης γενιάς θα πρέπει να υποστηρίζουν άμεσες αλληλεπιδράσεις ανθρώπου με μηχανή και μηχανής με μηχανή μέσω κειμένου, ομιλίας και εικόνας, καθώς και επαυξημένης και εικονικής πραγματικότητας για να ευθυγραμμιστούν με τη γενικότερη ανάγκη για ψηφιοποίηση, καθώς και με τις ανάγκες των κάθετων βιομηχανιών. Η τελευταία απαίτηση επιβάλλει τη σύγκλιση επικοινωνίας και υπολογισμών, με αποτέλεσμα μια βαθιά αλλαγή στη συνολική αρχιτεκτονική του δικτύου.

Πολλά μοντέλα υπολογισμών έχουν προταθεί τα τελευταία χρόνια από την ερευνητική κοινότητα που διαμορφώνουν το λεγόμενο "υπολογιστικό συνεχές", με υπολογιστικά συστήματα εγκατεστημέναστην άκρη του δικτύου έως το νέφος, απώτερος σκοπός των οποίων είναι να αντιμετωπίσουν ζητήματα των εφαρμογών με απαίτηση υψηλού εύρους ζώνης, γεωγραφικής διασποράς, εξαιρετικά χαμηλής χρονικής απόκρισης και αυξημένης ιδιωτικότητας. Τα πιο δημοφιλή παραδείγματα, ωστόσο, είναι οι τεχνολογίες Υπολογιστικού Νέφους (Mobile Cloud Computing - MCC) [15, 16], Υπολογιστικής Ομίχλης (Mobile Fog Computing - MFC) [14] και τα Υπολογιστικά Συστήματα στην Άκρη του Δικτύου (Mobile/Multi-Access Edge Computing - MEC) [17]. Ο κοινός παρονομαστής μεταξύ αυτών των παραδειγμάτων είναι η ανάπτυξη δυνατοτήτων που μοιάζουν με το υπολογιστικό νέφος στην άκρη του δικτύου με τη μορφή κέντρων δεδομένων (data senters), ενώ διακρίνονται από αρχιτεκτονική άποψη σχετικά με τη θέση όπου τοποθετείται η υπολογιστική τους ισχύς. Ειδικότερα, στο μοντέλο υπολογισμών στην άκρη του δικτύου, η υπολογιστική ισχύς και η ευφυΐα υλοποιούνται ακριβώς στην άκρη του δικτύου, ενώ στην περίπτωση του υπολογισμού ομίχλης, αυτή η λειτουργία μπορεί να προσφέρεται σε διαφορετικές θέσεις μεταξύ της άκρης του δικτύου και του δικτύου κορμού (core network) που συνδέεται με το νέφος. Είναι, επομένως, δυνατό να δημιουργηθεί μια ιεραρχική πολυεπίπεδη αρχιτεκτονική, διασυνδεδεμένη με την υποδομή ασύρματου δικτύου, η οποία επιτρέπει τη συνεργασία των επι-

μέρους κέντρων δεδομένων μεταξύ τους. Οποιοσδήποτε πελάτης – από τρίτους παρόχους υπηρεσιών έως τελικούς χρήστες, αλλά και τους ίδιους τους παρόχους υποδομής – μπορεί να χρησιμοποιήσει αυτό το υπολογιστικό συνεχές και να εκφορτώσει τις υπολογιστικές του εργασίες για απομακρυσμένη εκτέλεση, αξιοποιώντας την υπάρχουσα υποκείμενη υποδομή ασύρματου δικτύου.

2.Α. Υπολογιστικά Συστήματα στην Άκρη του Δικτύου (Multi-Access Edge Computing - MEC)

Ειδικότερα, το MEC έχει εισαχθεί για να φέρει τις υπηρεσίες και τους πόρους του νέφους πιο κοντά στον τελικό χρήστη, όπου ο όρος "πιο κοντά" υποδηλώνει την άμεση εφαρμογή του εντός του Δικτύου Ραδιοπρόσβασης (Radio Access Network - RAN). Ειδικότερα, οι ενδεικτικές τοποθεσίες ανάπτυξης που εξετάζονται για το MEC από το MEC ISG περιλαμβάνουν, κυψέλες LTE/5G BS (eNodeBs/gNodeB), ελεγκτές ασύρματης πρόσβασης 3G (Radio Network Controllers - RNC) και δίκτυα πολλαπλών ραδιο-τεχνολογιών (3G/LTE/WLAN) [39], ενσωματώνοντας επίσης άλλους δικτυακούς πόρους και πόρους αποθήκευσης με τη μορφή της πλατφόρμας MEC. Συνεπώς, λόγω της πυκνής εγκατάστασης των διακομιστών MEC και της εγγύτητάς τους στους χρήστες, το MEC παρέχει μια πολλά υποσχόμενη λύση στα προβλήματα επεκτασιμότητας, υποστήριξης κινητικότητας, ασφάλειας και ιδιωτικότητας, εκτός από την υποστήριξη επικοινωνιών και εκτελέσεων απομακρυσμένων υπολογισμών μεγάλου όγκου, για τα οποία προοριζόταν αρχικά. Τα δίκτυα κινητών υπολογισμών επόμενης γενιάς θα πρέπει να μπορούν να εξυπηρετούν πληθώρα κινούμενων συσκευών και, ως εκ τούτου, απαιτείται η δυναμική και απρόσκοπτη διαχείριση του αριθμού και της κίνησής τους για τη διατήρηση μιας υψηλής ποιότητας υπηρεσίας. Επιπλέον, το MEC ακολουθεί τις γενικές αρχές των κατανεμημένων αρχιτεκτονικών, παρόμοια με την κατανεμημένη αρχιτεκτονική των ασύρματων δικτύων, ενισχύοντας την ασφάλεια του συνολικού δικτύου και μειώνοντας μεμονωμένα σημεία αστοχίας. Είναι αξιοσημείωτο, ωστόσο, ότι ανεξάρτητα από τα ελκυστικά και κυρίαρχα χαρακτηριστικά του MEC σε σύγκριση με άλλα μοντέλα υπολογισμών, είναι σημαντικό να λαμβάνεται υπόψη και να χρησιμοποιείται ως συμπλήρωμα του μοντέλου υπολογιστικού νέφους και όχι ως αντικατάστασης του τελευταίου. Το MEC αποτελεί μια ακόμα κοινή δεξαμενή πόρων που θα πρέπει να χρησιμοποιείται αποτελεσματικά, συνετά και με φειδώ για να καρπωθούμε τα οφέλη του, παρόμοια με τους πόρους φάσματος στο πλαίσιο των ασύρματων επικοινωνιών. Διαφορετικά, η υπερεκμετάλλευσή του θα οδηγήσει σταδιακά σε υποβάθμιση της απόδοσής του.

3. Ενσωμάτωση ευφυίας

Η σημαντική αύξηση της κυκλοφορίας δεδομένων και των εργασιών υπολογισμού οδηγεί στη μετατροπή των ραδιοπόρων και των υπολογιστικών πόρων σε κρίσιμο σημείο συμφόρησης των ασύρματων δικτύων επικοινωνίας και κινητών υπολογισμών επόμενης γενιάς. Ένα είδος νοημοσύνης των δικτύων επόμενης γενιάς έγκειται στην ικανότητά τους να εκτελούν δυναμική διαχείριση και βελτιστοποίηση των πόρων αυτών. Δεδομένης της κατανεμημένης φύσης τους, αυτό το είδος νοημοσύνης θα πρέπει να εκτείνεται σε όλο το επίπεδο χρήστη, στο τμήμα του δικτύου ραδιοπρόσβασης και υπολογιστικού άκρου, στο δίκτυο κορμού και το νέφος, με την έννοια ότι κάθε δικτυακή οντότητα θα πρέπει να μπορεί να λαμβάνει αυτόνομες αποφάσεις σχετικά με την προσωπική εκμετάλλευση των πόρων της. Εν τω μεταξύ, από οικονομική άποψη και από πλευράς αγοράς, τα δίκτυα επόμενης γενιάς αποτελούν ένα ανταγωνιστικό περιβάλλον, όπου πολλοί ενδιαφερόμενοι, π.χ. διαχειριστές δικτύων κινητής τηλεφωνίας, πάροχοι υπηρεσιών υποδομής ή υπηρεσιών νέφους, συνεργάζονται ή ακόμη και ανταγωνίζονται στην παροχή παρόμοιων υπηρεσιών επιδιώκοντας τους προσωπικούς τους στόχους. Οι τελευταίοι στόχοι μπορεί να είναι διαφορετικοί και/ή αλληλοεξαρτώμενοι, όπως η μεγιστοποίηση της ενεργειακής ή φασματικής απόδοσης του δικτύου, ο μετριασμός των παρεμβολών, η ελαχιστοποίηση της χρονικής καθυστέρησης ή η αύξηση του κέρδους, για να αναφέρουμε μόνο μερικά από τα διάφορα

παραδείγματα. Ταυτόχρονα, η πολυδιάστατη φύση του προβλήματος διαχείρισης πόρων σχετικά με τον τύπο τους και τις απαιτήσεις ποιότητας υπηρεσίας των χρηστών που πρέπει να ικανοποιηθούν, κάνει εμφανή την ανάγκη για κοινά επιστημονικά εργαλεία, μεθοδολογίες και προσεγγίσεις που με ακρίβεια και ρεαλισμό μοντελοποιούν τη συμπεριφορά του υπό διερεύνηση δικτύου.

Ο απώτερος στόχος, ωστόσο, στην πραγματοποίηση της νοημοσύνης θα πρέπει να είναι η παροχή ολιστικών λύσεων στα συγκλίνοντα προβλήματα διαχείρισης ραδιοπόρων και υπολογιστικών πόρων. Το MEC βασίζεται σε μεγάλο βαθμό στην ασύρματη διεπαφή που πρακτικά εξυπηρεί στην εκφόρτωση εργασιών υπολογισμού όταν εξετάζονται εφαρμογές για κινητές συσκευές. Αυτό σημαίνει ότι η απόδοση των κινητών υπολογισμών είναι συνυφασμένη με την ποιότητα της ασύρματης επικοινωνίας, και ως εκ τούτου, τα αντίστοιχα προβλήματα διαχείρισης πόρων θα πρέπει να μελετηθούν από κοινού.

3.Α. Μοντελοποίηση μέσω Θεωρίας Παιγνίων (Game Theory - GT)

Μια καθιερωμένη μέθοδος στη βιβλιογραφία για τη διατύπωση και επίλυση κατανεμημένων προβλημάτων διαχείρισης πόρων είναι η Θεωρία Παιγνίων (Game Theory - GT) [40]. Στην πιο συχνά χρησιμοποιούμενη μορφή της, το πρόβλημα διαχείρισης πόρων διατυπώνεται ως ένα μη συνεργατικό παίγνιο μεταξύ των παικτών, όπου κάθε παίκτης θεωρείται μια άπληστη οντότητα που επιδιώκει ανεξάρτητα να μεγιστοποιήσει τη χρησιμότητα/ωφέλειά της. Ωστόσο, υπάρχουν συνεργατικές μορφές παιγνίων όπου οι μεμονωμένοι παίκτες επιδιώκουν έναν κοινό στόχο από την προσωπική τους οπτική ή την οπτική του δικτύου. Οι παίκτες που συμμετέχουν στο παίγνιο μπορούν να αντιστοιχηθούν σε οποιαδήποτε δικτυακή οντότητα ή ενδιαφερόμενο μέρος του δικτύου. Οι παίκτες μοιράζονται και συνεπώς ανταγωνίζονται για μια κοινή δεξαμενή πόρων (common pool of resource), η οποία με τη σειρά της μπορεί να αποτελείται από ραδιοπόρους ή υπολογιστικούς πόρους. Επίσης, οι παίκτες μπορεί να ανταγωνίζονται για το πλήθος των εγγεγραμένων σε μια υπηρεσία χρηστών, στην περίπτωση που κάνουμε λόγο σε ανταγωνιμσό μεταξύ παρόχων.

Τα κύρια πλεονεκτήματα του κατανεμημένου πλαισίου διαχείρισης πόρων που ισχύουν γενικά αλλά και ειδικότερα στο πλαίσιο της Θεωρίας Παιγνίων είναι (i) η ικανότητα των χρηστών να αποφασίζουν αυτόνομα και με γνωστικό τρόπο τον πιο ωφέλιμο τρόπο λειτουργίας τους, (ii) η εξάλειψη του μοναδικού σημείου αστοχίας (single point of failure) που χαρακτηρίζει τις κεντρικοποιημένες λύσεις, (iv) η μείωση της υπολογιστικής πολυπλοκότητας των λύσεων, η οποία μοιράζεται μεταξύ πολλών αυτόνομων οντοτήτων, (v) η βελτίωση των επιπέδων ασφάλειας και απορρήτου καθώς η διαδικασία λήψης αποφάσεων μοιράζεται μεταξύ διαφορετικών συσκευών, οι οποίες ανταλλάσσουν περιορισμένο αριθμό πληροφοριών, (vi) η υποστήριξη της ομαλής λειτουργίας του συνολικού συστήματος όταν εμπλέκονται πάροχοι και χρήστες με ετερογενή οικονομικά κίνητρα.

3.Β. Μοντελοποίηση μέσω Θεωρίας Συμβολαίων (Contract Theory - CT)

Ωστόσο, είναι γνωστό ότι τα θεωρητικά μοντέλα παιγνίων υποθέτουν τον ορθολογισμό (rationality) των παικτών που συμμετέχουν στο παίγνιο, κάτι που είναι μη πρακτικό ή ακόμα και αδύνατο καθώς το μέγεθος του δικτύου μεγαλώνει. Ένα νέο πλαίσιο από τον τομέα των οικονομικών που έχει εξεταστεί τα τελευταία χρόνια είναι η Θεωρία Συμβολαίων (Contract Theory - CT) [41]. Η Θεωρία Συμβολαίων, η οποία εμπίπτει στον τομέα της οικονομίας της εργασίας (labor economics), παρέχει τα μαθηματικά θεμέλια για τη δημιουργία αμοιβαία αποδεκτών συμβολαίων ή συμφωνιών μεταξύ οικονομικών παραγόντων, π.χ. εργοδότη και εργαζόμενου, υπό την ύπαρξη ελλιπούς πληροφόρησης (συχνά αναφερόμενης και ως ασύμμετρης πληροφόρησης). Η ελλιπής πληροφόρηση αναφέρεται στα άγνωστα από τον εργοδότη προσωπικά χαρακτηριστικά των εργαζόμενων, τα οποία μάλιστα είναι αυτά που καθορίζουν τη δημιουργία του τελικού συμβολαίου. Υπό το πρίσμα αυτό, ο εργοδότης δημιουργεί πακέτα συμβολαίων με βάση τη στατιστική γνώση περί των προσωπικών πληροφοριών των πιθανών υποψήφιων εργαζόμε-

νων, δηλαδή τους πιθανούς τύπους των εργαζόμενων όπως αναφέρεται σαν ορολογία, για να τους παρακινήσει να συνδράμουν τη δουλειά τους και, ως εκ τούτου, να αποκαλύψουν τον τύπο τους.

Κατά συνέπεια, η Θεωρία Συμβολαίων μπορεί να παρέχει μια πιο ρεαλιστική μοντελοποίηση των αλληλεξαρτώμενων συμπεριφορών, αλληλεπιδράσεων και αποφάσεων των διαφορετικών δικτυακών οντοτήτων και των ενδιαφερομένων μερών, χωρίς να προϋποθέτει πλήρη γνώση μεταξύ τους και ενώ προσπαθεί να συμφιλιώσει τους δυνητικά αντικρουόμενους στόχους τους. Χαρακτηριστικό παράδειγμα τέτοιας περίπτωσης από την πλευρά του δικτύου αποτελεί η προσπάθειά του να αυξήσει τη χωρητικότητά του καθώς και την αποτελεσματική χρήση των πόρων του φάσματος με τη βοήθεια τεχνολογιών όπως οι Επικοινωνίες Συσκευής προς Συσκευή (Device-to-Device - D2D), τα Γνωστικά Συστήματα Ραδιοεπικοινωνιών (Cognitive Radio - CR) ή μικρές κυψέλες (small cells). Προκειμένου να μεγιστοποιήσουν την ωφέλειά τους, οι χρήστες είναι πιο πιθανό να αποφύγουν τη συνεργασία με άλλες γειτονικές συσκευές, μοιράζοντας από κοινού τους πόρους τους, δηλαδή τη χωρητικότητα της μπαταρίας, την υπολογιστική ισχύ και το διαθέσιμο φάσμα τους. Επιπλέον, είναι πιο πιθανό να παρακάμψουν την επικοινωνία με ένα σταθμό βάσης μικρής κυψέλης και χαμηλής ισχύος, ελαχιστοποιώντας τον κίνδυνο έκθεσης σε υψηλότερες παρεμβολές λόγω των μειωμένων πόρων φάσματος της μικρής κυψέλης σε σύγκριση με μια μακροκυψέλη. Γενικά, οποιοσδήποτε σταθμός βάσης μικρής κυψέλης ή μακροκυψέλης, πάροχος υπηρεσιών ή υποδομής μπορεί να παίξει το ρόλο του εργοδότη που είναι υπεύθυνος για το σχεδιασμό των πακτέων συμβολαίων που προορίζονται για τους υποψήφιους εργαζόμενους, όπως συσκευές τελικού χρήστη ή άλλοι σταθμοί βάσης [42, 43, 44]. Σύμφωνα με αυτήν την ιδέα, μια μεγάλη ποικιλία προβλημάτων βελτιστοποίησης μπορούν να διαμορφωθούν και να επιλυθούν, επανεξετάζοντας τις συνολικές παραδοσιακές προσεγγίσεις διαχείρισης πόρων στα ασύρματα δίκτυα επικοινωνιών και κινητών υπολογισμών.

4. Προκλήσεις και Κίνητρα

Από τη μέχρι στιγμής συζήτηση, είναι σαφές ότι τα ασύρματα δίκτυα επόμενης γενιάς παρουσιάζουν πολλαπλούς βαθμούς ελευθερίας όσον αφορά τον έλεγχο του ασύρματου περιβάλλοντος και του περιβάλλοντος υπολογισμών για την επίτευξη της απαιτούμενης ποιότητας υπηρεσίας από την οπτική γωνία των χρηστών ή/και του δικτύου. Ωστόσο, αυτό το αυξημένο επίπεδο ευελιξίας φέρνει νέες προκλήσεις που πρέπει να εξεταστούν προσεκτικά. Η παρούσα διατριβή επιχειρεί να αναπτύξει νέες προσεγγίσεις που προσδίδουν ένα πραγματικό και ρεαλιστικό πνεύμα στη μοντελοποίηση προβλημάτων διαχείρισης πόρων. Παράλληλα επικεντρώνεται στην παροχή ολιστικών λύσεων, λαμβάνοντας υπόψιν πολλαπλούς τύπους πόρων που σχετίζονται με τις ασύρματες επικοινωνίες και τους κινητούς υπολογισμούς. Συγκεκριμένα, οι βασικοί πυλώνες πάνω στους οποίους έχει οικοδομηθεί αυτή η διατριβή συνοψίζονται ως εξής:

- **Διαχείριση πόρων & βελτιστοποίηση:** Η κατανομή πόρων είναι κρίσιμη από τις προηγούμενες γενιές ασύρματων δικτύων και γίνεται ακόμη πιο επιτακτική καθώς η πολυπλοκότητα του δικτύου αυξάνεται ως προς τον αριθμό των χρηστών και των εφαρμογών, την αυστηρότητα των απαιτήσεων ποιότητας υπηρεσίας, τις τεχνολογίες που αναπτύσσονται και τον τύπο των πόρων. Η απλή υιοθέτηση ήδη προτεινόμενων λύσεων σε παραδοσιακά προβλήματα διαχείρισης πόρων, όπως το τυπικό πρόβλημα μεγιστοποίησης του συνολικού ρυθμού μετάδοσης στη ζεύξη καθόδου/ανόδου, είναι αδύνατη λόγω της ασυμβατότητας με τις βασικές τεχνολογίες ενεργοποίησης του δικτύου επόμενης γενιάς 5G, όπως για παράδειγμα τις νέες τεχνικές πολλαπλής πρόσβασης, τις αναδιαμορφώσιμες έξυπνες επιφάνειες, τα υπολογιστικά συστήματα στην άκρη του δικτύου. Επιπλέον, η νοημοσύνη πίσω από τις προτεινόμενες λύσεις διαχείρισης πόρων πρέπει να εξελιχθεί για να αντιμετωπίσει την πολυπλοκότητα του υποκείμενου δικτυακού περιβάλλοντος. Ως εκ τούτου, η διαχείριση πόρων και η βελτιστοποίηση αποτελούν την κύρια κινητήρια δύναμη πίσω από αυτή τη διατριβή.

- **Κατανεμημένη λήψη αποφάσεων:** Η κατανεμημένη φύση του δικτύου επόμενης γενιάς 5G όχι μόνο προωθεί αλλά και επιβάλλει τη διατύπωση προβλημάτων διαχείρισης πόρων με κατανεμημένο τρόπο. Τέτοιες λύσεις επιτρέπουν τη μοντελοποίηση της ετερογένειας στη συμπεριφορά και της υποκειμενικότητας στην αντίληψη της ποιότητας υπηρεσίας από τις δικτυακές οντότητες, ενώ παρέχουν ευέλικτες και επεκτάσιμες εναλλακτικές καθώς μεγαλώνει η πολυπλοκότητα του δικτύου. Η ύπαρξη κεντρικών οντοτήτων που συσσωρεύουν τη γνώση του υποκείμενου δικτύου δεν είναι ρεαλιστική στα περισσότερα σύγχρονα σενάρια εφαρμογών. Έτσι, τα επιστημονικά πλαίσια που επιτρέπουν την αυτόνομη λήψη αποφάσεων από τις διαφορετικές οντότητες οδηγούν σε πιο βιώσιμες λύσεις.

- **Αντικρουόμενοι στόχοι:** Από οικονομικής άποψης και από πλευράς αγοράς, τα δίκτυα επόμενης γενιάς 5G αποτελούν ένα ανταγωνιστικό περιβάλλον, όπου πολλοί χρήστες και άλλα ενδιαφερόμενα μέρη (stakeholders) που εμπλέκονται στην παροχή υπηρεσιών επικοινωνίας και κινητών υπολογισμών θα πρέπει να συντονίζονται. Ως εκ τούτου, είναι σημαντικό να μοντελοποιήσουμε ταυτόχρονα την οικονομική και τεχνολογική τους αλληλεπίδραση και να λάβουμε υπόψιν τους διαφορετικούς και δυνητικά αντικρουόμενους στόχους τους για να επιτύχουμε περισσότερο ρεαλιστικές λύσεις στο τελικό πρόβλημα διαχείρισης πόρων και βελτιστοποίησης. Σε αυτό το πλαίσιο, αποτελεσματικά θεωρητικά πλαίσια από τον τομέα των οικονομικών μπορούν να χρησιμοποιηθούν για να συμβιβάσουν τους στόχους και να καταλήξουν σε αμοιβαία αποδεκτές συμφωνίες μεταξύ διαφόρων ενδιαφερόμενων μερών.

- **Ελλιπής πληροφόρηση:** Πέραν της σημαντικής ετερογένειάς του, το αναδυόμενο δίκτυο επόμενης γενιάς 5G αποτελεί ένα εξαιρετικά δυναμικό περιβάλλον (δηλαδή, στοχαστικό ή χρονικά μεταβλητό), πράγμα που επιβάλλει πρόσθετους πρακτικούς περιορισμούς στο επίπεδο γνώσης που μπορεί να έχει μια δικτυακή οντότητα σχετικά με τις ενέργειες των υπόλοιπων δικτυακών οντοτήτων με τις οποίες ανταγωνίζεται. Ως εκ τούτου, η εφαρμοσιμότητα και η ακρίβεια των παραδοσιακών κατανεμημένων προσεγγίσεων λήψης αποφάσεων που βασίζονται στην ορθολογικότητα των παικτών, δηλαδή των ανταγωνιζόμενων δικτυακών οντοτήτων, πάσχουν από τις ελλιπείς και μερικώς διαθέσιμες πληροφορίες που διαθέτει κάθε παίκτης. Οι λύσεις που περιορίζονται στις πληροφορίες που διαθέτει κάθε παίκτης σχετικά με τις δικές τους αποφάσεις ή/και τις ελλιπείς και αβέβαιες πληροφορίες για το τριγύρω περιβάλλον του είναι πολύ σημαντικές.

- **Ολιστικές λύσεις:** Τα δίκτυα επόμενης γενιάς 5G παρέχουν αρκετούς βαθμούς ελευθερίας σχετικά με τη φύση και τον τύπο των προς διαχείριση πόρων, που κυμαίνονται από πόρους ασύρματου δικτύου (π.χ. φάσμα, ισχείς και ρυθμοί μετάδοσης δεδομένων, μετατοπίσεις φάσης και πλάτη RIS) έως υπολογιστικούς πόρους (π.χ. υπολογιστική συχνότητα και ισχύς). Η μονομερής αντιμετώπιση προβλημάτων διαχείρισης πόρων δεν επιτρέπει την πλήρη εκμετάλλευση του δυναμικού και της προοπτικής του υποκείμενου ασύρματου δικτύου επικοινωνίας και υπολογισμών. Για να αποκαλυφθούν τα όρια του δικτύου, απαιτείται μια πιο ολιστική αντιμετώπιση των προβλημάτων κατανομής πόρων προσθέτοντας περισσότερους βαθμούς ελευθερίας και καταφεύγοντας σε πιο επεκτάσιμα και γενικά μοντέλα σχεδιασμού προβλημάτων. Η προστιθέμενη αξία των ολιστικών λύσεων είναι πολλαπλή και δεν περιορίζεται μόνο στον τομέα των δικτύων και των υπολογισμών, αλλά μπορεί επίσης να παρέχει πληροφορίες για την αντιμετώπιση παρόμοιων προβλημάτων συνδυαστικής βελτιστοποίησης σε άλλους κλάδους.

5. Συμβολή διατριβής

Η παρούσα διατριβή στοχεύει να αντιμετωπίσει τις προαναφερθείσες προκλήσεις που προκύπτουν στα αναδυόμενα δίκτυα ασύρματης επικοινωνίας και κινητών υπολογισμών επόμενης

γενιάς, προτείνοντας ρεαλιστικές λύσεις σε διάφορα σενάρια χρήσης. Η κύρια εστίαση δίνεται στη διαδικασία λήψης αποφάσεων των διαφορετικών δικτυακών οντοτήτων, όπου μεμονωμένες συσκευές χρήστη και απομακρυσμένοι διακομιστές πρέπει να ενεργούν αυτόνομα και να κάνουν επιλογές σχετικά με τη χρήση των πόρων και την επένδυσή τους εντός του λειτουργικού τους περιβάλλοντος. Οι βασικές συνεισφορές αυτής της διατριβής συνοψίζονται ως εξής:

- **Πολυδιάστατη μοντελοποίηση συστήματος:** Τα ασύρματα δίκτυα επόμενης γενιάς 5G έχουν εξελιχθεί σε ένα σύνθετο σύστημα πολυάριθμων διασυνδέσεων μεταξύ χρηστών και διαφορετικών τύπων παρόχων (π.χ. υποδομής, υπηρεσίας) λόγω της ενεργού συμμετοχής των χρηστών σε πολλαπλές υπηρεσίες ασύρματης επικοινωνίας και κινητών υπολογισμών. Μια σημαντική καινοτομία αυτής της διατριβής έγκειται στο γεγονός ότι οι διαφορετικές δικτυακές οντότητες μπορούν να προσδιορίσουν πολλαπλούς βαθμούς ελευθερίας κατά τη διαδικασία κατανομής πόρων. Για να επιτευχθεί αυτό, εξετάζονται διάφορα επίπεδα δικτύου, αρχιτεκτονικές και ποικίλες υπηρεσίες, μετατοπίζοντας, με αυτόν τον τρόπο, τη μοντελοποίηση του υποκείμενου συστήματος πέρα από τις παραδοσιακές «επίπεδες» τοπολογίες. Στη συνέχεια, αρκετοί πόροι προς διάθεση εξετάζονται ταυτόχρονα σε κάθε σενάριο εφαρμογής και πρόβλημα διαχείρισης πόρων, προχωρώντας σταθερά από περιβάλλοντα αμιγούς ασύρματης επικοινωνίας σε συγκλίνοντα περιβάλλοντα επικοινωνίας και κινητών υπολογισμών.

- **Κατανομή πόρων και σχεδιασμός μηχανισμών κινήτρων σε ασύρματα δίκτυα NOMA:** Αρχικά, μελετώνται προβλήματα κατανομής πόρων πολλαπλών μεταβλητών σε ετερογενή και πολυεπίπεδα ασύρματα δίκτυα επικοινωνιών. Με στόχο την αντιμετώπιση του προβλήματος της ελλιπούς/μερικής πληροφόρησης των σταθμών βάσης σχετικά με την κατάσταση καναλιού, καθώς και της αντίφασης μεταξύ των χρηστών και των σταθμών βάσης σχετικά με το επίπεδο ισχύος μετάδοσης στη ζεύξη ανόδου, εισάγεται μια συνεργατική προσέγγιση μεταξύ των δύο αυτών μερών, η οποία βασίζεται στις αρχές της Θεωρίας Συμβολαίων. Οι σταθμοί βάσης σχεδιάζουν ένα σύνολο συμβολαίων που αποτελούνται από ενδεικτικά επίπεδα ισχύος για τη ζεύξη ανόδου μαζί με μια αντίστοιχη ανταμοιβή προς τους χρήστες, κάνοντας χρήση της στατιστικής τους γνώσης σχετικά με την κατάσταση του καναλιού των χρηστών. Τα επίπεδα ισχύος των συμβολαίων επιλέγονται με τέτοιο τρόπο ώστε να επιτρέπουν την αποκωδικοποίηση των μεταδιδόμενων σημάτων των χρηστών από τους δέκτες των σταθμών βάσης, κάνοντας χρήση των τεχνικών NOMA και SIC. Οι χρήστες επιλέγουν αυτόνομα ένα συμβόλαιο από το σύνολο των συμβολαίων, το οποίο ταιριάζει καλύτερα στις συνθήκες καναλιού τους. Επιπλέον των παραπάνω, αναπτύσσεται ένας αλγόριθμος Ενισχυτικής Μάθησης (Reinforcement Learning - RL) προκειμένου κάθε χρήστης να προσδιορίζει αυτόνομα και κατανεμημένα την περισσότερο ωφέλιμη για αυτόν συσχέτισή του με έναν από τους διαθέσιμους σταθμούς βάσης.

- **Κατανομή πόρων σε ασύρματα δίκτυα NOMA υποστηριζόμενα από RIS:** Πηγαίνοντας ένα βήμα παραπέρα όσον αφορά την υποκείμενη αρχιτεκτονική δικτύου και τις χρησιμοποιούμενες τεχνολογίες, στοχεύουμε να συνυπολογίσουμε και να κατανείμουμε βέλτιστα τους πόρους στα τμήματα ασύρματης πρόσβασης (access network) και οπισθόζευξης (backhaul network) ενός δικτύου υποβοηθούμενου από Μη Επανδρωμένα Εναέρια Οχήματα (Unmanned Aerial Vehicle - UAV) και RIS. Αξιοποιώντας τη δομική ιεραρχία του δικτύου, διαμορφώνεται ένα παίγνιο Stackelberg μεταξύ του σταθμού βάσης που φέρει το UAV και των χρηστών για την κατανεμημένη επίλυση του ακόλουθου συνδυαστικού προβλήματος κατανομής πόρων. Το UAV, ενεργώντας ως ηγέτης, καθορίζει τις μετατοπίσεις φάσης του RIS έτσι ώστε η ισχύς του σήματος του συνόλου των χρηστών στη ζεύξη ανόδου να μεγιστοποιείται. Επίσης, το UAV, σε δεύτερη φάση, υπολογίζει από κοινού την κατανομή εύρους ζώνης συχνοτήτων και ελέγχου ισχύος στη ζεύξη ανόδου του οπισθοζευκτικού δικτύου προς το δίκτυο κορμού (core network). Σε τρίτη φάση, οι χρήστες, ενεργώντας

ως ακόλουθοι, βελτιστοποιούν την προσωπική τους ισχύ μετάδοσης στη ζεύξη ανόδου του δικτύου πρόσβασης προς το UAV, επίσης με κατανεμημένο τρόπο. Η δεύτερη και τρίτη φάση επαναλαμβάνονται έως ότου βρεθεί το σημείο ισορροπίας του παιγνίου Stackelberg, στο οποίο επιτυγχάνεται η μεγιστοποίηση της ενεργειακής/φασματικής απόδοσης του δικτύου πρόσβασης και οπισθόζευξης από άκρο σε άκρο.

- **Κατανομή πόρων και σχεδιασμός μηχανισμών κινήτρων σε δίκτυα υπολογισμών πολλαπλών επιπέδων:** Σεβόμενοι την ανάγκη για από κοινού μηχανισμούς κατανομής πόρων σε ασύρματα δίκτυα επικοινωνιών και δίκτυα κινητών υπολογισμών, εξετάζεται μια πολυεπίπεδη τοπολογία κινητών υπολογισμών και μελετάται το από κοινού πρόβλημα της εκφόρτωσης εργασιών υπολογισμού και κατανομής ισχύος μετάδοσης/εκφόρτωσης. Σε αντίθεση με την υπάρχουσα βιβλιογραφία, όπου μοντελοποιούνται δίκτυα υπολογισμών ενός επιπέδου, δηλαδή αποτελούμενα είτε από ένα επίπεδο υπολογισμών άκρης, ομίχλης ή νέφους, επιδιώκεται ταυτόχρονα η χρήση ενός ευρέος φάσματος υπολογιστικών δυνατοτήτων και επιλογών. Δεδομένης της εγωιστικής συμπεριφοράς των χρηστών για εκφόρτωση στην άκρη του δικτύου λόγω της εγγύτητας του τελευταίου, σχεδιάζεται ένας μηχανισμός κινήτρων που βασίζεται στη Θεωρία Συμβολαίων για να παρακινήσει τους χρήστες να επιτρέψουν ένα ποσοστό των αρχικών εκφορτωμένων εργασιών τους στο επίπεδο της άκρης να προωθηθούν περαιτέρω και να επεξεργαστούν στο επίπεδο της ομίχλης. Έχοντας καθορίσει αυτό το ποσοστό, το τελικό ποσοστό εκφόρτωσης υπολογιστικών εργασιών των χρηστών στην άκρη του δικτύου, καθώς και το επίπεδο ισχύος στη ζεύξη ανόδου κατά την εκφόρτωση, υπολογίζονται με κατανεμημένο τρόπο, διατυπώνοντας ένα μη συνεργατικό παίγνιο μεταξύ των χρηστών. Με τη χρήση πολλαπλών επιπέδων υπολογισμών, προκύπτει μια ενεργειακά αποδοτική λύση, ενώ επεκτείνεται η υπολογιστική ικανότητα του επιπέδου υπολογισμών άκρης.

- **Κατανομή πόρων σε RSMA υπολογιστικά συστήματα πολλαπλών διακομιστών στην άκρη του δικτύου:** Τέλος, με στόχο την περαιτέρω μελέτη της κατανομής των εργασιών υπολογισμού οριζόντια, δηλαδή εντός του ίδιου επιπέδου υπολογισμών θεωρώντας πολλαπλούς διακομιστές, μοντελοποιείται ένα δίκτυο υπολογιστικών συστημάτων στην άκρη του δικτύου πολλαπλών διακομιστών. Οι χρήστες αξιοποιούν τα διαφορετικά διαθέσιμα δίκτυα ραδιοπρόσβασης για να εκφορτώσουν τις υπολογιστικά απαιτητικές και χρονικά κρίσιμες εφαρμογές τους σε πολλαπλούς διακομιστές MEC ταυτόχρονα. Για την αντιμετώπιση του κρίσιμου προβλήματος διαχείρισης παρεμβολών υπό την προκύπτουσα τοπολογία δικτύου πολλαπλών διακομιστών πολλαπλών χρηστών, καθώς και υποκινούμενοι από τις εξελίξεις στις τεχνικές μη ορθογωνικής πολλαπλής πρόσβασης, εξετάζεται η εφαρμογή της τεχνικής RSMA. Υπό αυτό το πρίσμα, επιδιώκεται η ελαχιστοποίηση του αθροίσματος της μέγιστης μετρούμενης χρονικής καθυστέρησης από την πλευρά των χρηστών μεταξύ των διαφορετικών διακομιστών MEC μέσω της από κοινού βελτιστοποίησης των ποσοστών εκφόρτωσης υπολογιστικών εργασιών, του ρυθμού και της ισχύος μετάδοσης/εκφόρτωσης στη ζεύξη ανόδου από τους χρήστες, καθώς και της κατανομής υπολογιστικών πόρων από τους διάφορους διακομιστές MEC προς τους χρήστες. Το παραπάνω από κοινού πρόβλημα βελτιστοποίησης επιλύεται αναλυτικά, χρησιμοποιώντας κλασσικές μεθόδους βελτιστοποίησης που βασίζονται στις συνθήκες Karush-Kuhn-Tucker (KKT). Η μελέτη και επίλυση του προβλήματος αυτού συμπληρώνει τον απώτερο σκοπό της παρούσας διατριβής να παράσχει μια ολιστική προσέγγιση και άποψη ως προς την κατανομή πόρων σε συγκλίνοντα ασύρματα δίκτυα επικοινωνιών και κινητών υπολογισμών.

- **Αξιολόγηση των προτεινόμενων πλαισίων με αριθμητικά αποτελέσματα μέσω μοντελοποίησης και προσομοίωσης:** Παρουσιάζονται εκτεταμένα αριθμητικά αποτελέσματα που προκύπτουν μέσω κατάλληλης μοντελοποίησης και προσομοίωσης του δικτυακού πε-

ριβάλλοντος και του εξεταζόμενου προβλήματος για να καταδειχθεί η αποτελεσματικότητα και η αποδοτικότητα των προτεινόμενων πλαισίων και των λύσεων που προκύπτουν.

Στη συνέχεια, περιγράφονται αναλυτικά οι επιμέρους εργασίες που συνθέτουν τα διάφορα κεφάλαια της παρούσας διατριβής, δίνοντας έμφαση στο υποκείμενο περιβάλλον δικτύου που μελετάται, το συγκεκριμένο πρόβλημα κατανομής πόρων και λήψης αποφάσεων που στοχεύεται, καθώς και στη μέθοδο επίλυσης αυτού.

6. Κατανομή πόρων και σχεδιασμός μηχανισμών κινήτρων σε ασύρματα δίκτυα NOMA

Παρά την πληθώρα ερευνητικών εργασιών που έχουν υιοθετήσει και εκμεταλλευτεί την εφαρμογή του NOMA σε ετερογενή ασύρματα δίκτυα, εξακολουθούν να υπάρχουν σημαντικές προκλήσεις που πρέπει να αντιμετωπιστούν, σχετικά με την υλοποίησή του. Δεδομένης της εγγενούς παρεμβολής που προκαλείται από διαφορετικούς χρήστες που μεταδίδουν μηνύματα μέσω των ίδιων πόρων, οι προηγμένες τεχνικές διαχείρισης παρεμβολών είναι ζωτικής σημασίας για την εγγύηση του κέρδους απόδοσης του NOMA. Το τελευταίο, με τη σειρά του, εξαρτάται σε μεγάλο βαθμό από το από κοινού πρόβλημα δρομολόγησης χρηστών και ελέγχου ισχύος μετάδοσης, τονίζοντας την ανάγκη για από κοινού μεθόδους βελτιστοποίησης των παραπάνω. Ωστόσο, μία από τις βασικές προκλήσεις που αντιμετωπίζουν οι υπάρχουσες μέθοδοι κατανομής πόρων, που επηρεάζει άμεσα την αποτελεσματικότητα και την εφαρμογή τους, είναι η έλλειψη πλήρους γνώσης των πληροφοριών κατάστασης καναλιού στο σταθμό βάσης. Λόγω της εγγενούς αβεβαιότητας που εισάγουν τα ταχέως μεταβαλλόμενα κανάλια και της αυξημένης επιβάρυνσης του οπισθοζευκτικού δικτύου που προκαλείται από την πληθώρα συνδεδεμένων συσκευών των χρηστών, πλήρης γνώση του CSI είναι πρακτικά δύσκολο να επιτευχθεί. Στην περίπτωση που υπάρχει στατιστική γνώση του CSI διαθέσιμη στο σταθμό βάσης, τότε η εκτίμηση της συσκευής του χρήστη σχετικά με το κέρδος του καναλιού μπορεί να χρησιμοποιηθεί για την καθοδήγηση της διαδικασίας κατανομής πόρων. Υπό αυτή την έννοια, το πρόβλημα της κατανομής πόρων υπό στατιστική γνώση του CSI μπορεί να μοντελοποιηθεί και να αντιμετωπιστεί ως πρόβλημα ελλιπούς πληροφόρησης από την πλευρά του σταθμού βάσης.

Στο αντίστοιχο κεφάλαιο της διατριβής, εισάγεται μια συνεργιστική προσέγγιση μεταξύ των σταθμών βάσης και των συσκευών των χρηστών που εξυπηρετεί στην αντιμετώπιση του προβλήματος της ελλιπούς γνώσης του CSI από την πλευρά των σταθμών βάσης, ενώ το πρόβλημα κατανομής πόρων επιλύεται από την πλευρά των χρηστών. Ένας τέτοιος μηχανισμός κατανομής πόρων με επίκεντρο τον χρήστη στοχεύει επιπρόσθετα να βελτιώσει την ικανοποίηση των χρηστών και να διευκολύνει την τυχόν προσωρινή ανάπτυξη ενός δικτύου, π.χ. δίκτυα υποβοηθούμενα από μη επανδρωμένα εναέρια οχήματα, έναντι ενός συνεχώς εξελισσόμενου ετερογενούς περιβάλλοντος. Η εργασία μας στοχεύει στην παροχή ενός ενοποιημένου πλαισίου για την αντιμετώπιση των ερευνητικών κενών που σχετίζονται με την κατανεμημένη (δηλαδή, με επίκεντρο τον χρήστη) λήψη αποφάσεων, την ελλιπή πληροφόρηση, τους αντιφατικούς στόχους μεταξύ των χρηστών και των σταθμών βάσης και την παροχή ολιστικών λύσεων όσον αφορά το από κοινού πρόβλημα δρομολόγησης/συσχετισμού των χρηστών με σταθμούς βάσης και ελέγχου ισχύος στη ζεύξη ανόδου σε ετερογενή ασύρματα δίκτυα επικοινωνίας που βασίζονται στο NOMA. Για το σκοπό αυτό, υιοθετούνται τα πλαίσια της Θεωρίας Συμβολαίων και της ενισχυτικής μάθησης (RL) προκειμένου να αποτυπωθούν και να μοντελοποιηθούν σωστά οι σχέσεις μεταξύ των δικτυακών οντοτήτων που εμπλέκονται σε αυτή τη διαδικασία κατανομής πόρων.

Συγκεκριμένα, οι κύριες συνεισφορές αυτής της εργασίας μπορούν να συνοψιστούν ως εξής:

- Εισάγεται ένας μηχανισμός RL για να καταστήσει δυνατή την κατανεμημένη και αυτόνομη συσχέτιση χρήστη με κάποιον σταθμό βάσης. Κάθε χρήστης επιλέγει ένα σταθμό βάσης με το οποίο θα συσχετιστεί, με στόχο τη βελτιστοποίηση της παρεχόμενης αντιμοιβής από το περιβάλλον επικοινωνίας που αποτυπώνει τα χαρακτηριστικά της αντίστοιχης συσχέτισης. Τα χαρακτηριστικά αυτά περιλαμβάνουν τη μακροπρόθεσμη φήμη

των σταθμών βάσης που διαμορφώνεται από την εκφρασμένη υποκειμενική γνώμη των χρηστών σχετικά με την υπηρεσία που απολαμβάνουν όταν συνδέονται με αυτούς. Για να εκμαιεύσουμε με ειλικρίνεια την υποκειμενική γνώμη των χρηστών, προτείνεται η καινοτόμα χρήση του μηχανισμού Bayesian Truth Serum, επιτρέποντας περαιτέρω την έκφραση της φήμης των σταθμών βάσης ως Μπεϋζιανή Πεποίθηση (Bayesian Belief).

- Προτείνεται ένας μηχανισμός ελέγχου ισχύος μεταξύ κάθε σταθμού βάσης και των συσχετισμένων με αυτόν χρηστών, ο οποίος βασίζεται στη Θεωρία Συμβολαίων προκειμένου να ληφθεί υπόψιν και να μοντελοποιηθεί η περίπτωση ελλιπούς γνώσης του CSI από την πλευρά του σταθμού βάσης. Οι χρήστες διακρίνονται σε διαφορετικούς τύπους ανάλογα με τις συνθήκες καναλιού τους. Έτσι, οι σταθμοί βάσης σχεδιάζουν διαφορετικά συμβόλαια προσαρμοσμένα στους διαφορετικούς τύπους χρηστών έχοντας στατιστική γνώση για την ύπαρξή τους. Τα συμβόλαια περιλαμβάνουν την προσφορά των χρηστών προς τον εκάστοτε σταθμό βάσης, η οποία αντιστοιχίζεται στην ισχύ μετάδοσής τους στη ζεύξη ανόδου, και μια ανταμοιβή που παρέχεται πίσω στους χρήστες από το σταθμό βάσης. Η συνολική διαδικασία ελέγχου ισχύος στην ζεύξη ανόδου βελτιστοποιείται επαναληπτικά, ενώ πραγματοποιείται η διαδικασία συσχέτισης χρήστη με σταθμό βάσης που βασίζεται στο RL.
- Παρουσιάζονται αναλυτικά αριθμητικά αποτελέσματα, που προκύπτουν μέσω μοντελοποίησης και προσομοίωσης για να καταδειχθεί η σωστή λειτουργία και αποτελεσματικότητα του προτεινόμενου πλαισίου. Ειδικότερα, μελετώνται τα εγγενή χαρακτηριστικά του μηχανισμού ελέγχου ισχύος με χρήση της Θεωρίας Συμβολαίων στις περιπτώσεις πλήρους και ελλιπούς γνώσης του CSI, ενώ η λειτουργία του μηχανισμού συσχέτισης χρήστη σε σταθμό βάσης που βασίζεται στο RL εξετάζεται ως προς τη σύγκλιση στα σημεία της περισσότερο ωφέλιμης συσχέτισης. Πραγματοποιείται συγκριτική αριθμητική αξιολόγηση της προτεινόμενης προσέγγισης έναντι άλλων μηχανισμών συσχέτισης χρήστη με σταθμό βάσης, καταδεικνύοντας τα οφέλη του συνολικού προτεινόμενου πλαισίου όσον αφορά τον επιτυγχανόμενο ρυθμό δεδομένων και τη δικαιοσύνη (fairness) μεταξύ των χρηστών εντός του ετερογενούς ασύρματου δικτύου.

7. Κατανομή πόρων σε ασύρματα δίκτυα NOMA υποστηριζόμενα από RIS

Κάνοντας ένα βήμα παραπέρα ως προς την ετερογένεια της τοπολογίας του ασύρματου δικτύου και, ειδικότερα, εστιάζοντας στις επικοινωνίες που υποβοηθούνται από UAVs, αρκετές τεχνολογίες αναπτύχθηκαν πρόσφατα από την ερευνητική κοινότητα και τους φορείς τυποποίησης, οδηγώντας στη σταδιακή ωρίμανση των επικοινωνιών αυτής της μορφής. Χαρακτηριστικό παράδειγμα μιας τέτοιας τεχνολογίας είναι η ανάπτυξη του Ολοκληρωμένου Δικτύου Πρόσβασης και Οπισθόζευξης (Integrated Access and Backhaul - IAB) [94]. Η τεχνολογία αυτή προτείνει ότι οι σταθμοί βάσης επόμενης γενιάς (gNBs), που αναφέρονται ως IAB nodes, αναμεταδίδουν ασύρματα την κίνηση μέσω πολλαπλών βημάτων (multi-hop) μέχρι να φτάσει τελικά στον IAB donor, ο οποίος συνδέεται στο δίκτυο κορμού μέσω υποδομής οπτικών ινών [95]. Η κύρια ιδέα πίσω από την τεχνολογία IAB είναι η αποτελεσματική χρήση των φασματικών πόρων 5G New Radio (NR) σε όλα τα τμήματα του δικτύου πρόσβασης και οπισθόζευξης (συμπεριλαμβανομένων πολλαπλών ενδιάμεσων hops), χρησιμοποιώντας προηγμένες τεχνικές βελτιστοποίησης πόρων και πολλαπλής πρόσβασης. Η αρχιτεκτονική του δικτύου IAB θεωρείται ως βασικός ενεργοποιητής του οράματος για πλήρως αναδιαμορφώσιμα και ενεργειακά αποδοτικά ασύρματα δίκτυα. Επιπρόσθετα της τεχνολογίας IAB, μια άλλη τεχνολογία που έχει λάβει πρόσφατα αξιοσημείωτη προσοχή και σχετίζεται βαθιά με τα χαρακτηριστικά αναδιαμόρφωσης και ενεργειακής απόδοσης των μελλοντικών ασύρματων δικτύων, είναι το RIS.

Στο αντίστοιχο κεφάλαιο της διατριβής, αξιοποιούμε τα κοινά οφέλη των παραπάνω τεχνολογιών και σχεδιάζουμε και προτείνουμε ένα πλαίσιο διαχείρισης πόρων από άκρο σε άκρο,

προσαρμοσμένο στα ασύρματα δίκτυα IAB που υποστηρίζονται από RIS και UAVs. Αυτός ο τύπος δικτύων προσαρμόζεται στις μελλοντικές υποβοηθούμενες από UAVs αστικές επικοινωνίες, όπου τα UAVs χρησιμεύουν ως αναπόσπαστο μέρος της υποδομής του δικτύου για την παροχή συνδεσιμότητας από άκρο σε άκρο σε αντίξοες καταστάσεις. Σε αυτό το πλαίσιο, εξετάζουμε τις επικοινωνίες στη ζεύξη ανόδου και αντιμετωπίζουμε το πρόβλημα μεγιστοποίησης της ενεργειακής απόδοσης από άκρο σε άκρο λαμβάνοντας υπόψιν και ελέγχοντας από κοινού: α) τις μετατοπίσεις φάσης των ανακλαστικών στοιχείων του RIS, β) το διαχωρισμό του εύρους ζώνης μεταξύ των τμημάτων του δικτύου πρόσβασης και οπισθόζευξης, γ) την ισχύ μετάδοσης στη ζεύξη ανόδου των χρηστών προς το UAV και δ) την ισχύ μετάδοσης στη ζεύξη ανόδου του UAV (IAB node) προς το δίκτυο κορμού (IAB donor). Για να αντιμετωπίσουμε αυτό το πρόβλημα βελτιστοποίησης πολλαπλών μεταβλητών με κατανεμημένο τρόπο, καταφεύγουμε στην υιοθέτηση της Θεωρίας Παιγνίων και, ιδιαίτερα, στη χρήση των παιγνίων Stackelberg, εκμεταλλευόμενοι της εγγενούς ιεραρχίας που υπάρχει στο δίκτυο μεταξύ των χρηστών και του UAV. Συμπληρωματικά με τα παραπάνω, και για την καλύτερη αποκάλυψη των πλεονεκτημάτων και των συμβιβασμών (tradeoffs) της προκύπτουσας λύσης του προβλήματος όταν στοχεύουμε στην ενεργειακή απόδοση, αναλύουμε και αξιολογούμε επίσης την εφαρμογή του προτεινόμενου πλαισίου κάτω από ένα διαφορετικό στόχο βελτιστοποίησης, δηλαδή τη βελτιστοποίηση του ρυθμού δεδομένων από άκρο σε άκρο.

Συγκεκριμένα, οι κύριες συνεισφορές αυτής της εργασίας μπορούν να συνοψιστούν ως εξής:

- Παρουσιάζεται το μοντέλο συστήματος που περιλαμβάνει ένα δίκτυο IAB υποβοηθούμενο από ένα RIS και ένα UAV, λαμβάνοντας υπόψιν τις επικοινωνίες στη ζεύξη ανόδου των μερών του δικτύου ασύρματης πρόσβασης και οπισθόζευξης.

- Διατυπώνεται το πρόβλημα της διαχείρισης πόρων από άκρο σε άκρο του δικτύου IAB προς τη βελτιστοποίηση της ενεργειακής του απόδοσης. Το πρόβλημα αντιμετωπίζεται μέσω μιας κατανεμημένης παιγνιο-θεωρητικής προσέγγισης Stackelberg. Το προτεινόμενο πλαίσιο περιλαμβάνει τρία στάδια, στα οποία ελέγχονται και βελτιστοποιούνται δυναμικά οι ακόλουθες παράμετροι: α) οι μετατοπίσεις φάσης των στοιχείων του RIS, β) ο διαχωρισμός του εύρους ζώνης μεταξύ των τμημάτων του δικτύου ασύρματης πρόσβασης και οπισθόζευξης και γ) οι ισχείς μετάδοσης των χρηστών και δ) οι ισχύς μετάδοσης του UAV στη ζεύξη ανόδου. Το UAV, ενεργώντας ως ηγέτης του παιγνίου Stackelberg, καθορίζει στο πρώτο στάδιο τις μετατοπίσεις φάσης των στοιχείων RIS που μεγιστοποιούν την ισχύ του σήματος του αθροίσματος των χρηστών στην άνω ζεύξη, ακολουθώντας μια ευριστική προσέγγιση χαμηλής πολυπλοκότητας. Στη συνέχεια, το UAV υπολογίζει τον διαχωρισμό του εύρους ζώνης και την ισχύ μετάδοσης στη ζεύξη ανόδου προς τον IAB donor. Στο τρίτο στάδιο, οι χρήστες, δηλαδή οι ακόλουθοι του παιγνίου Stackelberg, βελτιστοποιούν τις ισχείς μετάδοσης στη ζεύξη ανόδου προς το UAV με κατανεμημένο τρόπο.

- Η εφαρμοσιμότητα και προσαρμοστικότητα του προτεινόμενου πλαισίου διαχείρισης πόρων αποδεικνύεται επίσης για την αντιμετώπιση του προβλήματος βελτιστοποίησης του ρυθμού δεδομένων του δικτύου IAB από άκρο σε άκρο. Η λύση λαμβάνεται ακολουθώντας μια παρόμοια κατανεμημένη προσέγγιση μέσω των παιγνίων Stackelberg, αντίστοιχη με αυτή που προτείνεται για τη βελτιστοποίηση της ενεργειακής απόδοσης. Αυτός ο εναλλακτικός στόχος βελτιστοποίησης χρησιμεύει ως βάση για την ανάδειξη των πλεονεκτημάτων και των συμβιβασμών (tradeoffs) της προκύπτουσας λύσης όταν στοχεύεται η ενεργειακή απόδοση του δικτύου IAB.

- Η συνολική απόδοση του δικτύου αξιολογείται και παρουσιάζονται εκτεταμένα αριθμητικά αποτελέσματα που καταδεικνύουν τα οφέλη που εισάγονται στην ενεργειακή απόδοση τόσο των χρηστών όσο και του UAV, από την από κοινού εκμετάλλευση των τεχνολογιών UAV, IAB και RIS.

8. Κατανομή πόρων και σχεδιασμός μηχανισμών κινήτρων σε δίκτυα υπολογισμών πολλαπλών επιπέδων

Για να διευκολυνθούν οι περιορισμένες σε υπολογιστική ισχύ και μπαταρία συσκευές χρήστη ώστε να ανταποκρίνονται στις απαιτήσεις ποιότητας υπηρεσίας των εφαρμογών, η έννοια της εκφόρτωσης εργασιών με υψηλές ανάγκες για υπολογιστικούς πόρους έχει γίνει εξαιρετικά δημοφιλής. Ειδικά, μεταξύ των διαφορετικών υπολογιστικών δυνατοτήτων και επιλογών που υπάρχουν εντός του υπολογιστικού συνεχούς, το MEC, που συχνά υλοποιείται εντός του δικτύου ραδιοπρόσβασης, έχει φέρει επανάσταση στην επιτυχή ολοκλήρωση εφαρμογών χαμηλής χρονικής απόκρισης. Ωστόσο, λόγω των ελκυστικών ιδιοτήτων του, η υπερεκμετάλλευση των διακομιστών στην άκρη του δικτύου θα οδηγήσει σταδιακά σε υποβάθμιση της απόδοσής τους. Για να μετριαστεί αυτό το πρόβλημα και να βελτιωθεί η συνολική χρήση των πόρων του συστήματος, θα πρέπει να επιδιωχθεί μια ετερογενής αρχιτεκτονική υπολογισμών πολλαπλών επιπέδων, όπου διαφορετικές υπολογιστικές οντότητες διαφόρων δυνατοτήτων συνεργάζονται σε όλο το δίκτυο. Πράγματι, η ποικιλομορφία των εκφορτωμένων εργασιών ως προς την ανάγκη για υπολογιστικούς πόρους, καθώς και η ετερογένεια των απαιτήσεων απόδοσης των αντίστοιχων εφαρμογών των χρηστών σχετικά με την ευαισθησία ή μη ως προς τη χρονική καθυστέρηση και την κατανάλωση ενέργειας, δημιουργούν ένα στέρεο έδαφος για τη σωστή χρήση των διαφορετικών επιλογών υπολογισμών στο υπολογιστικό συνεχές. Ωστόσο, παρά την πιθανή ικανότητα των εργασιών με ανεκτικότητα στη χρονική καθυστέρηση να υποβάλλονται σε επεξεργασία στην ομίχλη (ή ακόμα και στο νέφος) χωρίς να υποβαθμίζουν την παρεχόμενη ποιότητα υπηρεσίας, τα ελκυστικά χαρακτηριστικά του υπολογισμού στην άκρη του δικτύου σχετικά με την εγγύτητά του στους χρήστες σε συνδυασμό με την εγωιστική συμπεριφορά των χρηστών, μπορεί να αποδειχθούν τροχοπέδη στην υλοποίηση του οραματιζόμενου πολυεπίπεδου δικτύου υπολογισμών.

Στο αντίστοιχο κεφάλαιο της διατριβής, στοχεύουμε να αντιμετωπίσουμε ακριβώς αυτήν την πρόκληση σε ένα περιβάλλον υπολογισμών δύο επιπέδων, που αποτελείται από υπολογιστικά συστήματα στην άκρη του δικτύου και από υπολογιστική ομίχλης, τα οποία διακρίνονται από αρχιτεκτονική άποψη ως προς τη θέση όπου τοποθετείται η υπολογιστική τους ισχύς εντός του δικτύου. Πρώτον, σχεδιάζεται και προτείνεται ένας μηχανισμός κινήτρων που βασίζεται στην Πολυδιάστατη Θεωρία Συμβολαίων (Multi-Dimensional Contract Theory). Το υπολογιστικό σύστημα στην άκρη του δικτύου επιδιώκει να παρακινήσει τους χρήστες που εκφορτώνουν εργασίες σε αυτό να επιτρέπουν σε μέρος των εκφορτωμένων εργασιών τους να προωθούνται περαιτέρω και να υποβάλλονται σε επεξεργασία στην ομίχλη με βάση τα ξεχωριστά και ετερογενή χαρακτηριστικά των εφαρμογών τους. Απώτερος στόχος είναι η βελτίωση της αποδοτικότητας χρήσης πόρων σε όλο το δίκτυο και η αύξηση της συνολικής του ικανότητας εξυπηρέτησης, ιδίως υπό την παρουσία υπηρεσιών ανεκτικών ως προς τη χρονική καθυστέρηση. Το αποτέλεσμα της παραπάνω οικονομικής αλληλεπίδρασης μεταξύ των επιπέδων χρηστών-άκρης-ομίχλης χρησιμοποιείται στη συνέχεια για να αντιμετωπιστεί το δύσκολο πρόβλημα της ενορχήστρωσης πόρων εντός του περιβάλλοντος υπολογισμών πολλαπλών επιπέδων. Δεδομένου του ποσοστού των αρχικών εκφορτωμένων εργασιών στην άκρη του δικτύου που επιτρέπεται να προωθηθούν περαιτέρω στην ομίχλη, αντιμετωπίζεται το από κοινού πρόβλημα εκφόρτωσης υπολογιστικών εργασιών και ελέγχου ισχύος στη ζεύξη ανόδου μεταξύ των χρηστών και του υπολογιστικού συστήματος στην άκρη του δικτύου, θεωρώντας πως τα σήματα των χρηστών πολυπλέκονται μέσω της τεχνικής NOMA. Σεβόμενοι την ανάγκη για κατανεμημένες προσεγγίσεις διαχείρισης πόρων, το από κοινού πρόβλημα διαχείρισης ραδιοπόρων και εκφόρτωσης υπολογιστικών εργασιών διαμορφώνεται ως ένα παίγνιο Stackelberg και επιλύεται με κατανεμημένο τρόπο από τις διάφορες οντότητες του δικτύου.

Συγκεκριμένα, οι κύριες συνεισφορές αυτής της εργασίας μπορούν να συνοψιστούν ως εξής:

- Παρουσιάζεται το μοντέλο συστήματος που περιλαμβάνει ένα διεπίπεδο περιβάλλον υπολογισμών, αποτελούμενο από ένα διακομιστή άκρης και ένα διακομιστή ομίχλης. Μο-

ντελοποιούνται οι υπολογισμοί που πραγματοποιούνται στις συσκευές των χρηστών και στους διακομιστές άκρης και ομίχλης, καθώς και οι επικοινωνίες μεταξύ χρηστών και του διακομιστή άκρης, και μεταξύ του διακομιστη άκρης και διακομιστή ομίχλης.

- Σχεδιάζεται ένας μηχανισμός κινήτρων μεταξύ του διακομιστή άκρης και των χρηστών ακολουθώντας τις αρχές της πολυδιάστατης Θεωρίας Συμβολαίων. Με βάση την ετερογένεια των εφαρμογών των χρηστών και τις πολυδιάστατες ιδιωτικές πληροφορίες τους, ο διακομιστης άκρης σχεδιάζει ένα σύνολο συμβολαίων, καθένα από τα οποία περιλαμβάνει τις απαιτούμενες προσφορές από τους χρήστες προς αυτόν και τις ανάλογες αντιμοιβές που θα πάρουν πίσω. Η προσφορά κάθε χρήστη αντιπροσωπεύει το ποσοστό της υπολογιστικής εργασίας που είχε αρχικά εκφορτωθεί στην άκρη του δικτύου και μπορεί να μεταδοθεί περαιτέρω και να υποβληθεί σε επεξεργασία στην ομίχλη.

- Διατυπώνεται το από κοινού πρόβλημα εκφόρτωσης υπολογιστικών εργασιών και ελέγχου ισχύος στη ζεύξη ανόδου μεταξύ των χρηστών και του διακομιστή άκρης με τη μορφή ενός παιγνίου Stackelberg. Ο διακομιστής άκρης, δηλαδή ο ηγέτης του παιγνίου, καθορίζει τις βέλτιστες ποσότητες εργασιών των χρηστών που θα εκφορτωθούν στην άκρη του δικτύου, έχοντας επίγνωση του ποσοστού υπολογιστικής εργασίας κάθε χρήστη που πρόκειται να υποβληθεί για περαιτέρω επεξεργασία στην ομίχλη. Στη συνέχεια, οι χρήστες, δηλαδή οι ακόλουθοι του παιγνίου, των οποίων τα σήματα πολυπλέκονται μέσω της τεχνικής NOMA, υπολογίζουν τις βέλτιστες ισχείς μετάδοσης των σημάτων τους στη ζεύξη ανόδου προς το διακομιστή άκρης. Ο ηγέτης του παιγνίου Stackelberg επιδιώκει να μεγιστοποιήσει την αντιληπτή σε αυτόν ικανοποίηση λόγω εκφόρτωσης των εργασίων των χρηστών μείον την ενεργειακή επιβάρυνση του δικτύου από άκρο σε άκρο, δηλαδή από τους τους χρήστες έως και την ομίχλη. Οι ακόλουθοι, δηλαδή οι χρήστες, επιδιώκουν με τη σειρά τους τη μεγιστοποίηση της προσωπικής τους ενεργειακής απόδοσης παίζοντας ένα μη συνεργατικό παίγνιο μεταξύ τους. Η συνολική διαδικασία κατανομής πόρων εκτελείται επαναληπτικά μέχρι να επιτευχθεί η ισορροπία Stackelberg.

- Με βάση τα παραπάνω θεωρητικά θεμέλια, μελετώνται τα εγγενή λειτουργικά χαρακτηριστικά τόσο του μηχανισμού κινήτρων όσο και της διαδικασίας κατανομής πόρων μέσω μοντελοποίησης και προσομοίωσης. Επιπλέον, αναδεικνύεται η αποτελεσματικότητα απόδοσης του προτεινόμενου συμβολαίου υπό στατιστική γνώση του τύπου των εργασιών εκφόρτωσης των χρηστών σε σύγκριση με την περίπτωση αναφοράς όπου υπάρχει πλήρης πληροφόρηση σχετικά με τον τύπο αυτόν, ενώ αναδεικνύεται, ταυτόχρονα, η υπεροχή της προτεινόμενης προσέγγισης κατανομής πόρων έναντι διαφορετικών στρατηγικών εκφόρτωσης.

9. Κατανομή πόρων σε RSMA υπολογιστικά συστήματα πολλαπλών διακομιστών στην άκρη του δικτύου

Σε αυτό το κεφάλαιο, εμβαθύνουμε στην οριζόντια κατανομή των εκφορτωμένων υπολογιστικών εργασιών από τους χρήστες, δηλαδή σε πολλαπλούς διακομιστές εντός του ίδιου επιπέδου υπολογισμών. Συγκεκριμένα, με κίνητρο την κατανεμημένη ανάπτυξη πολλαπλών διακομιστών MEC εντός του δικτύου ραδιοπρόσβασης και τις εξελίξεις στις τεχνικές μη ορθογωνικής πολλαπλής πρόσβασης επόμενης γενιάς, προτείνουμε οι χρήστες να χρησιμοποιούν τα διαφορετικά διαθέσιμα δίκτυα ραδιοπρόσβασης στην εμβέλειά τους και να εκφορτώνουν ταυτόχρονα σε πολλούς διακομιστές MEC υπολογιστικές εργασίες με υψηλές απαιτήσεις για υπολογιστικούς πόρους και ευαισθησία ως προς τη χρονική καθυστέρηση. Για να αντιμετωπίσουμε το κρίσιμο πρόβλημα της διαχείρισης παρεμβολών μεταξύ διακομιστών που προέρχονται από τις ταυτόχρονες μεταδόσεις ενός χρήστη σε πολλούς διακομιστές, εξετάζουμε την εφαρμογή της τεχνικής RSMA, η οποία θεωρείται βασικός ενεργοποιητής των δικτύων επόμενης γενιάς. Η διαί-

ρεση ρυθμού έγκειται στο διαχωρισμό του μηνύματος ενός χρήστη σε δύο ή περισσότερα μέρη που μπορούν να αποκωδικοποιηθούν ευέλικτα σε έναν ή περισσότερους δέκτες, αντίστοιχα. Το κοινό μήνυμα (common message) - όπως ονομάζεται - προορίζεται και αποκωδικοποιείται από όλους τους εμπλεκόμενους διακομιστές στη μετάδοση, σε αντίθεση με ένα ιδιωτικό μήνυμα (private message) που προορίζεται για κάθε διακομιστή MEC ξεχωριστά. Ως αποτέλεσμα, κατά την αποκωδικοποίηση του ιδιωτικού μηνύματος, οι παρεμβολές που προέρχονται από τα ιδιωτικά μηνύματα των άλλων διακομιστών αντιμετωπίζονται ως θόρυβος. Με τον έξυπνο έλεγχο του διαχωρισμού μεταξύ των κοινών και των ιδιωτικών μηνυμάτων, επιτυγχάνεται μια αποδεκτή αντιστάθμιση μεταξύ αποτελεσματικής χρήσης φάσματος, διαχείρισης παρεμβολών πολλών διακομιστών και πολυπλοκότητας επεξεργασίας σήματος στους δέκτες.

Προφανώς, η απόδοση του MEC είναι σε μεγάλο βαθμό συνυφασμένη με την κατανομή των ραδιοπόρων σύμφωνα με την τεχνική RSMA για την επίτευξη της στοχευμένης απαίτησης σε χρονική απόκριση της εφαρμογής κάθε χρήστη και επομένως θα πρέπει να μελετηθεί από κοινού. Κατά συνέπεια, προκύπτει το δύσκολο πρόβλημα της από κοινού εκφόρτωσης υπολογιστικών εργασιών και κατανομής ραδιοπόρων και υπολογιστικών πόρων μεταξύ των χρηστών και των πολλαπλών διακομιστών MEC, το οποίο παραμένει κυρίως άλυτο στη βιβλιογραφία και προσπαθούμε να αντιμετωπίσουμε. Συγκεκριμένα στο αντίστοιχο κεφάλαιο της παρούσας διατριβής, προτείνουμε μια ολιστική λύση για την ελαχιστοποίηση του αθροίσματος της μέγιστης χρονικής καθυστέρησης των χρηστών μεταξύ των διαφορετικών διακομιστών MEC, που προέρχεται τόσο από την εκφόρτωση όσο και από την επεξεργασία των υπολογιστικών εργασιών στους διάφορους διακομιστές. Για το σκοπό αυτό, βελτιστοποιούνται από κοινού οι αναλογίες εκφόρτωσης υπολογιστικών εργασιών από τους χρήστες στους διαφορετικούς διακομιστές MEC, οι ρυθμοί και οι ισχείς μετάδοσης των χρηστών στη ζεύξη ανόδου, καθώς και οι υπολογιστικοί πόροι που κατανέμονται από τους διακομιστές προς τον κάθε χρήστη ανάλογα με το μέγεθος της εκφορτωμένης σε αυτούς υπολογιστικής εργασίας. Το διαμορφωμένο min-max-sum πρόβλημα - όπως χαρακτηρίζεται με όρους βελτιστοποίησης - μετασχηματίζεται ισοδύναμα και αποσυντίθεται σε δύο ανεξάρτητα υποπροβλήματα, αυτό του ελέγχου ρυθμού και ισχύος μετάδοσης και αυτό της κατανομής υπολογιστικών πόρων. Η βέλτιστη λύση για τις αναλογίες εκφόρτωσης υπολογιστικών εργασιών σε κάθε διακομιστή MEC προέρχεται φυσικά από την προαναφερθείσα διαδικασία μετασχηματισμού και αποσύνθεσης του αρχικού προβλήματος. Με αυτόν τον τρόπο, καταλήγουμε σε μια σχεδόν βέλτιστη λύση στο αρχικό πρόβλημα που αποδεικνύεται ιδιαίτερα αποτελεσματική από άποψη πολυπλοκότητας και χρονικής καθυστέρησης που αισθάνονται οι χρήστες σε σύγκριση με τους συμβατικούς μη γραμμικούς αλγόριθμους βελτιστοποίησης.

Συγκεκριμένα, οι κύριες συνεισφορές αυτής της εργασίας μπορούν να συνοψιστούν ως εξής:

- Διατυπώνεται το πρόβλημα της ελαχιστοποίησης του αθροίσματος της μέγιστης χρονικής καθυστέρησης των χρηστών που προέρχεται από την εκφόρτωση και την επεξεργασία της υπολογιστικής εργασίας τους μεταξύ των διαφορετικών διακομιστών MEC. Ο στόχος είναι να βελτιστοποιηθούν από κοινού οι αναλογίες εκφόρτωσης υπολογιστικών εργασιών των χρηστών στους διαφορετικούς διακομιστές MEC, οι ρυθμοί και ισχείς μετάδοσής τους στη ζεύξη ανόδου, καθώς και οι υπολογιστικοί πόροι που κατανείμονται από κάθε διακομιστή MEC προς τους εξυπηρετούμενους χρήστες του.

- Ο ισοδύναμος μετασχηματισμός του αρχικά διατυπωμένου min-max-sum προβλήματος αναλύεται για να οδηγήσει σε μια αντικειμενική συνάρτηση συνεχούς μορφής και να εξαγάγει τις βέλτιστες συνθήκες που ισχύουν για το πρόβλημα βελτιστοποίησης.

- Οι συνθήκες KKT χρησιμοποιούνται για την αποσύνθεση του μετασχηματισμένου προβλήματος σε δύο ανεξάρτητα υποπροβλήματα, οι λύσεις των οποίων παρέχουν χωριστά μη βέλτιστες λύσεις για το πρόβλημα ελέγχου των ραδιοπόρων (δηλαδή, των ισχύων και ρυθμών μετάδοσης στη ζεύξη ανόδου) και βέλτιστες λύσεις για το πρόβλημα κατανομής

υπολογιστικών πόρων από τη μεριά των διακομιστών MEC. Η βέλτιστη αναλογία εκφόρτωσης υπολογιστικών εργασιών στους διαφορετικούς διακομιστές MEC προέρχεται επίσης άμεσα από την ισοδύναμη ανάλυση μετασχηματισμού και αποσύνθεσης του αρχικού προβλήματος.

- Λαμβάνονται αριθμητικά αποτελέσματα μέσω μοντελοποίησης και προσομοίωσης για να καταδειχθεί η αποτελεσματικότητα της προτεινόμενης λύσης όσον αφορά την πολυπλοκότητα και τη χρονική καθυστέρηση που αντιλαμβάνονται οι χρήστες, καθώς και να επιδειχθεί η συνολική αποτελεσματικότητα του συστήματος έναντι άλλων παραδοσιακών τεχνικών πολλαπλής πρόσβασης.

10. Συμπεράσματα διατριβής

Ειδικότερα, τα συμπεράσματα στα οποία καταλήξαμε μέσω της παρούσας διατριβής είναι τα ακόλουθα:

- **Η Θεωρία Συμβολαίων μπορεί να αποτελέσει ένα ισχυρό εργαλείο για να επιτρέψει την κατανεμημένη λήψη αποφάσεων σε περίπτωση ελλιπούς πληροφόρησης.**
  Γενικά, η Θεωρία Συμβολαίων παρέχει τις αρχές και τα μαθηματικά θεμέλια για τη λειτουργία μιας αγοράς υπό την ύπαρξη ελλιπούς πληροφόρησης, όπως για παράδειγμα ένα συμβόλαιο εργασίας μεταξύ ενός εργοδότη (ή εντολέα όπως ονομάζεται με συμβολαιοθεωρητικούς όρους) και πολλών εργαζόμενων (ή πρακτόρων). Αξιοποιώντας τη στατιστική γνώση σχετικά με τις προσωπικές πληροφορίες των εργαζόμενων, ο εργοδότης σχεδιάζει ένα μενού από συμβόλαια και κάθε εργαζόμενος επιλέγει αυτόνομα ένα από τα διάφορα συμβόλαια που ταιριάζει καλύτερα στις προσωπικές του πληροφορίες. Το συγκεκριμένο μοντέλο χρησιμοποιήθηκε με επιτυχία σε αυτή τη διατριβή, προκειμένου να διατυπωθεί και να επιλυθεί το τυπικό πρόβλημα ελέγχου ισχύος στη ζεύξη ανόδου σε ένα ετερογενές ασύρματο δίκτυο με πολλαπλούς σταθμούς βάσης που βασίζεται στο NOMA, ειδικότερα για την περίπτωση μη ύπαρξης πλήρους γνώσης του CSI από την πλευρά των σταθμών βάσης. Οι χρήστες, από την πλευρά τους, έχοντας πιθανώς καλύτερη εκτίμηση σχετικά με τη συνθήκη του ασύρματου καναλιού τους, έχουν τη δυνατότητα να αυτοπροσαρμόζονται και να επιλέγουν αυτόνομα το επίπεδο ισχύος μετάδοσης στη ζεύξη ανόδου που τους ταιριάζει καλύτερα από τα διάφορα συμβόλαια που έχουν σχεδιαστεί από τους σταθμούς βάσης. Με αυτόν τον τρόπο, εξασφαλίζεται ταυτόχρονα ότι το επιλεχθέν συμβόλαιο πληροί τις απαιτήσεις των σταθμών βάσης για επιτυχή εφαρμογή της τεχνικής SIC και αποκωδικοποίησης του σήματος που φτάνει σε αυτούς.

- **Η Θεωρία Συμβολαίων μπορεί να χρησιμοποιηθεί με επιτυχία για να συμβιβάσει τους αντικρουόμενους στόχους των δικτυακών οντοτήτων.**
  Σχεδιάζοντας αμοιβαία επωφελή συμβόλαια, ο εκάστοτε εντολέας μπορεί να συμβιβάσει τον αντικρουόμενο στόχο του με τους πράκτορες που συμμετέχουν στο συμβόλαιο. Για το σκοπό αυτό, προσφέρεται ένα είδος ανταμοιβής στους πράκτορες που είναι ανάλογο με τις προσωπικές τους πληροφορίες και την προσφορά που επιλέγουν αυτόνομα να παράσχουν στον εντολέα, ως μέσο αντιστάθμισης της προσφοράς τους ή ακόμη και παρακίνησης για να καταβάλουν μεγαλύτερη προσπάθεια από αυτή που σκοπεύουν. Αυτή η ιδέα της συμφιλίωσης αντικρουόμενων στόχων μεταξύ των χρηστών και των παρόχων υπηρεσιών υπολογισμών έχει εφαρμοστεί με επιτυχία στο πλαίσιο ενός πολυεπίπεδου δικτύου κινητών υπολογισμών. Συγκεκριμένα, η νέα ιδέα που παρουσιάζεται σε αυτή τη διατριβή έγκειται στην επαρκή παρακίνηση των εγωιστικά και άπληστα συμπεριφερόμενων χρηστών να χρησιμοποιήσουν ολόκληρο το φάσμα του υπολογιστικού συνεχούς (που περιλαμβάνει τα επίπεδα άκρης και ομίχλης στην παρούσα διατριβή). Λόγω των ελκυστικών ιδιοτήτων τους σε σχέση με την εγγύτητά τους με τους χρήστες και την επαρκή

υπολογιστική τους ικανότητα, οι χρήστες παρουσιάζουν την τάση να προτιμούν περισσότερο τα υπολογιστικά συστήματα στην άκρη του δικτύου συγκριτικά με τις υπολογιστικές υπηρεσίες ομίχλης, οδηγώντας σταδιακά σε συμφόρηση και υποβάθμιση της απόδοσης των πρώτων. Σχεδιάζοντας σωστά συμβόλαια, τα οποία παρέχουν μια καλή αντιστάθμιση μεταξύ νομισματικού κόστους και ικανοποίησης ως προς την ποιότητα της παρεχόμενης υπηρεσίας, οι πάροχοι υπολογιστικών υπηρεσιών μπορούν να αλλάξουν τις προτιμήσεις των χρηστών και να αυξήσουν τη χωρητικότητα και την αποτελεσματικότητα του δικτύου.

- **Η Θεωρία Παιγνίων είναι ένα ακόμη ισχυρό εργαλείο που επιτρέπει την κατανεμημένη λήψη αποφάσεων μεταξύ πολλαπλών ετερογενών δικτυακών οντοτήτων.**
  Δεδομένης της ήδη κατανεμημένης φύσης των ασύρματων δικτύων επόμενης γενιάς 5G και του εγγενούς ανταγωνισμού για την κοινή χρήση κάποιας κοινής δεξαμενής πόρων, όπως το φάσμα ή η υπολογιστική ισχύς ενός απομακρυσμένου διακομιστή, έχουμε εφαρμόσει εκτενώς τις αρχές της Θεωρίας Παιγνίων στις εργασίες μας και στα πλαίσια κατανομής πόρων και λήψης αποφάσεων που προτείνουμε. Ειδικότερα, η εφαρμογή παιγνιοθεωρητικών προσεγγίσεων έχει αξιοποιηθεί ιδιαίτερα για να επιτρέψει τον κατανεμημένο έλεγχο ισχύος στη ζεύξη ανόδου σε ασύρματα δίκτυα επικοινωνιών, ενώ οι χρήστες ανταγωνίζονται για το κοινό φάσμα μέσω του οποίου πραγματοποιούνται οι μεταδόσεις τους. Άλλα παιγνιο-θεωρητικά μοντέλα επιτρέπουν την ιεραρχική μοντελοποίηση των παικτών στο παίγνιο με τη μορφή ηγέτη/ηγετών και ακόλουθου/ακολούθων. Σε αυτό το είδος παιγνίου, ο ηγέτης παίρνει μια απόφαση που είναι παρατηρήσιμη από τον ακόλουθο, ο οποίος στη συνέχεια παίρνει αυτόνομα την προσωπική του απόφαση. Αυτό το μοντέλο της Θεωρίας Παιγνίων έχει επίσης εφαρμοστεί ευρέως για να αποτυπώσει την ιεραρχία που υπάρχει μεταξύ των αποφάσεων ενός σταθμού βάσης ή απομακρυσμένου διακομιστή και των χρηστών του δικτύου. Κάθε ένα από τα κατανεμημένα διατυπωμένα και επιλυμένα προβλήματα από τις δικτυακές οντότητες μετατρέπεται σε πρόβλημα μεγιστοποίησης/ελαχιστοποίησης σε σχέση με μια καλά καθορισμένη συνάρτηση. Έπειτα, η Θεωρία Παιγνίων παρέχει ενδιαφέρουσες προσεγγίσεις λύσεων που οδηγούν σε λειτουργικά σημεία, όπως το σημείο ισορροπίας Nash, το οποίο παρέχει έναν συνήθη τρόπο μέτρησης της αποτελεσματικότητας των προτεινόμενων πλαισίων.

- **Η μοντελοποίηση της συμπεριφοράς ενός δικτύου είναι περίπλοκη, αλλά τα προτεινόμενα πλαίσια και οι λύσεις πρέπει να είναι χαμηλής πολυπλοκότητας.**
  Οι εφαρμογές στο πλαίσιο των δικτύων επόμενης γενιάς 5G απαιτούν στιγμιαίες μεταδόσεις και εκφόρτωση, καθώς και υπολογισμούς και λήψη αποφάσεων σε πραγματικό χρόνο για την ικανοποίηση των απαιτήσεων εξαιρετικά χαμηλής χρονικής απόκρισης και υψηλής αξιοπιστίας. Επιπλέον, από άποψη επεκτασιμότητας, ένας κεντρικοποιημένος αλγόριθμος υψηλής πολυπλοκότητας μπορεί να δημιουργήσει σημείο συμφόρησης για το δίκτυο από πλευράς εκτέλεσης αλλά και απαιτούμενης σηματοδοσίας (signaling) προς την κεντρική οντότητα που εκτελεί τον αλγόριθμο. Για το λόγο αυτό, απαιτούνται αποτελεσματικοί και αποδοτικοί αλγόριθμοι χαμηλής πολυπλοκότητας. Οι οικονομο-θεωρητικοί αλγόριθμοι και οι αλγόριθμοι ενισχυτικής μάθησης τείνουν να ταιριάζουν καλύτερα με την παραπάνω περιγραφή, κατανέμοντας τη διαδικασία και επιτρέποντας σε κάθε οντότητα να εκτελέσει μόνη της τους αντίστοιχους υπολογισμούς. Σε αυτή τη διατριβή, σχεδιάσαμε και προτείναμε πολύπλοκα μοντέλα που αποτυπώνουν τη συμπεριφορά, τις αλληλοεξαρτώμενες αλληλεπιδράσεις και τις αποφάσεις των συμμετεχόντων οντοτήτων με ρεαλιστικό τρόπο, αλλά απαιτούν υπολογισμούς χαμηλής πολυπλοκότητας για να συγκλίνουν πραγματικά στο βέλτιστο αποτέλεσμα.

- **Τα RIS μπορούν να βελτιώσουν τόσο τη φασματική όσο και την ενεργειακή απόδοση του δικτύου.**
  Τα RIS αποτελούνται από μεγάλο αριθμό ανακλαστικών στοιχείων κατασκευασμένων

από μετα-υλικά, τα οποία μπορούν να αντανακλούν τα προσκρουόμενα ηλεκτρομαγνητικά κύματα, καθορίζοντας τη μετατόπιση φάσης τους μέσω ενός έξυπνου ελεγκτή. Ο ελεγκτής μπορεί να ελεγχθεί δυναμικά με τρόπο που καθορίζεται από λογισμικό για να προσαρμόζει την τοποθέτηση των στοιχείων και να παρέχει προγραμματιζόμενες ιδιότητες στο περιβάλλον ραδιοδιάδοσης. Αυτή η ιδιότητα είναι απόλυτα ευθυγραμμισμένη με το ευρύτερο όραμα των δικτύων επόμενης γενιάς 5G για στιγμιαία αναδιαμόρφωση και προσαρμοστικότητα, ανάλογα με τις ανάγκες του δικτύου. Ταυτόχρονα, όμως, έχει επαληθευτεί - στο πλαίσιο της παρούσας διατριβής - ότι η χρήση των RIS μπορεί να επιτύχει τον απώτερο στόχο της καταπολέμησης των δυσμενών συνθηκών μετάδοσης λόγω της εξασθένισης των ασύρματων καναλιών. Συγκεκριμένα, έχει διερευνηθεί η προοπτική των RIS να βελτιώσουν την ενεργειακή και φασματική απόδοση τόσο στο κομμάτι του δικτύου ασύρματης πρόσβασης αλλά και οπισθόζευξης, αποδεικνύοντας την ανωτερότητα στην επιτυγχανόμενη απόδοση σε σύγκριση με το σενάριο αξιολόγησης όπου δεν γίνεται χρήση RIS εντός της τοπολογίας του δικτύου. Με αυτόν τον τρόπο, η συνδεσιμότητα δικτύου καθώς και η διάρκεια ζωής της μπαταρίας των μεμονωμένων δικτυακών οντοτήτων μπορούν να επεκταθούν.

- **Η χρήση όλου του φάσματος του υπολογιστικού συνεχούς οδηγεί σε ανώτερη απόδοση τόσο από άποψη ενέργειας όσο και χρονικής απόκρισης.**
  Εκτός από τις απαιτήσεις των εφαρμογών σχετικά με την ποιότητα παρεχόμενης υπηρεσίας, οι οποίες κατευθύνουν τις προτιμήσεις και τις αποφάσεις των χρηστών προς έναν πάροχο υπηρεσιών υπολογισμών (δηλαδή, άκρη, ομίχλη, νέφος), τα εγγενή εγωιστικά και άπληστα χαρακτηριστικά συμπεριφοράς των χρηστών παίζουν τον πιο σημαντικό ρόλο όταν ανταγωνίζονται για μια κοινή δεξαμενή πόρων. Η μοντελοποίηση της συμπεριφορικής και οικονομικής αλληλεπίδρασης μεταξύ των χρηστών και των ανταγωνιστικών παρόχων υπηρεσιών υπολογισμών είναι επιτακτική ανάγκη για να προσδώσουμε ένα ρεαλιστικό πνεύμα κατά τη δρομολόγηση των αιτημάτων για υπολογισμό και τη διαδικασία κατανομής πόρων στα διάφορα επίπεδα υπηρεσιών υπολογισμών. Αυτή είναι η βασική ιδέα πάνω στην οποία έχει οικοδομηθεί το προτεινόμενο πλαίσιο για τη χρήση όλου του φάσματος του υπολογιστικού συνεχούς, χρησιμοποιώντας Θεωρίες Συμβολαίων και Παιγνίων. Τα κύρια ευρήματα της εργασίας μας είναι ότι η σωστή χρήση πολλαπλών επιπέδων υπολογιστικών δυνατοτήτων επιτρέπει την 100% ικανοποίηση των απαιτήσεων των χρηστών ως προς τη χρονική καθυστέρηση, διατηρώντας παράλληλα χαμηλά επίπεδα κατανάλωσης ενέργειας στα διαφορετικά επίπεδα υπολογισμών συγκριτικά με άλλες επιλογές εκφόρτωσης, π.χ., εκτέλεση υπολογισμών αποκλειστικά τοπικά στις συσκευές των χρηστών, εκφόρτωση υπολογισμών αοπκλειστικά στην άκρη, εκφόρτωση υπολογισμών αποκλειστικά στην ομίχλη.

- **Η ταυτόχρονη εκφόρτωση υπολογισμών σε πολλούς διακομιστές μειώνει τη χρονική καθυστέρηση ενώ επιτρέπει βελτιωμένη προσαρμοστικότητα και ασφάλεια.**
  Η εκφόρτωση σε πολλαπλούς διακομιστές MEC αποτελεί μια ακόμη πολύτιμη στρατηγική για διάφορες εφαρμογές υπολογισμών. Αυτή η στρατηγική εκμεταλλεύεται τους γεωγραφικά κατανεμημένους διακομιστές εντός του δικτύου ραδιοπρόσβασης των δικτύων επόμενης γενιάς 5G για να μειώσει τη χρονική καθυστέρηση για τους χρήστες σε διαφορετικές περιοχές. Οι χρήστες περιορισμένης διαθεσιμότητας υπολογιστικών ή ενεργειακών πόρων μπορούν να εκφορτώσουν τμήματα της υπολογιστικής τους εργασίας σε έναν συνδυασμό διαθέσιμων διακομιστών MEC. Δεδομένου ότι κάθε διακομιστής MEC φέρει διαφορετικά χαρακτηριστικά, π.χ. υπολογιστική ισχύ και ακρίβεια στους υπολογισμούς, αυτή η στρατηγική επιτρέπει την προσαρμογή και την ευελιξία από την πλευρά του χρήστη ανάλογα με τις ανάγκες κάθε μέρους της εκφορτούμενης εργασίας. Συγκεκριμένα, οι βαριές εργασίες μηχανικής μάθησης, π.χ. η επεξεργασία εικόνας, μπορούν να επωφεληθούν από την εκφόρτωση σε πολλαπλούς διακομιστές MEC. Διαφορετικές ροές βίντεο που προέρχονται

από εφαρμογές οχημάτων, υγειονομικής περίθαλψης ή ασφάλειας - για να αναφέρουμε μερικά παραδείγματα - μπορούν να εκφορτωθούν σε διαφορετικούς διακομιστές MEC για επεξεργασία. Με αυτόν τον τρόπο, η συνολική πολυπλοκότητα της εργασίας μειώνεται και διάφορα επίπεδα ακρίβειας επεξεργασίας μπορούν να στοχευθούν για κάθε μέρος της εργασίας με βάση την υπολογιστική ικανότητα κάθε διακομιστή MEC. Ταυτόχρονα, η κατανομή υπολογισμών σε πολλούς διακομιστές μπορεί να βελτιώσει την ασφάλεια σε περίπτωση παραβίασης ενός από αυτούς. Συγκεκριμένα, όσον αφορά τη μειωμένη χρονική καθυστέρηση, αυτό το όφελος έχει πρακτικά εντοπιστεί και μετρηθεί στην παρούσα διατριβή ενώ πειραματιζόμαστε με διαφορετικές τεχνικές πολλαπλής πρόσβασης κατά τη ραδιομετάδοση από τους χρήστες.

- **Ο σχεδιασμός ολιστικών λύσεων είναι υψίστης σημασίας για την αξιοποίηση του πλήρους δυναμικού της αρχιτεκτονικής, της υποδομής και της τεχνολογίας του δικτύου.**
  Τα ασύρματα δίκτυα επικοινωνίας και κινητών υπολογισμών επόμενης γενιάς 5G περιλαμβάνουν έναν συνεχώς αυξανόμενο αριθμό βαθμών ελευθερίας όσον αφορά τους πόρους που πρέπει να διαχειρίζονται ταυτόχρονα, ο οποίος πηγάζει από τα διάφορα αρχιτεκτονικά παραδείγματα και τεχνολογίες που υιοθετούνται. Το φάσμα, η ισχύς και ο ρυθμός μετάδοσης δεδομένων, η συσχέτιση χρήστη με σταθμό βάσης ή απομακρυσμένο διακομιστή, οι μετατοπίσεις φάσης των στοιχείων των RIS, η εκφόρτωση υπολογισμών και η υπολογιστική ισχύς, αποτελούν μόνο μερικές από τις διαφορετικές παραμέτρους και πόρους που πρέπει να λαμβάνονται υπόψη κάθε φορά, ενώ ένα διαφορετικό υποσύνολο αυτών έχει βελτιστοποιηθεί από κοινού στα διάφορα κεφάλαια της παρούσας διατριβής. Τα αποτελέσματα αυτής της διατριβής έχουν επιβεβαιώσει την κυριαρχία των πλαισίων ολιστικής βελτιστοποίησης, σε σύγκριση με λύσεις συγκριτικής αξιολόγησης που αντιμετωπίζουν μονομερώς τη βελτιστοποίηση διαφορετικών τύπων πόρων, με αποτέλεσμα περισσότερο αποδοτικές λύσεις ως προς την αξιοποίηση του φάσματος, την ενέργεια αλλά και το χρόνο απόκρισης. Η δημιουργία πλαισίων βελτιστοποίησης χαμηλής πολυπλοκότητας για την αντιμετώπιση εντός πολυωνυμικού χρόνου τέτοιων συνδυαστικών προβλημάτων που πιθανότατα δεν φέρουν ούτε γραμμικές ούτε κυρτές ιδιότητες (δηλαδή χιλιοστά του δευτερολέπτου) είναι σημαντικής και πρακτικής σημασίας, αποκαλύπτοντας περαιτέρω την αποτελεσματικότητα της οικονομο-θεωρητικής μοντελοποίησης και πλαισίων λύσης.

Bibliography

[1] I. T. Union, "Imt traffic estimates for the years 2020 to 2030," 2015. Rep. ITU-R M.2370-0.

[2] Cisco, "Cisco annual internet report (2018–2023) white paper," 2020 [Online].

[3] G. Kakkavas, M. Diamanti, A. Stamou, V. Karyotis, F. Bouali, J. Pinola, O. Apilo, S. Papavassiliou, and K. Moessner, "Design, development, and evaluation of 5g-enabled vehicular services: The 5g-heart perspective," *Sensors*, vol. 22, no. 2, p. 426, 2022.

[4] G. Kakkavas, M. Diamanti, A. Stamou, V. Karyotis, S. Papavassiliou, F. Bouali, and K. Moessner, "5g network requirement analysis and slice dimensioning for sustainable vehicular services," in *2021 17th International Conference on Distributed Computing in Sensor Systems (DCOSS)*, pp. 495–502, 2021.

[5] J. An, K. Yang, J. Wu, N. Ye, S. Guo, and Z. Liao, "Achieving sustainable ultra-dense heterogeneous networks for 5g," *IEEE Communications Magazine*, vol. 55, no. 12, pp. 84–90, 2017.

[6] N. Wang, E. Hossain, and V. K. Bhargava, "Backhauling 5g small cells: A radio resource management perspective," *IEEE Wireless Communications*, vol. 22, no. 5, pp. 41–49, 2015.

[7] I. Bor-Yaliniz and H. Yanikomeroglu, "The new frontier in ran heterogeneity: Multi-tier drone-cells," *IEEE Communications Magazine*, vol. 54, no. 11, pp. 48–55, 2016.

[8] M. Jia, X. Gu, Q. Guo, W. Xiang, and N. Zhang, "Broadband hybrid satellite-terrestrial communication systems based on cognitive radio toward 5g," *IEEE Wireless Communications*, vol. 23, no. 6, pp. 96–106, 2016.

[9] X. Wang, L. Kong, F. Kong, F. Qiu, M. Xia, S. Arnon, and G. Chen, "Millimeter wave communication: A comprehensive survey," *IEEE Communications Surveys & Tutorials*, vol. 20, no. 3, pp. 1616–1653, 2018.

[10] K. M. S. Huq, S. A. Busari, J. Rodriguez, V. Frascolla, W. Bazzi, and D. C. Sicker, "Terahertz-enabled wireless system for beyond-5g ultra-fast networks: A brief survey," *IEEE Network*, vol. 33, no. 4, pp. 89–95, 2019.

[11] C. Pan, H. Ren, K. Wang, J. F. Kolb, M. Elkashlan, M. Chen, M. Di Renzo, Y. Hao, J. Wang, A. L. Swindlehurst, X. You, and L. Hanzo, "Reconfigurable intelligent surfaces for 6g systems: Principles, applications, and research directions," *IEEE Communications Magazine*, vol. 59, no. 6, pp. 14–20, 2021.

[12] M. Chen, Y. Hao, Y. Li, C.-F. Lai, and D. Wu, "On the computation offloading at ad hoc cloudlet: architecture and service modes," *IEEE Communications Magazine*, vol. 53, no. 6, pp. 18–24, 2015.

[13] H. Guo, J. Liu, and J. Zhang, "Computation offloading for multi-access mobile edge computing in ultra-dense networks," *IEEE Communications Magazine*, vol. 56, no. 8, pp. 14–19, 2018.

[14] R. Mahmud, R. Kotagiri, and R. Buyya, "Fog computing: A taxonomy, survey and future directions," in *Internet of Everything: Algorithms, Methodologies, Technologies and Perspectives* (B. Di Martino, K.-C. Li, L. T. Yang, and A. Esposito, eds.), pp. 103–130, Singapore: Springer Singapore, 2018.

[15] N. Zhang, N. Cheng, A. T. Gamage, K. Zhang, J. W. Mark, and X. Shen, "Cloud assisted hetnets toward 5g wireless networks," *IEEE Communications Magazine*, vol. 53, no. 6, pp. 59–65, 2015.

[16] M. Jo, T. Maksymyuk, B. Strykhalyuk, and C.-H. Cho, "Device-to-device-based heterogeneous radio access network architecture for mobile cloud computing," *IEEE Wireless Communications*, vol. 22, no. 3, pp. 50–58, 2015.

[17] T. Taleb, K. Samdanis, B. Mada, H. Flinck, S. Dutta, and D. Sabella, "On multi-access edge computing: A survey of the emerging 5g network edge cloud architecture and orchestration," *IEEE Communications Surveys & Tutorials*, vol. 19, no. 3, pp. 1657–1681, 2017.

[18] M. S. Elbamby, C. Perfecto, M. Bennis, and K. Doppler, "Toward low-latency and ultra-reliable virtual reality," *IEEE Network*, vol. 32, no. 2, pp. 78–84, 2018.

[19] C. Cox, *Orthogonal Frequency Division Multiple Access*, pp. 67–85. John Wiley & Sons, 2014.

[20] M. Diamanti, N. Fryganiotis, S. Papavassiliou, C. Pelekis, and E. E. Tsiropoulou, "On the minimum collisions assignment problem in interdependent networked systems," in *2022 IEEE Symposium on Computers and Communications (ISCC)*, pp. 1–6, 2022.

[21] L. Dai, B. Wang, Y. Yuan, S. Han, C. I, and Z. Wang, "Non-orthogonal multiple access for 5g: solutions, challenges, opportunities, and future research trends," *IEEE Communications Magazine*, vol. 53, no. 9, pp. 74–81, 2015.

[22] S. M. R. Islam, N. Avazov, O. A. Dobre, and K.-s. Kwak, "Power-domain non-orthogonal multiple access (noma) in 5g systems: Potentials and challenges," *IEEE Communications Surveys & Tutorials*, vol. 19, no. 2, pp. 721–742, 2017.

[23] Z. Liu and L.-L. Yang, "Sparse or dense: A comparative study of code-domain noma systems," *IEEE Transactions on Wireless Communications*, vol. 20, no. 8, pp. 4768–4780, 2021.

[24] M. S. Ali, H. Tabassum, and E. Hossain, "Dynamic user clustering and power allocation for uplink and downlink non-orthogonal multiple access (noma) systems," *IEEE Access*, vol. 4, pp. 6325–6343, 2016.

[25] B. Rimoldi and R. Urbanke, "A rate-splitting approach to the gaussian multiple-access channel," *IEEE Transactions on Information Theory*, vol. 42, no. 2, pp. 364–375, 1996.

[26] B. Clerckx, Y. Mao, R. Schober, and H. V. Poor, "Rate-splitting unifying sdma, oma, noma, and multicasting in miso broadcast channel: A simple two-user rate analysis," *IEEE Wireless Communications Letters*, vol. 9, no. 3, pp. 349–353, 2020.

[27] Z. Yang, M. Chen, W. Saad, and M. Shikh-Bahaei, "Optimization of rate allocation and power control for rate splitting multiple access (rsma)," *IEEE Transactions on Communications*, vol. 69, no. 9, pp. 5988–6002, 2021.

[28] Q. Wu and R. Zhang, "Towards smart and reconfigurable environment: Intelligent reflecting surface aided wireless network," *IEEE Communications Magazine*, vol. 58, no. 1, pp. 106–112, 2020.

[29] Q. Wu and R. Zhang, "Intelligent reflecting surface enhanced wireless network via joint active and passive beamforming," *IEEE Transactions on Wireless Communications*, vol. 18, no. 11, pp. 5394–5409, 2019.

[30] S. Hu, F. Rusek, and O. Edfors, "Beyond massive mimo: The potential of data transmission with large intelligent surfaces," *IEEE Transactions on Signal Processing*, vol. 66, no. 10, pp. 2746–2758, 2018.

[31] H. Guo, Y.-C. Liang, J. Chen, and E. G. Larsson, "Weighted sum-rate maximization for reconfigurable intelligent surface aided wireless networks," *IEEE Transactions on Wireless Communications*, vol. 19, no. 5, pp. 3064–3076, 2020.

[32] C. Huang, A. Zappone, G. C. Alexandropoulos, M. Debbah, and C. Yuen, "Reconfigurable intelligent surfaces for energy efficiency in wireless communication," *IEEE Transactions on Wireless Communications*, vol. 18, no. 8, pp. 4157–4170, 2019.

[33] M. Almekhlafi, M. A. Arfaoui, C. Assi, and A. Ghrayeb, "Enabling urllc applications through reconfigurable intelligent surfaces: Challenges and potential," *IEEE Internet of Things Magazine*, vol. 5, no. 1, pp. 130–135, 2022.

[34] T. Haustein, J. McMenamy, L. Thiele, and P. S. H. Leather, "Reconfigurable intelligent surface deployment in 5g and beyond 5g cellular networks," in *2022 IEEE 23rd International Workshop on Signal Processing Advances in Wireless Communication (SPAWC)*, pp. 1–5, 2022.

[35] S. Li, B. Duo, X. Yuan, Y.-C. Liang, and M. Di Renzo, "Reconfigurable intelligent surface assisted uav communication: Joint trajectory design and passive beamforming," *IEEE Wireless Communications Letters*, vol. 9, no. 5, pp. 716–720, 2020.

[36] M. S. Siraj, A. B. Rahman, M. Diamanti, E. E. Tsiropoulou, S. Papavassiliou, and J. Plusquellic, "Orchestration of reconfigurable intelligent surfaces for positioning, navigation, and timing," in *MILCOM 2022 - 2022 IEEE Military Communications Conference (MILCOM)*, pp. 148–153, 2022.

[37] M. S. Siraj, A. B. Rahman, M. Diamanti, E. E. Tsiropoulou, and S. Papavassiliou, "Alternative positioning, navigation, and timing enabled by games in satisfaction form and reconfigurable intelligent surfaces," *IEEE Systems Journal*, vol. 17, no. 3, pp. 5035–5046, 2023.

[38] M. S. Hossain, N. is Irtija, M. Diamanti, F. Sangoleye, E. E. Tsiropoulou, and S. Papavassiliou, "Reconfigurable intelligent surfaces-enabled edge computing: A location-aware task offloading framework," *ITU Journal on Future and Evolving Technologies*, vol. 3, no. 3, pp. 830–843, 2022.

[39] ETSI, "Multi-access edge computing (mec); phase 2: Use cases and requirements," Tech. Rep. GS MEC 002 V2.1.1, Sophia Antipolis Cedex, France, 2018 [Online].

[40] R. B. Myerson, *Game Theory: Analysis of Conflict*. Harvard University Press, 1997.

[41] P. Bolton and M. Dewatripont, *Contract Theory*. MIT Press, 2005.

[42] Y. Zhang, L. Song, W. Saad, Z. Dawy, and Z. Han, "Contract-based incentive mechanisms for device-to-device communications in cellular networks," *IEEE Journal on Selected Areas in Communications*, vol. 33, no. 10, pp. 2144–2155, 2015.

[43] L. Duan, L. Gao, and J. Huang, "Cooperative spectrum sharing: A contract-based approach," *IEEE Transactions on Mobile Computing*, vol. 13, no. 1, pp. 174–187, 2014.

[44] J. Du, E. Gelenbe, C. Jiang, H. Zhang, and Y. Ren, "Contract design for traffic offloading and resource allocation in heterogeneous ultra-dense networks," *IEEE Journal on Selected Areas in Communications*, vol. 35, no. 11, pp. 2457–2467, 2017.

[45] J. Von Neumann and O. Morgenstern, "Theory of games and economic behavior," in *Theory of games and economic behavior*, Princeton university press, 2007.

[46] J. Nash, "Non-cooperative games," *Annals of mathematics*, pp. 286–295, 1951.

[47] R. S. Gibbons, *Game theory for applied economists*. Princeton University Press, 1992.

[48] A. M. Colman, *Game theory and its applications: In the social and biological sciences*. Psychology Press, 2013.

[49] Q. Zhu and T. Başar, *Decision and Game Theory for Security*. Springer, 2013.

[50] S. Lasaulce and H. Tembine, *Game theory and learning for wireless networks: fundamentals and applications*. Academic Press, 2011.

[51] J. Tirole, "Market power and regulation," *Scientific Background on the Sveriges Riksbank Prize in Economic Sciences in Memory of Alfred Nobel*, pp. 1–6, 2014.

[52] O. Hart and B. Holmström, "The theory of contracts," in *Advances in economic theory: Fifth world congress*, vol. 71, p. 155, Cambridge, 1987.

[53] M. Eswaran and A. Kotwal, "A theory of contractual structure in agriculture," *The American Economic Review*, vol. 75, no. 3, pp. 352–367, 1985.

[54] J.-J. Laffont and J. Tirole, *Competition in telecommunications*. MIT press, 2001.

[55] M. Diamanti, G. Fragkos, E. E. Tsiropoulou, and S. Papavassiliou, "Resource orchestration in interference-limited small cell networks: A contract-theoretic approach," in *International Conference on Network Games, Control and Optimization*, pp. 101–109, Springer, 2021.

[56] M. Diamanti, E. E. Tsiropoulou, and S. Papavassiliou, "An incentivization mechanism for green computing continuum of delay-tolerant tasks," in *ICC 2022 - IEEE International Conference on Communications*, pp. 3538–3543, 2022.

[57] M. Diamanti, E. E. Tsiropoulou, and S. Papavassiliou, "Resource orchestration in uav-assisted noma wireless networks: A labor economics perspective," in *ICC 2021 - IEEE International Conference on Communications*, pp. 1–6, 2021.

[58] M. Diamanti and S. Papavassiliou, "Trading in collaborative mobile edge computing networks: A contract theory-based auction model," in *2022 18th International Conference on Distributed Computing in Sensor Systems (DCOSS)*, pp. 387–393, 2022.

[59] Z. Ding, Z. Yang, P. Fan, and H. V. Poor, "On the performance of non-orthogonal multiple access in 5g systems with randomly deployed users," *IEEE Signal Processing Letters*, vol. 21, no. 12, pp. 1501–1505, 2014.

[60] Z. Ding, P. Fan, and H. V. Poor, "Impact of user pairing on 5g nonorthogonal multiple-access downlink transmissions," *IEEE Transactions on Vehicular Technology*, vol. 65, no. 8, pp. 6010–6023, 2016.

[61] Z. Yang, Z. Ding, P. Fan, and N. Al-Dhahir, "A general power allocation scheme to guarantee quality of service in downlink and uplink noma systems," *IEEE Transactions on Wireless Communications*, vol. 15, no. 11, pp. 7244–7257, 2016.

[62] S. Timotheou and I. Krikidis, "Fairness for non-orthogonal multiple access in 5g systems," *IEEE Signal Processing Letters*, vol. 22, no. 10, pp. 1647–1651, 2015.

[63] W. Bao, H. Chen, Y. Li, and B. Vucetic, "Joint rate control and power allocation for non-orthogonal multiple access systems," *IEEE Journal on Selected Areas in Communications*, vol. 35, no. 12, pp. 2798–2811, 2017.

[64] J. Zhao, Y. Liu, K. K. Chai, A. Nallanathan, Y. Chen, and Z. Han, "Spectrum allocation and power control for non-orthogonal multiple access in hetnets," *IEEE Transactions on Wireless Communications*, vol. 16, no. 9, pp. 5825–5837, 2017.

[65] P. Charatsaris, M. Diamanti, E. E. Tsiropoulou, and S. Papavassiliou, "Efficient power control for integrated sensing and communication networks with dual connectivity," in *ICC 2023 - IEEE International Conference on Communications*, pp. 5910–5915, 2023.

[66] L. P. Qian, Y. Wu, H. Zhou, and X. Shen, "Joint uplink base station association and power control for small-cell networks with non-orthogonal multiple access," *IEEE Transactions on Wireless Communications*, vol. 16, no. 9, pp. 5567–5582, 2017.

[67] S. Zhang and G. Kang, "User association and power control for energy efficiency maximization in m2m-enabled uplink heterogeneous networks with noma," *Sensors*, vol. 19, p. 5307, Dec 2019.

[68] M. S. Elbamby, M. Bennis, W. Saad, M. Debbah, and M. Latva-aho, "Resource optimization and power allocation in in-band full duplex-enabled non-orthogonal multiple access networks," *IEEE Journal on Selected Areas in Communications*, vol. 35, no. 12, 2017.

[69] A. Celik, M.-C. Tsai, R. M. Radaydeh, F. S. Al-Qahtani, and M.-S. Alouini, "Distributed user clustering and resource allocation for imperfect noma in heterogeneous networks," 2019.

[70] Z. Yang, Z. Ding, P. Fan, and G. K. Karagiannidis, "On the performance of non-orthogonal multiple access systems with partial channel information," *IEEE Transactions on Communications*, vol. 64, no. 2, pp. 654–667, 2016.

[71] P. Xu and K. Cumanan, "Optimal power allocation scheme for non-orthogonal multiple access with α -fairness," *IEEE Journal on Selected Areas in Communications*, vol. 35, no. 10, pp. 2357–2369, 2017.

[72] Z. Wei, D. W. K. Ng, and J. Yuan, "Power-efficient resource allocation for mc-noma with statistical channel state information," in *2016 IEEE Global Communications Conference (GLOBECOM)*, pp. 1–7, 2016.

[73] F. Fang, H. Zhang, J. Cheng, S. Roy, and V. C. M. Leung, "Joint user scheduling and power allocation optimization for energy-efficient noma systems with imperfect csi," *IEEE Journal on Selected Areas in Communications*, vol. 35, no. 12, pp. 2874–2885, 2017.

[74] Z. Wei, D. W. K. Ng, J. Yuan, and H. Wang, "Optimal resource allocation for power-efficient mc-noma with imperfect channel state information," *IEEE Transactions on Communications*, vol. 65, no. 9, pp. 3944–3961, 2017.

[75] W. Lu, S. Hu, X. Liu, C. He, and Y. Gong, "Incentive mechanism based cooperative spectrum sharing for ofdm cognitive iot network," *IEEE Transactions on Network Science and Engineering*, pp. 1–1, 2019.

[76] R. Tang, J. Cheng, and Z. Cao, "Contract-based incentive mechanism for cooperative noma systems," *IEEE Communications Letters*, vol. 23, no. 1, pp. 172–175, 2019.

[77] A. Asheralieva and Y. Miyanaga, "Optimal contract design for joint user association and intercell interference mitigation in heterogeneous lte-a networks with asymmetric information," *IEEE Transactions on Vehicular Technology*, vol. 66, no. 6, pp. 5284–5300, 2017.

[78] Z. Hasan and V. K. Bhargava, "Relay selection for ofdm wireless systems under asymmetric information: A contract-theory based approach," *IEEE Transactions on Wireless Communications*, vol. 12, no. 8, pp. 3824–3837, 2013.

[79] A. Kaloxylos, A. Gavras, D. Camps, M. Ghoraishi, and H. Hrasnica, "Ai and ml–enablers for beyond 5g networks," 2021.

[80] D. Prelec, "A bayesian truth serum for subjective data," *science*, vol. 306, no. 5695, pp. 462–466, 2004.

[81] P. Sedlmeier and G. Gigerenzer, "Teaching bayesian reasoning in less than two hours.," *Journal of experimental psychology: general*, vol. 130, no. 3, p. 380, 2001.

[82] T. Van Erven and P. Harremos, "Rényi divergence and kullback-leibler divergence," *IEEE Transactions on Information Theory*, vol. 60, no. 7, pp. 3797–3820, 2014.

[83] L. M. Cabral, "The economics of trust and reputation: A primer," *New York University and CEPR*, vol. 2005, 2005.

[84] Y. Xu, J. Wang, and Q. Wu, "Distributed learning of equilibria with incomplete, dynamic, and uncertain information in wireless communication networks," *Game Theory Framework Applied to Wireless Comm. Net., IGI Global*, pp. 63–86, 2016.

[85] P. Vamvakas, E. E. Tsiropoulou, and S. Papavassiliou, "Dynamic provider selection & power resource management in competitive wireless communication markets," *Mobile Networks and Applications*, vol. 23, no. 1, pp. 86–99, 2018.

[86] C. Huang, R. Mo, and C. Yuen, "Reconfigurable intelligent surface assisted multiuser miso systems exploiting deep reinforcement learning," *IEEE Journal on Selected Areas in Communications*, vol. 38, no. 8, pp. 1839–1850, 2020.

[87] J. Nocedal and S. Wright, "Sequential quadratic programming," *Numerical Optimization, Springer*, pp. 529–562, 2006.

[88] T. Coleman, M. A. Branch, and A. Grace, "Optimization toolbox," *For use with MATLAB. User's guide for MATLAB*, vol. 5, 1999.

[89] P. A. Apostolopoulos, E. E. Tsiropoulou, and S. Papavassiliou, "Risk-aware data offloading in multi-server multi-access edge computing environment," *IEEE/ACM Transactions on Networking*, vol. 28, no. 3, pp. 1405–1418, 2020.

[90] M. Diamanti, G. Fragkos, E. E. Tsiropoulou, and S. Papavassiliou, "Unified user association and contract-theoretic resource orchestration in noma heterogeneous wireless networks," *IEEE Open Journal of the Communications Society*, vol. 1, pp. 1485–1502, 2020.

[91] ETSI, "Lte; evolved universal terrestrial radio access (eutra) and evolved universal terrestrial radio access network (eutran); overall description; stage 2," Tech. Rep. TS 136 300 V9.4.0, Sophia Antipolis Cedex, France, 2010 [Online].

[92] W. Khawaja, I. Guvenc, D. W. Matolak, U. Fiebig, and N. Schneckenburger, "A survey of air-to-ground propagation channel modeling for unmanned aerial vehicles," *IEEE Communications Surveys Tutorials*, vol. 21, no. 3, pp. 2361–2391, 2019.

[93] R. Jain, D. M. Chiu, and H. WR, "A quantitative measure of fairness and discrimination for resource allocation in shared computer systems," *CoRR*, vol. cs.NI/9809099, 01 1998.

[94] C. Madapatha, B. Makki, C. Fang, O. Teyeb, E. Dahlman, M.-S. Alouini, and T. Svensson, "On integrated access and backhaul networks: Current status and potentials," *IEEE Open Journal of the Communications Society*, vol. 1, pp. 1374–1389, 2020.

[95] 3GPP, "3rd generation partnership project; technical specification group radio access network; study on integrated access and backhaul; (release 16)," Tech. Rep. TR 38.874 V16.0.0, Sophia Antipolis Valbonne, France, 2018 [Online].

[96] J. Y. Lai, W.-H. Wu, and Y. T. Su, "Resource allocation and node placement in multihop heterogeneous integrated-access-and-backhaul networks," *IEEE Access*, vol. 8, pp. 122937–122958, 2020.

[97] W. Lei, Y. Ye, and M. Xiao, "Deep reinforcement learning-based spectrum allocation in integrated access and backhaul networks," *IEEE Transactions on Cognitive Communications and Networking*, vol. 6, no. 3, pp. 970–979, 2020.

[98] Q. Zhang, W. Ma, Z. Feng, and Z. Han, "Backhaul capacity aware interference mitigation framework in 6g cellular internet of things," *IEEE Internet of Things Journal*, pp. 1–1, 2021.

[99] N. Tafintsev, D. Moltchanov, M. Gerasimenko, M. Gapeyenko, J. Zhu, S.-p. Yeh, N. Himayat, S. Andreev, Y. Koucheryavy, and M. Valkama, "Aerial access and backhaul in mmwave b5g systems: Performance dynamics and optimization," *IEEE Communications Magazine*, vol. 58, no. 2, pp. 93–99, 2020.

[100] M.-J. Youssef, J. Farah, C. A. Nour, and C. Douillard, "Full-duplex and backhaul-constrained uav-enabled networks using noma," *IEEE Trans. on Veh. Tech.*, vol. 69, no. 9, pp. 9667–9681, 2020.

[101] L. Zhang and N. Ansari, "Optimizing the deployment and throughput of dbss for uplink communications," *IEEE Open Journal of Vehicular Technology*, vol. 1, pp. 18–28, 2020.

[102] A. Fouda, A. Ibrahim, I. Guvenc, and M. Ghosh, "Interference management in uav-assisted integrated access and backhaul networks," *IEEE Access*, vol. PP, pp. 1–1, 07 2019.

[103] P. Charatsaris, M. Diamanti, E. E. Tsiropoulou, and S. Papavassiliou, "Competitive energy allocation for aerial computation offloading: A colonel blotto game," in *GLOBECOM 2022 - 2022 IEEE Global Communications Conference*, pp. 970–975, 2022.

[104] B. Zheng, Q. Wu, and R. Zhang, "Intelligent reflecting surface-assisted multiple access with user pairing: Noma or oma?," *IEEE Communications Letters*, vol. 24, no. 4, pp. 753–757, 2020.

[105] Y. Guo, Z. Qin, Y. Liu, and N. Al-Dhahir, "Intelligent reflecting surface assisted noma over fading channels," in *GLOBECOM 2020 - 2020 IEEE Global Communications Conference*, pp. 1–6, 2020.

[106] M. Diamanti, M. Tsampazi, E. E. Tsiropoulou, and S. Papavassiliou, "Energy efficient multi-user communications aided by reconfigurable intelligent surfaces and uavs," in *2021 IEEE International Conference on Smart Computing (SMARTCOMP)*, pp. 371–376, 2021.

[107] M. Diamanti, E. E. Tsiropoulou, and S. Papavassiliou, "The joint power of noma and reconfigurable intelligent surfaces in swipt networks," in *2021 IEEE 22nd International Workshop on Signal Processing Advances in Wireless Communications (SPAWC)*, pp. 621–625, 2021.

[108] X. Gao, Y. Liu, X. Liu, and Z. Qin, "Resource allocation in irss aided miso-noma networks: A machine learning approach," in *GLOBECOM 2020 - 2020 IEEE Global Communications Conference*, pp. 1–6, 2020.

[109] M. Zeng, X. Li, G. Li, W. Hao, and O. A. Dobre, "Sum rate maximization for irs-assisted uplink noma," *IEEE Communications Letters*, vol. 25, no. 1, pp. 234–238, 2021.

[110] Y. Cheng, K. H. Li, Y. Liu, K. C. Teh, and H. Vincent Poor, "Downlink and uplink intelligent reflecting surface aided networks: Noma and oma," *IEEE Transactions on Wireless Communications*, pp. 1–1, 2021.

[111] J. Xiong, L. You, D. W. K. Ng, C. Yuen, W. Wang, and X. Gao, "Energy efficiency and spectral efficiency tradeoff in ris-aided multiuser mimo uplink systems," in *GLOBECOM 2020 - 2020 IEEE Global Communications Conference*, pp. 1–6, 2020.

[112] Z. Wei, Y. Cai, Z. Sun, D. W. Kwan Ng, and J. Yuan, "Sum-rate maximization for irs-assisted uav ofdma communication systems," in *IEEE Global Communications Conf. (GLOBECOM)*, pp. 1–7, 2020.

[113] X. Liu, Y. Liu, and Y. Chen, "Machine learning empowered trajectory and passive beamforming design in uav-ris wireless networks," *IEEE Journal on Selected Areas in Communications*, pp. 1–1, 2020.

[114] Q. Zhang, W. Saad, and M. Bennis, "Distributional reinforcement learning for mmwave communications with intelligent reflectors on a uav," in *IEEE Global Comm. Conf. (GLOBECOM)*, pp. 1–6, 2020.

[115] S. Jia, X. Yuan, and Y.-C. Liang, "Reconfigurable intelligent surfaces for energy efficiency in d2d communication network," *IEEE Wireless Communications Letters*, vol. 10, no. 3, pp. 683–687, 2021.

[116] P. D. Diamantoulakis, K. N. Pappi, and G. K. Karagiannidis, "Jointly optimal downlink/uplink design for wireless powered networks," in *2017 24th International Conference on Telecommunications (ICT)*, pp. 1–6, 2017.

[117] S. Boyd and L. Vandenberghe, *Convex Optimization, Cambridge*. Cambridge University Press, 2004.

[118] S. Schaible, *Fractional Programming*. Boston, MA: Springer US, 2013.

[119] W. Dinkelbach, "On nonlinear fractional programming," *Management Science*, vol. 13, no. 7, pp. 492–498, 1967.

[120] A. Zappone and E. Jorswieck, "Energy efficiency in wireless networks via fractional programming theory," *Foundations and Trends in Communications and Information Theory*, vol. 11, no. 3-4, pp. 185–396, 2015.

[121] F. Forgó, "On the existence of nash-equilibrium in n-person generalized concave game," *In: Komlósi S., Rapcsák T., Schaible S. (eds) Generalized Convexity. Lecture Notes in Econom. and Math. Syst.*, vol. 405, 1994.

[122] E. E. Tsiropoulou, P. Vamvakas, G. K. Katsinis, and S. Papavassiliou, "Combined power and rate allocation in self-optimized multi-service two-tier femtocell networks," *Computer Communications*, vol. 72, pp. 38–48, 2015.

[123] F. A. Potra and S. J. Wright, "Interior-point methods," *Journal of Computational and Applied Mathematics*, vol. 124, no. 1, pp. 281–302, 2000. Numerical Analysis 2000. Vol. IV: Optimization and Nonlinear Equations.

[124] T. H. Cormen, C. E. Leiserson, R. L. Rivest, and C. Stein, *Introduction to Algorithms*. Cambridge, MA: MIT Press, 2009.

[125] M. Diamanti, P. Charatsaris, E. E. Tsiropoulou, and S. Papavassiliou, "The prospect of reconfigurable intelligent surfaces in integrated access and backhaul networks," *IEEE Transactions on Green Communications and Networking*, vol. 6, no. 2, pp. 859–872, 2022.

[126] M. Mukherjee, S. Kumar, Q. Zhang, R. Matam, C. X. Mavromoustakis, Y. Lv, and G. Mastorakis, "Task data offloading and resource allocation in fog computing with multi-task delay guarantee," *IEEE Access*, vol. 7, pp. 152911–152918, 2019.

[127] H. Shah-Mansouri and V. W. S. Wong, "Hierarchical fog-cloud computing for iot systems: A computation offloading game," *IEEE Internet of Things Journal*, vol. 5, no. 4, pp. 3246–3257, 2018.

[128] Y. Wang, X. Tao, X. Zhang, P. Zhang, and Y. T. Hou, "Cooperative task offloading in three-tier mobile computing networks: An admm framework," *IEEE Transactions on Vehicular Technology*, vol. 68, no. 3, pp. 2763–2776, 2019.

[129] E. El Haber, T. M. Nguyen, and C. Assi, "Joint optimization of computational cost and devices energy for task offloading in multi-tier edge-clouds," *IEEE Transactions on Communications*, vol. 67, no. 5, pp. 3407–3421, 2019.

[130] L. Li and H. Zhang, "Delay optimization strategy for service cache and task offloading in three-tier architecture mobile edge computing system," *IEEE Access*, vol. 8, pp. 170211–170224, 2020.

[131] Y. Chen, S. He, F. Hou, Z. Shi, and J. Chen, "An efficient incentive mechanism for device-to-device multicast communication in cellular networks," *IEEE Transactions on Wireless Communications*, vol. 17, no. 12, pp. 7922–7935, 2018.

[132] Q. Ma, L. Gao, Y.-F. Liu, and J. Huang, "Incentivizing wi-fi network crowdsourcing: A contract theoretic approach," *IEEE/ACM Transactions on Networking*, vol. 26, no. 3, pp. 1035–1048, 2018.

[133] C. Su, F. Ye, T. Liu, Y. Tian, and Z. Han, "Computation offloading in hierarchical multi-access edge computing based on contract theory and bayesian matching game," *IEEE Transactions on Vehicular Technology*, vol. 69, no. 11, pp. 13686–13701, 2020.

[134] C. Yang, W. Lou, Y. Liu, and S. Xie, "Resource allocation for edge computing-based vehicle platoon on freeway: A contract-optimization approach," *IEEE Transactions on Vehicular Technology*, vol. 69, no. 12, pp. 15988–16000, 2020.

[135] J. Zhao, M. Kong, Q. Li, and X. Sun, "Contract-based computing resource management via deep reinforcement learning in vehicular fog computing," *IEEE Access*, vol. 8, pp. 3319–3329, 2020.

[136] Y. Li, J. Zhang, X. Gan, L. Fu, H. Yu, and X. Wang, "A contract-based incentive mechanism for delayed traffic offloading in cellular networks," *IEEE Transactions on Wireless Communications*, vol. 15, no. 8, pp. 5314–5327, 2016.

[137] Z. Xiong, J. Kang, D. Niyato, P. Wang, H. V. Poor, and S. Xie, "A multi-dimensional contract approach for data rewarding in mobile networks," *IEEE Transactions on Wireless Communications*, vol. 19, no. 9, pp. 5779–5793, 2020.

[138] W. Y. B. Lim, J. Huang, Z. Xiong, J. Kang, D. Niyato, X.-S. Hua, C. Leung, and C. Miao, "Towards federated learning in uav-enabled internet of vehicles: A multi-dimensional contract-matching approach," *IEEE Transactions on Intelligent Transportation Systems*, vol. 22, no. 8, pp. 5140–5154, 2021.

[139] Z. Wang, L. Gao, and J. Huang, "Multi-cap optimization for wireless data plans with time flexibility," *IEEE Transactions on Mobile Computing*, vol. 19, no. 9, pp. 2145–2159, 2020.

[140] G. Mitsis, E. E. Tsiropoulou, and S. Papavassiliou, "Data offloading in uav-assisted multi-access edge computing systems: A resource-based pricing and user risk-awareness approach," *Sensors*, vol. 20, no. 8: 2434, 2020.

[141] F. Fang, Y. Xu, Z. Ding, C. Shen, M. Peng, and G. K. Karagiannidis, "Optimal resource allocation for delay minimization in noma-mec networks," *IEEE Transactions on Communications*, vol. 68, no. 12, pp. 7867–7881, 2020.

[142] Y. Pan, M. Chen, Z. Yang, N. Huang, and M. Shikh-Bahaei, "Energy-efficient noma-based mobile edge computing offloading," *IEEE Communications Letters*, vol. 23, no. 2, pp. 310–313, 2019.

[143] K. Wang, Z. Ding, D. K. C. So, and G. K. Karagiannidis, "Stackelberg game of energy consumption and latency in mec systems with noma," *IEEE Transactions on Communications*, vol. 69, no. 4, pp. 2191–2206, 2021.

[144] Z. Han, D. Niyato, W. Saad, T. Başar, and A. Hjørungnes, *Game Theory in Wireless and Communication Networks: Theory, Models, and Applications*. New York, NY, USA: Cambridge University Press, 2011.

[145] S. S. Gill, "A manifesto for modern fog and edge computing: Vision, new paradigms, opportunities, and future directions," in *Operationalizing Multi-Cloud Environments: Technologies, Tools and Use Cases* (R. Nagarajan, P. Raj, and R. Thirunavukarasu, eds.), pp. 237–253, Cham: Springer International Publishing, 2022.

[146] M. Goudarzi, H. Wu, M. Palaniswami, and R. Buyya, "An application placement technique for concurrent iot applications in edge and fog computing environments," *IEEE Transactions on Mobile Computing*, vol. 20, no. 4, pp. 1298–1311, 2021.

[147] M. Heck, J. Edinger, D. Schaefer, and C. Becker, "Iot applications in fog and edge computing: Where are we and where are we going?," in *2018 27th International Conference on Computer Communication and Networks (ICCCN)*, pp. 1–6, 2018.

[148] G. Kakkavas, M. Diamanti, K. Nseboah Nyarko, M. Gabriel, V. Karyotis, K. Mößner, and S. Papavassiliou, "Realistic field trial evaluation of a tele-operated support service for remote driving over 5g," in *2022 IEEE Conference on Standards for Communications and Networking (CSCN)*, pp. 58–63, 2022.

[149] Y. Mao, C. You, J. Zhang, K. Huang, and K. B. Letaief, "A survey on mobile edge computing: The communication perspective," *IEEE Communications Surveys Tutorials*, vol. 19, no. 4, pp. 2322–2358, 2017.

[150] Q.-V. Pham, F. Fang, V. N. Ha, M. J. Piran, M. Le, L. B. Le, W.-J. Hwang, and Z. Ding, "A survey of multi-access edge computing in 5g and beyond: Fundamentals, technology integration, and state-of-the-art," *IEEE Access*, vol. 8, pp. 116974–117017, 2020.

[151] D. Pliatsios, P. Sarigiannidis, T. D. Lagkas, V. Argyriou, A.-A. A. Boulogeorgos, and P. Baziana, "Joint wireless resource and computation offloading optimization for energy efficient internet of vehicles," *IEEE Transactions on Green Communications and Networking*, vol. 6, no. 3, pp. 1468–1480, 2022.

[152] S. Mao, J. Wu, L. Liu, D. Lan, and A. Taherkordi, "Energy-efficient cooperative communication and computation for wireless powered mobile-edge computing," *IEEE Systems Journal*, pp. 1–12, 2020.

[153] Y. Liu, F. R. Yu, X. Li, H. Ji, and V. C. M. Leung, "Distributed resource allocation and computation offloading in fog and cloud networks with non-orthogonal multiple access," *IEEE Transactions on Vehicular Technology*, vol. 67, no. 12, pp. 12137–12151, 2018.

[154] P. A. Apostolopoulos, G. Fragkos, E. E. Tsiropoulou, and S. Papavassiliou, "Data offloading in uav-assisted multi-access edge computing systems under resource uncertainty," *IEEE Transactions on Mobile Computing*, pp. 1–1, 2021.

[155] X. Chen, L. Jiao, W. Li, and X. Fu, "Efficient multi-user computation offloading for mobile-edge cloud computing," *IEEE/ACM Transactions on Networking*, vol. 24, no. 5, pp. 2795–2808, 2016.

[156] G. Zheng, C. Xu, H. Long, and X. Zhao, "Mec in noma-hetnets: A joint task offloading and resource allocation approach," in *2021 IEEE Wireless Communications and Networking Conference (WCNC)*, pp. 1–6, 2021.

[157] B. Liu, C. Liu, and M. Peng, "Resource allocation for energy-efficient mec in noma-enabled massive iot networks," *IEEE Journal on Selected Areas in Communications*, vol. 39, no. 4, pp. 1015–1027, 2021.

[158] J. C. Bezdek and R. J. Hathaway, "Some notes on alternating optimization," in *Advances in Soft Computing — AFSS 2002* (N. R. Pal and M. Sugeno, eds.), (Berlin, Heidelberg), pp. 288–300, Springer Berlin Heidelberg, 2002.

[159] E. E. Tsiropoulou, G. K. Katsinis, and S. Papavassiliou, "Distributed uplink power control in multiservice wireless networks via a game theoretic approach with convex pricing," *IEEE Transactions on Parallel and Distributed Systems*, vol. 23, no. 1, pp. 61–68, 2012.

[160] H. Yu, Y. Li, M. Kountouris, X. Xu, and J. Wang, "Energy efficiency analysis of relay-assisted cellular networks," *EURASIP Journal on Advances in Signal Processing*, vol. 2014, no. 1, pp. 1–11, 2014.

[161] M. Diamanti, P. Charatsaris, E. E. Tsiropoulou, and S. Papavassiliou, "Incentive mechanism and resource allocation for edge-fog networks driven by multi-dimensional contract and game theories," *IEEE Open Journal of the Communications Society*, vol. 3, pp. 435–452, 2022.

[162] J.-J. Yu, M. Zhao, W.-T. Li, D. Liu, S. Yao, and W. Feng, "Joint offloading and resource allocation for time-sensitive multi-access edge computing network," in *2020 IEEE Wireless Communications and Networking Conference (WCNC)*, pp. 1–6, 2020.

[163] W. Zhou, L. Lin, J. Liu, D. Zhang, and Y. Xie, "Joint offloading decision and resource allocation for multiuser noma-mec systems," *IEEE Access*, vol. 7, pp. 181100–181116, 2019.

[164] K. Wang, F. Fang, D. B. d. Costa, and Z. Ding, "Sub-channel scheduling, task assignment, and power allocation for oma-based and noma-based mec systems," *IEEE Transactions on Communications*, vol. 69, no. 4, pp. 2692–2708, 2021.

[165] T. X. Tran and D. Pompili, "Joint task offloading and resource allocation for multi-server mobile-edge computing networks," *IEEE Transactions on Vehicular Technology*, vol. 68, no. 1, pp. 856–868, 2019.

[166] P. Wang, K. Li, B. Xiao, and K. Li, "Multi-objective optimization for joint task offloading, power assignment, and resource allocation in mobile edge computing," *IEEE Internet of Things J.*, pp. 1–1, 2021.

[167] C. Li, H. Wang, and R. Song, "Mobility-aware offloading and resource allocation in noma-mec systems via dc," *IEEE Communications Letters*, pp. 1–1, 2022.

[168] F. Fang, K. Wang, Z. Ding, and V. C. M. Leung, "Energy-efficient resource allocation for noma-mec networks with imperfect csi," *IEEE Transactions on Communications*, vol. 69, no. 5, pp. 3436–3449, 2021.

[169] C. Xu, G. Zheng, and X. Zhao, "Energy-minimization task offloading and resource allocation for mobile edge computing in noma heterogeneous networks," *IEEE Transactions on Vehicular Technology*, vol. 69, no. 12, pp. 16001–16016, 2020.

[170] J. Xue and Y. An, "Joint task offloading and resource allocation for multi-task multi-server noma-mec networks," *IEEE Access*, vol. 9, pp. 16152–16163, 2021.

[171] H. Xia, Y. Mao, B. Clerckx, X. Zhou, S. Han, and C. Li, "Weighted sum-rate maximization for rate-splitting multiple access based secure communication," 2022.

[172] Y. Mao, B. Clerckx, and V. O. Li, "Energy efficiency of rate-splitting multiple access, and performance benefits over sdma and noma," in *2018 15th International Symposium on Wireless Communication Systems (ISWCS)*, pp. 1–5, 2018.

[173] G. Zhou, Y. Mao, and B. Clerckx, "Rate-splitting multiple access for multi-antenna downlink communication systems: Spectral and energy efficiency tradeoff," *IEEE Transactions on Wireless Communications*, pp. 1–1, 2021.

[174] M. Diamanti, G. Kapsalis, E. E. Tsiropoulou, and S. Papavassiliou, "Energy-efficient rate-splitting multiple access: A deep reinforcement learning-based framework," *IEEE Open Journal of the Communications Society*, pp. 1–1, 2023.

[175] Y. Mao, B. Clerckx, and V. O. Li, "Rate-splitting for multi-user multi-antenna wireless information and power transfer," in *2019 IEEE 20th International Workshop on Signal Processing Advances in Wireless Communications (SPAWC)*, pp. 1–5, 2019.

[176] A. Mishra, Y. Mao, L. Sanguinetti, and B. Clerckx, "Rate-splitting assisted massive machine-type communications in cell-free massive mimo," *IEEE Communications Letters*, pp. 1–1, 2022.

[177] L. Yin and B. Clerckx, "Rate-splitting multiple access for dual-functional radar-communication satellite systems," in *2022 IEEE Wireless Communications and Networking Conference (WCNC)*, pp. 1–6, 2022.

[178] A. Bansal, N. Agrawal, and K. Singh, "Rate-splitting multiple access for uav-based ris-enabled interference-limited vehicular communication system," *IEEE Transactions on Intelligent Vehicles*, pp. 1–1, 2022.

[179] H. Liu, Y. Ye, Z. Bai, K. J. Kim, and T. A. Tsiftsis, "Rate splitting multiple access aided mobile edge computing in cognitive radio networks," 2022.

[180] T. P. Truong, N.-N. Dao, and S. Cho, "Hamec-rsma: Enhanced aerial computing systems with rate splitting multiple access," *IEEE Access*, vol. 10, pp. 52398–52409, 2022.

[181] S. Deng, H. Zhao, W. Fang, J. Yin, S. Dustdar, and A. Y. Zomaya, "Edge intelligence: The confluence of edge computing and artificial intelligence," *IEEE Internet of Things Journal*, vol. 7, no. 8, pp. 7457–7469, 2020.

[182] G. Kakkavas, K. N. Nyarko, C. Lahoud, D. Kühnert, P. Küffner, M. Gabriel, S. Ehsanfar, M. Diamanti, V. Karyotis, K. Mößner, and S. Papavassiliou, "Teleoperated support for remote driving over 5g mobile communications," in *2022 IEEE International Mediterranean Conference on Communications and Networking (MeditCom)*, pp. 280–285, 2022.

[183] G. Kakkavas, M. Diamanti, M. Gabriel, C. Lahoud, P. Akula, V. Karyotis, K. Mößner, and S. Papavassiliou, "Demo proposal: Tele-operated support over 4g/5g mobile communications," in *2021 IEEE International Mediterranean Conference on Communications and Networking (MeditCom)*, pp. 1–2, 2021.

[184] M. Luptacik *et al.*, *Mathematical optimization and economic analysis*. Springer, 2010.

[185] M. Diamanti, C. Pelekis, E. E. Tsiropoulou, and S. Papavassiliou, "Delay minimization for rate-splitting multiple access-based multi-server mec offloading," *IEEE/ACM Transactions on Networking*, pp. 1–13, 2023.

[186] K. Seong, M. Mohseni, and J. M. Cioffi, "Optimal resource allocation for ofdma downlink systems," in *2006 IEEE International Symposium on Information Theory*, pp. 1394–1398, 2006.

[187] G. Debreu, "Market equilibrium," *Proceedings of the National Academy of Sciences*, vol. 42, no. 11, pp. 876–878, 1956.

[188] K. P. Naveen and R. Sundaresan, "Double-auction mechanisms for resource trading markets," *IEEE/ACM Transactions on Networking*, vol. 29, no. 3, pp. 1210–1223, 2021.

[189] M. Goonewardena, S. M. Perlaza, A. Yadav, and W. Ajib, "Generalized satisfaction equilibrium for service-level provisioning in wireless networks," *IEEE Transactions on Communications*, vol. 65, no. 6, pp. 2427–2437, 2017.

[190] V. Smith, C.-K. Chiang, M. Sanjabi, and A. S. Talwalkar, "Federated multi-task learning," *Advances in neural information processing systems*, vol. 30, 2017.

[191] Z. Yang, M. Chen, W. Saad, C. S. Hong, and M. Shikh-Bahaei, "Energy efficient federated learning over wireless communication networks," *IEEE Transactions on Wireless Communications*, vol. 20, no. 3, pp. 1935–1949, 2021.

[192] P. Charatsaris, M. Diamanti, and S. Papavassiliou, "On the accuracy-energy tradeoff for hierarchical federated learning via satisfaction equilibrium," in *2023 19th International Conference on Distributed Computing in Smart Systems and the Internet of Things (DCOSS-IoT)*, pp. 422–428, 2023.

[193] F. Meng, P. Chen, L. Wu, and J. Cheng, "Power allocation in multi-user cellular networks: Deep reinforcement learning approaches," *IEEE Transactions on Wireless Communications*, vol. 19, no. 10, pp. 6255–6267, 2020.

[194] Y. S. Nasir and D. Guo, "Multi-agent deep reinforcement learning for dynamic power allocation in wireless networks," *IEEE Journal on Selected Areas in Communications*, vol. 37, no. 10, pp. 2239–2250, 2019.